



جامعة أم القرى

كلية العلوم التطبيقية

قسم الكيمياء

## تأثير بعض المركبات العضوية على السلوك الكهروكيميائي

و التآكلي للألومنيوم و سبائكه في الأوساط الحامضية.

رسالة مقدمة من

بدرية علي الجمالي

و ذلك كجزء من المتطلبات للحصول على درجة الماجستير في الكيمياء

(كيمياء فيزيائية)

الأشراف

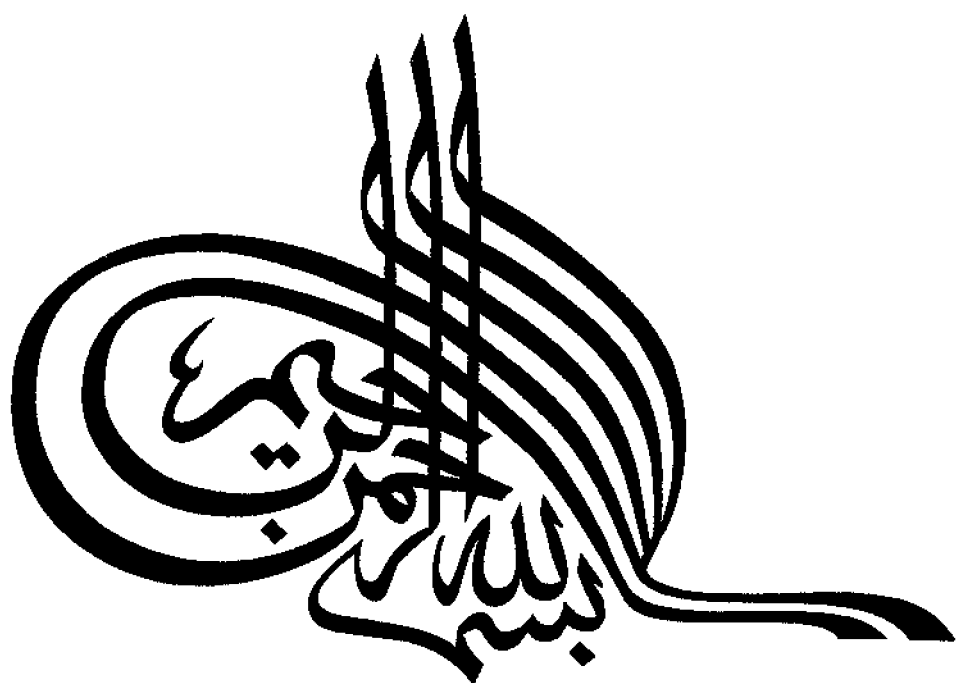
أ. د. عبدالرحمن السيد محمد

أستاذ الكيمياء الفيزيائية

جامعة أم القرى - كلية العلوم التطبيقية

مكة المكرمة

يوضع هذا النموذج أمام الصفحة المقابلة لصفحة عنوان الأطروحة في كل نسخة من الرسالة .



## الملخص العربي

تشتمل الرسالة على دراسة تأثير بعض المواد العضوية على السلوك الكهروكيميائي والتآكلي لكل من الألومنيوم وسبائك الألومنيوم في بعض المحاليل الحامضية، وقد تم اختيار الألومنيوم وسبائكه نظراً للأهمية التكنولوجية الكبيرة فهما يستخدمان على نطاق واسع في صناعة المعلبات وأواني الطهي والطائرات.

**الجزء الأول:** يستعرض الأبحاث التي نشرت في مجال تأثير بعض المثبطات العضوية على السلوك الكهروكيميائي والتآكلي لكل من الألومنيوم وسبائكه في الأوساط الحامضية. وقد وُجد أن هناك عدد قليل من الأبحاث التي أجريت بخصوص بعض مركبات التراي آزول على كل من الألومنيوم وسبائكه، ومن ناحية أخرى لا توجد أبحاث سبق لإجراءها لدراسة تأثير كل من مركبي الأدينين والأدونيدين بصفة خاصة على الألومنيوم وسبائكه.

**الجزء العملي:** يستعرض طريقة إعداد الأقطاب، تحضير المحاليل، وصف الأجهزة المستخدمة في عمليات القياس (الطريقة الجلفانوستاتيكية) وتحضير محاليل مثبطات المواد العضوية التي تم دراستها.

**الجزء الثالث:** يتناول عرض النتائج التي أمكن الحصول عليها في أشكال بيانية وجداول.

**الجزء الرابع:** يختص بمناقشة النتائج وينقسم إلى:

١. تأثير مركبات مشتق البيروول، الأدينين والأدونيدين على السلوك الكهروكيميائي والتآكلي للألومنيوم وسبائك الألومنيوم في محاليل ٠,٥ مولار لكل من حمض الهيدروكلوريك، البيروكلوريك والكبريتيك وقد تم تلخيص هذه الدراسة كالآتي:

أ - السلوك في محلول حمض الهيدروكلوريك:

قد دُرِس كل من الاستقطاب المهبطي والاستقطاب المصعدي على الألومنيوم وسبائكه بطريقة الجهد الثابت في وجود وعدم وجود بعض المركبات العضوية السابق ذكرها بتركيزات تتراوح بين  $10^{-1}$  -  $10^{-2}$  مول/لتر، وقد وُجد أن قيم جهود التآكل لزيحت في الاتجاه الموجب، وأن قيم الفوق جهدية للهيدروجين والذوبان الأنودي قد زادت، ولهذا تُعَدُّ هذه المركبات مثبطات مختلطة أي مهبطية ومصعدية ما عدا مشتق البيروول الذي أظهر فعل مثبط مصعدي فقط على السبيكة رقم (١).

ب - السلوك في محلول حمض البيروكلوريك:

أظهرت النتائج أن مشتق البيروول له فعل مثبط على كل من الألومنيوم النقي وسبائكه ما عدا السبيكة رقم (١) عند تركيز  $10^{-4}$  مول/لتر التي أظهرت زيادة في معدل التآكل عند هذا التركيز. كما وُجد أيضاً أن كلا من مركبي الأدينين و الأدونيدين لهما فعل مثبط على الألومنيوم النقي والسبيكة رقم (٢) ولكن كفاءة المثبط تقل نسبياً عند

التركيز العالي ( $10^{-1}$  مولار)، ولكن نفس هذه المركبات وُجِدَ أنَّها تزيد من معدل التآكل على السبيكة رقم (١) ومعدل التآكل هذا يزداد بزيادة تركيز أي من المركبين. وبالمقارنة بين تأثير كل من الأدينين و الأدونيزين وُجِدَ أن الأدونيزين له فعل مُثَبِّط على الألومنيوم النقي أعلى من الأدينين وذلك بسبب كبر حجم جزيء الأدونيزين.

#### ج - السلوك في محلول حمض الكبريتيك:

أظهرت النتائج أن مشتق البيروول له فعل مُثَبِّط على كل من الألومنيوم النقي والسبيكة رقم (٢) ولكن كفاءة المثبط على الألومنيوم النقي أعلى بالمقارنة بالسبيكة رقم (٢) هذا وقد تمَّ مقارنة قيم كفاءة المثبط لهذا المركب على الألومنيوم النقي في كل من الأحماض الثلاثة فُوجِدَ أن كفاءة المثبط في حمض الكبريتيك أقل منه في حمض الهيدروكلوريك والبيروكلوريك ويُعزى ذلك إلى المنافسة بين امتزاز أيون الكبريتات وجزيئات المثبط على سطح القطب، وقد لوحظ أيضاً أن مركبات الأدينين والأدونيزين لها فعل مُثَبِّط على كل العمليات المبهطية والمصعدية كما أن معدل التآكل على كل من الألومنيوم وسبائكته يقل بزيادة تركيز أيأ من هذه المركبات وقد تمَّ تفسير هذا السلوك على أساس أن امتزاز جزيئات أيأ من الأدينين أو الأدونيزين يؤدي إلى إعاقه امتزاز أيون الكبريتات على السطح.

٢. تأثير بعض مشتقات التراي آزول على السلوك الكهروكيميائي والتآكلي لكل من الألومنيوم وسبائكته في  $0.5$  مولار لمحاليل كل من حمض الهيدروكلوريك والبيروكلوريك والكبريتيك وقد تمَّ تلخيص هذه الدراسة كالآتي:

#### أ - السلوك في محلول حمض الهيدروكلوريك:

لُوحِظَ أن كفاءة المثبط على الألومنيوم النقي تزداد بزيادة التركيز لمشتق التراي آزول المتصل به مجموعة بيريديل في الموضع خمسة ولكن في حالة السبائك تزداد كفاءة المثبط بزيادة التركيز حتى  $5 \times 10^{-4}$  مولار فقط وعند التركيز الأعلى يكون له تأثير عكسي أي زيادة معدل التآكل على كل من السبيكتين. وقد وُجِدَ أن إضافة مركب التراي آزول المتصل به مجموعة توليل له فعل مُثَبِّط عالي جداً على الألومنيوم النقي بالمقارنة مع السبائك، كما أن له فعل مُثَبِّط أكبر على السبيكة رقم (١) مقارنة بالسبيكة رقم (٢). وقد أظهرت النتائج أيضاً أن المركب الثالث لمشتق التراي آزول المتصل به مجموعة نيتروفينيل يؤدي إلى إزاحة جهد التآكل إلى قيم أكثر إيجابية لكل من الألومنيوم النقي وسبائكته ومعدل التآكل يقل بزيادة التركيز ولكن كفاءة المثبط لهذا المركب على الألومنيوم النقي أعلى من كفاءة المثبط على السبائك. وبالمقارنة بين كفاءة التثبيط للمركبات الثلاثة على الألومنيوم النقي وُجِدَ أن مركب التراي آزول المتصل به مجموعة نيتروفينيل له فعل مُثَبِّط أقل من المركبين الآخرين ويُعزى ذلك إلى اختزال مجموعة النيترو على سطح القطب.

#### ب - السلوك في محلول حمض البيروكلوريك:

أظهرت النتائج أن مركب التراي آزول المتصل به مجموعة بيريديل ليس له تأثير على العمليات المبهطية ولكن له فعل مُثَبِّط على العمليات المصعدية للسبيكة رقم (١) بينما الفعل المثبط لهذا المركب على السبيكة رقم (٢) أعلى من الألومنيوم النقي. كما تبين من النتائج أن معدل التآكل لكل من الألومنيوم النقي والسبيكة رقم (٢) يقل بزيادة تركيز مركب التراي آزول المتصل به مجموعة توليل كما أن لهذا المركب تأثير عكسي على السبيكة رقم (١) أي

يزيد من معدل التآكل. في حين وُجِدَ أنَّ مركب التتراي آزول المتصل به مجموعة نيتروفينيل أظهر فعل مُثَبِّط على كل من الألومنيوم النقي وسبائكته ولكن كفاءة المُثَبِّط على كل من الألومنيوم النقي والسبيكة رقم (٢) (٩٥ %) أعلى من على السبيكة رقم (١) (٤٨ %).

#### ج - السلوك في محلول حمض الكبريتيك:

بالمقارنة بين النتائج التي تمَّ الحصول عليها لكل من الألومنيوم النقي و السبائك في وجود مركب التتراي آزول المتصل به مجموعة بيردليل تبين أنَّ هذا المركب يؤدي إلى نقص معدل التآكل ويزداد هذا النقص بزيادة التركيز، كما أنَّ تأثير هذا المركب على الألومنيوم النقي أقوى من تأثيره على السبائك وكفاءة المُثَبِّط أعلى منه للسبائك. وقد تبين أيضاً أنَّ استخدام مركب التتراي آزول المتصل به مجموعة توليل يؤدي إلى نقص معدل التآكل لكل من الألومنيوم وسبائكته وهذا المركب له فعل مُثَبِّط مختلط ( مهبطي ومصعدي ). وكذلك وُجِدَ أنَّ هذا المركب لم يغير في ميكانيكية تفاعل تصاعد غاز الهيدروجين على سطح القطب. كما تمَّ دراسة التأثير المعطل لمركب التتراي آزول المتصل به مجموعة نيتروفينيل، حيث وُجِدَ أنَّ هذا المركب له فعل مُثَبِّط على كل من العمليات المهبطية والمصعدية، كما أنَّ له فعل مُثَبِّط أكبر على الألومنيوم النقي مقارنة بالسبائك خاصة في تعطيل تفاعل تصاعد غاز الهيدروجين. وبالمقارنة بين الفعل المُثَبِّط لهذا المركب في كل من حمض الكبريتيك والهيدروكلوريك خاصة على السبائك وُجِدَ أنَّ الفعل المُثَبِّط لهذا المركب يكون أكبر في حمض الكبريتيك بالنسبة له في حمض الهيدروكلوريك عند نفس التركيز، ويرجع ذلك إلى احتمال عدم إمكانية اختزال مجموعة النيترو في حمض الكبريتيك.

Umm Al-Qura University  
Faculty of Applied Science  
Chemistry Department

***EFFECT OF SOME ORGANIC COMPOUNDS ON  
THE ELECTROCHEMICAL AND CORROSION  
BEHAVIOUR OF ALUMINIUM AND ALUMINIUM  
ALLOYS IN ACIDIC MEDIA.***

By

***Badriah Ali Al-Jahdali***

(B. Sc. in Chemistry)

A thesis

Submitted in Partial Fulfillment of the Requirements for the  
Master Degree in Chemistry  
(Physical Chemistry)

*Supervisor*

***Prof. Dr. A. El-Sayed Mohamed***

Professor of Physical Chemistry  
Umm Al-Qura University  
Faculty of Applied Science  
Makkah Al-Mukarramah

1421 H



وَمَا تَوْفِيقِي إِلَّا بِاللَّهِ







*To my dear parents*



# ACKNOWLEDGEMENT

My thanks to Allah for his guidance and to help me in my studies and for all those efforts to achieve this thesis: studying, working and writing and peace be upon our prophet Mohammed.

First and foremost, I send my deepest appreciation to my dear parents and my dear family for their patience and comprehending the essence of the scientific research and also, for their supporting me in my academic career. I, also, offer my thanks to my dear brother Hamzah with all the compliments and what he bears for my sake.

Also, I would like to express my deepest appreciation to my supervisor Prof. Dr. Abdel-Rahman El-Sayed Mohamed, Professor of physical chemistry, Chemistry Department, Faculty of Applied Science, Umm Al-Qura University, Makkah Al-Mukarramah, For suggesting the problem, his continuous supervision, sincere guidance and concentrate discussion of this work.

I would like to thank Prof. Dr. Abdel-Badia Goda, Professor of organic chemistry and Dr. A. M. El-Sayed Assistant Professor of organic chemistry, Chemistry Department, Faculty of Science at Sohag, South Valley University, Egypt for supplying triazole derivatives and pyrrole derivative compounds used as inhibitors in this investigations.

I offer my thanks to Professor Marzoug S. Al-Thebeiti, head of the chemistry department, for his help and encouragement and to facilitate all obstructs my way of research.

Last, but not least, I owe very special thanks to special person who support me during the all days that ago, relay I wish I could express the gratitude I feel in so many different ways. It's hard to say the meaningful things; but I know that "thanks" is one emotion that flows directly into the heart. And it's a very wonderful feeling that never goes away.

# CONTENTS

Subject	Page
Introduction	1
The aim of the work	16
Experimental	18
Aluminium and aluminium alloys specimens	18
Electrolytic cell	19
Equipments for potential measurements	21
Electrolytes	22
a. Acids solutions	22
b. Corrosion inhibitors solutions	22
c. Preparation and purification of some organic compounds used as inhibitors:	23
c.1.Preparation of 3-amino-4-cyano-2-benzoyl-N-phenyl pyrrole	23
c.2.Preparation of triazole derivatives	24
d. Preparation of solutions of the organic compounds	25
Results	
<i>1.Effect of some organic compounds on the electrochemical and         corrosion behaviour of aluminium and its alloys in 0.5 M         solutions of HCl, HClO<sub>4</sub> and H<sub>2</sub>SO<sub>4</sub>.</i>	26
1.1. Tafel lines for cathodic hydrogen evolution reaction	26
1.2. Parameters for hydrogen evolution reaction	55
1.3. Open circuit corrosion potential ( $E_{\text{corr.}}$ )	55
1.4. Corrosion currents ( $i_{\text{corr.}}$ )	56
1.5. Inhibition efficiency	57
1.6. Change in overpotential of cathodic hydrogen evolution	58
1.7. Parameters for anodic dissolution reaction	59
1.8. Adsorption isotherm	59

<b>2.Effect of some triazole derivatives on the electrochemical and corrosion behaviour of both pure aluminium and its alloys in 0.5 M solutions of HCl, HClO<sub>4</sub> and H<sub>2</sub>SO<sub>4</sub>.</b>	79
2.1. Tafel lines for cathodic hydrogen evolution reaction	79
2.2. Parameters for hydrogen evolution reaction	108
2.3. Open circuit corrosion potentials (E <sub>corr.</sub> )	108
2.4. Corrosion currents (i <sub>corr.</sub> )	109
2.5. Inhibition efficiency	110
2.6. Change in the hydrogen overpotential reaction	110
2.7. Change in the overpotential of anodic dissolution reaction	
2.8. Adsorption isotherm	112
<b>Discussion</b>	131
<b>1.Effect of adenine, adenosine and pyrrole derivative on the electrochemical and corrosion behaviour of pure aluminium and its alloys in 0.5 M solutions of HCl, HClO<sub>4</sub> and H<sub>2</sub>SO<sub>4</sub>.</b>	131
1.1. Behaviour in HCl solution	131
1.2. Behaviour in HClO <sub>4</sub> solution	138
1.3. Behaviour in H <sub>2</sub> SO <sub>4</sub> solution	142
1.4. Adsorption isotherms	145
<b>2.Effect of some triazole derivatives on the electrochemical and corrosion behaviour of pure aluminium and its alloys in 0.5 M solutions of HCl, HClO<sub>4</sub> and H<sub>2</sub>SO<sub>4</sub>.</b>	147
2.1. Behaviour in HCl solution	147
2.2. Behaviour in HClO <sub>4</sub> solution	153
2.3. Behaviour in H <sub>2</sub> SO <sub>4</sub> solution	160
2.4. Adsorption isotherms	165
<b>Summary</b>	167
<b>References</b>	176
<b>Arabic summary</b>	

[illegible]

# INTRODUCTION

***INTRODUCTION***

## INTRODUCTION

Aluminium and its alloys are widely used in various industrial and space operations. Aluminium has high electronegative potential (-1.67 V). However the resistance of Al against corrosion in aqueous media can be attributed to a rapidly formed surface oxide film. Therefore the presence of aggressive ions like chloride creates extensive localized attack. Iron is always present in aluminium it is the dominant impurity in commercial grades and still a major one in pure grades. Silicon is the second most abundant impurity of aluminium and one of the most common additions to aluminium alloys to which it imparts fluidity in casting and welding and high mechanical properties<sup>(1)</sup>.

The solid solution of iron in aluminium has been examined by X-rays and the solubility limits in the aluminium lattice are found to be 0.052 wt.% iron at 655°C, 0.025 wt.% at 600°C, 0.006 wt.% at 500°C and practically 0 at 400°C. In equilibrium at room temperature the lattice is free of iron and it is all present as  $\text{FeAl}_3$ . The solubility of silicon in aluminium is 1.65 wt. % at 577°C, 0.8 wt. % at 500°C, 0.29 wt. % at 400°C and 0.05 to 0.08 wt. % at 250°C. Thus on quenching from the liquid state a material such as aluminium 99.5 % containing 0.25 wt. % silicon a solid solution of silicon in aluminium is formed<sup>(2)</sup>.

In analyzing the effect of iron and manganese, it was reported that the addition of iron is harmful to the corrosion resistance of aluminium, whereas the addition of manganese does not adversely affect its corrosion properties<sup>(1,3,4)</sup>. These observations have been explained in terms of the corrosion potentials of aluminium and  $\text{MnAl}_6$  are similar, while that of

$\text{FeAl}_3$  is more cathodic<sup>(3,4)</sup>. The beneficial effect of manganese in commercial Al-Mn alloys has been also rationalized by Anderson and Stumpf<sup>(5)</sup>. Zamin<sup>(6)</sup> suggested that corrosion resistance increases with an increase in the Mn/Fe ratio in the commercial Al-Mn alloys ( alloys containing 0.4-1.2 % Mn, 0.4-0.8 % Fe, 0.15 % Si and some with small amount of magnesium have been fabricated and evaluated ), but remains unaffected by the magnesium addition.

Aleikina<sup>(7)</sup> studied the corrosion disintegration of Al-Ni alloys in 0.1N HCl with  $\text{Ni-Al}_3(\beta)$ ,  $\text{Ni}_2\text{Al}_3(\gamma)$ ,  $\text{NiAl}(\delta)$ , and  $\text{Ni}_3\text{Al}(\epsilon)$  phases and with cast alloys with a gradual 10 % increase in nickel content. He determined the rate of disintegration of the alloy from the volume of hydrogen liberated and the amount of alloy components passing into solution. Cote, Howlette and Lamb<sup>(8)</sup> studied the behaviour of coarse particles of five intermetallic compounds,  $\text{CuAl}_2$ ,  $\beta\text{-AlMg}$ ,  $\text{TiAl}_3$ ,  $\beta\text{-AlFeSi}$  and  $\text{AlZnMg}$  in high purity aluminium alloys during  $\text{H}_2\text{SO}_4$  anodizing under constant d. c. potential. They were examined by optical microscopy and electron probe microanalysis. They found that silicon was inter as were  $\text{TiAl}_3$  and  $\beta\text{-AlFeSi}$ , while  $\text{CuAl}_3$ ,  $\beta\text{-AlMg}$ , and  $\text{AlZnMg}$  were anodizing faster than the matrix and readily dissolved in the electrolyte. Isasi and Metzger<sup>(9)</sup> also found that , at low copper contents the structure and impurity related corrosion phenomena in nitric and sulphuric acids solutions were similar to those in hydrochloric acid solution.

Inhibition is a preventive measure against corrosive attack on metallic materials. It consists of the use of chemical compounds which, when added in small concentrations to an aggressive environment, are able to decrease corrosion of the exposed metal.

By considering the electrochemical nature of corrosion processes, constituted by at least two electrochemical partial reactions, inhibition may also be defined on an electrochemical bases. Inhibitors will reduce the rates of either or both of these partial reactions( anodic oxidation and / or cathodic reduction). As a consequence we could have anodic, cathodic, and mixed inhibitors. Other tentative classifications of inhibitors have been made by taking into consideration their chemical nature (organic or inorganic substance), their characteristics (oxidizing or nonoxidizing compounds), or their technological field of application (pickling, descaling acid cleaning, cooling water system, etc.).

Inhibitors can be used in electrolytes at different pH values, from acid to near-neutral or alkaline solution. Because of the very different situations created by changing various factors such as medium and inhibitor in the system metal/aggressive medium/inhibitor, various inhibition mechanisms must be considered<sup>(10-15)</sup>.

An accurate analysis of the different modes of inhibiting electrode reactions including corrosion was carried out by Fischer<sup>(16)</sup>. He distinguished among various mechanism of action, such as:

- Interface inhibition.
- Electrolyte layer inhibition.
- Membrane inhibition.
- Passivation.

Subsequently, Lorenz and Mansfeld<sup>(17)</sup> proposed a clear distinction between interface and interphase inhibition, presenting two different types of retardation mechanisms of electrode reactions including corrosion.



Interface inhibition presumes a strong interaction between the inhibitor and the corroding surface of the metal<sup>(10,16,18)</sup>. In this case the inhibitor adsorbs as a potential-dependent two-dimensional layer. This layer can affect the basic corrosion reactions in different ways:

- By a geometric blocking effect of the electrode surface due to the adsorption of a stable inhibitor at a relative high degree of coverage of the metal surface.
- By a blocking effect of active surface sites due to the adsorption of a stable inhibitor at a relatively low degree of coverage.
- By a reactive coverage of the metal surface. In this case the adsorption process is followed by electrochemical or chemical reactions of the inhibitor at the interface.

According to Lorenz and Mansfeld<sup>(17)</sup>, interface inhibition occurs in corroding systems exhibiting a bare metal surface in contact with the corrosive medium. This condition is often realized for active metal dissolution in acid solutions.

Interphase inhibition presumes a three-dimensional layer between the corroding substrate and the electrolyte<sup>(16,19,20)</sup>. Such layers generally consist of weakly soluble corrosion products and/or inhibitors. Interphase inhibition is mainly observed in neutral media, with the formation of porous or nonporous layers. Clearly, the inhibition efficiency depends on the properties of the formed three-dimensional layer.

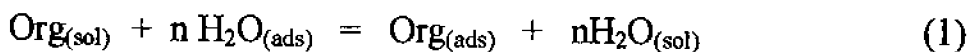
In the following chapters we discuss inhibition mechanisms, which vary according to the different conditions considered.

### **Acid solutions:**

Usually, corrosion of metals and alloys in aqueous acid solutions is very severe; nevertheless, this kind of attack can be inhibited by a large number of organic substances. These include triple-bonded hydrocarbons, acetylenic alcohols, sulfoxides, sulfides and mercaptans, aliphatic, aromatic or heterocyclic compounds containing nitrogen, and many other families of simple organic compounds or of condensation products formed by the reaction between two different species such as aldehydes and amines.

Generally, it is assumed that the first stage in the action mechanism of the inhibitors in aggressive acid media is adsorption of the inhibitors onto the metal surface. The processes of adsorption of inhibitors are influenced by the nature and surface charge of the metal, by the chemical structure of the organic inhibitor, and by the type of aggressive electrolyte. Physical (or electrostatic) adsorption and chemisorption are the principal types of interaction between an organic inhibitor and a metal surface.

In the adsorption of organic inhibitors the water molecules adsorbed at the metal surface in contact with the aqueous solution are involved. As a consequence, the adsorption of an organic substance at the metal / solution interface may be written<sup>(21)</sup> according to the following displacement reaction:



Which  $n$  is the number of water molecules removed from the metal surface for each molecule of inhibitor adsorbed. According to Bockris and Swinkels<sup>(21)</sup>,  $n$  is assumed to be independent of coverage or charge of the electrode.

Clearly, the value of  $n$  will depend on the cross-sectional area of the organic molecule with respect to that of the water molecule. Adsorption of the organic molecule occurs because the interaction energy between the inhibitor and the metal surface is higher than the interaction energy between the water molecules and the metal surface<sup>(14)</sup>.

In the following the various adsorption phenomena and the influencing parameters are discussed.

### **Physical adsorption:**

Physical adsorption is the result of electrostatic attractive forces between inhibiting organic ions or dipoles and the electrically charged surface of the metal. The surface charge of the metal is due to the electric field at the outer Helmholtz plane of the electrical double layer existing at the metal/solution interface. The surface charge can be defined by the potential of the metal ( $E_{\text{corr.}}$ ) vs. its zero charge potential (ZCP) ( $E_{q=0}$ )<sup>(22)</sup>. When the difference  $E_{\text{corr.}} - E_{q=0} = \phi$  is negative, cation adsorption is favored. Adsorption of anions is favored when  $\phi$  becomes positive or negative charge, but also to dipoles whose orientation is determined by the value of the  $\phi$  potential.

According to Antropov<sup>(22)</sup>, at equal values of  $\phi$  for different metals,

similar behaviour of a given inhibiting species should be expected in the same environment. This has been verified for adsorption of organic charged species on mercury and iron electrode, at the same  $\phi$  potential for both metals.

In studying the adsorption of ions at the metal/solution interface, it was first assumed that ions maintained their total charge during the adsorption, giving rise in this way to a pure electrostatic bond. Lorenz<sup>(23-25)</sup> suggested that a partial charge is present the adsorption of ions, in this case a certain amount of covalent bond in the adsorption process must be considered. The partial charge concept was studied by Vetter and Schulze<sup>(26-29)</sup>, who defined, as electrosorption valence, the coefficient for the potential dependence and charge flow of electrosorption processes. The term electrosorption valence was chosen because of its analogy with the electrode reaction valence which into Faraday's law as well as the Nernst equation.

Considering the concepts discussed above in relation to corrosion inhibition, when an inhibited solution contains adsorbable anions, such as halide ions, these are adsorbed on the metal surface by creating oriented dipoles and consequently increase the adsorption of the organic cations on the dipoles. In these cases a positive synergistic effect arises, thus, the degree of inhibition in the presence of both adsorbable anions and inhibitor cations is higher than the sum of the individual effects. This could explain the higher inhibitions compared to sulfuric acid solutions<sup>(30)</sup>. A similar interpretation has been given<sup>(30)</sup> for the increase in inhibition by quaternary ammonium ions in sulfuric acid solution when the solution contains bromide ions.

A very detailed discussion of electrostatic adsorption has been given by Foroulis<sup>(11)</sup>, who also considered the importance of structural parameters, such as hydrocarbon chain length and the nature and position of substituents in aromatic rings, in influencing the electrical charge of the organic ions, since these factors could change the degree of inhibition.

The inhibiting species whose action is to be attributed to electrostatic adsorption interact rapidly with the electrode surface, but they are also easily removed from the surface. The electrostatic adsorption process has a low activation energy, and it proves to be relatively independent of temperature<sup>(31)</sup>. On the other hand, electrostatic adsorption appears to depend on:

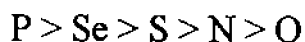
- The electrical characteristics of the organic inhibitors.
- The position of the corrosion potential with respect to the zero-charge potential.
- The type of adsorbable anions present in the aggressive solution.

### **Chemisorption:**

Another type of metal/inhibitor interaction is chemisorption. This process involves charge sharing or charge transfer from the inhibitor molecules to the metal surface in order to form a coordinate bond type.

The chemisorption process takes place more slowly than electrostatic adsorption and with a higher activation energy. It depends on the temperature, higher degree of inhibition should be expected at higher temperatures. Chemisorption is specific for certain metals and is not completely reversible<sup>(31)</sup>. The bonding occurring with electron transfer

clearly depends on the nature of the metal and the nature of the organic inhibitor. In fact, electron transfer is typical for transition metals having vacant, low-energy electron orbitals. Concerning inhibitors, electron transfer can be expected with compounds having relatively loosely bound electrons. This situation may arise because of the presence, in the adsorbed inhibitor, of multiple bonds or aromatic rings, whose electrons have a  $\pi$  character. Clearly, even the presence of heteroatoms with lone-pair of electrons in the adsorbed molecule will favor electron transfer. Most organic inhibitors are substances with at least one functional group regarded as the reaction center of the chemisorption process. In this case, the strength of the adsorption bond is related to the heteroatom electron density and to the functional group polarizability. For example, the inhibition efficiency of homologous series of organic substances differing only in the heteroatom is usually in the following sequence:



An interpretation may be found in the easier polarizability and lower electronegativity of the elements on the left in the above sequence. On this bases, a surface bond of the Lewis acid-base type, normally with the inhibitor as electron donor and the metal as electron acceptor, has been postulated<sup>(31)</sup>.

The principle of soft and hard acids and bases (SHAB)<sup>(32)</sup> has also been applied to explain adsorption bonds and inhibition effects<sup>(33)</sup>. Softness and hardness are usually associated with high or low polarizability. The SHAB principle states that hard acids prefer to coordinate with soft bases. Metal atoms  $M^\circ$  on oxide-free surfaces are considered soft acids which in

acid solutions are able to form strong bonds with soft bases, such as sulfur-containing organic inhibitors. By comparison, nitrogen-containing or oxygen-containing organic compounds are considered hard bases and may establish weaker bonds with metal surface in acid solutions. From these considerations, the importance of the concepts of functional group electron density, polarizability, and electronegativity with respect to inhibition efficiency is confirmed.

Hydrochloric acid solutions are used for pickling of aluminium or for chemical or electrochemical etching of aluminium foil and lithographic panels which substitute metallic zinc<sup>(34)</sup>. Since the metal dissolution in such solutions is rather large, it is necessary to inhibit it by the addition of additives, which should provide a good quality pickled metal surface.

The inhibition of aluminium corrosion and its alloys in hydrochloric acid solutions by using different organic compounds were studied by several authors<sup>(35-48)</sup>. Makwana, Patel and Vora<sup>(35)</sup> found that the inhibitive power of 4-HOC<sub>6</sub>H<sub>4</sub>CO<sub>2</sub>H (I), 2-HSC<sub>6</sub>H<sub>4</sub>CO<sub>2</sub>H (II) and BZSH (III) decreased in the order: III > II > I. The excellent inhibitive action of III was attributed to chemisorption at the cathodic sites. Desai, Patel and Shah<sup>(36)</sup> found that cyclohexanol, cyclohexanone and cyclohexylamine act as corrosion inhibitors for aluminium alloy in hydrochloric acid solution. Ramakrishnaiah and Subramanyan<sup>(37)</sup> studied the inhibition of aluminium corrosion in 1M HCl and 0.1M NaOH. They found that, the inhibition occur only in the HCl-Amino acid system, this was attributed to the existence of cationic form of the amino acids  $\text{RCH}(\text{NH}_3^+)\text{CO}_2\text{H}$  which becomes adsorbed on the negatively charged aluminium surface.

Desai, Shah and Deasi<sup>(38)</sup> studied aniline and its mono- and di-N-substituted amines as corrosion inhibitors for aluminium alloys in hydrochloric acid solution. They found that the values of activation energy in the presence of inhibitors are lower than those in uninhibited 1N HCl, the difference effect is positive in inhibited 2N HCl but negative in uninhibited 2N HCl. Talati and Gandhi<sup>(39,40)</sup> and Patel, Pandya and Lal<sup>(41)</sup> studied the inhibition of the corrosion of Al-Cu alloy in HCl solution by some organic compounds such as N-heterocyclic compounds, some dyes and toluidines. They found that the efficiency of the N-heterocyclic compounds as inhibitors increased in the order 4-picoline < 3-picoline < 2-picoline < pyridine < piperidine < acridine while for toluidines compounds, increases as: p-toluidine < o-toluidine < m-toluidine. Yadav, Chaudhary and Agarwal<sup>(42)</sup> studied aliphatic amines as corrosion inhibitors for aluminium alloys in an acidic chloride solution of pH = 1 in the presence and absence of tungstate ions. They found that, the inhibitive efficiency decreases in the order: ethanol amine > diethanol amine > triethanol amine, and these three amines are partially effective on the anodes while predominantly inhibit the cathodic reaction. Abo-El-Khair and Mostafa<sup>(43)</sup> studied the inhibitive effect of N-vinyl pyrrolidone and ploy-N-vinyl pyrrolidone on the dissolution of aluminium in 1.15 N HCl solution. They observed that the percent inhibition of aluminium increases with the increase of inhibitor concentration approaching complete protection (95 %) at 44°C for N-vinyl pyrrolidone.

Abd El-Nabey, Essa and Shaban<sup>(44)</sup> studied phthalazine derivatives as inhibitors for the acid corrosion of aluminium. They found that, these compounds are cathodic inhibitors and the efficiency of the inhibitor decrease with increase in the number of carbon atoms in the sugar moiety



of the molecule. Talati and Daraji<sup>(45)</sup> found that the inhibitive efficiency of triphenyl methane dyes for Al-Mg alloys in hydrochloric acid solution increases with the rise in temperature, and the inhibitors act as cathodic type inhibitors. Fouada et al.<sup>(46,47)</sup> studied the inhibition of the dissolution of aluminium in hydrochloric acid using weight loss, thermometric and galvanostatic methods. They found that biacetyl monoxime hydrazone derivatives inhibited both cathodic and anodic reactions. They suggested that the adsorbability of some  $\beta$ -diketo compounds investigated as inhibitors is dependent on the basicity of the oxygen and nitrogen sites involved. They also found that the activation energy of the dissolution reaction increases with decreasing acid concentration and increasing inhibitor concentration.

In recent years new data have been obtained on the pitting corrosion of aluminium due to the presence of chloride ions in different aqueous solutions<sup>(48-54)</sup>. Generally, local corrosion attack can be prevented by the action of adsorptive inhibitors which prevent the adsorption of the aggressive anions, and by the formation of a more resistant oxide film on the metallic surface<sup>(55)</sup>. A number of organic compounds have been introduced as aluminium corrosion inhibitors in acidic media<sup>(56,57)</sup>. Investigation of various aliphatic and aromatic amines as well as nitrogen-heterocyclic compounds<sup>(15,58-61)</sup>, showed that their inhibitory action is connected with several factors such as:

- (i) The structure of molecules.
- (ii) The number and type of adsorption sites.
- (iii) The distribution of charge in the molecule.
- (iv) The type of interaction between organic molecules, and the metallic surface.

A number of organic compounds are also described as aluminium corrosion inhibitors in neutral and acidic media, the majority being nitrogen-containing compounds<sup>(56,62-65)</sup>, recently, Isobe et al.<sup>(66)</sup> have shown that the addition of benzotriazole or 8-hydroxyquinoline is effective for preventing pitting corrosion of aluminium alloys. The latter compound is able to form insoluble chelates and it is used successfully to protect iron<sup>(67)</sup>, zinc<sup>(68)</sup> and copper<sup>(69)</sup>.

In a previous study<sup>(70)</sup> we showed that 8-hydroxyquinoline and benzotriazole are two effective corrosion inhibitors for a 2024 aluminium alloy, mainly in the cathodic range. The mixture of the two compounds presents a synergistic effect for the corrosion protection of this alloy over both anodic and cathodic ranges. The action of benzotriazole is mainly limited to the copper-rich intermetallic compounds which are responsible for the degradation of the alloy.

Garrigues et al.<sup>(71)</sup> studied the corrosion inhibition of pure aluminium in acidic solutions containing 8-hydroxyquinoline. They investigated that does not modify the corrosion mechanism of aluminium. This result is explained by the solubility of the aluminium chelate in acidic media. The influence of benzotriazole on the efficiency of anodizing of Al-3.5wt.%Cu alloy at constant current density in 0.1M ammonium pentaborate electrolyte has been investigated by paez et al.<sup>(72)</sup>. They found that the addition of benzotriazole to this solution significantly increases the efficiency of anodic film growth. El-Warraky et al.<sup>(73)</sup> studied the synergistic effect between either benzotriazole or thiourea and iodide ions to retard the dissolution of Al-bronze alloy in deaerated solution of acidified 4% NaCl of pH 1.8-2 at 60°C. This is shown by the weight loss

and polarization techniques. Iodide ions alone has no effect on the dissolution of the alloy but addition of 100 ppm KI to 300 ppm of both benzotriazole and thiourea improved the inhibition efficiency to 92% and 78.8%, respectively, and also decreased the anodic current density in both media. Adsorption of benzotriazole on the Al surface was studied by Popova et al.<sup>(74)</sup> at 150 and 293 K. They investigated the thermal stability of the adsorbed layer. The temperatures adsorption results in the production of a thick condensed layer of benzotriazole. Strong intermolecular hydrogen bonds are observed, with increasing sample temperature, the benzotriazole molecules diffuse into the Al pore structure.

Substituted N-arylpyrroles containing carbaldehyde groups on a pyrrole ring and their inhibitive effects on the corrosion of aluminium in perchloric acid were investigated by Metikos-Hukovic et al.<sup>(75)</sup>. They showed that the organic compounds examined had inhibiting properties at 40°C. The high inhibition effect of the N-aryl-2,5-dimethyl pyrroles containing carbaldehyde groups on a pyrrole ring on corrosion of Al in acidic media was explained on the basis of the electronic structure of the molecule and by the condensation characteristic of the carbaldehydes. The adsorption behaviour of triethanol amine on aluminium and its alloys covered with naturally formed oxide films in acidic 0.5M NaCl solution was investigated by Hukovic and Babic<sup>(56)</sup>. The results of polarization measurements show that in all cases the addition of triethanol amine induces a decrease in the cathodic currents without affecting the anodic polarization behaviour and accordingly the investigated inhibitor can be treated as a cathodic type inhibitor.

The effect of 1,10-phenanthroline, bathophenanthroline,

bathophenanthroline disulphonic disodium salts hydrate, 2,2'-bipyridyl and 2,4,6-tris(2-pyridyl)-1,3,5-triazine and their complexes with  $\text{Cu}^{2+}$  and  $\text{Fe}^{3+}$  ions on the corrosion of pure aluminium and its alloys in 1M HCl solution was studied by El-Sayed<sup>(76)</sup> using electrochemical impedance spectroscopy. He found that the free inhibitors are found to be predominantly anodic type of pure Al and cathodic of its alloys. The adsorption of most inhibitors is also found to obey Langmuir's adsorption isotherm, thereby indicating that the main process of inhibition is by adsorption. Addition of most investigated additives as a complex with  $\text{Cu}^{2+}$  and  $\text{Fe}^{3+}$  ions enhances efficiency of pure Al particularly at cathodic potential and of its alloys at anodic potential. The inhibiting effect of benzotriazole on the corrosion of  $\alpha$ -Al bronze (Cu-7% Al) in 3.4% NaCl was studied by Ashour et al.<sup>(77)</sup>. The investigated additive showed good inhibition effects on the anodic dissolution of Cu than on the cathodic reduction of oxygen. It is also shown that the interaction of benzotriazole with a  $\text{Cu}_2\text{O}$ -covered alloy surface is faster than on reduced alloy surface, although the protection efficiency on the latter is slightly better than on the former.

## THE AIM OF THE PRESENT WORK

The study of the corrosion of aluminium and its alloys is a subject of pronounced practical significance because they find widespread applications in many industries. The use of inhibitors is one of the most practical methods for protection against corrosion, especially in acidic media. The progress in this field has phenomenal in recent years and is born out by the output of literature. Acid solutions are generally used for the removal of rust and scale in several industrial processes. Inhibitors are generally used in these processes to control the metal dissolution. HCl and H<sub>2</sub>SO<sub>4</sub> are widely used in the pickling of aluminium and its alloys. Most of the well known acid inhibitors are organic compounds containing nitrogen, sulphur and oxygen atoms.

The present work is devoted to study the inhibiting action of a new organic compounds containing nitrogen, sulphur and aromatic rings on the corrosion of aluminium and its alloys in HCl, H<sub>2</sub>SO<sub>4</sub> and HClO<sub>4</sub> solutions using current density-potential measurements under galvanostatic technique.

The trend of study to be carried out in the present work involves the following points:

- 1)- Investigation and comparison of the inhibiting action of heterocyclic compounds containing nitrogen atoms such as: Adenine, Adenosine and Pyrrole derivative on the corrosion of the pure aluminium and the investigated aluminium-alloys in HCl, HClO<sub>4</sub> and H<sub>2</sub>SO<sub>4</sub> solutions.

2)- Effect of heterocyclic compounds containing nitrogen atoms such as: 3-mercapto-4-phenyl-5-4-pyridyl-1,2,4-triazole, 3-mercapto-4-phenyl-5-p-tolyl-1,2,4-triazole and 3-mercapto-4-phenyl-5-p-nitrophenyl-1,2,4-triazole on the electrochemical and corrosion behaviour of pure aluminium and its investigated alloys in the above mentioned acids solutions has been studied. The objective of the investigation was to study the effect of various aryl groups attached to five position of triazole derivative (4-pyridyl, p-tolyl and p-nitrophenyl) on corrosion of Al and its investigated alloys in acidic solutions.

IMENTAL EXPERIMENTAL EXPERIME

EXPERIMENTAL EXPERIMENTAL

IMENTAL EXPERIMENTAL EXPERIME

EXPERIMENTAL EXPERIMENTAL

IMENTAL EXPERIMENTAL EXPERIME

EXPERIMENTAL EXPERIMENTAL

IMENTAL EXPERIMENTAL EXPERIME

EXPERIMENTAL EXPERIMENTAL

IMENTAL EXPERIMENTAL EXPERIME

EXPERIMENTAL EXPERIMENTAL

IMENTA KPERIME

EXPERIMENTAL

IMENTA KPERIME

EXPERIMENTAL EXPERIMENTAL

IMENTAL EXPERIMENTAL EXPERIME

EXPERIMENTAL EXPERIMENTAL

IMENTAL EXPERIMENTAL EXPERIME

EXPERIMENTAL EXPERIMENTAL

IMENTAL EXPERIMENTAL EXPERIME

EXPERIMENTAL EXPERIMENTAL

IMENTAL EXPERIMENTAL EXPERIME

EXPERIMENTAL EXPERIMENTAL

## EXPERIMENTAL

### Aluminium and aluminium alloys specimens:

Aluminium specimens were cut from specpure aluminium rods (99.999% Johnson Matthey, London). The aluminium alloys were provided from the Egyptian aluminium Company, and have the following composition by wt. %:

<i>Alloys</i>	<i>% Alloying elements.</i>		
	<i>Si</i>	<i>Fe</i>	<i>Al</i>
<i>I</i>	0.08	0.1	99.82
<i>II</i>	0.25	0.32	99.43

All the measurements were performed on a planar disk electrodes ( $A = 0.277 \text{ cm}^2$ ), of both pure aluminium and its alloys. The aluminium and its alloys were prepared by cutting the rod and setting it in an Araldite holder.

Prior to each experiment the electrode surface was polished with successive grades of emery paper, degreased in absolute ethanol (AR grade), and finally washed in running distilled water before being inserted in the polarization cell.

Prior to each electrochemical measurement, the electrode was activated by cathodic polarization in the used-electrolyte solution at 1 mA



for 5 min. with vigorous hydrogen evolution to remove any surface contamination and air formed oxide and then it was left for 60 min. (after the current was switched off) in the solution to reach a steady state open circuit potential ( $E_{ocp}$ ).

A platinum sheet and a saturated calomel electrode were used as the counter electrode and reference electrode, respectively.

### Electrolytic cell:

Galvanostatic polarization experiments were carried out in a cell shown diagrammatically in Figure (1), it is made of Pyrex glass without any rubber connections. It consists of a vessel of about 250 ml capacity provided with a three openings. Two of these are used for fitting the working electrode and the platinum counter electrode (platinum sheet 2cm x 1cm). The latter electrode is fitted into a compartment separated from the main bulk of the electrolyte by means of a G-4 sintered glass disc to effect the separation of the anode and cathode compartments. The potential of the working electrode was measured relative to a saturated calomel electrode, which is also separated from the main electrolyte through sintered glass disc. The end of the reference electrode was elongated in the form of a Haber-Luggin capillary, which was placed at a distance of about 0.1mm from the working electrode. The electrolytic cell was cleaned before each run by chromic/sulphuric mixture at 80°C for at least four hours and then left over night. After sucking out the cleaning mixture the cell was then washed with double distilled water, methanol and a little amount from the used-electrolyte solution.

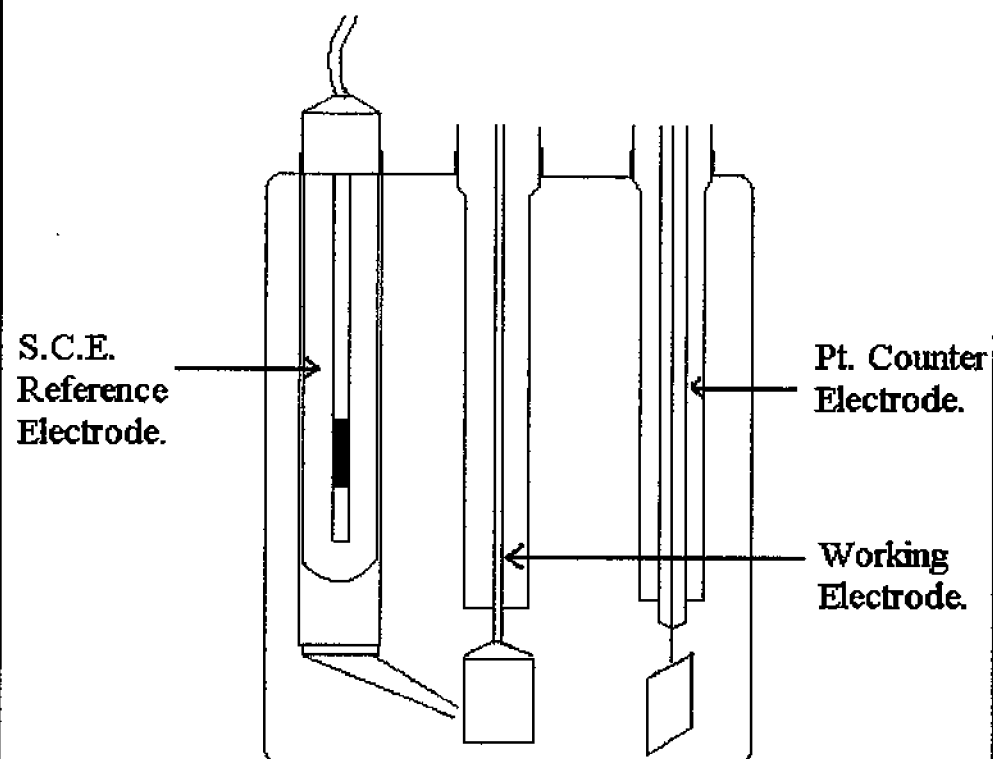


Figure (1): Electrolytic cell.

### **Equipments for potential measurements:**

Anodic and cathodic galvanostatic polarization experiments were carried out on aluminium and its alloys in three different acids solutions with and without the addition of organic compounds as inhibitors.

In the galvanostatic polarization runs, the potentials were measured with the aid of a digital potentiometer (BBC, GOERZ METRAWATT, MA5D), using a saturated calomel electrode (SCE) half cell. The current was applied from a PASCO Model SF-9586 KILOVOLT power supply which was connected in series with a digital multimeter Model YF-3502.

All galvanostatic polarization experiments were carried out in an electrolytic cell which will be describe elsewhere.

The measurements for the galvanostatic cathodic polarization to be reported here were obtained in descending direction of current density (starting with the higher current density). It was observed by Vijh<sup>(78)</sup> that data in descending direction were more reproducible than those in the ascending direction. During measurements the current density was varied in the range  $36 \mu\text{A}/\text{cm}^2$  to  $360 \mu\text{A}/\text{cm}^2$  for pure Al and  $180$ - $1260 \mu\text{A}/\text{cm}^2$  for its alloys. On using the galvanostatic technique to study the corrosion behaviour of pure aluminium and the investigated alloys without profound changes in the spontaneously formed oxide, the quasi steady state method was used<sup>(79)</sup>. In this method the value of the electrode potential after approximately one minute was recorded. Vijh<sup>(78)</sup> found that the time required for the steady state values of potential ranges from 2-30 minutes. For studying the inhibitive action of some organic compounds on

the corrosion of aluminium and some Al-alloys in 0.5M solutions of HCl, H<sub>2</sub>SO<sub>4</sub> and HClO<sub>4</sub>, the steady state method for galvanostatic cathodic polarization was used in this investigation. All experiments were conducted after attaining steady state open circuit corrosion potentials in the examined solutions.

All the measurements were carried out at a definite constant temperature, namely  $25\pm 1^{\circ}\text{C}$ , and each measurement was repeated until reproducibility of results was satisfactory.

Corrosion currents ( $i_{\text{corr.}}$ ) were determined by extrapolation of the cathodic Tafel curves to the corrosion potential ( $E_{\text{corr.}}$ ), Tafel parameters for hydrogen evolution reaction were obtained directly from the Tafel plots.

### **Electrolytes:**

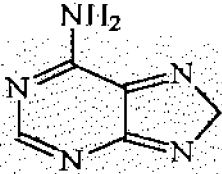
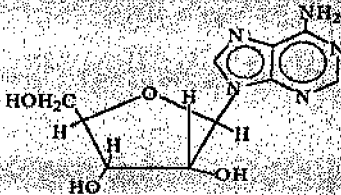
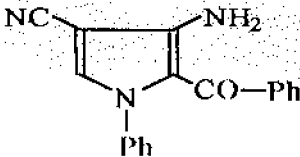

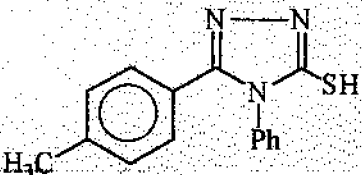
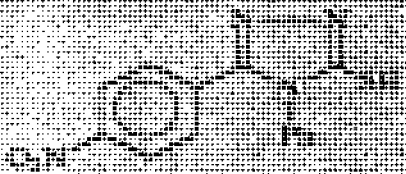
#### ***a. acids solutions:***

A stock of 0.5M solutions of HCl, HClO<sub>4</sub> and H<sub>2</sub>SO<sub>4</sub> were prepared by dilution of the Analar reagent grade concentrated acids to one liter.

#### ***b. corrosion inhibitors solutions:***

Adenine, adenosine, pyrrole derivative and triazole derivatives were used as additives, (corrosion inhibitors), the structures of the inhibitors are given in Table (1).

**Table(1):** The investigated organic compounds used as inhibitors.

<u>Name</u>	<u>Structure</u>	<u>M.wt</u>
Adenine.		135
Adenosine.		267
3-amino-4-cyano-2-benzoyl-N-phenyl pyrrole		287
3-mercapto-4-phenyl-5-p-tolyl-1,2,4-triazole.		258
3-mercapto-4-phenyl-5-p-tolyl-1,2,4-triazole.		267
3-mercapto-4-phenyl-5-p-tolyl-1,2,4-triazole.		258

### ***C. preparation and purification of some organic compounds used as inhibitors:***

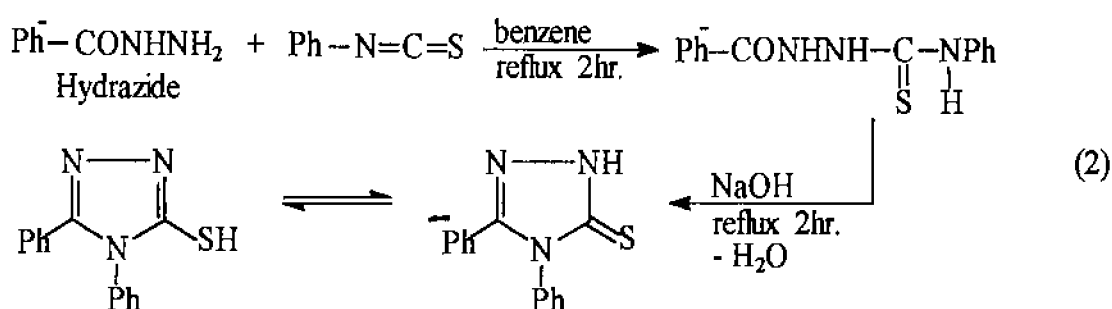
#### ***c.1. preparation of 3-amino-4-cyano-2-benzoyl-N-phenyl pyrrole:***

To 5gm of anhydrous potassium carbonate in 80 ml dry dioxane was

added, an equimolar ratio (0.2 mol) of anilinomethylene malononitrile and phenyl bromide with stirring. The reaction mixture was treated with a catalytic amount of tetrabutyl ammonium bromide (TBAB). The reaction mixture was stirred for 4h at 25-30°C. The mixture was filtered, the filtrate washed thoroughly with water, dried over  $\text{MgSO}_4$  and evaporated in vacuo.

The residue was washed with water, and crystallized from ethanol to give 50.06g (88%) of this compound, m.p. 225°C<sup>(80)</sup>.

### c.2. preparation of triazole derivatives:



Benzoic acid hydrazide (0.25mol, 34gm) and phenyl isothiocyanate (0.25mol, 30ml) in benzene (150 ml) were refluxed for 2hr. The solvent was evaporated till dryness, then sodium hydroxide (0.3mol, 12 gm) in water (150 ml) was added and was heated under reflux for 2hr. The reaction mixture was cooled and dilute HCl was added drop by drop, then 4,5-diphenyl-3-mercapto-1,2,4-triazole was formed, crystallized from dioxane. Yield 95%, m.p. 289°C<sup>(81)</sup>.

However, adenine and adenosine are reagent grade (Merck) and used without further purification.

***d. preparation of solutions of the organic compounds:***

the inhibitive solution was prepared by dissolving the appropriate amount by weight in 10 ml B.D.H. methanol. The desired volume of the inhibitor solution was added to the electrolyte by means of a graduated micropipette. All inhibitors are completely soluble in the used concentrations, no suspensions were employed.

***RESULTS***

## RESULTS

[illegible]



## RESULTS

### ***1. Effect of some organic compounds on the electrochemical and corrosion behaviour of aluminium and its alloys in 0.5M solutions of HCl, HClO<sub>4</sub> and H<sub>2</sub>SO<sub>4</sub>.***

#### **1.1. Tafel lines for cathodic hydrogen evolution reaction:**

Cathodic overvoltage ( $\eta_c$ ) values were obtained by subtracting the reversible hydrogen electrode potential from the steady state values attained at each cathodic current density. Values of  $\eta_c$  at different current density from 36-360  $\mu\text{A}/\text{cm}^2$  for pure Al and from 180-1260  $\mu\text{A}/\text{cm}^2$  in case of Al-alloys in the investigated acids solutions as well as those containing various concentrations of adenine, adenosine and pyrrole derivative within the concentration range  $10^{-6}$ - $10^{-4}$  M of pyrrole derivative and  $10^{-5}$ - $10^{-3}$  M in case of adenine and adenosine are given in Tables 2-10. On the other hand, all Tafel lines seen to be run parallel to each other.

Tafel lines for hydrogen evolution reaction (h.e.r.) at both Al and its alloys in the presence of the investigated organic additives are shown in Figs.2-19. These curves indicate that  $\eta_c$  is a linear function of the logarithm of current density (c.d.) for the current density ranging from 36-360  $\mu\text{A}/\text{cm}^2$  for pure Al and from 180-1260  $\mu\text{A}/\text{cm}^2$  for its alloys.

These results also indicate that  $\eta_c$  values for pure Al and alloy II are increased in the negative direction in the presence of Adenine, Adenosine and pyrrole derivative within the examined concentration range in all

investigated acids solutions. On the other hand,  $\eta_c$  values in case of alloy I are increased in the negative direction in the presence of adenine and adenosine only in  $H_2SO_4$  and  $HCl$ .  $\eta_c$  values for alloy I are shifted in the positive direction (decreased in  $\eta_c$ ) in the presence of pyrrole derivative in  $H_2SO_4$  and  $HCl$  solutions and at higher concentration only ( $10^{-4}$  M) in  $HClO_4$ . The data exhibited that adenine and adenosine have influence to decrease  $\eta_c$  value of alloy I at all examined concentrations in  $HClO_4$ .

Table (2): Hydrogen overvoltage ( $\eta_c$ ) values of Al and Al-alloys in 0.5 M HCl solution in the presence of adenine.

Electrode	Additive concn. (M)	$-\eta_c$ (mV)														
		c.d. $\mu\text{A}/\text{cm}^2$														
Aluminium	0	99	91	83	75	67	55	43	31	2	—					
	$1 \times 10^{-5}$	214	205	196	187	178	166	148	128	98	50					
	$1 \times 10^{-4}$	270	260	250	240	230	218	205	180	150	104					
	$5 \times 10^{-4}$	345	335	325	315	304	292	278	254	220	174					
	$1 \times 10^{-3}$	405	395	385	375	364	350	335	310	280	230					
Alloy I		c.d. $\mu\text{A}/\text{cm}^2$														
	0	1260	1170	1080	990	900	810	720	630	540	450	360	270	180		
	$1 \times 10^{-5}$	134	130	126	121	116	110	103	94	85	76	66	48	25		
	$1 \times 10^{-4}$	151	147	143	138	133	127	120	111	103	93	80	65	42		
	$5 \times 10^{-4}$	163	159	155	150	145	139	132	123	115	105	94	79	56		
Alloy II	$1 \times 10^{-3}$	177	172	168	162	157	151	144	136	127	116	106	92	68		
		184	179	174	169	164	158	151	143	135	125	113	99	74		
	0	106	102	97	92	86	80	73	65	56	46	33	18	—		
	$1 \times 10^{-5}$	128	124	119	114	108	102	95	87	78	68	55	40	15		
	$1 \times 10^{-4}$	140	135	130	125	120	114	107	98	89	79	67	52	28		
	$5 \times 10^{-4}$	148	143	138	132	128	122	115	106	97	87	75	60	34		
	$1 \times 10^{-3}$	160	155	150	144	140	134	127	118	109	99	87	72	47		



Table (4): Hydrogen overvoltage ( $\eta_c$ ) values of Al and Al-alloys in 0.5 M HCl solution in the presence of 3-amino-4-cyano-2-benzoyl-N-phenyl pyrrole.

Electrode	Additive concn. (M)	$-\eta_c$ (mV)													
		360	324	288	252	216	180	144	108	72	36				
Aluminium	0	99	91	83	75	67	55	43	31	2	—				
	$1 \times 10^{-6}$	118	110	102	94	85	73	60	44	18	—				
	$1 \times 10^{-5}$	195	186	177	168	158	146	133	115	90	45				
	$5 \times 10^{-5}$	210	201	192	183	173	161	148	130	106	60				
	$1 \times 10^{-4}$	227	218	208	199	189	177	164	146	120	77				
Alloy I		1260	1170	1080	990	900	810	720	630	540	450	360	270	180	
	0	134	130	126	121	116	110	103	94	85	76	66	48	25	
	$1 \times 10^{-6}$	122	118	114	109	104	98	91	84	76	67	56	41	21	
	$1 \times 10^{-5}$	118	114	110	105	100	94	87	80	72	62	50	35	13	
	$5 \times 10^{-5}$	109	105	101	96	91	85	78	69	60	51	41	24	4	
Alloy II	$1 \times 10^{-4}$	89	85	81	76	71	65	58	49	39	29	19	5	—	
	0	106	102	97	92	86	80	73	65	56	46	33	18		
	$1 \times 10^{-6}$	142	138	133	128	122	116	109	101	92	82	69	54	29	
	$1 \times 10^{-5}$	166	161	156	152	146	140	133	125	116	106	93	78	54	
	$5 \times 10^{-5}$	178	173	168	164	158	152	145	137	128	118	105	90	66	
Alloy II	$1 \times 10^{-4}$	187	182	177	172	166	160	154	145	135	125	114	99	72	











Table (9): Hydrogen overvoltage ( $\eta_c$ ) values of Al and Al-alloys in 0.5 M H<sub>2</sub>SO<sub>4</sub> solution in the presence of adenosine.

Electrode	Additive concn. (M)	$-\eta_c$ (mV)														
		c.d. $\mu\text{A}/\text{cm}^2$														
Aluminium	0	141	131	121	111	101	90	70	47	18	—					
	$1 \times 10^{-5}$	195	187	182	171	160	149	137	117	95	50					
	$1 \times 10^{-4}$	214	207	199	189	178	167	155	135	113	68					
	$5 \times 10^{-4}$	236	228	221	211	200	188	177	157	135	90					
	$1 \times 10^{-3}$	252	245	238	228	217	204	194	174	152	110					
Alloy I		1260	1170	1080	990	900	810	720	630	540	450	360	270	180		
	0	140	135	129	121	116	108	102	94	85	74	60	41	16		
	$1 \times 10^{-5}$	166	162	157	149	143	135	129	121	112	101	90	76	54		
	$1 \times 10^{-4}$	200	195	190	182	175	168	162	154	145	134	123	108	85		
	$5 \times 10^{-4}$	212	207	202	194	187	180	174	166	157	146	135	120	98		
	$1 \times 10^{-3}$	225	220	215	207	200	193	187	179	170	160	148	134	110		
Alloy II	0	148	140	135	130	123	117	110	100	90	78	65	51	29		
	$1 \times 10^{-5}$	175	168	163	156	150	142	134	127	118	100	88	68	44		
	$1 \times 10^{-4}$	191	184	179	172	166	157	149	142	132	120	106	84	59		
	$5 \times 10^{-4}$	206	199	194	187	181	172	164	156	146	136	120	95	70		
	$1 \times 10^{-3}$	221	214	209	201	196	187	179	171	161	145	130	110	82		



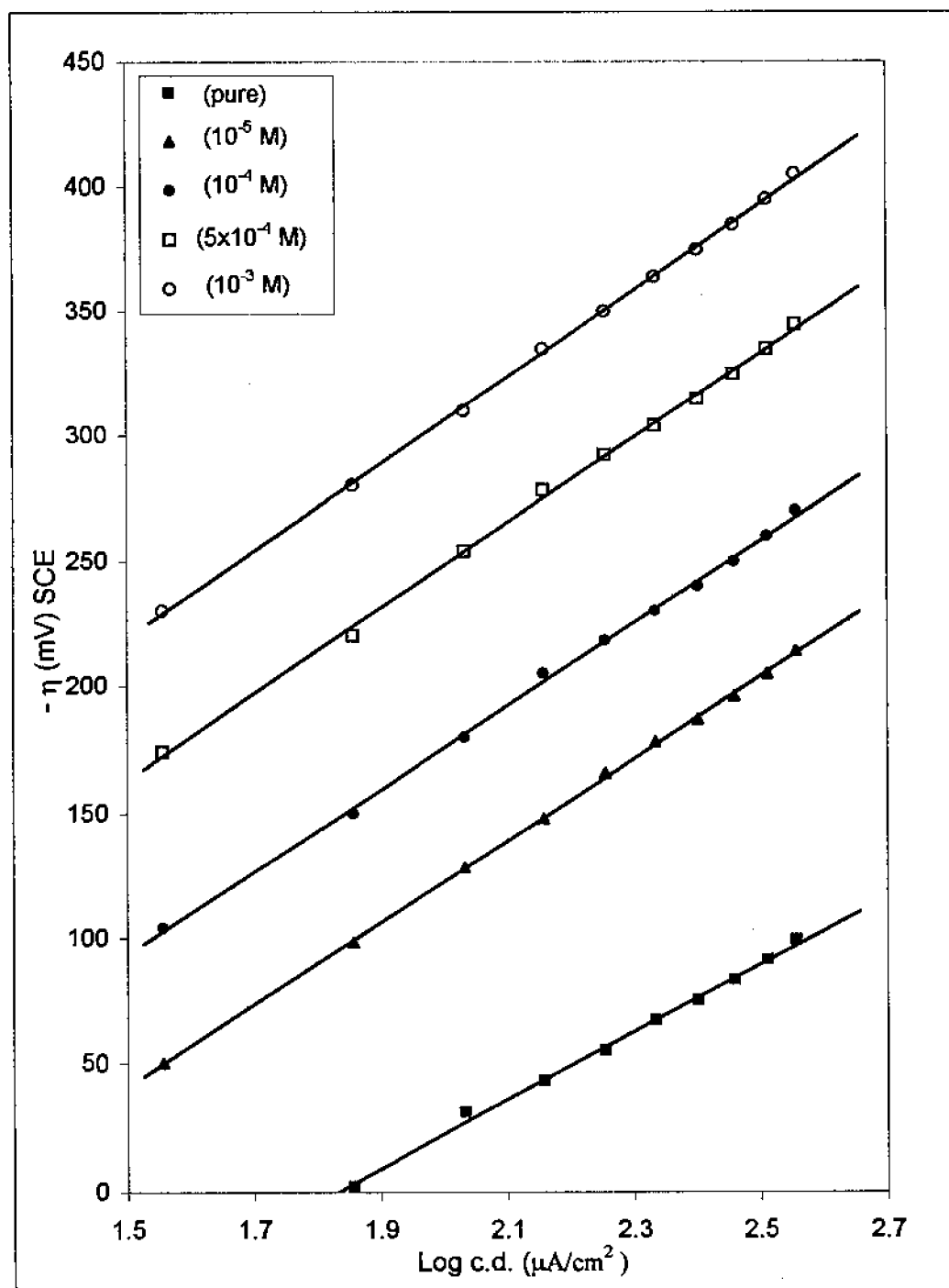


Figure (2): Cathodic Tafel lines for pure aluminium in 0.5 M HCl solution in presence of adenine.

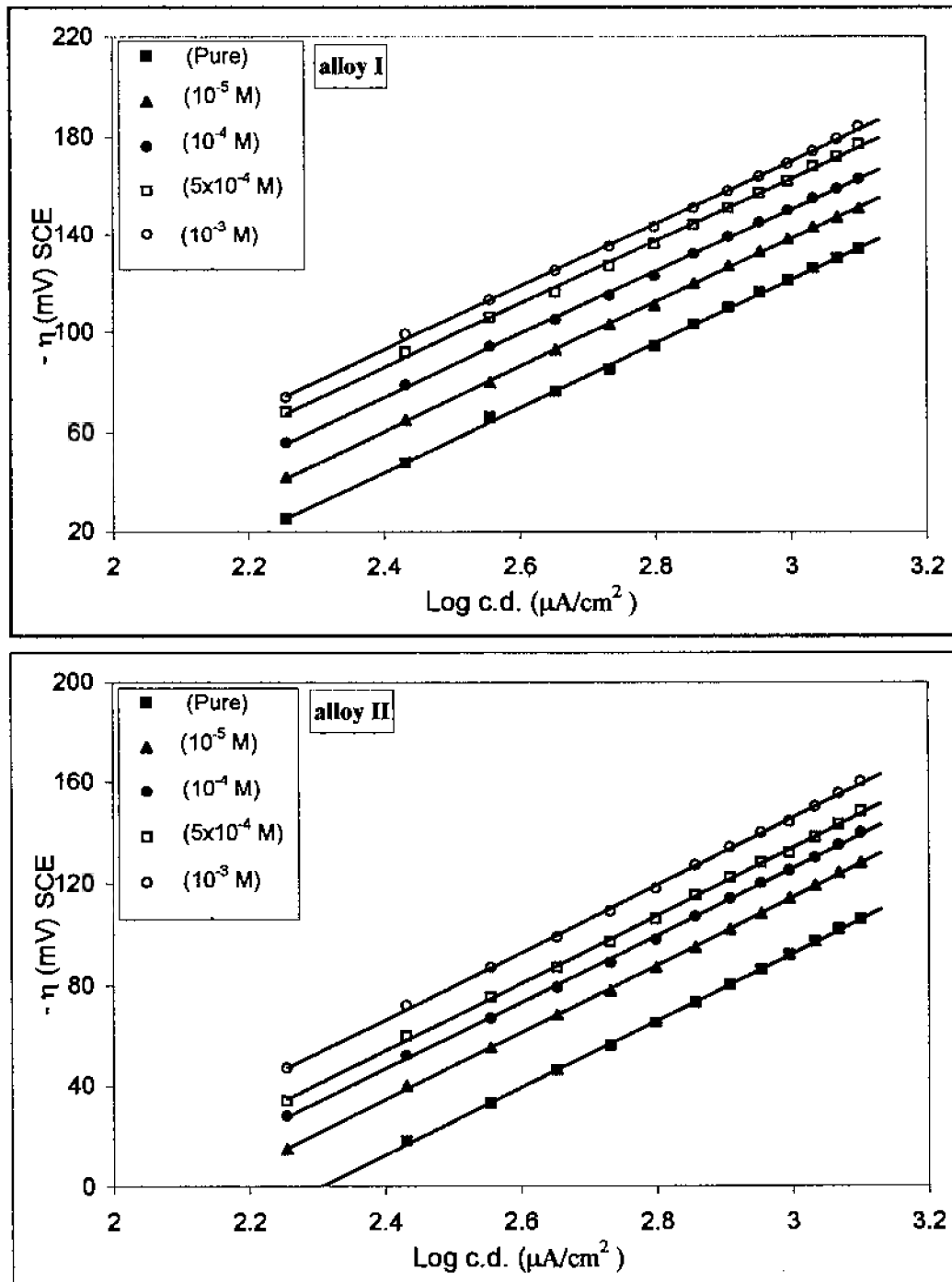


Figure (3): Cathodic Tafel lines for Al-alloys in 0.5M HCl solution in presence of adenine.

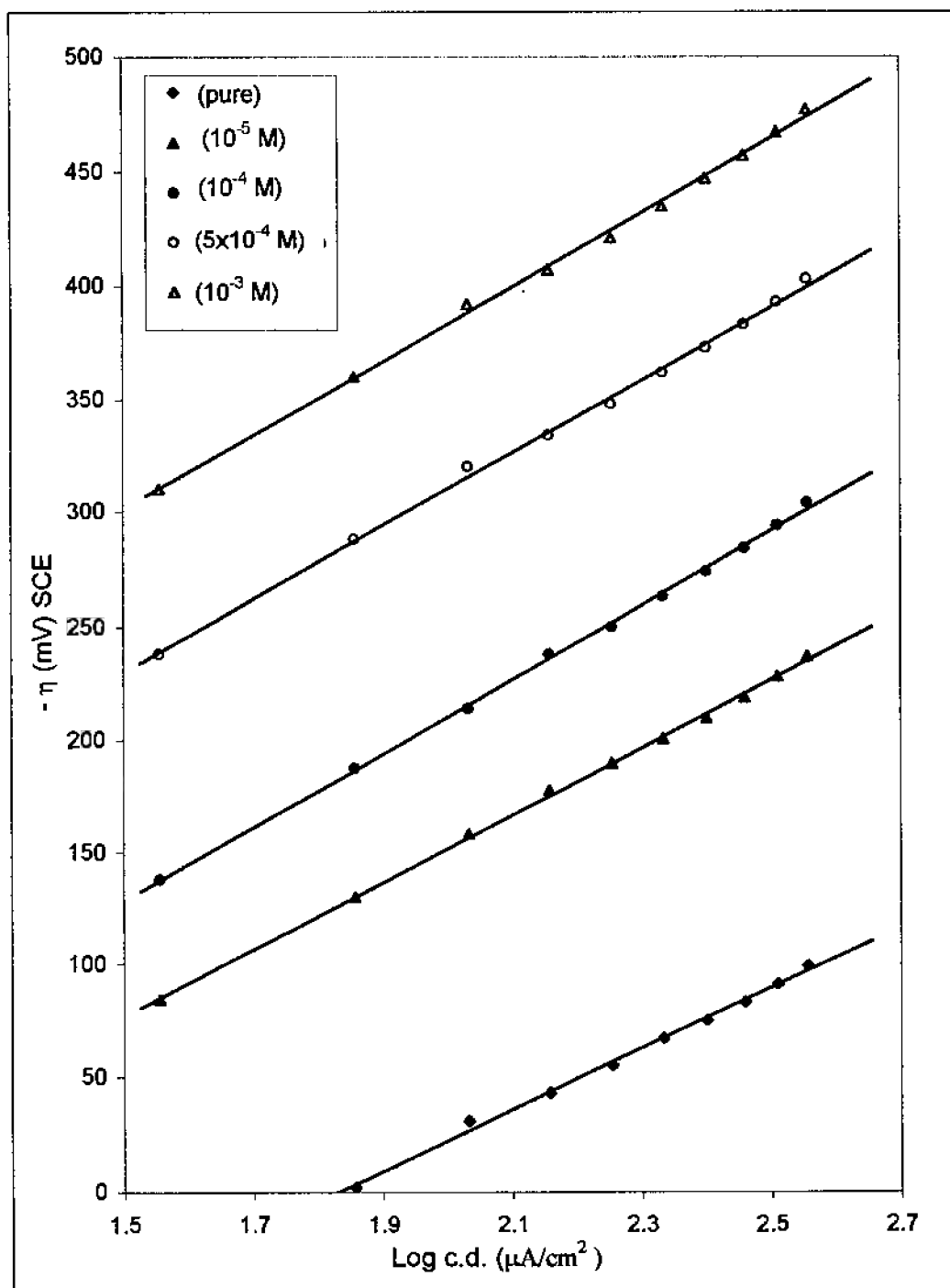


Figure (4): Cathodic Tafel lines for pure aluminium in 0.5 M HCl solution in presence of adenosine.

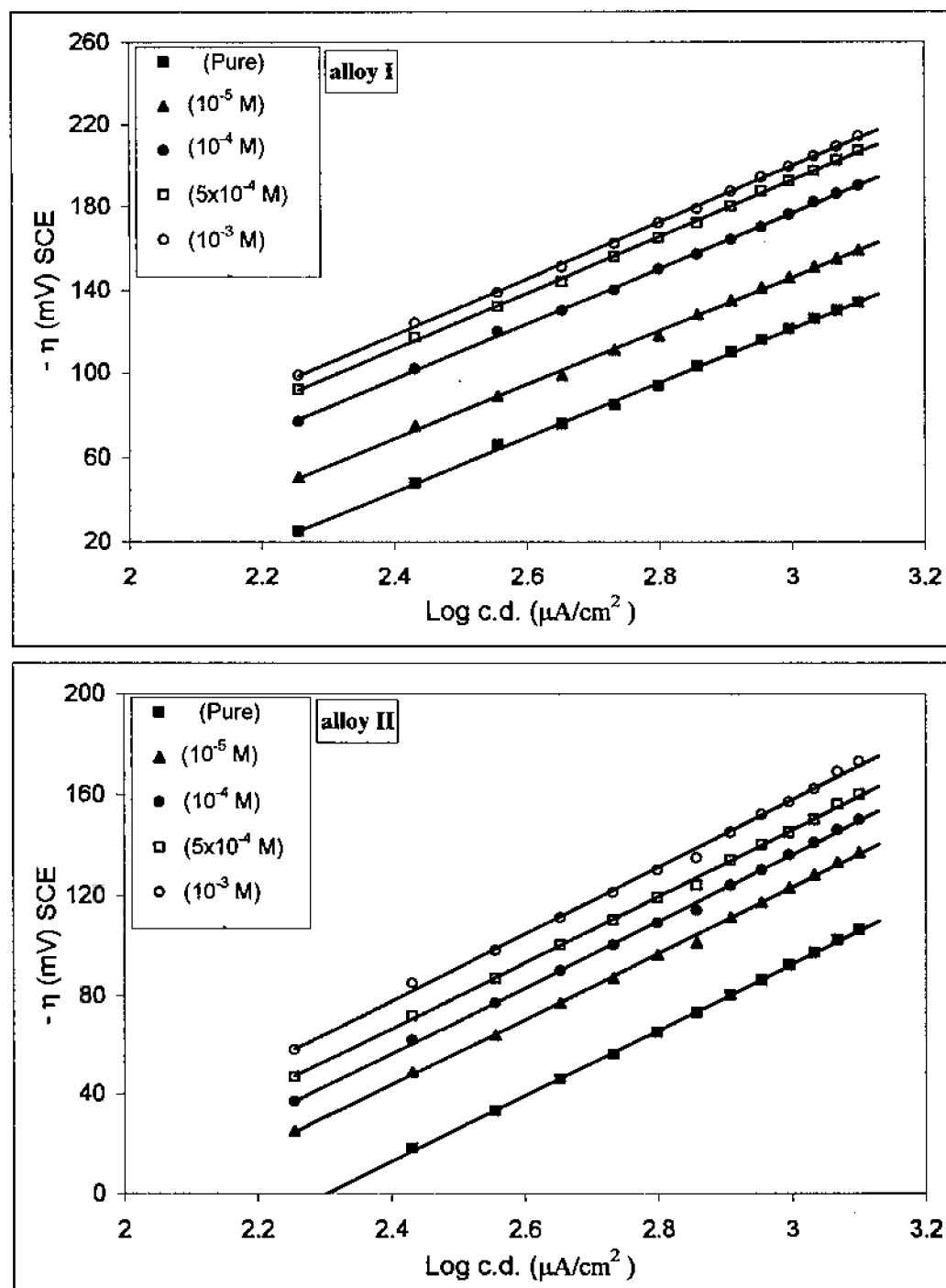


Figure (5): Cathodic Tafel lines for Al-alloys in 0.5M HCl solution in presence of adenosine.

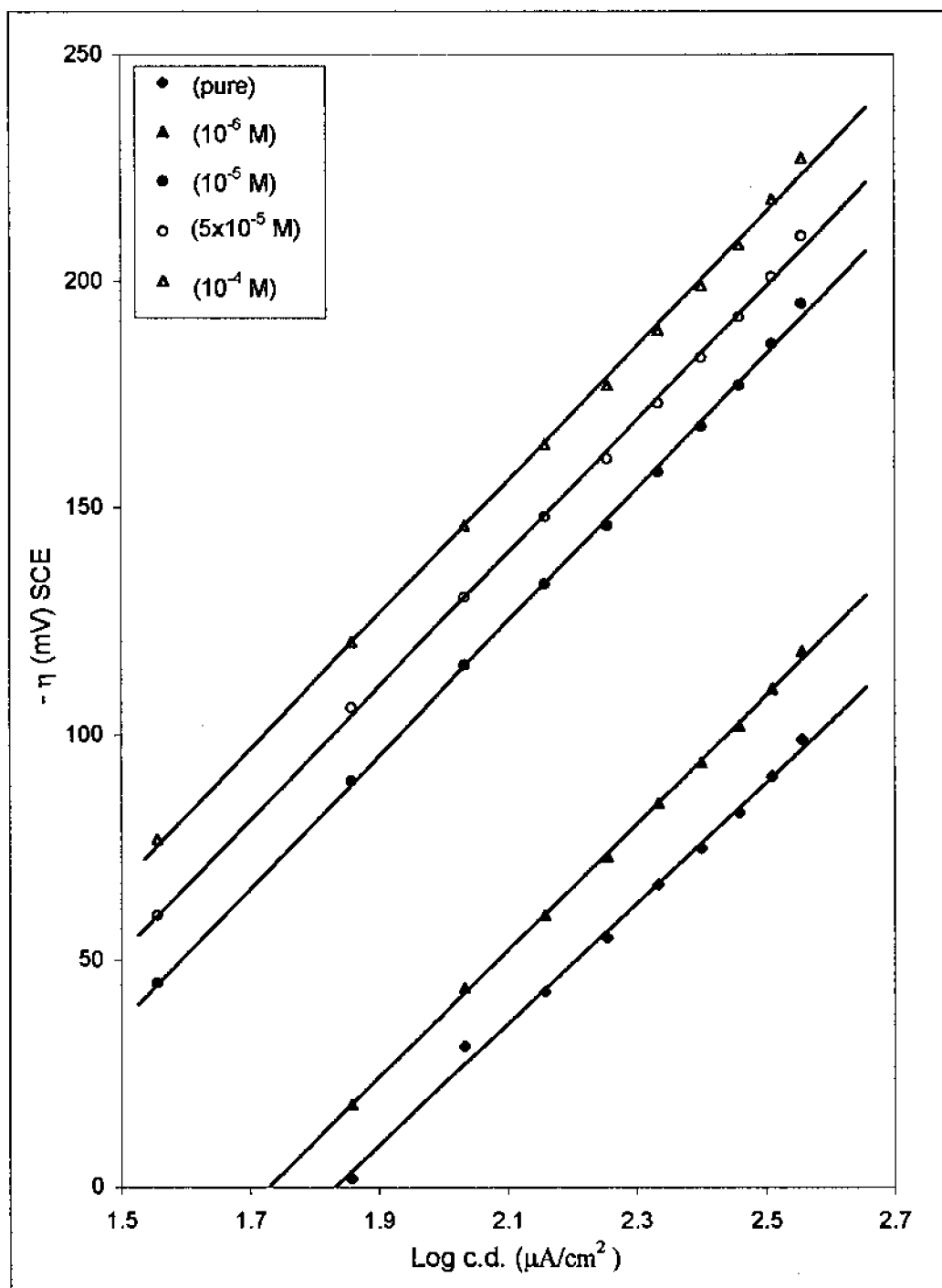


Figure (6): Cathodic Tafel lines for pure aluminium in 0.5 M HCl solution in presence of 3-amino-4-cyano-2-benzoyl-N-phenyl pyrrole.



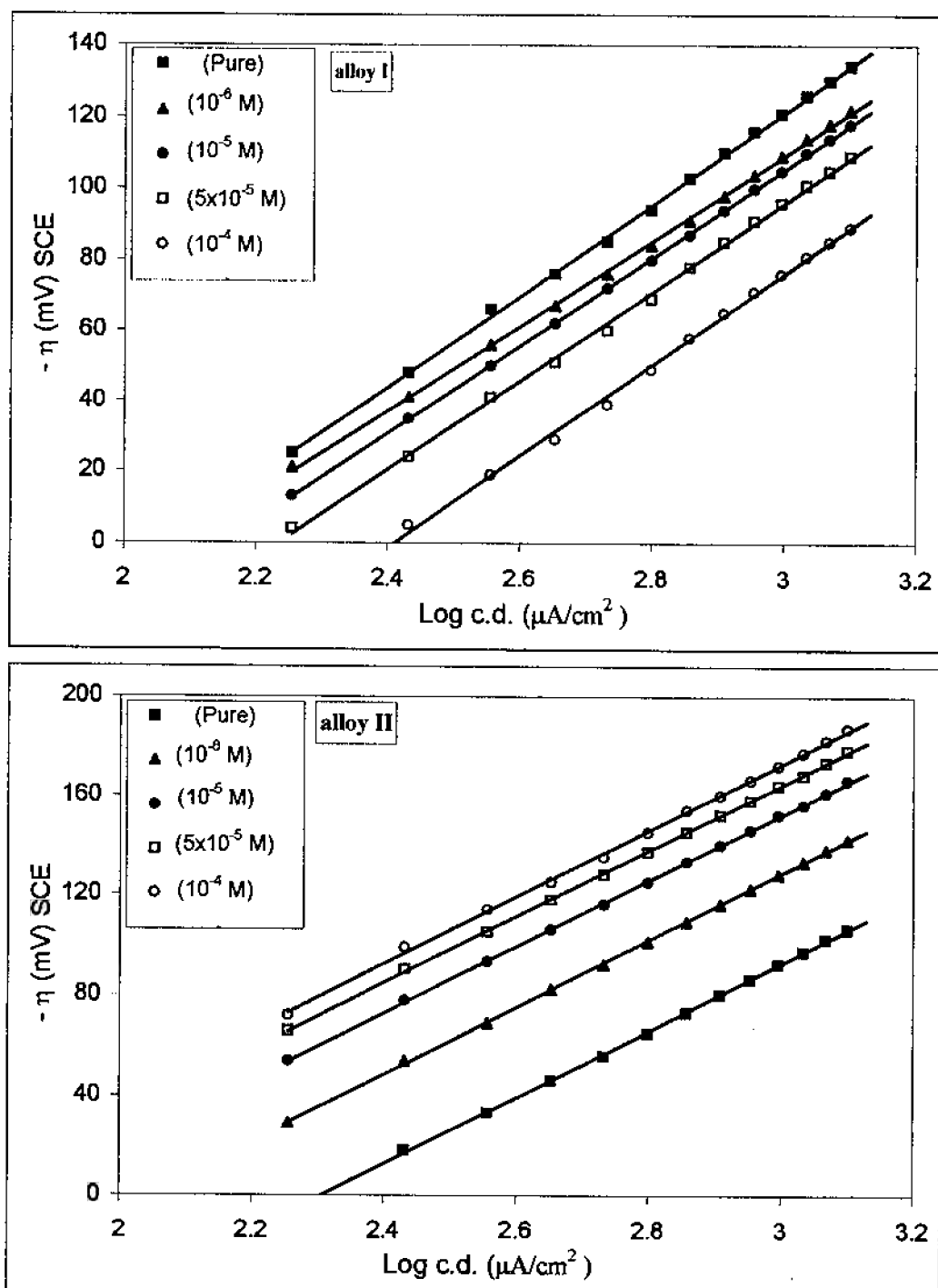


Figure (7): Cathodic Tafel lines for Al-alloys in 0.5 M HCl solution in presence of 3-amino-4-cyano-2-benzoyl-N-phenyl pyrrole.

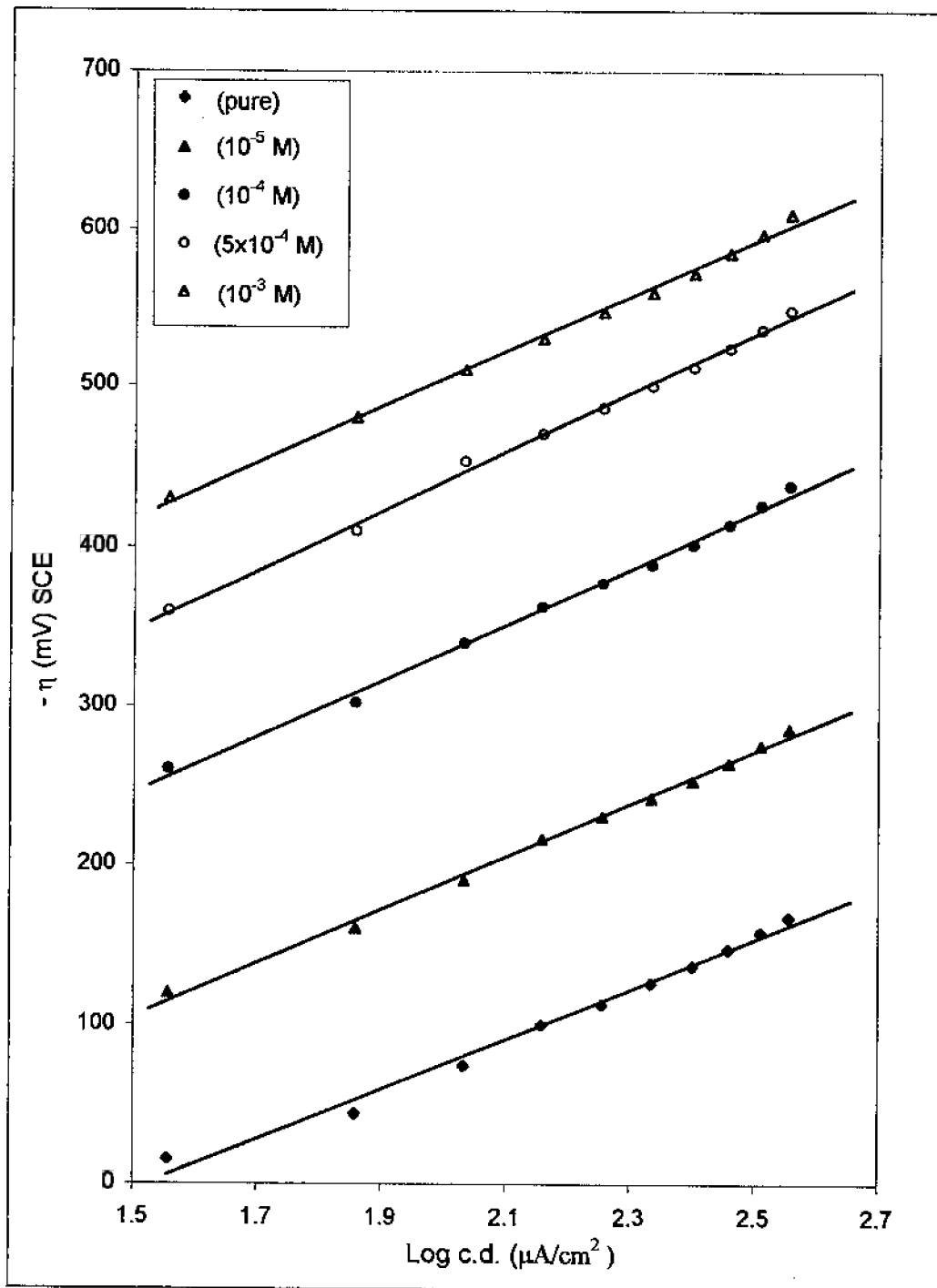


Figure (8): Cathodic Tafel lines for pure aluminium in 0.5 M  $\text{HClO}_4$  solution in presence of adenine.

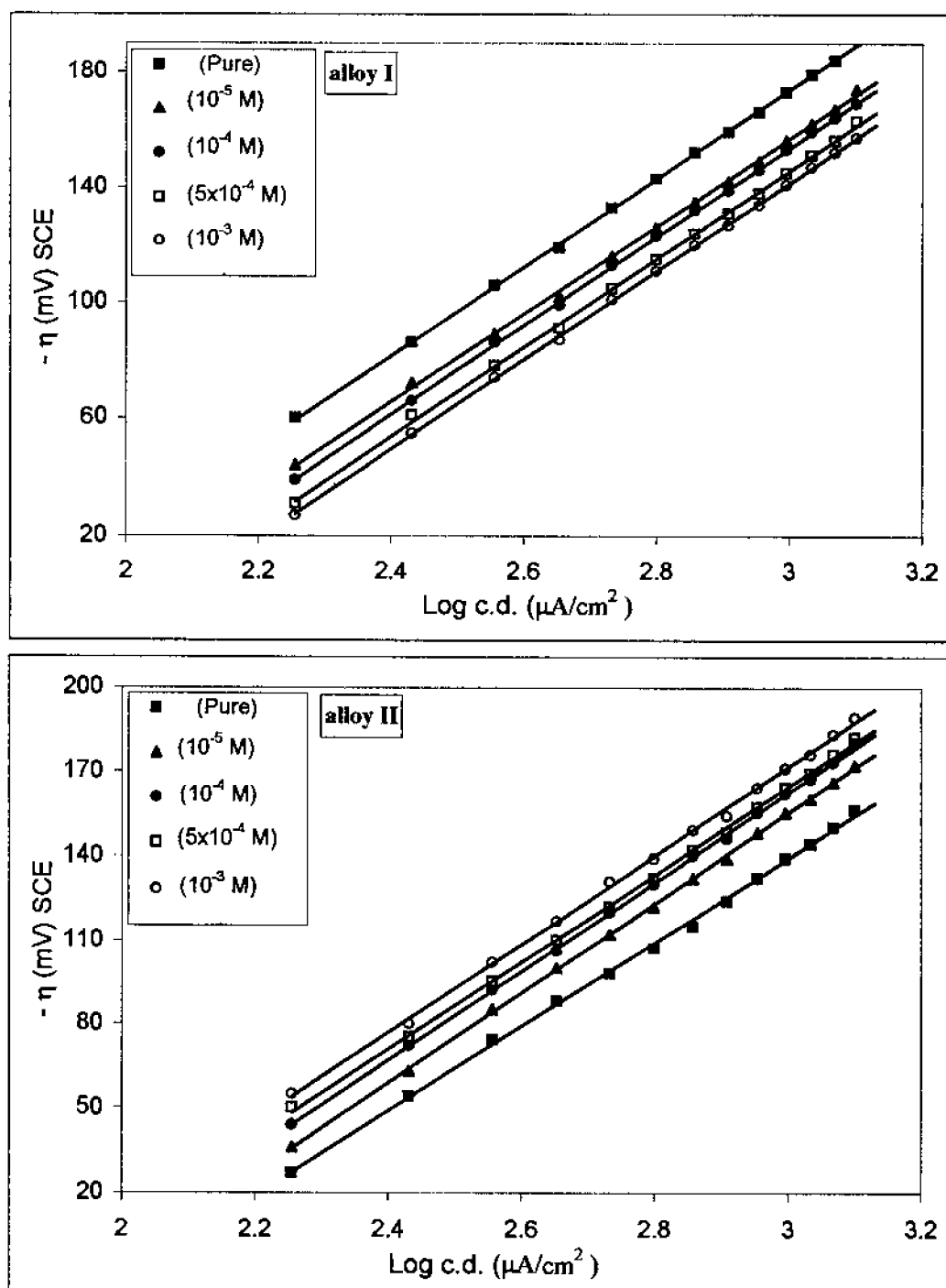


Figure (9): Cathodic Tafel lines for Al-alloys in 0.5 M HClO<sub>4</sub> solution in presence of adenine.

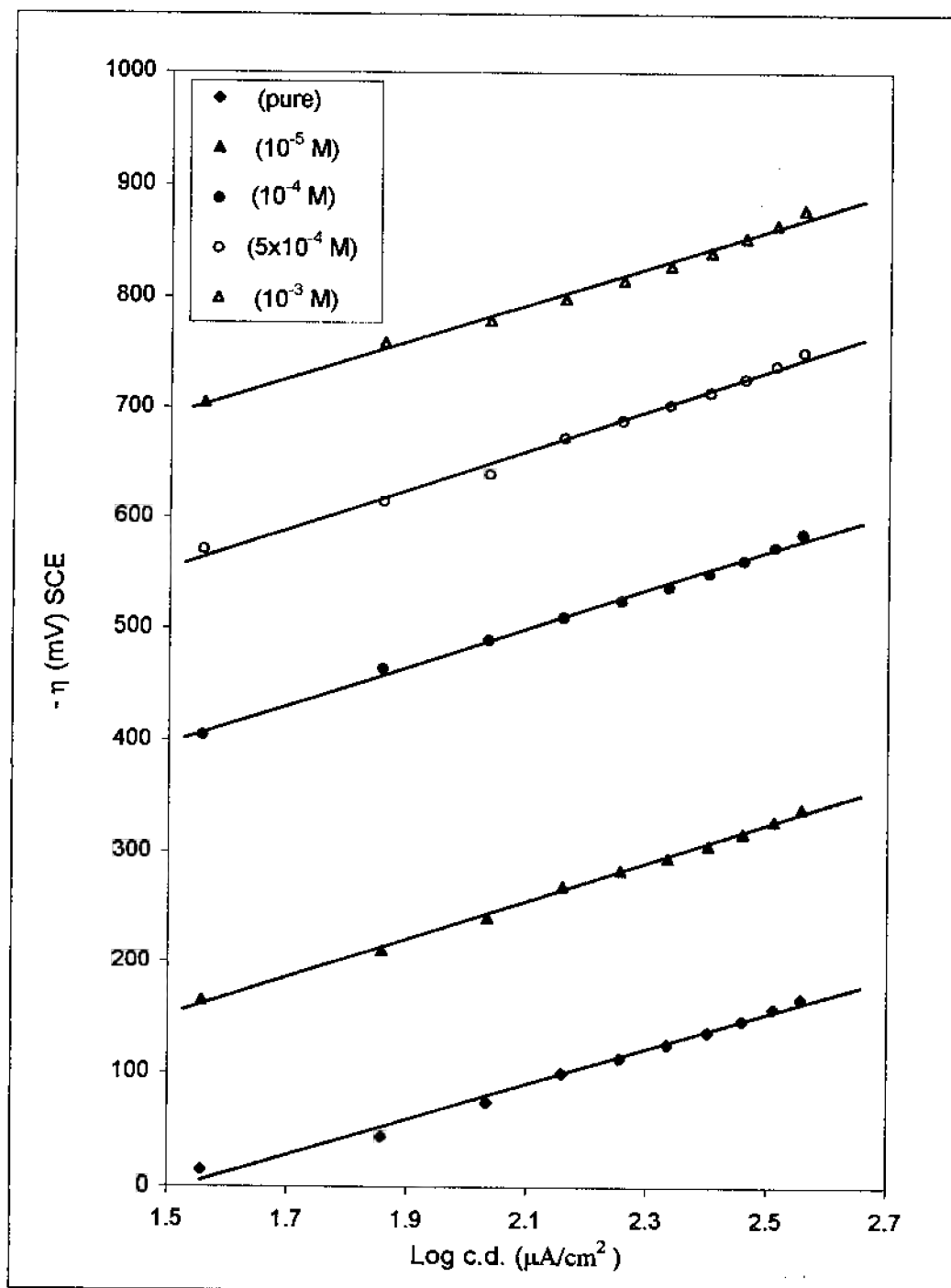


Figure (10): Cathodic Tafel lines for pure aluminium in 0.5 M HClO<sub>4</sub> solution in presence of adenosine.

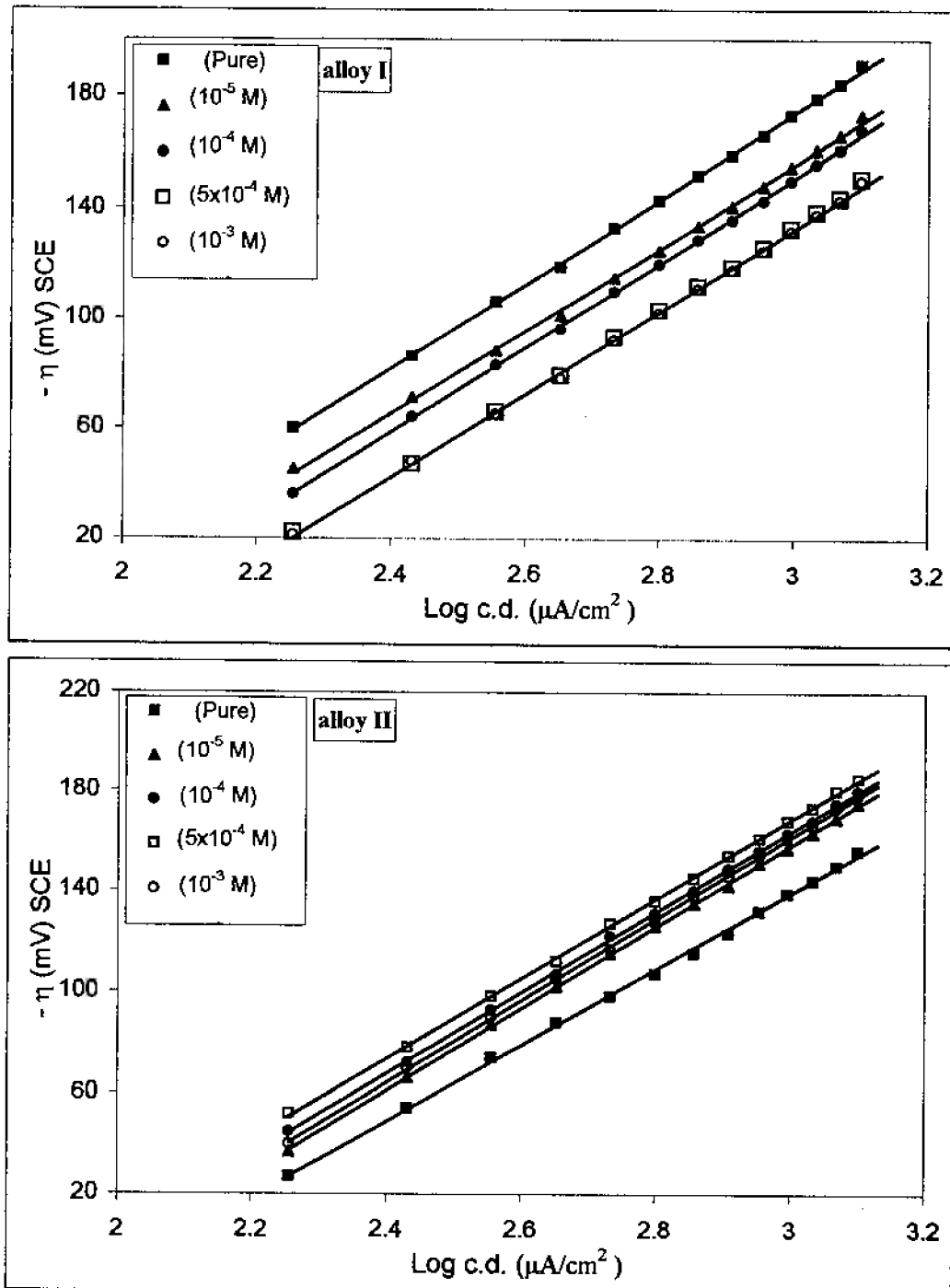


Figure (11): Cathodic Tafel lines for Al-alloys in 0.5 M  $\text{HClO}_4$  solution in presence of adenosine.

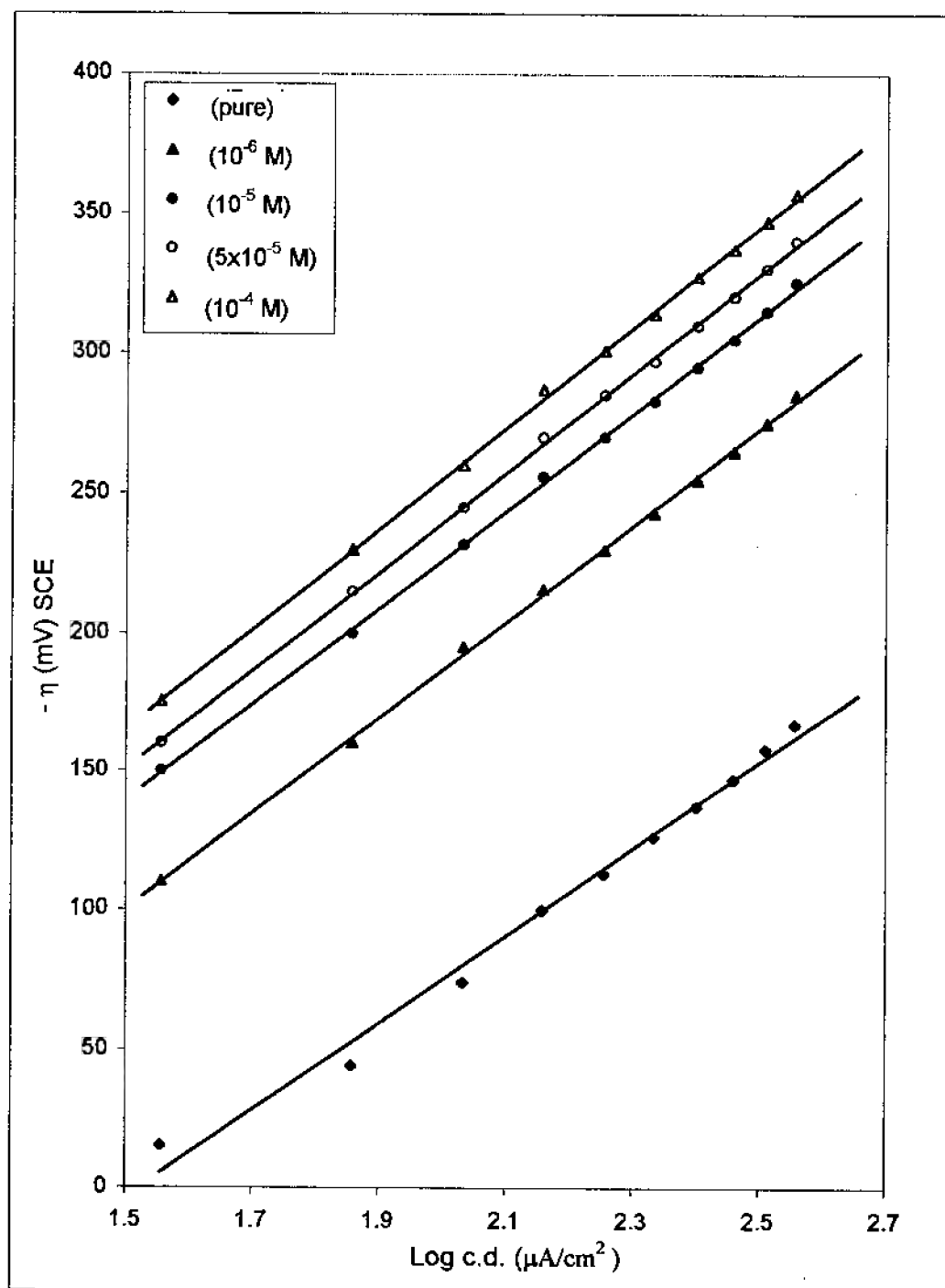


Figure (12): Cathodic Tafel lines for pure aluminium in 0.5 M  $\text{HClO}_4$  solution in presence of 3-amino-4-cyano-2-benzoyl-N-phenyl pyrrole.

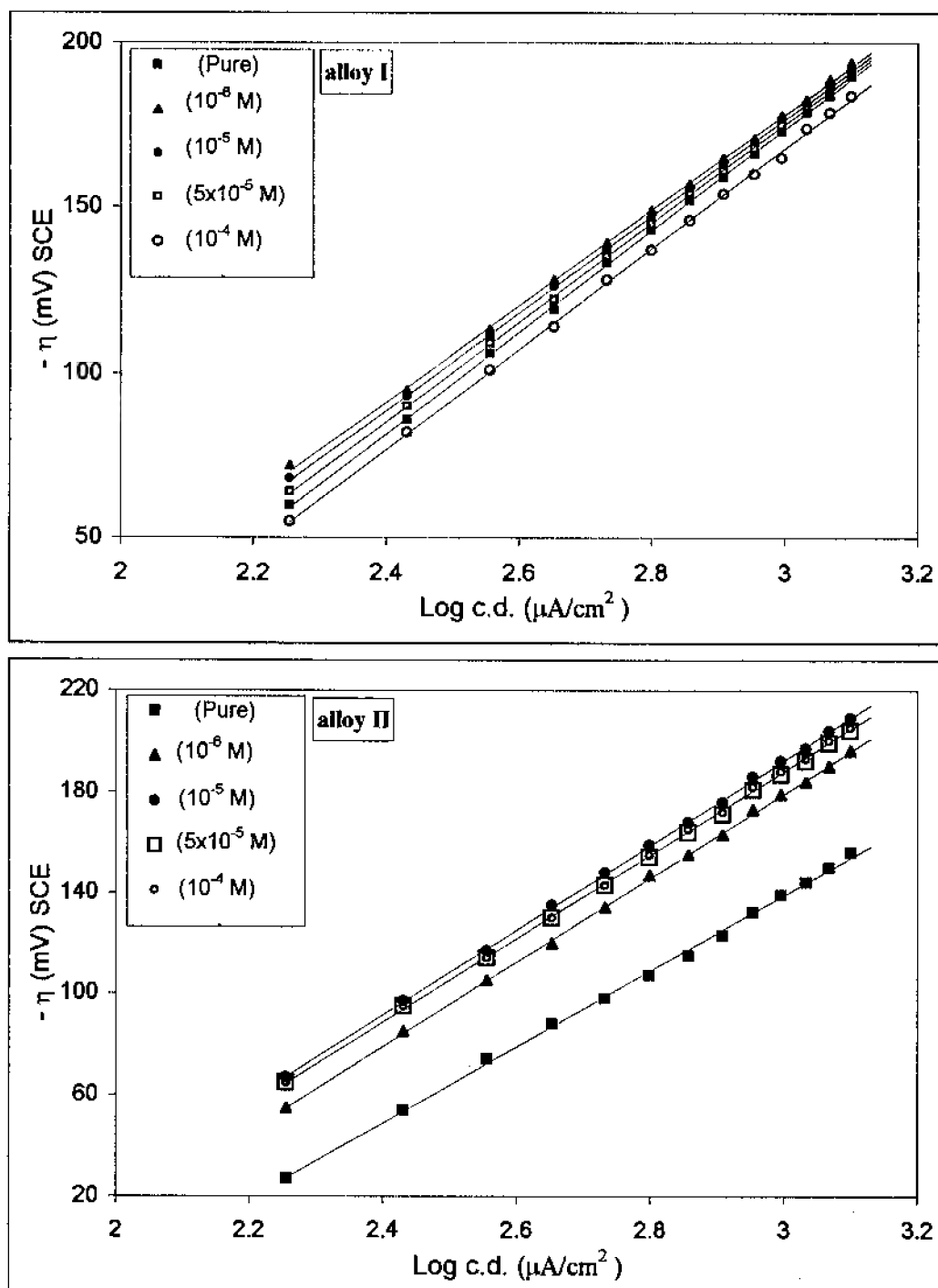


Figure (13): Cathodic Tafel lines for Al-alloys in 0.5 M  $\text{HClO}_4$  solution in presence of 3-amino-4-cyano-2-benzoyl-N-phenyl pyrrole.

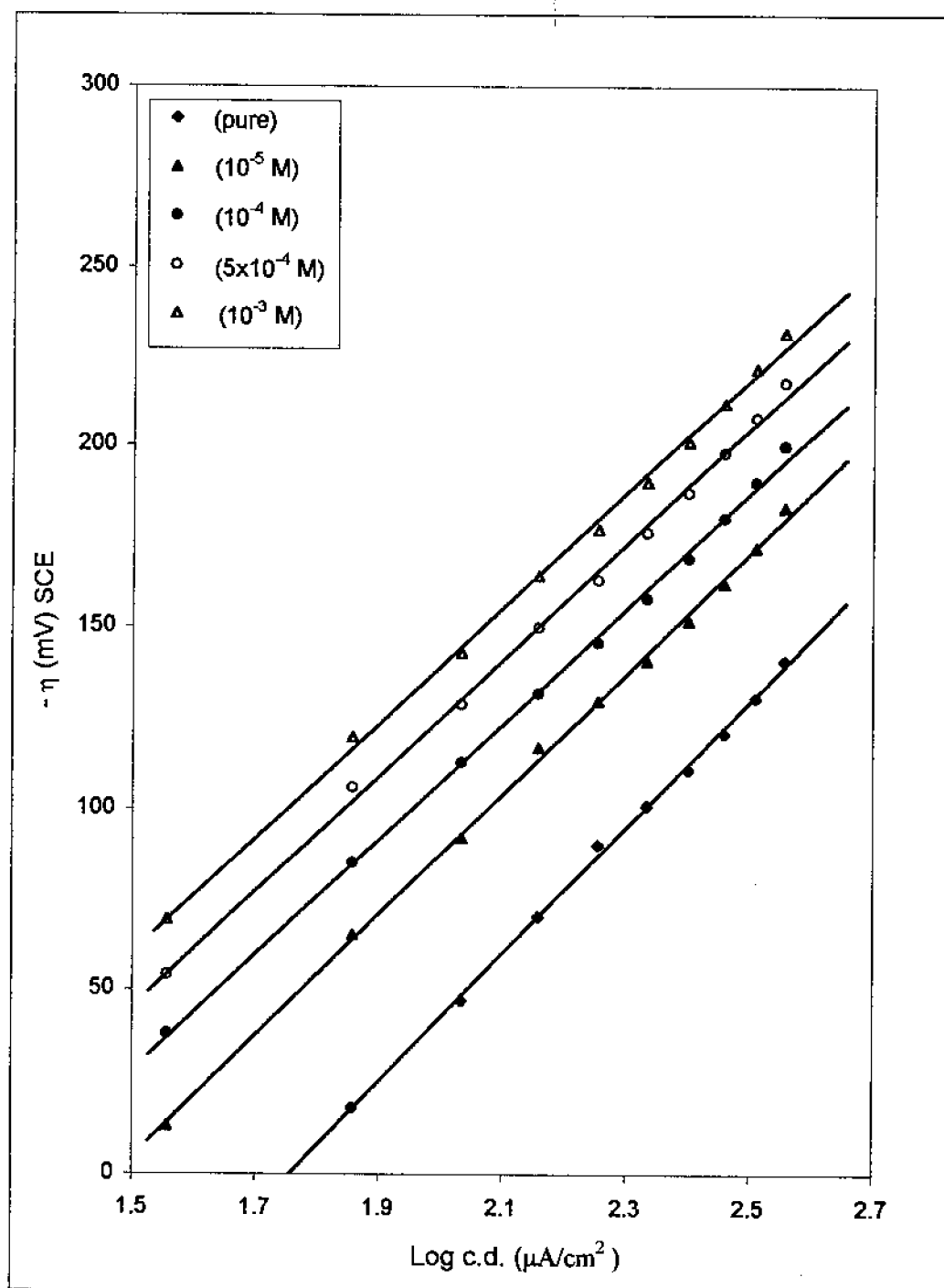


Figure (14): Cathodic Tafel lines for pure aluminium in 0.5 M  $\text{H}_2\text{SO}_4$  solution in presence of adenine.



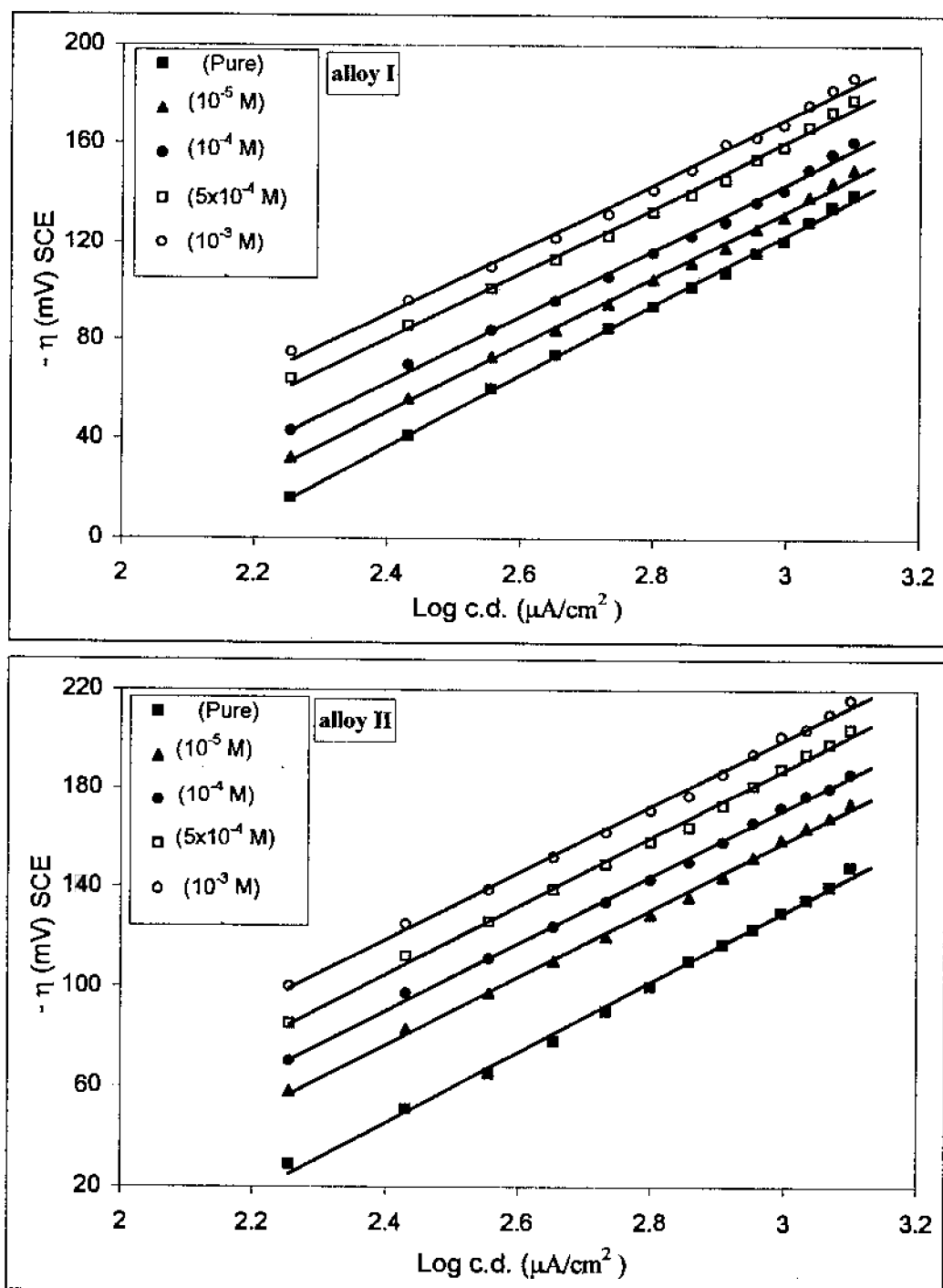


Figure (15): Cathodic Tafel lines for Al-alloys in 0.5 M  $\text{H}_2\text{SO}_4$  solution in presence of adenine.

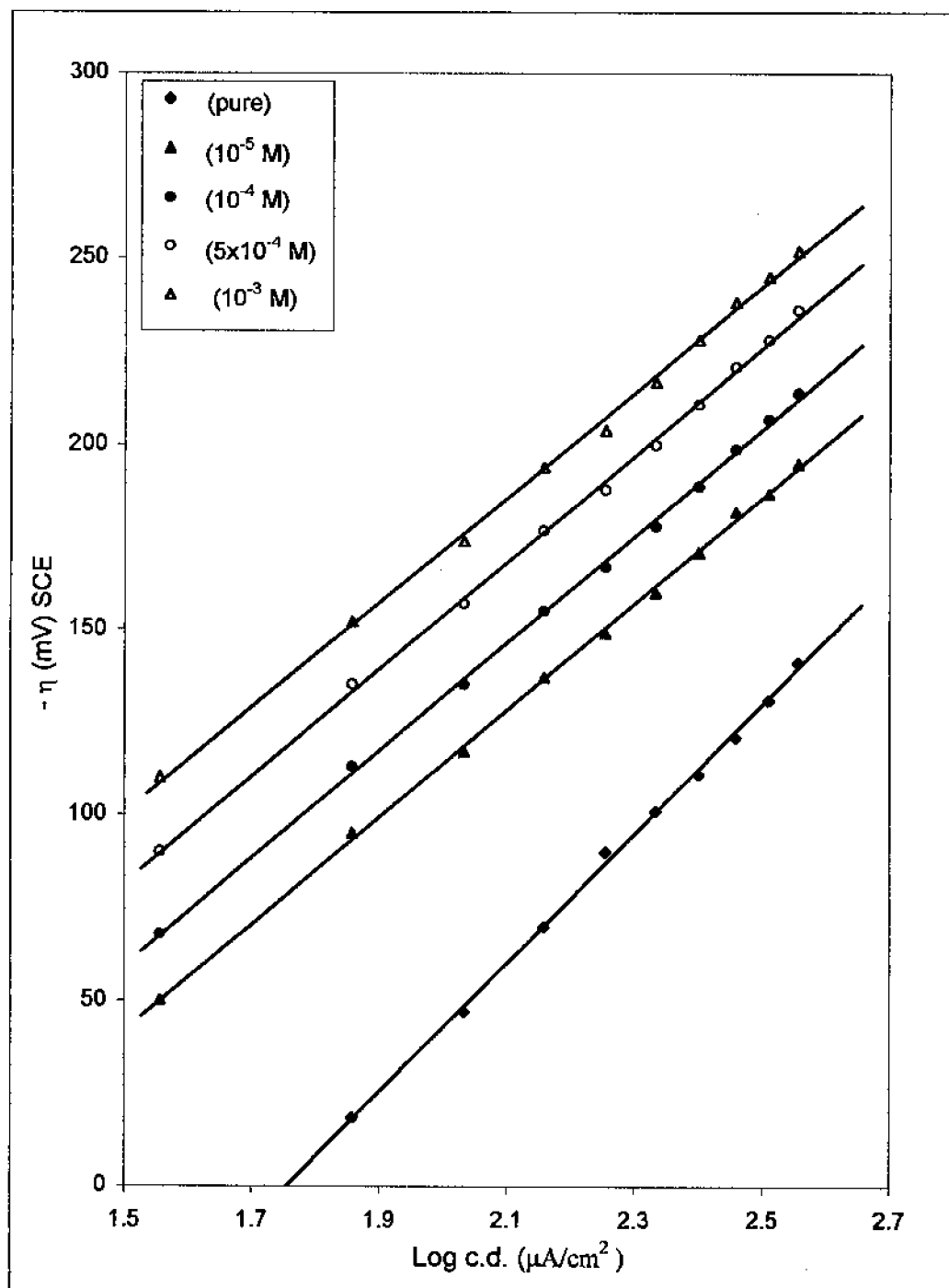


Figure (16): Cathodic Tafel lines for pure aluminium in 0.5 M  $\text{H}_2\text{SO}_4$  solution in presence of adenosine.

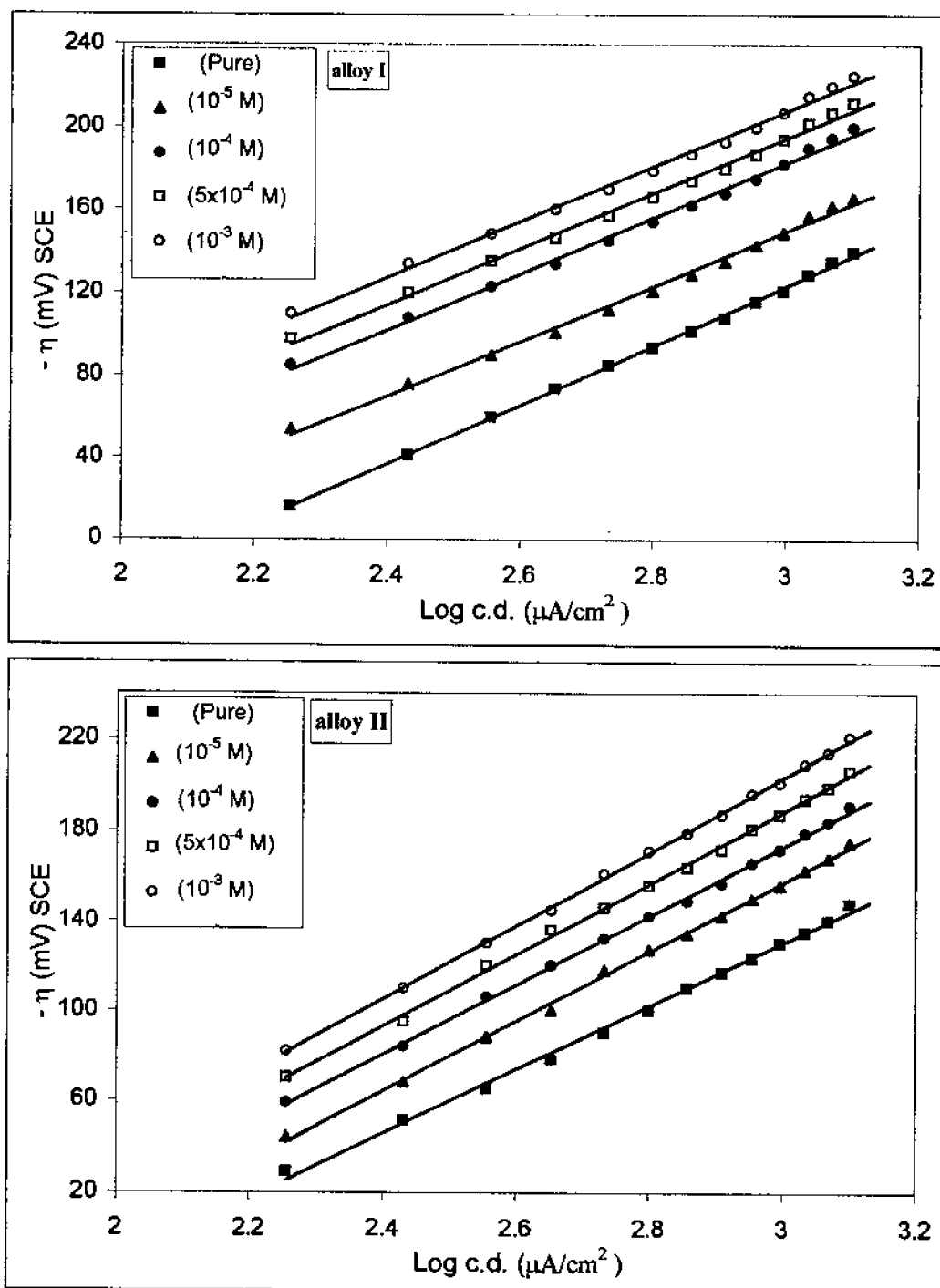


Figure (17): Cathodic Tafel lines for Al-alloys in 0.5 M  $H_2SO_4$  solution in presence of adenosine.

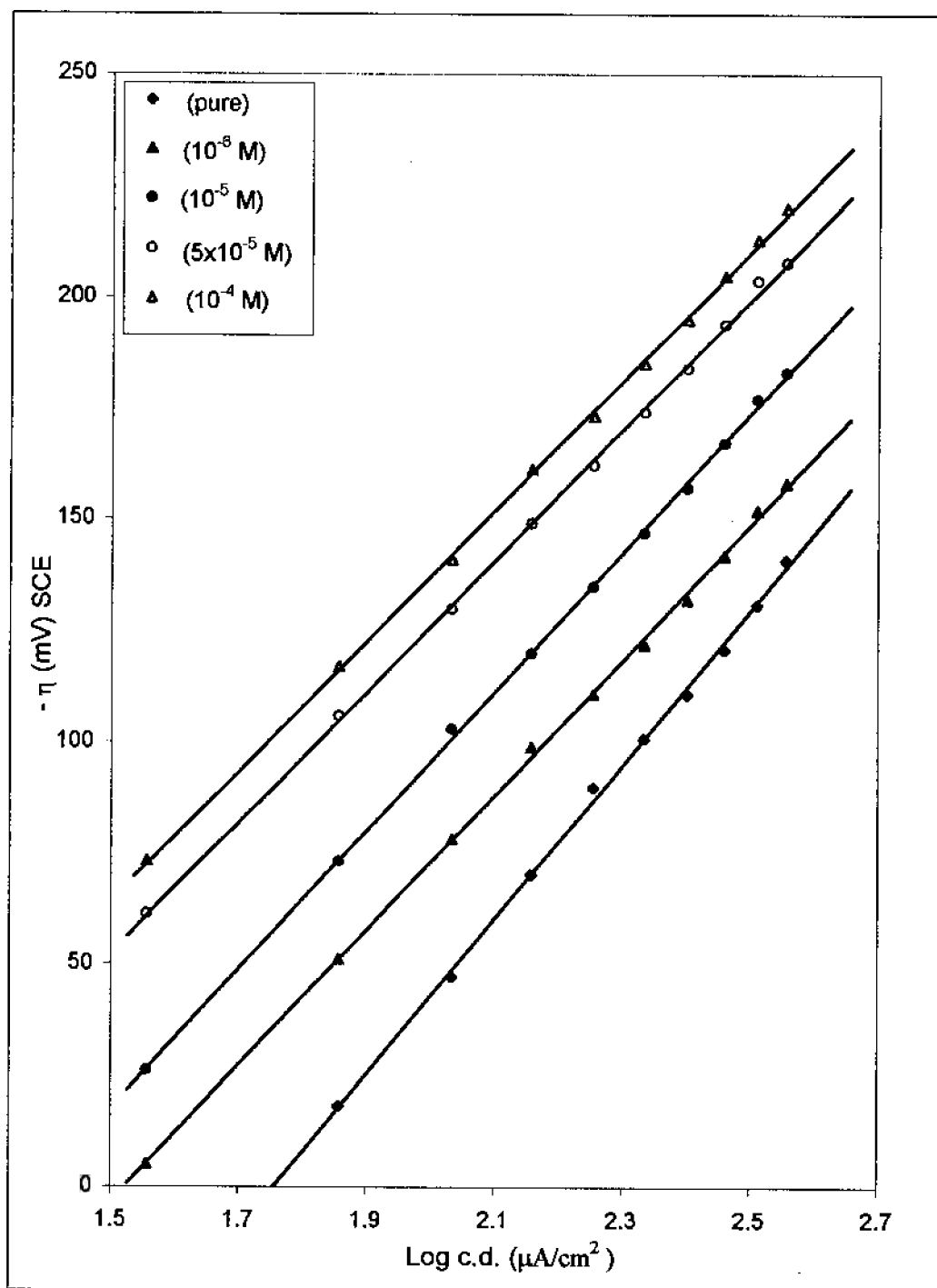


Figure (18): Cathodic Tafel lines for pure aluminium in 0.5 M  $\text{H}_2\text{SO}_4$  solution in presence of 3-amino-4-cyano-2-benzoyl-N-phenyl pyrrole.

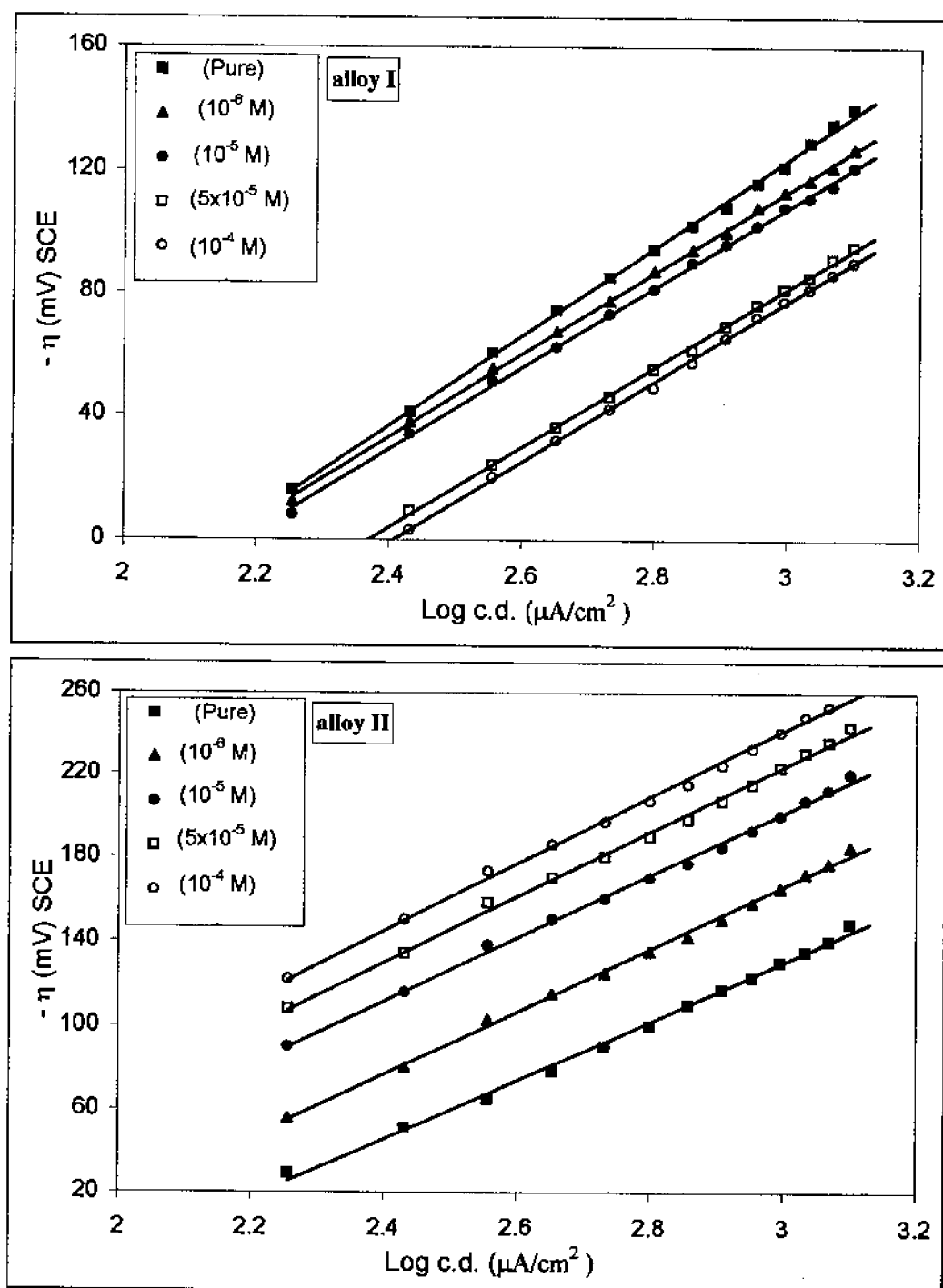


Figure (19): Cathodic Tafel lines for Al-alloys in 0.5 M  $H_2SO_4$  solution in presence of 3-amino-4-cyano-2-benzoyl-N-phenyl pyrrole.

### **1.2. Parameters for hydrogen evolution reaction:**

Tables 11-19 show the parameters for hydrogen evolution reaction (h.e.r) at both Al and its alloys in 0.5M solutions of HCl, HClO<sub>4</sub> and H<sub>2</sub>SO<sub>4</sub> as well as those containing various concentrations of adenine, adenosine and pyrrole derivative.

The parameters for hydrogen evolution reaction include Tafel slope ( $b_c$ ) and transfer coefficient ( $\alpha$ ). It is seen that values of the Tafel slope ( $b_c$ ) and transfer coefficient ( $\alpha$ ) for hydrogen evolution reaction at both Al and its alloys approximately the same in the absence and presence of all investigated organic compounds. Values of ( $b_c$ ) range from 146 to 183 mV for pure Al and from 129 to 166 mV for alloys I and II. Transfer coefficient values range from 0.330 to 0.404 for pure aluminium while those of its alloys are ranging from 0.355 to 0.457.

### **1.3. Open circuit corrosion potential ( $E_{corr}$ ):**

Steady state open circuit corrosion potentials ( $E_{corr}$ ) for Al and its alloys were measured in pure 0.5 M solutions of HCl, HClO<sub>4</sub> and H<sub>2</sub>SO<sub>4</sub> as well as those containing various concentrations of adenine, adenosine and pyrrole derivative. These values are given in Tables 11-19. From these Tables, it can be seen that the value of  $E_{corr}$  is shifted in the positive direction in the presence of the investigated organic compounds. The potential shift increases with the increase in the concentration of the additive. For the same concentration of investigated organic compounds, the positive shift in  $E_{corr}$  in H<sub>2</sub>SO<sub>4</sub> solution increases in the order:

$$\text{Adenosine} < \text{Adenine} < \text{Pyrrole derivative.}$$

#### 1.4. Corrosion currents ( $i_{\text{corr.}}$ ):

Corrosion currents ( $i_{\text{corr.}}$ ) of both Al and its alloys in 0.5 M solutions of HCl, HClO<sub>4</sub> and H<sub>2</sub>SO<sub>4</sub> in the absence and presence of various concentrations of organic compounds are determined by the method described by Kaesche and Hackerman<sup>(61)</sup> by extrapolation back of the cathodic polarization curves to open circuit corrosion potential.

Cathodic polarization curves are used rather than anodic polarization curves for several reasons: Anodic dissolution may be nonuniform because of differences in individual corrosion rates of various crystal face. Also, with increased dissolution of the metal, the surface changes in an underfined manner so that the geometrical surface area is no longer a good approximation of the true surface area.

Corrosion currents ( $\mu\text{A}/\text{cm}^2$ ) determined by the above mentioned method, in 0.5 M solutions of HCl, HClO<sub>4</sub> and H<sub>2</sub>SO<sub>4</sub> and those obtained in the presence of the investigated organic compounds at concentrations ranging from  $10^{-6}$ - $10^{-4}$  M of pyrrole derivative and from  $10^{-5}$ - $10^{-3}$  M in case of adenine and adenosine are given in Tables 11-19.

From these results it is seen that all investigated organic compounds (except pyrrole derivative in case of alloy I) in HCl solution decrease the corrosion current of both Al and its alloys. With one and the same series of compounds, the maximum decrease in corrosion current is attained with adenosine. Similar behaviour is observed for pure Al in HClO<sub>4</sub> in the presence of all investigated compounds. For alloy I the corrosion current decreases only in the presence of pyrrole derivative at lower

concentrations, while the higher concentration ( $10^{-4}\text{M}$ ) has influence to increase the corrosion current. For alloy II, the investigated compounds exhibited decrease in corrosion current in  $\text{HClO}_4$  solution. The maximum decrease in corrosion current is attained with pyrrole derivative. All the investigated compounds (except alloy I in the presence of pyrrole derivative) have influence to decrease the corrosion current of pure Al and its alloys in  $\text{H}_2\text{SO}_4$  solution. Pyrrole derivative showed an increase in the corrosion current for alloy I in the same investigated acid solution.

### **1.5. Inhibition efficiency:**

The inhibition efficiency expressed as percent inhibition (% I) is defined as:

$$\% I = \frac{i_{\text{uninh.}} - i_{\text{inh.}}}{i_{\text{uninh.}}} \times 100 \quad (3)$$

where  $i_{\text{uninh.}}$  and  $i_{\text{inh.}}$  are the uninhibited and inhibited corrosion currents. The inhibited corrosion currents are those determined in the presence of the various organic compounds used in this investigation and can be considered as corrosion inhibitors. The uninhibited corrosion currents were determined in pure (inhibitor free) 0.5 M solutions of  $\text{HCl}$ ,  $\text{HClO}_4$  and  $\text{H}_2\text{SO}_4$  under the same conditions of temperature ( $25^\circ\text{C}$ ). Values of the inhibition efficiency in the presence of the various organic compounds within the concentration range  $10^{-6}$ - $10^{-4}$  M in case of pyrrole derivative and  $10^{-5}$ - $10^{-3}$  M in case of adenine and adenosine are given in Tables 11-19 together with  $E_{\text{corr.}}$  and  $i_{\text{corr.}}$  values. These results show that all the investigated additives (except pyrrole derivative for alloy I) in  $\text{HCl}$  solution



increase the inhibition efficiency as the inhibitor concentration is increased. But pyrrole derivative shows negative values of % I on alloy I.

The data show that for all studied organic compounds on pure Al, the inhibition efficiency increases with the increase of the inhibitor concentration in  $\text{HClO}_4$  solution. However, % I increases of alloy II as the adenine concentration is increased, while in the presence of pyrrole derivative and adenosine, %I increases as the concentration of additive is increased only at lower concentrations, but at higher concentration of adenosine ( $10^{-3}$  M) it decreases. For alloy I in  $\text{HClO}_4$ , the addition of investigated organic compounds (except pyrrole derivative) has negative influence on inhibition efficiency. The inhibition efficiency increases (except pyrrole derivative in case of alloy I) as the concentration of all studied organic compounds is increased in  $\text{H}_2\text{SO}_4$  solution.

#### **1.6. Change in overpotential of cathodic hydrogen evolution ( $\Delta\eta_c$ ):**

The addition of investigated organic compounds has influence to increase the value of  $\Delta\eta_c$  in the negative direction and the value increases with increasing the concentration of the inhibitor in all investigated acids solutions on pure Al and alloy II. The values of  $\Delta\eta_c$  at different examined additives on pure Al are higher than those of alloy II under the same conditions. In case of alloy I, addition of all investigated organic compounds (except pyrrole derivative at lower concentrations,  $10^{-6}$  -  $5 \times 10^{-5}$  M) has influence to increase the values of  $\Delta\eta_c$  in the positive direction in  $\text{HClO}_4$ . Such positive shift increases with the increase in concentration of adenine and adenosine. Also,  $\Delta\eta_c$  values increase in the positive direction

with increasing the concentration of pyrrole derivative in both HCl and H<sub>2</sub>SO<sub>4</sub> solutions on alloy I.

### **1.7. Parameters for anodic dissolution reaction ( $\Delta\eta_a$ ):**

Tables 11-19 show the parameters for anodic dissolution reaction at both Al and its alloys in 0.5 M solutions of HCl, HClO<sub>4</sub> and H<sub>2</sub>SO<sub>4</sub> in the absence and presence of various concentrations of pyrrole derivative, adenine and adenosine at concentrations 10<sup>-6</sup>-10<sup>-4</sup> M of pyrrole derivative and 10<sup>-5</sup>-10<sup>-3</sup> M of both adenine and adenosine.

These parameters include Tafel slope ( $b_a$ ) and change in overpotential of anodic dissolution ( $\Delta\eta_a$ ). It is observed that values of the Tafel slope ( $b_a$ ) at both Al and its alloys approximately the same in the absence and presence of all investigated organic compounds. Values of ( $b_a$ ) range from 148-158 mV for pure Al, 59-79 mV for alloy I and 46-65 mV for alloy II in H<sub>2</sub>SO<sub>4</sub> solution. 132-164 mV for pure Al, 61-89 mV for alloy I and 28-42 mV for alloy II in HClO<sub>4</sub> solution. 76-87 mV for pure Al, 47-59 mV for alloy I and 26-32 mV for alloy II in HCl solution.

The same above mentioned Tables show the values of  $\Delta\eta_a$  in the presence of the investigated compounds. It is seen that the most values of  $\Delta\eta_a$  increase with increasing the concentration of all investigated compounds in the studied acids solutions.

### **1.8. Adsorption isotherm:**

For primary interface inhibition, the degree of coverage ( $\theta_{org.}$ ) is

given by equation:

$$\theta_{\text{org.}} = \frac{i_{\text{uninh.}} - i_{\text{inh.}}}{i_{\text{uninh.}}} \quad (4)$$

and agree with the value of %I given by equation(3), values of  $\theta_{\text{org.}}$  determined by equation(4) are recorded in Tables 11-19. From these values  $C/\theta$  plotted against  $C$  (mol/L) of various organic inhibitors at 25°C are shown in Figs.20-28 straight lines are obtained. These can be considered as the adsorption isotherms for such organic inhibitors at both Al and alloys I and II in the investigated acids solutions.

Table (11): Effect of adenine on the electrochemical and corrosion behaviour of aluminium and its alloys in 0.5 M HCl solution.

Electrode	Additive concn. (M)	-E <sub>corr.</sub> mV (SCE)	i <sub>corr.</sub> $\mu\text{A}/\text{cm}^2$	% I (inh.effec.)	Surf. Coverage ( $\theta$ )	$\Delta\eta_c$ (mV) at 360 $\mu\text{A}/\text{cm}^2$	$\Delta\eta_a$ (mV) at 162 $\mu\text{A}/\text{cm}^2$	Tafel slopes.		Transfer coeff. ( $\alpha$ )
								b <sub>a</sub> (mV)	b <sub>c</sub> (mV)	
Aluminium	0	922	68	—	—	—	—	76	147	0.40
	$1 \times 10^{-5}$	916	18	73.5	0.735	-115	+ 16	79	170	0.35
	$1 \times 10^{-4}$	910	10	85.3	0.853	-171	+ 20	77	174	0.34
	$5 \times 10^{-4}$	905	4	94.1	0.941	-246	+ 26	82	176	0.34
	$1 \times 10^{-3}$	895	3	95.6	0.956	-306	+ 27	82	176	0.34
Alloy I	0	774	122	—	—	—	—	47	131	0.45
	$1 \times 10^{-5}$	772	84	31.1	0.311	-14	+ 3	47	130	0.45
	$1 \times 10^{-4}$	770	68	44.3	0.443	-28	+ 5	47	129	0.46
	$5 \times 10^{-4}$	768	61	50.0	0.500	-40	+ 5	47	129	0.46
	$1 \times 10^{-3}$	766	58	52.5	0.525	-47	+ 8	47	130	0.45
Alloy II	0	767	200	—	—	—	—	31	131	0.45
	$1 \times 10^{-5}$	765	145	27.5	0.275	-22	+ 3	31	135	0.44
	$1 \times 10^{-4}$	763	119	40.5	0.405	-34	+ 6	31	134	0.44
	$5 \times 10^{-4}$	760	106	47.0	0.470	-42	+ 8	32	135	0.44
	$1 \times 10^{-3}$	752	78	61.0	0.610	-54	+ 10	32	134	0.44

Table (12): Effect of adenosine on the electrochemical and corrosion behaviour of aluminium and its alloys in 0.5 M HCl solution.

Electrode	Additive concn. (M)	$-E_{\text{corr.}}$ mV (SCE)	$i_{\text{corr.}}$ $\mu\text{A}/\text{cm}^2$	% I (inh. effec.)	Surf. Coverage ( $\theta$ )	$\Delta\eta_c$ (mV) at 360 $\mu\text{A}/\text{cm}^2$	$\Delta\eta_a$ (mV) at 162 $\mu\text{A}/\text{cm}^2$	Tafel slopes.		Transfer coeff. ( $\alpha$ )
								$b_a$ (mV)	$b_c$ (mV)	
Aluminium	0	922	68	—	—	—	—	77	147	0.401
	$1 \times 10^{-5}$	913	23	66.2	0.662	-138	+ 24	79	161	0.366
	$1 \times 10^{-4}$	906	12	82.4	0.824	-205	+ 29	79	166	0.355
	$5 \times 10^{-4}$	900	5	92.6	0.926	-304	+ 34	79	164	0.360
	$1 \times 10^{-3}$	893	2	97.1	0.971	-378	+ 38	76	166	0.355
Alloy I	0	774	122	—	—	—	—	47	131	0.450
	$1 \times 10^{-5}$	771	75	38.5	0.385	-23	+ 2	50	129	0.457
	$1 \times 10^{-4}$	770	42	65.6	0.656	-54	+ 4	50	133	0.444
	$5 \times 10^{-4}$	768	40	67.2	0.672	-66	+ 7	49	134	0.440
	$1 \times 10^{-3}$	766	35	71.3	0.713	-73	+ 10	50	136	0.434
Alloy II	0	767	200	—	—	—	—	32	131	0.450
	$1 \times 10^{-5}$	760	122	39.0	0.390	-31	+ 3	31	133	0.444
	$1 \times 10^{-4}$	755	94	53.0	0.530	-44	+ 4	26	134	0.440
	$5 \times 10^{-4}$	750	82	59.0	0.590	-54	+ 5	26	134	0.440
	$1 \times 10^{-3}$	745	67	66.5	0.665	-65	+ 6	26	134	0.440

Table (13): Effect of 3-amino-4-cyano-2-benzoyl-N-phenyl pyrrole on the electrochemical and corrosion behaviour of aluminium and its alloys in 0.5 M HCl solution.

Electrode	Additive concn. (M)	-E <sub>corr.</sub> mV (SCE)	i <sub>corr.</sub> $\mu\text{A}/\text{cm}^2$	% I (inh. effec.)	Surf. Coverage ( $\theta$ )	$\Delta\eta_c$ (mV) at 360 $\mu\text{A}/\text{cm}^2$	$\Delta\eta_a$ (mV) at 162 $\mu\text{A}/\text{cm}^2$	Tafel slopes.		Transfer coeff. ( $\alpha$ )
								b <sub>a</sub> (mV)	b <sub>c</sub> (mV)	
Aluminium	0	922	68	—	—	—	—	76	147	0.401
	$1 \times 10^{-6}$	920	56	17.6	0.176	-19	+12	84	162	0.364
	$1 \times 10^{-5}$	914	23	66.2	0.662	-96	+17	77	162	0.364
	$5 \times 10^{-5}$	906	19	72.1	0.721	-111	+30	86	163	0.362
	$1 \times 10^{-4}$	900	16	76.5	0.765	-128	+35	87	163	0.362
Alloy I	0	774	122	—	—	—	—	47	131	0.450
	$1 \times 10^{-6}$	766	145	-18.9	—	+10	+5	55	133	0.444
	$1 \times 10^{-5}$	762	156	-27.9	—	+16	+8	58	131	0.450
	$5 \times 10^{-5}$	761	183	-50.0	—	+25	+12	59	133	0.444
	$1 \times 10^{-4}$	761	259	-112.3	—	+47	+15	59	131	0.450
Alloy II	0	767	200	—	—	—	—	31	131	0.450
	$1 \times 10^{-6}$	764	112	44.0	0.440	-36	+4	30	134	0.440
	$1 \times 10^{-5}$	762	76	62.0	0.620	-60	+6	31	134	0.440
	$5 \times 10^{-5}$	760	60	70.0	0.700	-72	+7	30	133	0.444
	$1 \times 10^{-4}$	758	49	75.5	0.755	-81	+8	31	131	0.450

Table (14): Effect of adenine on the electrochemical and corrosion behaviour of aluminium and its alloys in 0.5 M HClO<sub>4</sub> solution.

Electrode	Additive concn. (M)	-E <sub>corr.</sub> mV (SCE)	i <sub>corr.</sub> $\mu\text{A}/\text{cm}^2$	% I (inh. effec.)	Surf. Coverage ( $\theta$ )	$\Delta\eta_c$ (mV) at 360 $\mu\text{A}/\text{cm}^2$	$\Delta\eta_a$ (mV) at 162 $\mu\text{A}/\text{cm}^2$	Tafel slopes.		Transfer coeff. ( $\alpha$ )
								b <sub>a</sub> (mV)	b <sub>c</sub> (mV)	
Aluminium	0	925	34	—	—	—	—	164	175	0.337
	$1 \times 10^{-5}$	914	11	67.6	0.676	-119	+23	138	175	0.337
	$1 \times 10^{-4}$	912	5	85.3	0.853	-271	+26	136	175	0.337
	$5 \times 10^{-4}$	902	2	94.1	0.941	-381	+29	139	178	0.331
	$1 \times 10^{-3}$	900	2	94.1	0.941	-443	+32	140	179	0.330
Alloy I	0	725	78	—	—	—	—	67	158	0.373
	$1 \times 10^{-5}$	726	94	-20.5	—	+17	+8	89	154	0.383
	$1 \times 10^{-4}$	719	103	-32.1	—	+20	+24	68	154	0.383
	$5 \times 10^{-4}$	717	114	-46.2	—	+28	+27	67	154	0.383
	$1 \times 10^{-3}$	716	122	-56.4	—	+32	+31	67	155	0.381
Alloy II	0	712	135	—	—	—	—	32	160	0.369
	$1 \times 10^{-5}$	678	111	17.8	0.178	-11	+7	33	159	0.371
	$1 \times 10^{-4}$	660	77	43.0	0.430	-18	+7	36	159	0.371
	$5 \times 10^{-4}$	653	61	54.8	0.548	-21	+6	34	159	0.371
	$1 \times 10^{-3}$	641	55	59.3	0.593	-28	+7	34	159	0.371

Table (15): Effect of adenosine on the electrochemical and corrosion behaviour of aluminium and its alloys in 0.5M HClO<sub>4</sub> solution.

Electrode	Additive concn. (M)	-E <sub>corr.</sub> mV (SCE)	i <sub>corr.</sub> $\mu\text{A}/\text{cm}^2$	% I (inh. effec.)	Surf. Coverage ( $\theta$ )	$\Delta\eta_c$ (mV) at 360 $\mu\text{A}/\text{cm}^2$	$\Delta\eta_a$ (mV) at 162 $\mu\text{A}/\text{cm}^2$	Tafel slopes.		Transfer coeff. ( $\alpha$ )
								b <sub>a</sub> (mV)	b <sub>c</sub> (mV)	
Aluminium	0	925	34	—	—	—	—	132	175	0.337
	$1 \times 10^{-5}$	891	16	52.9	0.529	-172	+ 9	142	180	0.328
	$1 \times 10^{-4}$	815	4	88.2	0.882	-419	+ 9	152	179	0.330
	$5 \times 10^{-4}$	749	2	94.1	0.941	-584	+ 8	160	183	0.322
	$1 \times 10^{-3}$	681	1	97.1	0.971	-712	+ 42	162	179	0.330
Alloy I	0	725	78	—	—	—	—	68	158	0.373
	$1 \times 10^{-5}$	722	99	-26.9	—	+ 18	+ 7	63	156	0.378
	$1 \times 10^{-4}$	717	106	-35.9	—	+ 23	+ 17	63	156	0.378
	$5 \times 10^{-4}$	719	137	-75.6	—	+ 40	+ 29	63	156	0.378
	$1 \times 10^{-3}$	715	141	-80.8	—	+ 41	+ 34	61	156	0.378
Alloy II	0	712	135	—	—	—	—	28	160	0.369
	$1 \times 10^{-5}$	685	87	35.6	0.356	-13	+ 3	37	160	0.369
	$1 \times 10^{-4}$	675	78	42.2	0.422	-19	+ 3	41	160	0.369
	$5 \times 10^{-4}$	665	70	48.1	0.481	-24	+ 6	41	160	0.369
	$1 \times 10^{-3}$	662	84	37.8	0.378	-16	+ 9	39	160	0.369



Table (16): Effect of 3-amino-4-cyano-2-benzoyl-N-phenyl pyrrole on the electrochemical and corrosion behaviour of aluminium and its alloys in 0.5 M  $\text{HClO}_4$  solution.

Electrode	Additive concn. (M)	-E <sub>corr.</sub> mV (SCE)	i <sub>corr.</sub> $\mu\text{A}/\text{cm}^2$	% I (inh. effec.)	Surf. Coverage ( $\theta$ )	$\Delta\eta_c$ (mV) at 360 $\mu\text{A}/\text{cm}^2$	$\Delta\eta_a$ (mV) at 162 $\mu\text{A}/\text{cm}^2$	Tafel slopes.		Transfer coeff. ( $\alpha$ )
								$b_a$ (mV)	$b_c$ (mV)	
Aluminium	0	925	34	—	—	—	—	133	175	0.337
	$1 \times 10^{-6}$	915	10	70.6	0.706	-118	+ 4	135	176	0.335
	$1 \times 10^{-5}$	905	6	82.4	0.824	-158	+ 7	144	176	0.335
	$5 \times 10^{-5}$	900	5	85.3	0.853	-173	+ 11	144	175	0.337
	$1 \times 10^{-4}$	891	4	88.2	0.882	-190	+ 14	148	179	0.330
Alloy I	0	725	78	—	—	—	—	67	158	0.373
	$1 \times 10^{-6}$	710	74	5.1	0.051	-7	0	66	151	0.391
	$1 \times 10^{-5}$	701	69	11.5	0.115	-5	+ 7	67	151	0.391
	$5 \times 10^{-5}$	688	65	16.7	0.167	-3	+ 14	66	151	0.391
	$1 \times 10^{-4}$	686	82	-5.1	—	+ 5	+ 22	67	156	0.378
Alloy II	0	712	135	—	—	—	—	30	160	0.369
	$1 \times 10^{-6}$	667	71	47.4	0.474	-31	+ 5	37	166	0.355
	$1 \times 10^{-5}$	641	52	61.5	0.615	-43	+ 9	42	166	0.355
	$5 \times 10^{-5}$	636	55	59.3	0.593	-40	+ 11	42	165	0.358
	$1 \times 10^{-4}$	635	54	60.0	0.600	-40	+ 11	41	165	0.358

Table (17): Effect of adenine on the electrochemical and corrosion behaviour of aluminium and its alloys in 0.5 M H<sub>2</sub>SO<sub>4</sub> solution.

Electrode	Additive concn. (M)	-E <sub>corr.</sub> mV (SCE)	i <sub>corr.</sub> $\mu\text{A}/\text{cm}^2$	% I (inh. effec.)	Surf. Coverage ( $\theta$ )	$\Delta\eta_c$ (mV) at 360 $\mu\text{A}/\text{cm}^2$	$\Delta\eta_a$ (mV) at 162 $\mu\text{A}/\text{cm}^2$	Tafel slopes.		Transfer coeff. ( $\alpha$ )
								b <sub>a</sub> (mV)	b <sub>c</sub> (mV)	
Aluminium	0	915	51	—	—	—	—	158	162	0.364
	1x10 <sup>-5</sup>	913	25	51.0	0.510	-42	+ 2	150	160	0.369
	1x10 <sup>-4</sup>	910	19	62.7	0.627	-59	+ 5	150	160	0.369
	5x10 <sup>-4</sup>	907	15	70.6	0.706	-77	+ 5	150	160	0.369
	1x10 <sup>-3</sup>	903	10	80.4	0.804	-91	+ 10	150	165	0.358
Alloy I	0	760	126	—	—	—	—	59	133	0.444
	1x10 <sup>-5</sup>	755	115	8.7	0.087	-13	+ 4	67	139	0.424
	1x10 <sup>-4</sup>	754	87	31.0	0.310	-24	+ 10	70	140	0.421
	5x10 <sup>-4</sup>	747	63	50.0	0.500	-41	+ 11	70	139	0.424
	1x10 <sup>-3</sup>	743	56	55.6	0.556	-50	+ 12	70	138	0.428
Alloy II	0	745	130	—	—	—	—	47	145	0.407
	1x10 <sup>-5</sup>	733	67	48.5	0.485	-32	+ 3	46	141	0.418
	1x10 <sup>-4</sup>	724	60	53.8	0.538	-46	+ 7	49	140	0.421
	5x10 <sup>-4</sup>	715	49	62.3	0.623	-61	+ 8	51	142	0.415
	1x10 <sup>-3</sup>	708	42	67.7	0.677	-74	+ 9	52	140	0.421

Table (18): Effect of adenosine on the electrochemical and corrosion behaviour of aluminium and its alloys in 0.5 M H<sub>2</sub>SO<sub>4</sub> solution.

Electrode	Additive concn. (M)	-E <sub>corr.</sub> mV (SCE)	i <sub>corr.</sub> $\mu\text{A}/\text{cm}^2$	% I (inh. effec.)	Surf. Coverage ( $\theta$ )	$\Delta\eta_c$ (mV) at 360 $\mu\text{A}/\text{cm}^2$	$\Delta\eta_a$ (mV) at 162 $\mu\text{A}/\text{cm}^2$	Tafel slopes.		Transfer coeff. ( $\alpha$ )
								b <sub>a</sub> (mV)	b <sub>c</sub> (mV)	
Aluminium	0	915	51	—	—	—	—	150	162	0.364
	1x10 <sup>-5</sup>	913	28	45.1	0.451	-54	+ 15	154	146	0.404
	1x10 <sup>-4</sup>	910	20	60.8	0.608	-73	+ 25	153	148	0.399
	5x10 <sup>-4</sup>	908	13	74.5	0.745	-95	+ 35	158	148	0.399
	1x10 <sup>-3</sup>	906	8	84.3	0.843	-111	+ 44	158	146	0.404
Alloy I	0	760	126	—	—	—	—	61	133	0.444
	1x10 <sup>-5</sup>	753	70	44.4	0.444	-30	+ 4	63	137	0.431
	1x10 <sup>-4</sup>	750	47	62.7	0.627	-63	+ 8	70	136	0.434
	5x10 <sup>-4</sup>	748	30	76.2	0.762	-75	+ 12	70	136	0.434
	1x10 <sup>-3</sup>	745	24	81.0	0.810	-88	+ 14	74	136	0.434
Alloy II	0	745	130	—	—	—	—	49	145	0.407
	1x10 <sup>-5</sup>	740	103	20.8	0.208	-23	+ 8	54	153	0.386
	1x10 <sup>-4</sup>	734	85	34.6	0.346	-41	+ 9	54	154	0.383
	5x10 <sup>-4</sup>	724	70	46.2	0.462	-55	+ 6	60	154	0.383
	1x10 <sup>-3</sup>	715	54	58.5	0.585	-65	+ 8	65	152	0.388

Table (19): Effect of 3-amino-4-cyano-2-benzoyl-N-phenyl pyrrole on the electrochemical and corrosion behaviour of aluminium and its alloys in 0.5 M H<sub>2</sub>SO<sub>4</sub> solution.

Electrode	Additive concn. (M)	-E <sub>corr.</sub> mV (SCE)	i <sub>corr.</sub> $\mu\text{A}/\text{cm}^2$	% I (inh. effec.)	Surf. Coverage ( $\theta$ )	$\Delta\eta_c$ (mV) at 360 $\mu\text{A}/\text{cm}^2$	$\Delta\eta_a$ (mV) at 162 $\mu\text{A}/\text{cm}^2$	Tafel slopes.		Transfer coeff. ( $\alpha$ )
								b <sub>a</sub> (mV)	b <sub>c</sub> (mV)	
Aluminium	0	915	51	—	—	—	—	153	162	0.364
	1x10 <sup>-6</sup>	908	35	31.4	0.314	-17	+ 9	153	157	0.376
	1x10 <sup>-5</sup>	903	22	56.9	0.569	-42	+ 18	150	156	0.378
	5x10 <sup>-5</sup>	891	16	68.6	0.686	-67	+ 22	149	157	0.376
	1x10 <sup>-4</sup>	887	15	70.6	0.706	-79	+ 41	148	158	0.373
Alloy I	0	766	126	—	—	—	—	61	133	0.444
	1x10 <sup>-6</sup>	753	156	-23.8	—	+ 5	+ 11	74	132	0.447
	1x10 <sup>-5</sup>	752	154	-22.2	—	+ 9	+ 14	76	132	0.447
	5x10 <sup>-5</sup>	734	241	-91.3	—	+ 36	+ 15	77	130	0.454
	1x10 <sup>-4</sup>	733	251	-99.2	—	+ 40	+ 21	79	130	0.454
Alloy II	0	745	130	—	—	—	—	50	145	0.407
	1x10 <sup>-6</sup>	725	88	32.3	0.323	-38	0	48	150	0.393
	1x10 <sup>-5</sup>	710	38	70.8	0.708	-73	+ 3	48	148	0.399
	5x10 <sup>-5</sup>	697	43	66.9	0.669	-93	+ 3	46	151	0.391
	1x10 <sup>-4</sup>	690	49	62.3	0.623	-108	+ 8	52	151	0.391

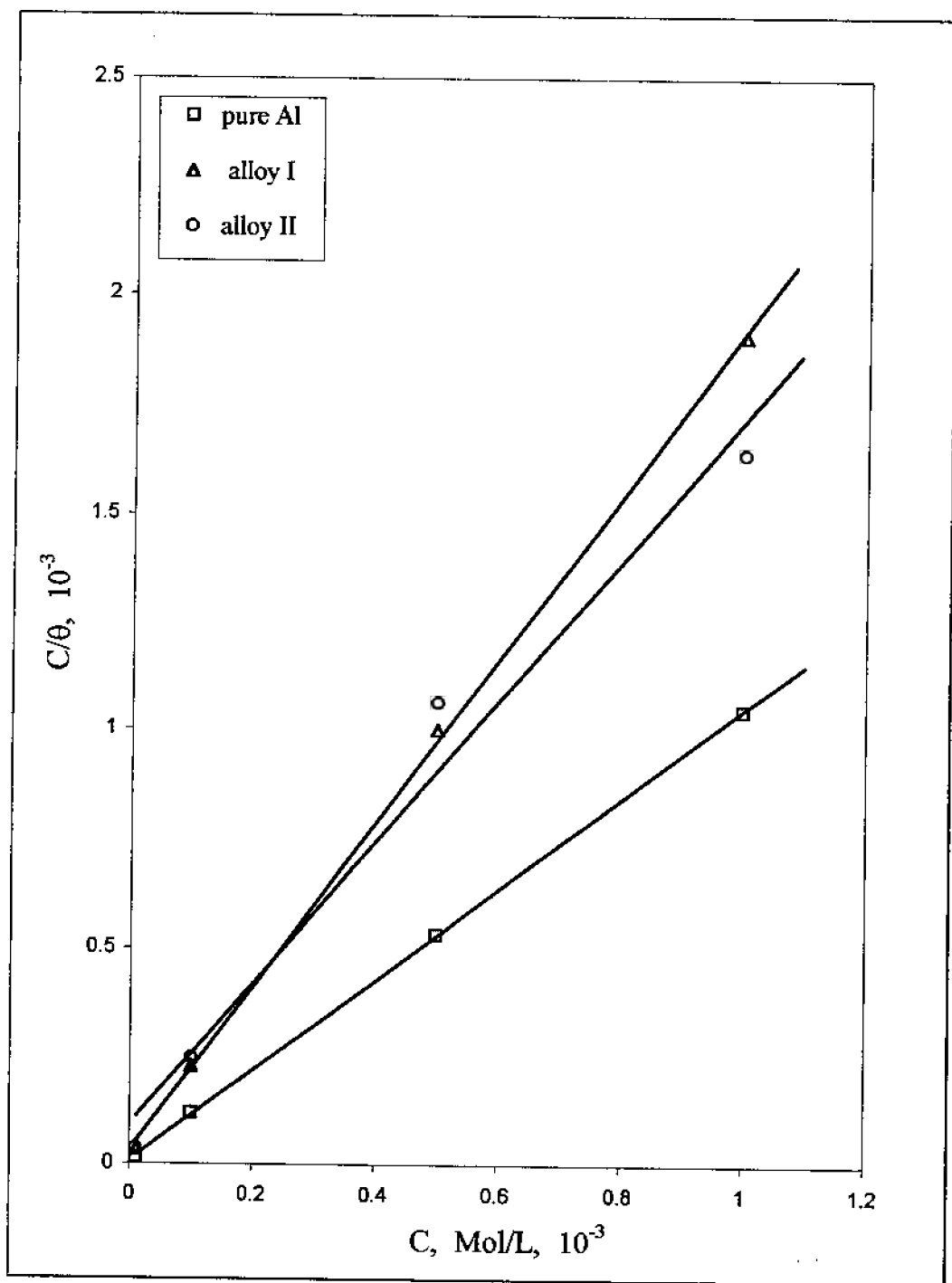


Figure (20): adsorption isotherm for adenine on pure Al and its alloys in 0.5 M HCl solution.

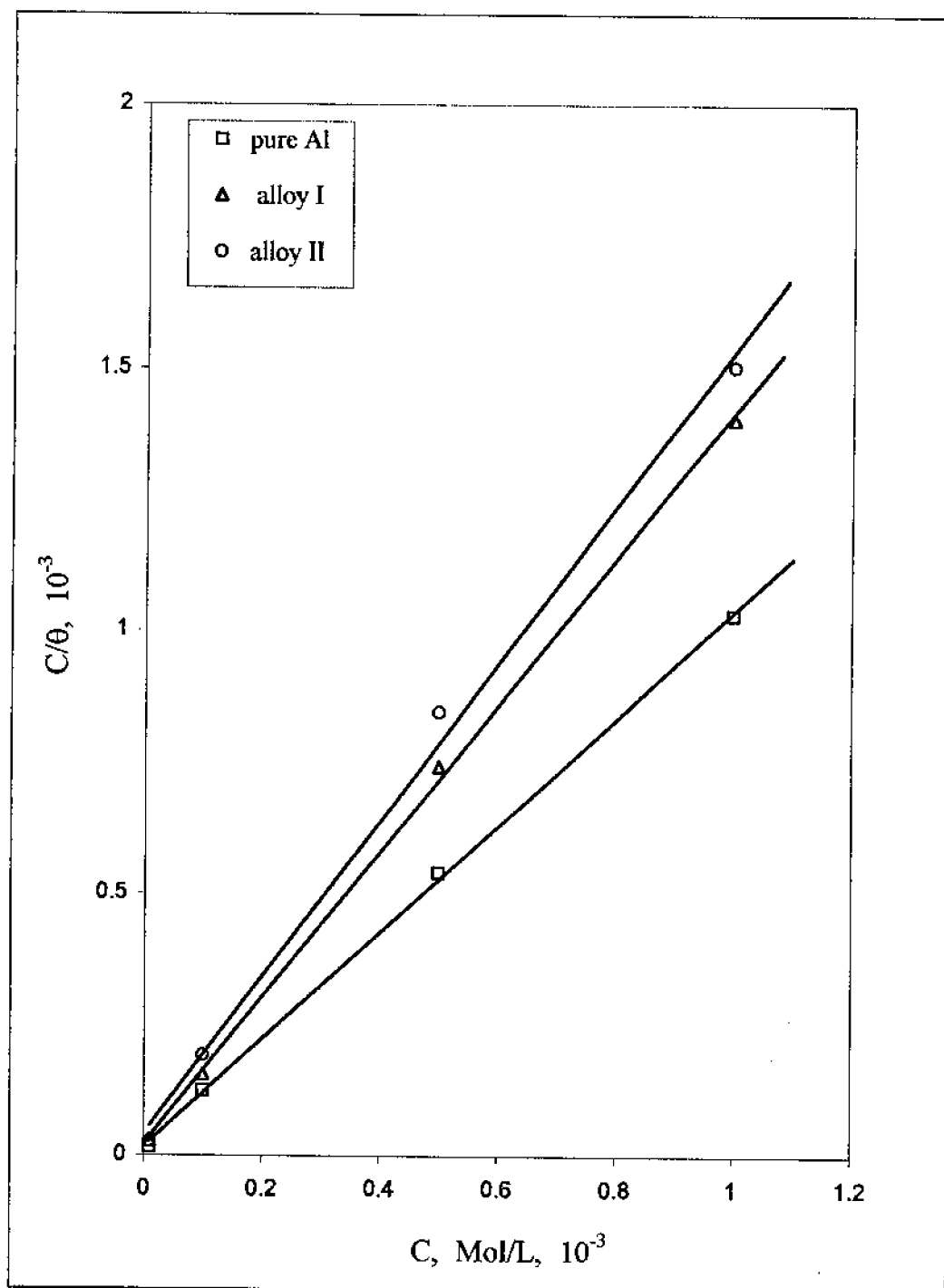


Figure (21): adsorption isotherm for adenosine on pure Al and its alloys in 0.5 M HCl solution.

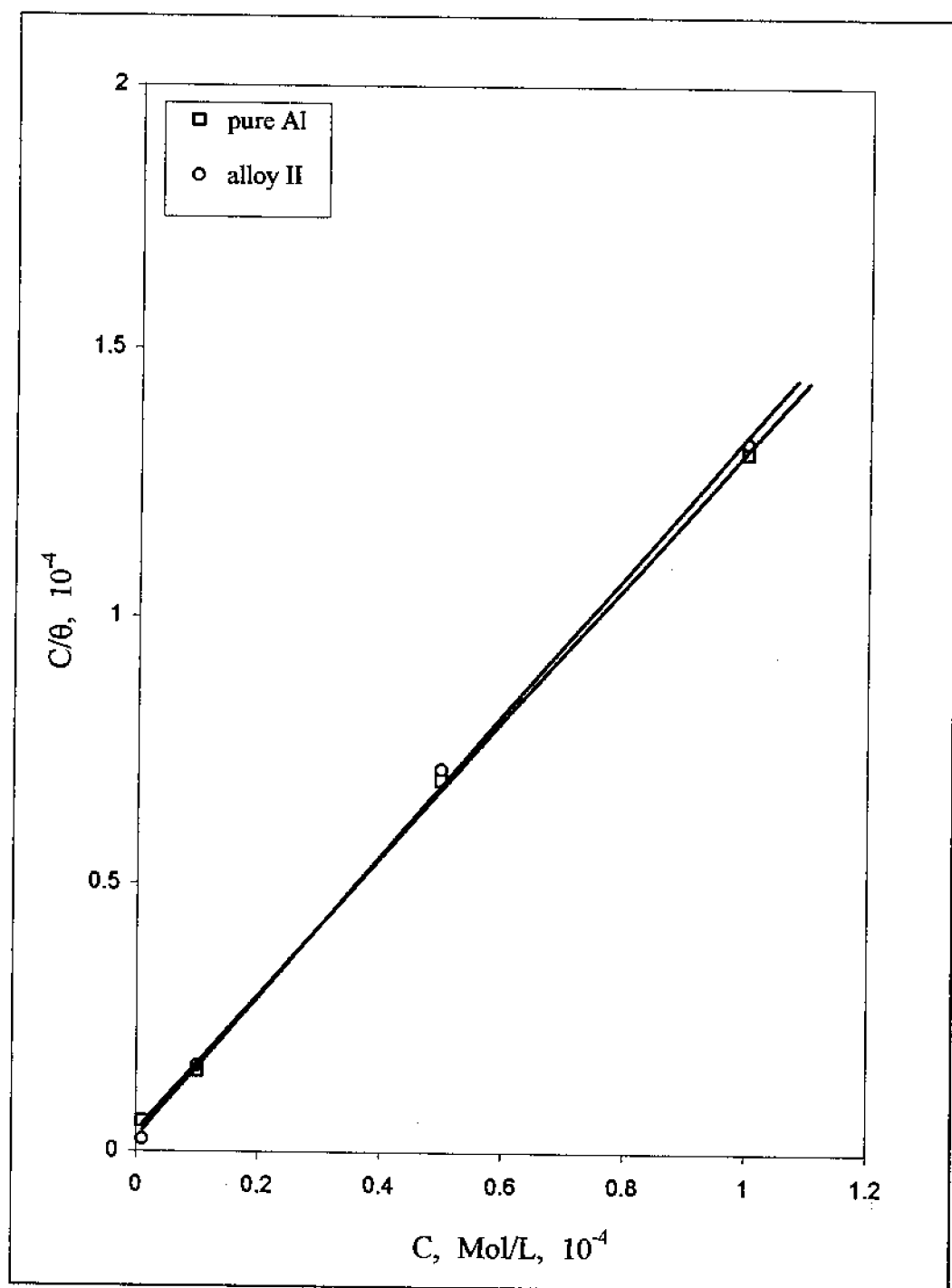


Figure (22): adsorption isotherm for 3-amino-4-cyano-2-benzoyl-N-phenyl pyrrole on pure Al and its alloys in 0.5 M HCl solution.

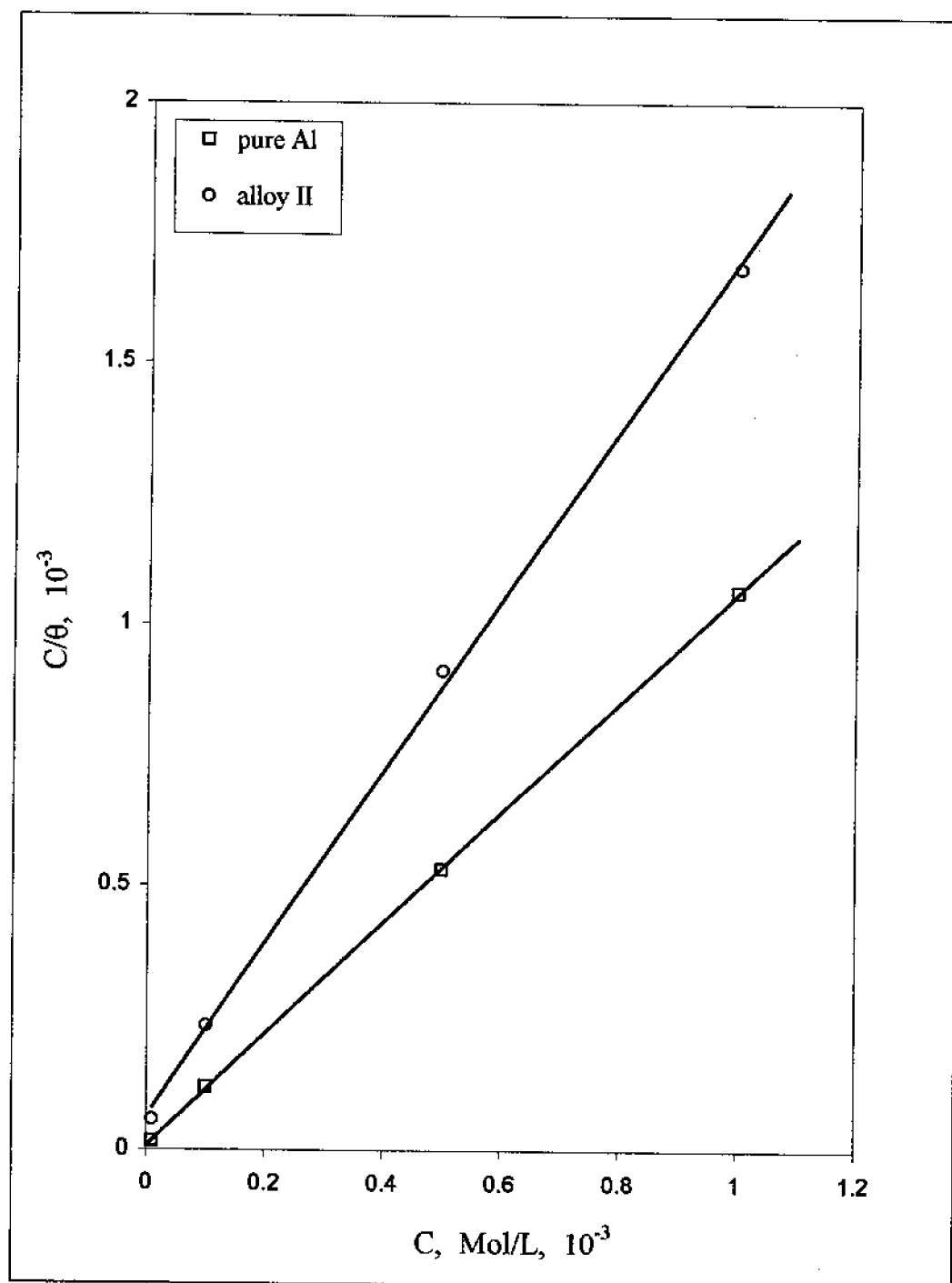


Figure (23): adsorption isotherm for adenine on pure Al and its alloys in 0.5 M  $\text{HClO}_4$  solution.



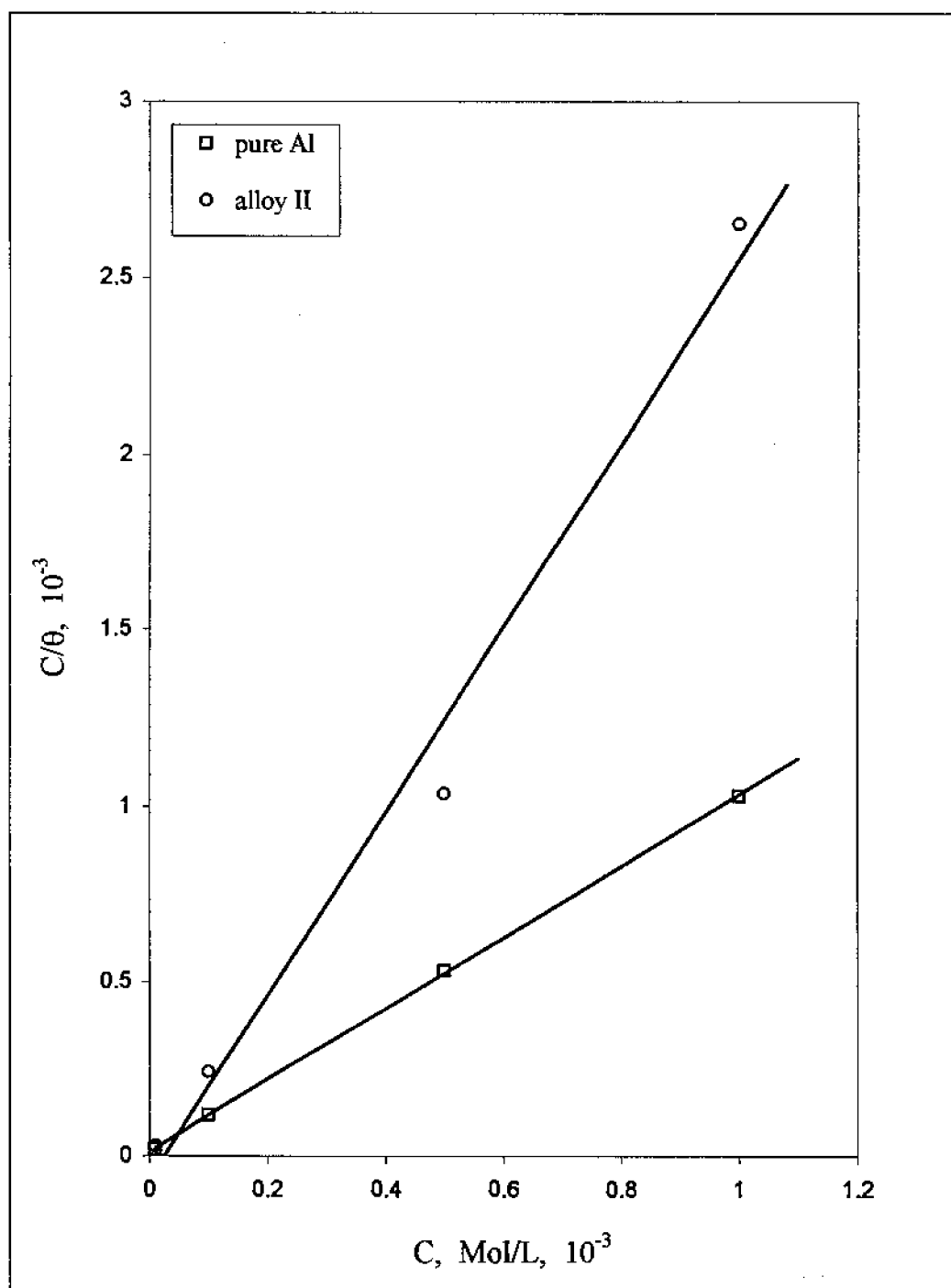


Figure (24): adsorption isotherm for adenosine on pure Al and its alloys in 0.5 M HClO<sub>4</sub> solution.

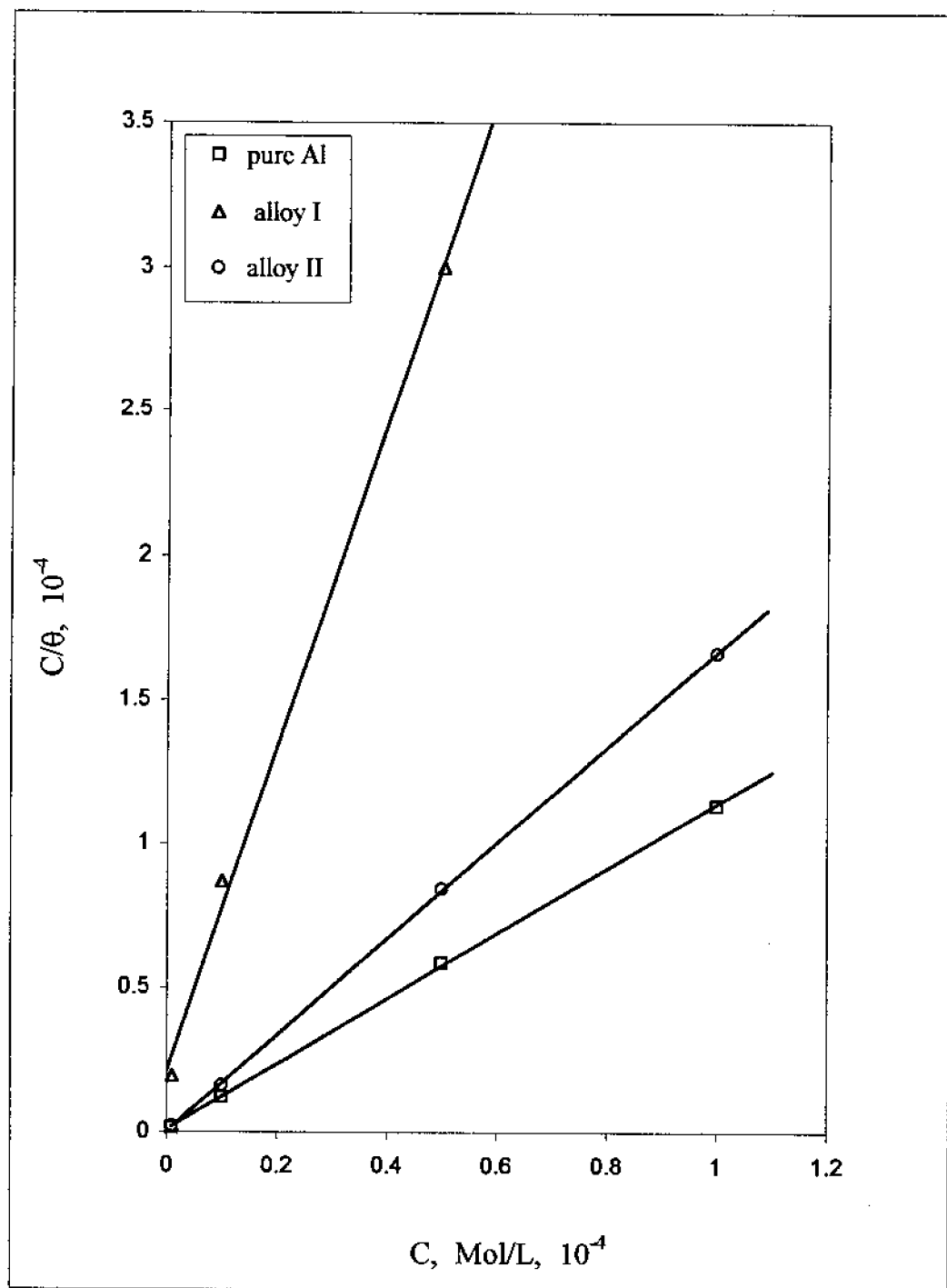


Figure (25): adsorption isotherm for 3-amino-4-cyano-2-benzoyl-N-phenyl pyrrole on pure Al and its alloys in 0.5 M HClO<sub>4</sub> solution.

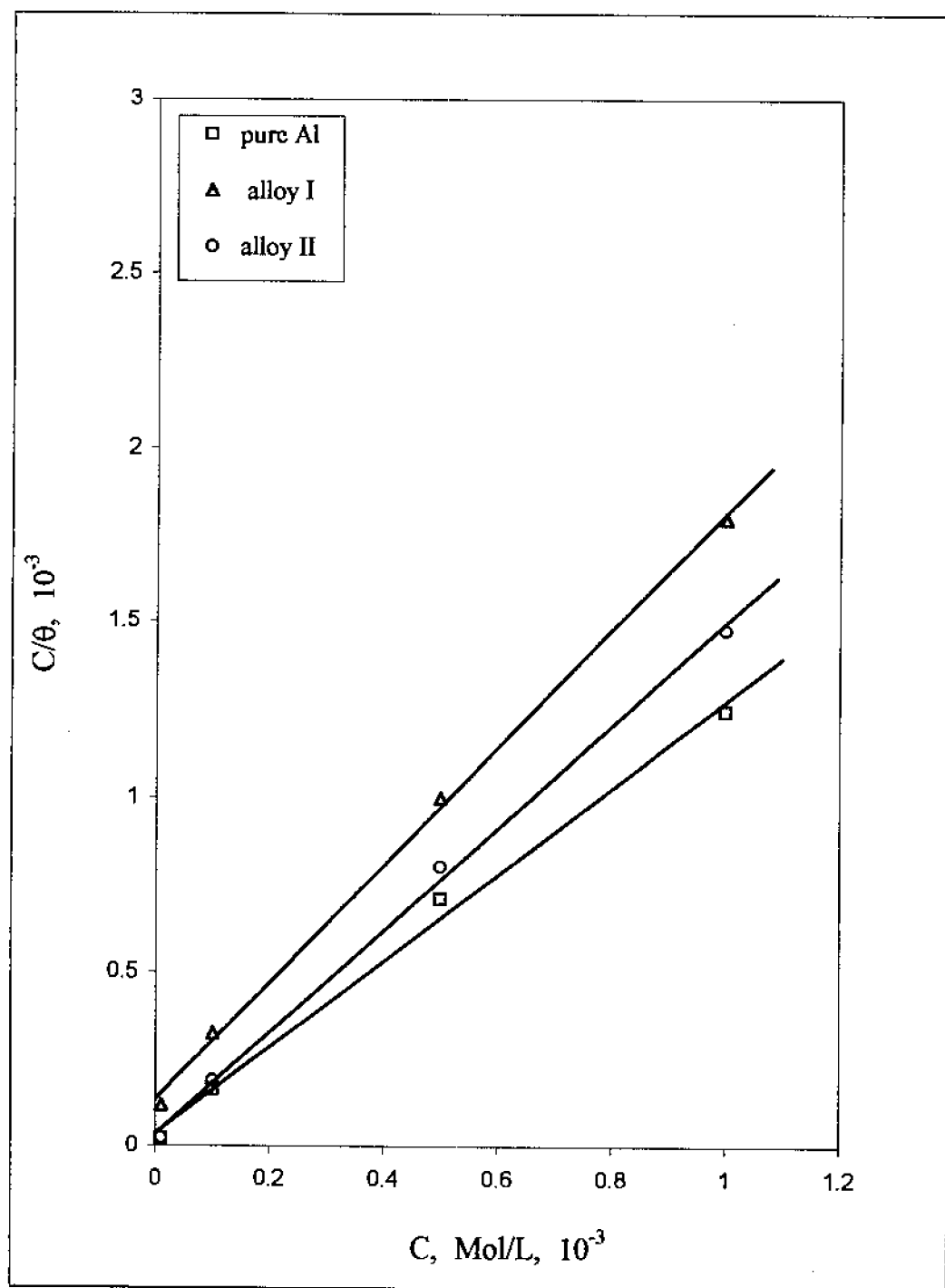


Figure (26): adsorption isotherm for adenine on pure Al and its alloys in 0.5 M  $\text{H}_2\text{SO}_4$  solution.

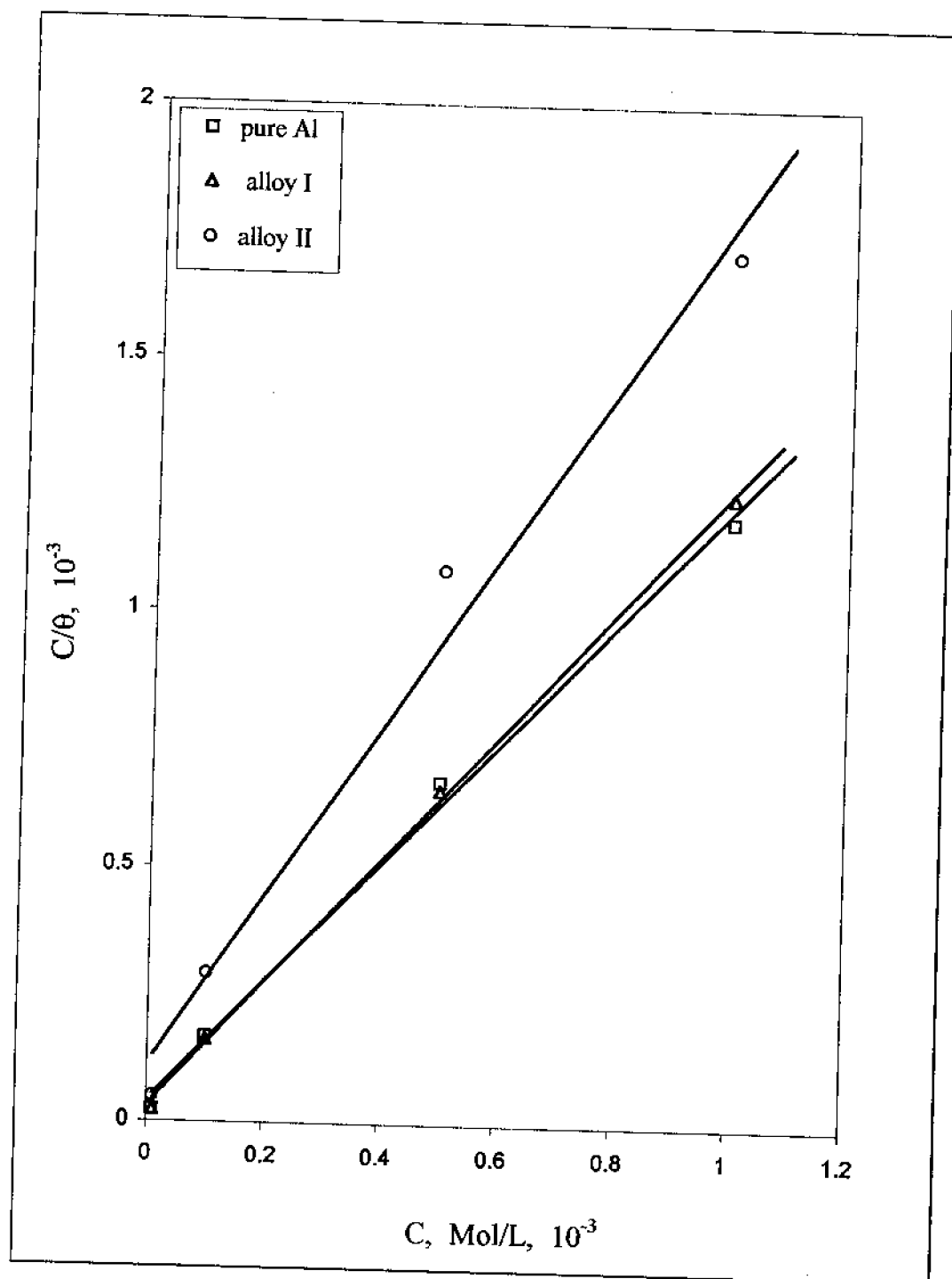


Figure (27): adsorption isotherm for adenosine on pure Al and its alloys in 0.5 M  $\text{H}_2\text{SO}_4$  solution.

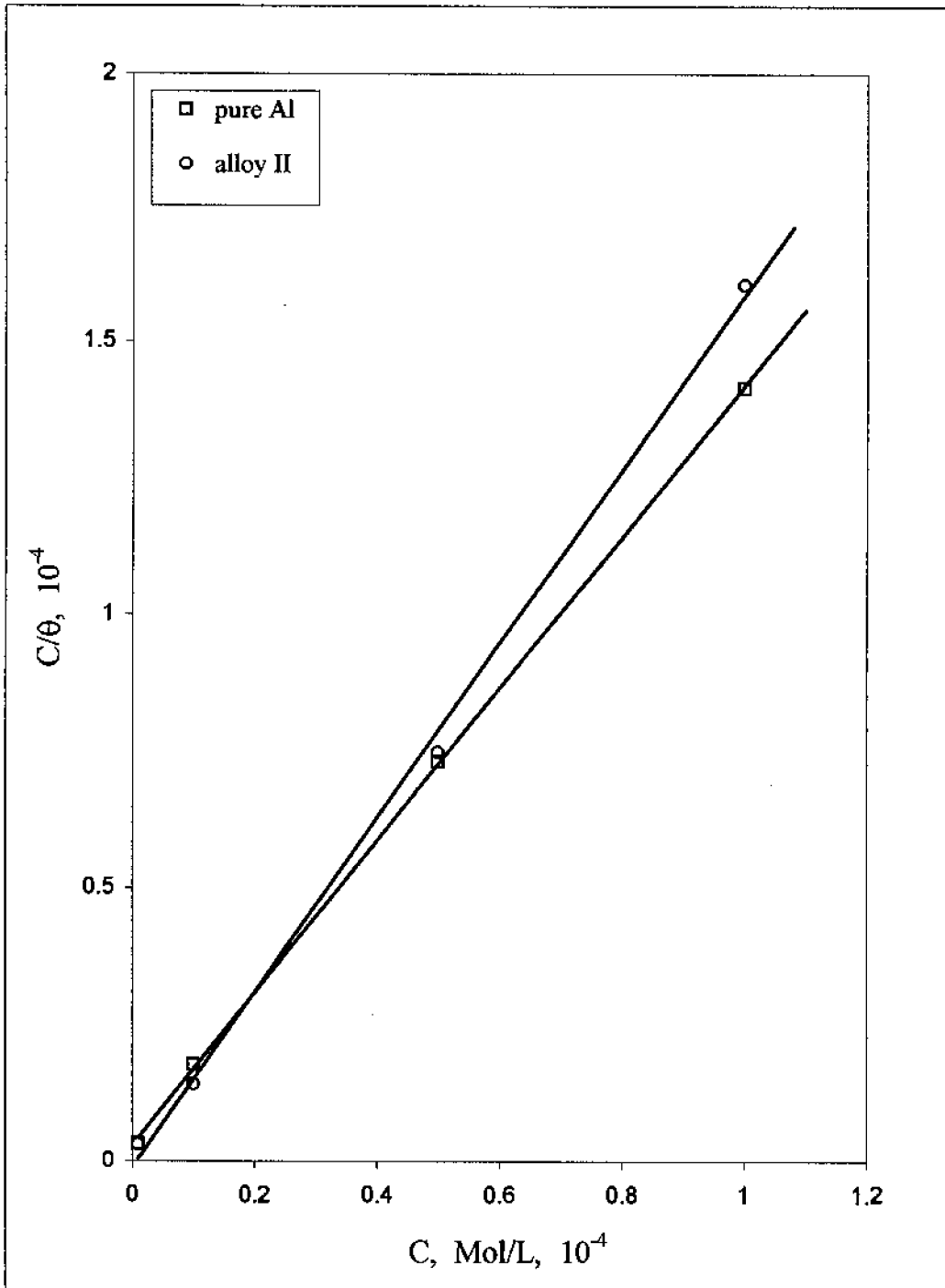


Figure (28): adsorption isotherm for 3-amino-4-cyano-2-benzoyl-N-phenyl pyrrole on pure Al and its alloys in 0.5 M H<sub>2</sub>SO<sub>4</sub> solution.

## 2. *Effect of some triazole derivatives on the electrochemical and corrosion behaviour of both pure aluminium and its alloys in 0.5 M solutions of HCl, HClO<sub>4</sub> and H<sub>2</sub>SO<sub>4</sub>.*

### 2.1. Tafel lines for cathodic hydrogen evolution reaction:

Tables 20-28 show the values of  $\eta_c$  for (h.e.r.) at both pure aluminium and its alloys in 0.5 M solutions of HCl, HClO<sub>4</sub> and H<sub>2</sub>SO<sub>4</sub> and those containing 3-mercapto-4-phenyl-5-4-pyridyl-1,2,4-triazole, 3-mercapto-4-phenyl-5-p-tolyl-1,2,4-triazole and 3-mercapto-4-phenyl-5-p-nitrophenyl-1,2,4-triazole within the concentration range  $10^{-6}$ - $10^{-4}$  M. These values are obtained at current densities ranging from 36-360  $\mu\text{A}/\text{cm}^2$  for pure aluminium and from 180-1260  $\mu\text{A}/\text{cm}^2$  in case of Al-alloys.

From these results it is seen that 3-mercapto-4-phenyl-5-4-pyridyl-1,2,4-triazole increases the value of  $\eta_c$  of pure Al and its alloys in HCl solution up to  $5 \times 10^{-5}$  M. However at higher concentration ( $10^{-4}$  M) it decreases (shift in the positive direction). It is found that  $\eta_c$  increases with increasing concentration of 3-mercapto-4-phenyl-5-p-tolyl-1,2,4-triazole in HCl solution for pure Al and its investigated alloys. But, the value of  $\eta_c$  decreases relatively only at higher concentrations (at  $5 \times 10^{-5}$  and  $10^{-4}$  M in case of alloy I and at  $10^{-4}$  M in case of alloy II) of 3-mercapto-4-phenyl-5-p-nitrophenyl-1,2,4-triazole in HCl solution of Al-alloys.

3-mercapto-4-phenyl-5-4-pyridyl-1,2,4-triazole increases the value of  $\eta_c$  at pure Al and alloy II, but it has no effect on such value (except  $10^{-6}$  M) in case of alloy I in HClO<sub>4</sub> solution. It is observed that value of  $\eta_c$

increases as an increase in concentration of 3-mercapto-4-phenyl-5-p-tolyl-1,2,4-triazole in  $\text{HClO}_4$  solution of pure Al and alloy II, but it decreases (sharply shifted in the positive direction) in case of alloy I. 3-mercapto-4-phenyl-5-p-nitrophenyl-1,2,4-triazole increases the value of  $\eta_c$  for pure Al and its investigated alloys at all examined concentrations in  $\text{HClO}_4$  solution.

In  $\text{H}_2\text{SO}_4$  solution, all investigated triazole derivatives showed an increase of  $\eta_c$  value of pure Al and its investigated alloys, and  $\eta_c$  value increases with increasing concentration of the inhibitor. The extent of increase is greater at pure Al in the presence of all examined additives than of alloys I and II.

Tafel lines ( $\eta$ -log c.d. relation) for h.e.r. at both pure Al and its alloys in 0.5 M solutions of HCl,  $\text{HClO}_4$  and  $\text{H}_2\text{SO}_4$  in the absence and presence of the investigated triazole derivatives within the concentration range  $10^{-6}$ - $10^{-4}$  M are shown in Figs.29-46.

From these curves, it is observed that  $\eta_c$  is a linear function of log c.d. for the current density range 36-360  $\mu\text{A}/\text{cm}^2$  for pure Al and from 180-1260  $\mu\text{A}/\text{cm}^2$  for its alloys. In most cases Tafel lines wither they are shifted in the positive or negative direction run parallel to each other. In all cases, the increase in  $\eta_c$  is greater for pure Al than for its alloys at the same concentration of triazole derivative.

Table (20): Hydrogen overvoltage (  $\eta_c$  ) values of Al and Al-alloys in 0.5 M HCl solution in the presence of 3-mercapto-4-phenyl-5-4-pyridyl-1,2,4-triazole.

Electrode	Additive concn. (M)	$-\eta_c$ (mV)														
		c.d. $\mu\text{A}/\text{cm}^2$														
Aluminium	0	99	91	83	75	67	55	43	31	2	—					
	$1 \times 10^{-6}$	173	164	155	146	137	125	113	90	66	21					
	$1 \times 10^{-5}$	307	297	288	278	268	256	243	222	195	144					
	$5 \times 10^{-5}$	628	618	608	597	586	574	560	534	504	447					
	$1 \times 10^{-4}$	113	105	97	89	81	70	58	42	18	—					
Alloy I		c.d. $\mu\text{A}/\text{cm}^2$														
	0	1260	1170	1080	990	900	810	720	630	540	450	360	270	180		
	$1 \times 10^{-6}$	134	130	126	121	116	110	103	94	85	76	66	48	25		
	$1 \times 10^{-5}$	145	141	137	132	127	121	114	105	98	87	77	61	40		
	$5 \times 10^{-5}$	153	149	145	140	135	129	122	115	106	95	85	69	48		
Alloy II		165	161	157	152	147	141	134	125	119	109	97	82	60		
	$1 \times 10^{-4}$	158	154	150	145	140	134	127	120	112	102	90	75	54		
	0	106	102	97	92	86	80	73	65	56	46	33	18	—		
	$1 \times 10^{-6}$	126	120	116	111	106	100	94	87	79	70	60	44	24		
	$1 \times 10^{-5}$	139	132	128	123	118	112	106	99	91	82	72	57	37		
	$5 \times 10^{-5}$	156	150	146	141	136	130	126	117	109	100	90	77	54		
	$1 \times 10^{-4}$	121	115	111	106	102	95	89	82	74	65	55	39	19		





Table (22): Hydrogen overvoltage ( $\eta_c$ ) values of Al and Al-alloys in 0.5 M HCl solution in the presence of 3-mercapto-4-phenyl-5-p-nitrophenyl-1,2,4-triazole.

Electrode	Additive concn. (M)	$-\eta_c$ (mV)													
		c.d. $\mu\text{A}/\text{cm}^2$													
Aluminium	0	99	91	83	75	67	55	43	31	2	—				
	$1 \times 10^{-6}$	130	122	114	106	98	87	75	56	32	10				
	$1 \times 10^{-5}$	188	179	170	161	152	140	128	108	80	40				
	$5 \times 10^{-5}$	263	254	245	236	227	215	202	180	154	108				
	$1 \times 10^{-4}$	280	271	262	253	243	230	216	201	170	122				
Alloy I		c.d. $\mu\text{A}/\text{cm}^2$													
	0	1260	1170	1080	990	900	810	720	630	540	450	360	270	180	
	$1 \times 10^{-6}$	134	130	126	121	116	110	103	94	85	76	66	48	25	
	$1 \times 10^{-5}$	152	148	144	139	134	128	121	112	105	94	84	68	46	
	$5 \times 10^{-5}$	159	155	151	146	141	135	128	119	112	101	91	76	54	
Alloy II	$1 \times 10^{-4}$	145	141	137	133	128	122	115	106	99	88	78	63	40	
		140	136	132	128	123	117	110	101	94	83	73	58	37	
	0	106	102	97	92	86	80	73	65	56	46	33	18	—	
	$1 \times 10^{-6}$	132	127	123	119	114	108	102	95	86	78	65	50	30	
	$1 \times 10^{-5}$	140	135	129	125	120	114	107	101	94	84	72	56	35	
	$5 \times 10^{-5}$	148	143	138	134	128	122	116	109	102	93	81	65	43	
	$1 \times 10^{-4}$	128	123	117	112	107	102	95	89	82	70	58	42	20	

Table (23): Hydrogen overvoltage ( $\eta_c$ ) values of Al and Al-alloys in 0.5 M HClO<sub>4</sub> solution in the presence of 3-mercapto-4-phenyl-5-4-pyridyl-1,2,4-triazole.

Electrode	Additive concn. (M)	$-\eta_c$ (mV)											
		c.d. $\mu\text{A}/\text{cm}^2$											
Aluminium	0	167	158	147	137	126	113	100	75	45	20		
	$1 \times 10^{-6}$	219	209	199	187	175	161	147	122	88	40		
	$1 \times 10^{-5}$	278	268	256	245	233	220	207	180	146	84		
	$5 \times 10^{-5}$	305	300	294	283	274	261	244	213	194	150		
	$1 \times 10^{-4}$	362	352	341	330	322	310	293	275	254	206		
		1260	1170	1080	990	900	810	720	630	540	450	360	270
Alloy I	0	191	184	179	173	166	159	152	143	133	119	106	86
	$1 \times 10^{-6}$	184	178	173	169	160	155	146	138	128	115	102	82
	$1 \times 10^{-5}$	179	171	168	162	155	149	142	132	122	108	94	75
	$5 \times 10^{-5}$	182	175	171	165	158	153	145	136	126	112	97	79
	$1 \times 10^{-4}$	182	175	171	165	158	153	145	136	126	112	97	79
		156	150	144	139	132	123	118	107	98	88	74	59
Alloy II	0	187	182	177	171	166	158	150	141	131	121	107	91
	$1 \times 10^{-6}$	236	231	226	220	214	205	197	188	178	167	153	135
	$1 \times 10^{-5}$	260	255	250	245	238	230	222	213	203	193	180	160
	$5 \times 10^{-5}$	305	300	295	288	282	275	267	258	247	236	222	203
	$1 \times 10^{-4}$												







Table (27): Hydrogen overvoltage ( $\eta_c$ ) values of Al and Al-alloys in 0.5 M  $H_2SO_4$  solution in the presence of 3-mercapto-4-phenyl-5-p-tolyl-1,2,4-triazole.

Electrode	Additive concn. (M)	$-\eta_c$ (mV)														
		c.d. $\mu\text{A}/\text{cm}^2$														
Aluminium	0	141	131	121	111	101	90	70	47	18	—					
	$1 \times 10^{-6}$	165	155	145	135	125	114	102	80	54	10					
	$1 \times 10^{-5}$	238	228	218	208	198	188	175	160	134	90					
	$5 \times 10^{-5}$	326	316	306	296	286	274	261	236	208	160					
	$1 \times 10^{-4}$	365	355	345	335	323	310	295	275	250	200					
Alloy I		c.d. $\mu\text{A}/\text{cm}^2$														
	0	140	135	129	121	116	108	102	94	85	74	60	40	16		
	$1 \times 10^{-6}$	165	160	154	146	141	133	127	119	110	99	88	66	42		
	$1 \times 10^{-5}$	187	182	176	168	163	155	149	141	132	121	110	88	60		
	$5 \times 10^{-5}$	204	199	193	185	180	172	166	158	149	138	127	104	80		
Alloy II	$1 \times 10^{-4}$	218	213	207	199	194	186	180	172	163	152	141	120	98		
	0	148	140	135	130	123	117	110	90	88	78	65	50	25		
	$1 \times 10^{-6}$	159	151	146	140	133	127	120	108	99	89	76	54	30		
	$1 \times 10^{-5}$	178	172	167	159	152	146	140	131	120	110	97	80	55		
	$5 \times 10^{-5}$	227	221	216	210	201	195	190	181	169	159	146	127	103		
	$1 \times 10^{-4}$	262	256	251	243	236	230	223	213	204	194	181	164	140		





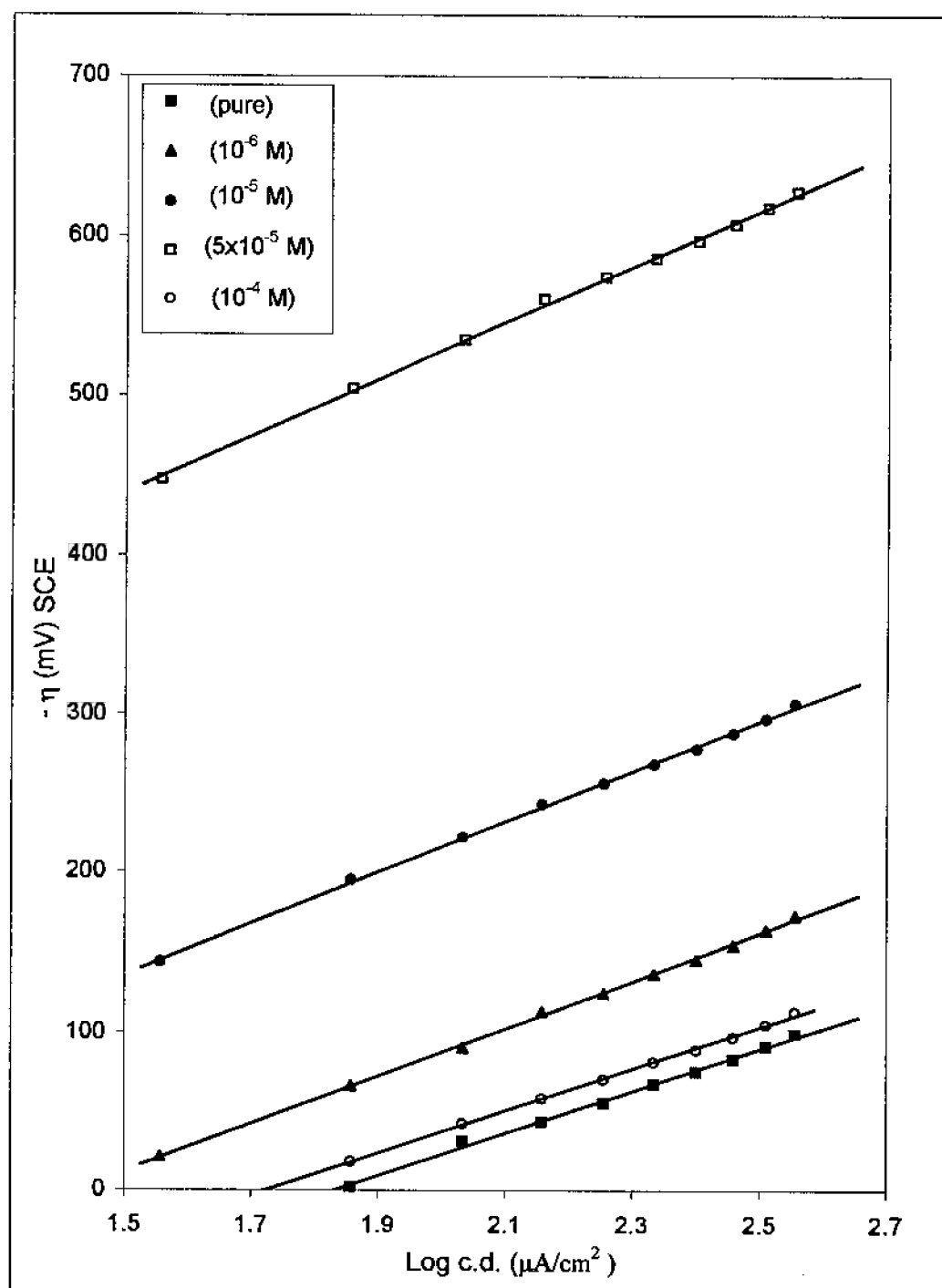


Figure (29): Cathodic Tafel lines for pure aluminium in 0.5 M HCl solution in presence of 3-mercapto-4-phenyl-5-4-pyridyl-1,2,4-triazole.

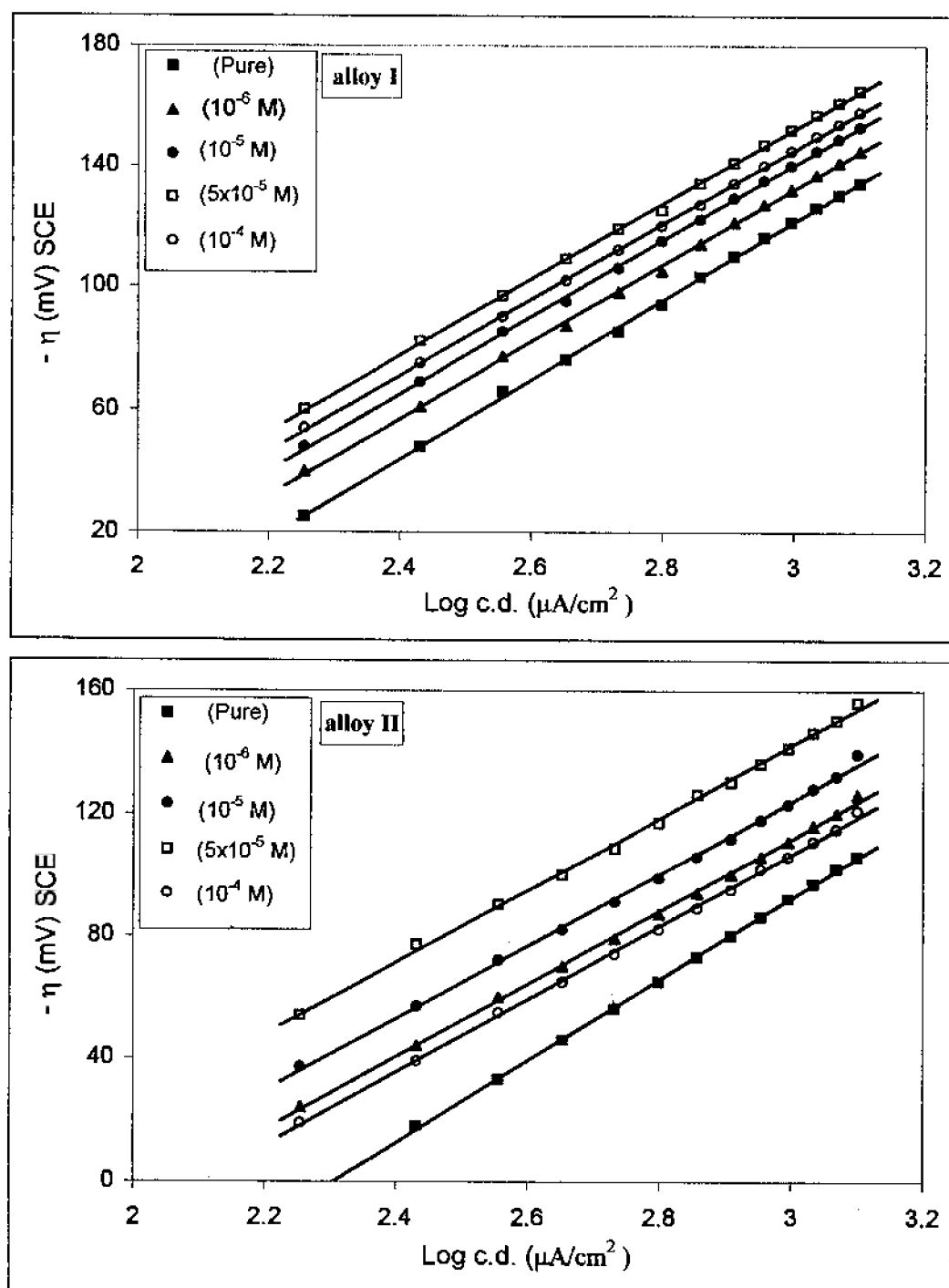


Figure (30): Cathodic Tafel lines for Al-alloys in 0.5M HCl solution in presence of 3-mercapto-4-phenyl-5-4-pyridyl-1,2,4-triazole.

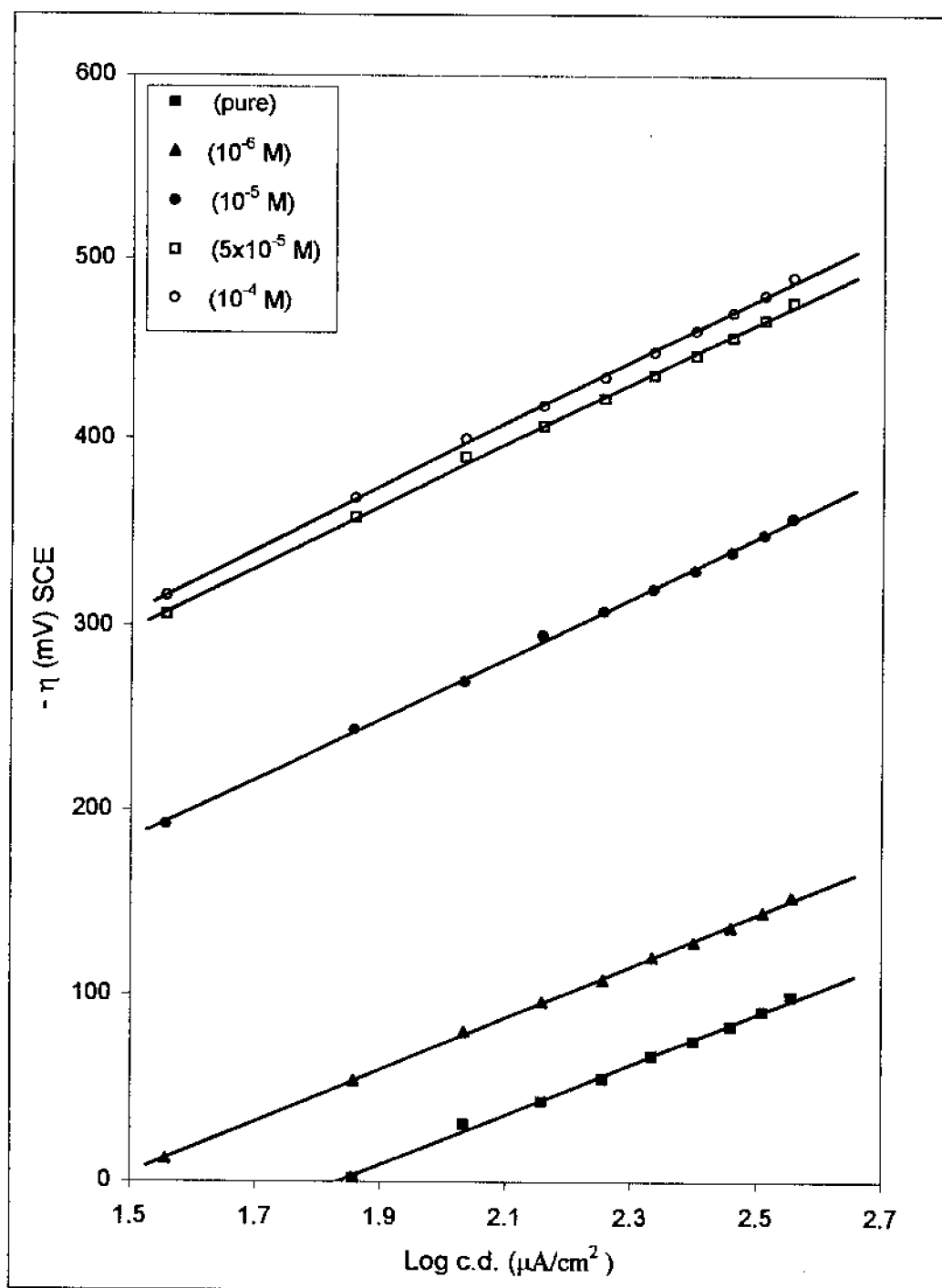


Figure (31): Cathodic Tafel lines for pure aluminium in 0.5 M HCl solution in presence of 3-mercapto-4-phenyl-5-p-tolyl-1,2,4-triazole.

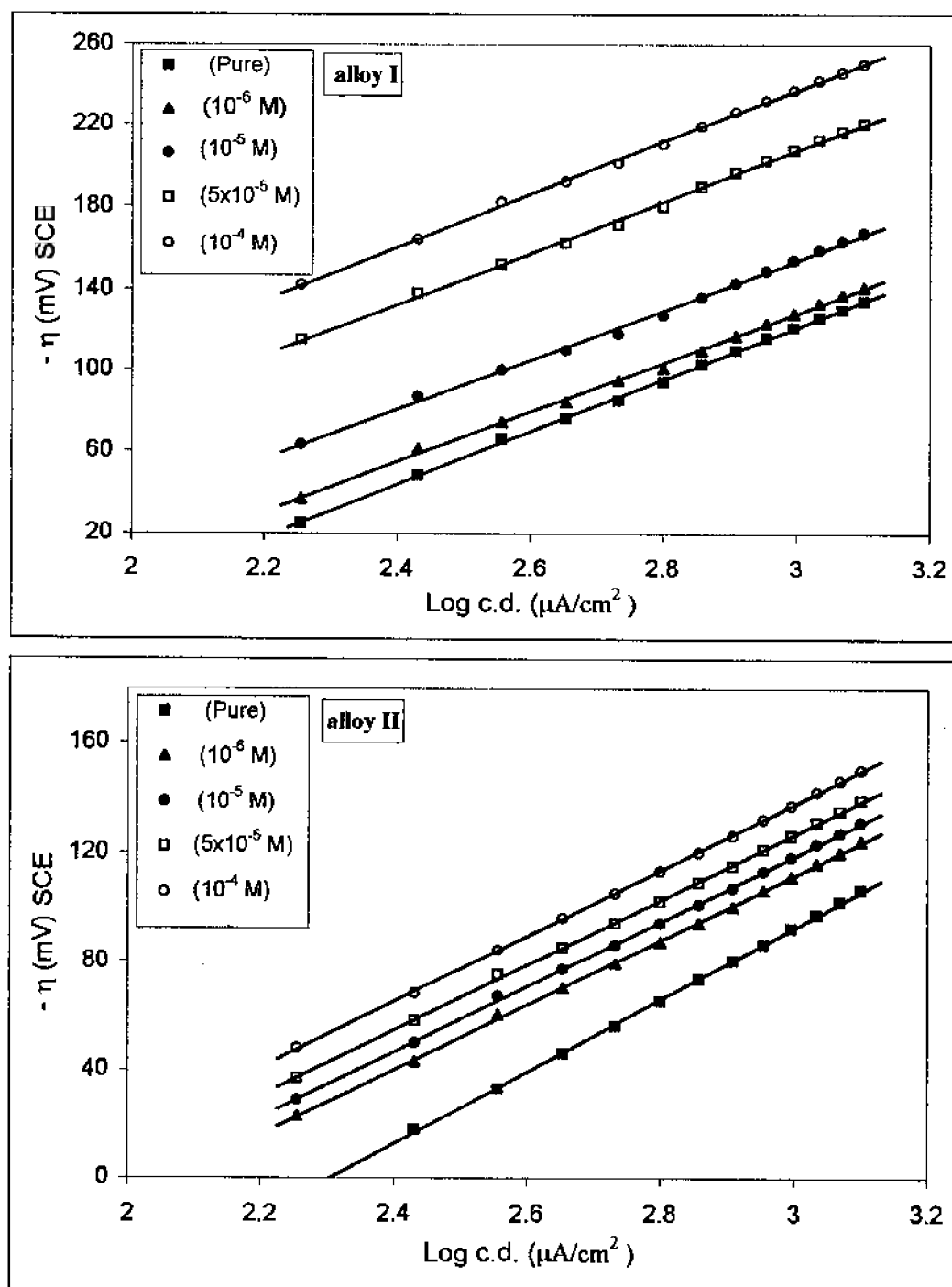


Figure (32): Cathodic Tafel lines for Al-alloys in 0.5M HCl solution in presence of 3-mercapto-4-phenyl-5-p-tolyl-1,2,4-triazole.

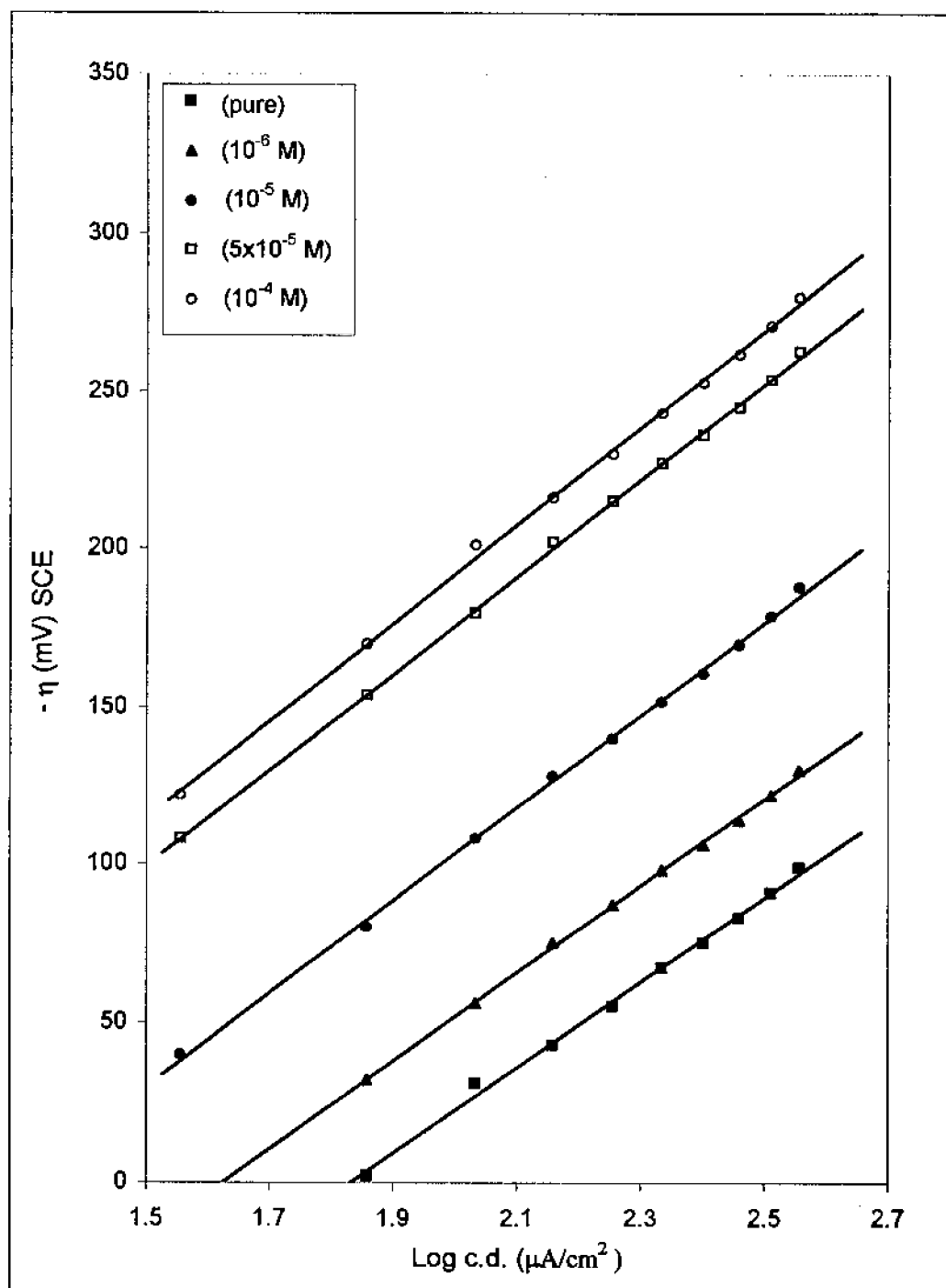


Figure (33): Cathodic Tafel lines for pure aluminium in 0.5 M HCl solution in presence of 3-mercapto-4-phenyl-5-p-nitrophenyl-1,2,4-triazole.

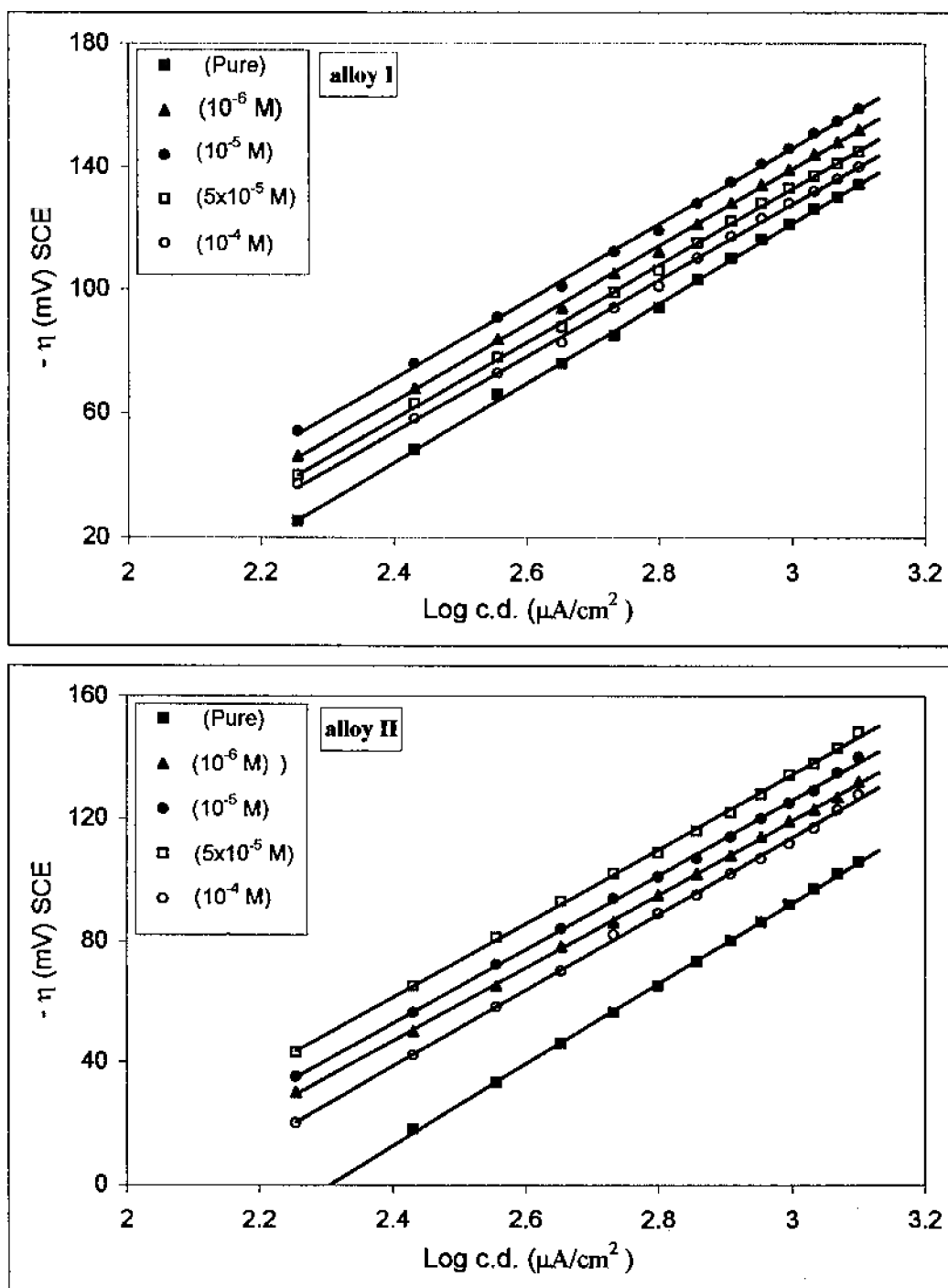


Figure (34): Cathodic Tafel lines for Al-alloys in 0.5M HCl solution in presence of 3-mercapto-4-phenyl-5-p-nitrophenyl-1,2,4-triazole.

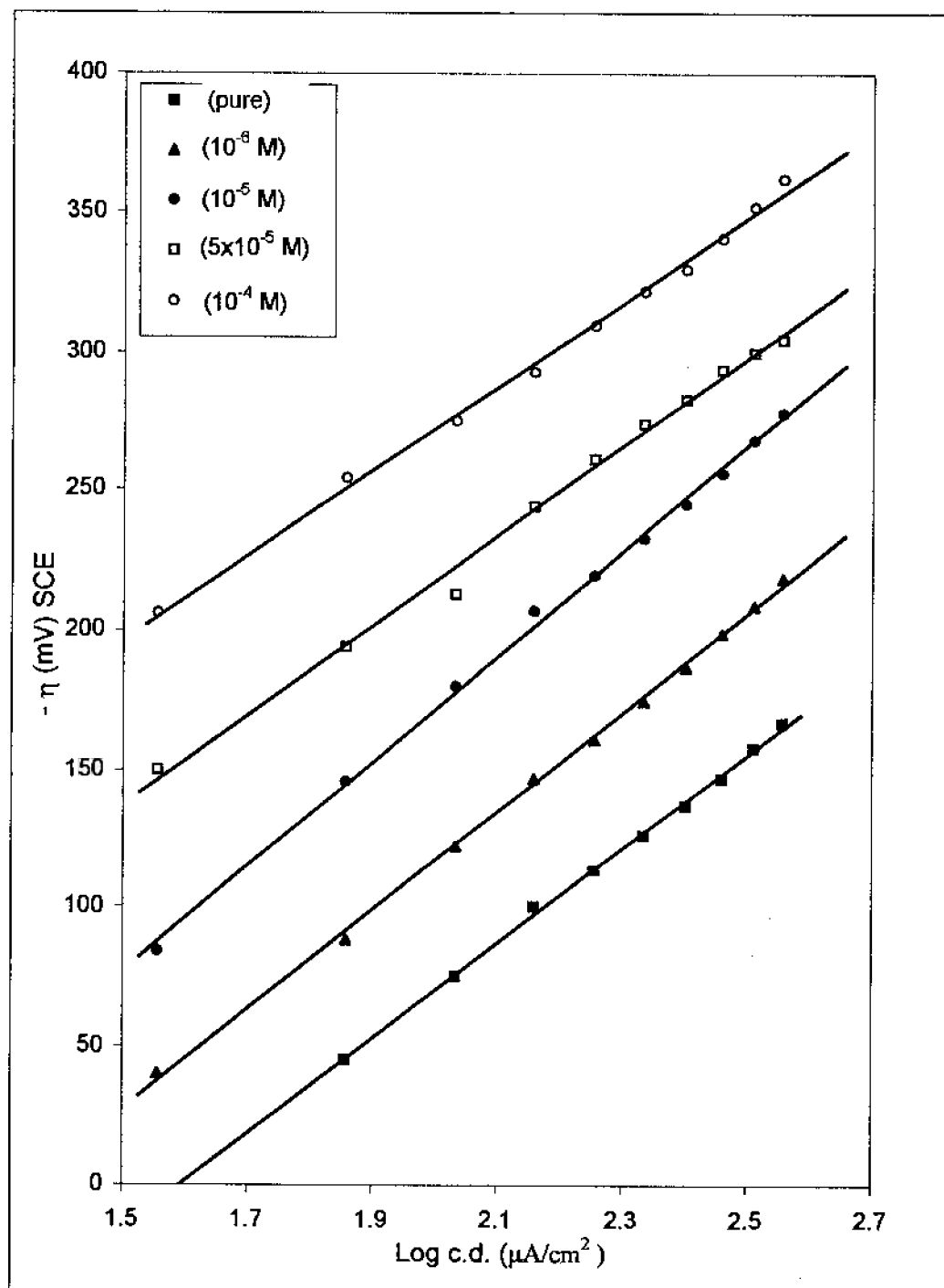


Figure (35): Cathodic Tafel lines for pure aluminium in 0.5M  $\text{HClO}_4$  solution in presence of 3-mercapto-4-phenyl-5-4-pyridyl-1,2,4-triazole.

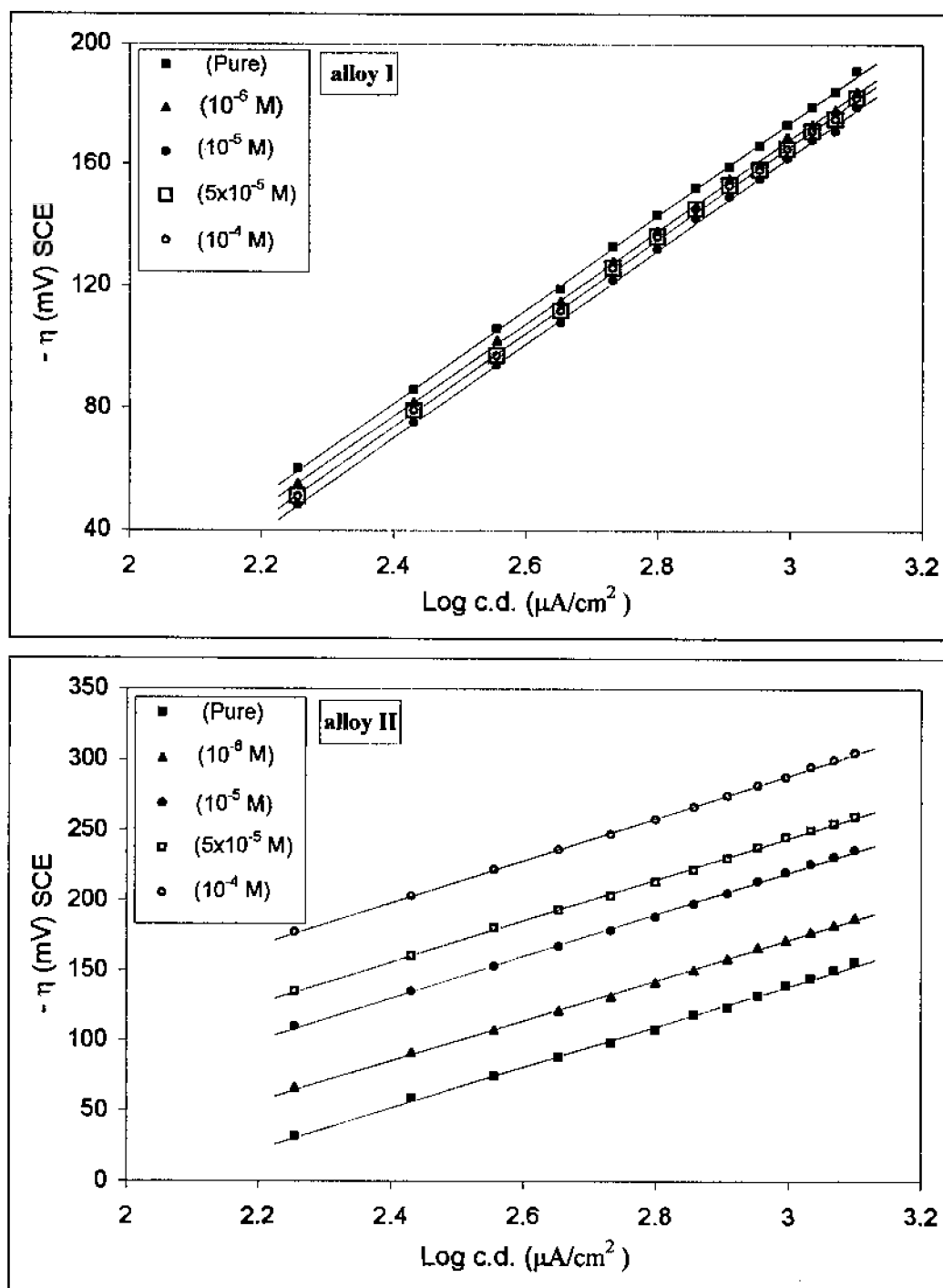


Figure (36): Cathodic Tafel lines for Al-alloys in 0.5 M  $\text{HClO}_4$  solution in presence of 3-mercapto-4-phenyl-5-4-pyridyl-1,2,4-triazole.



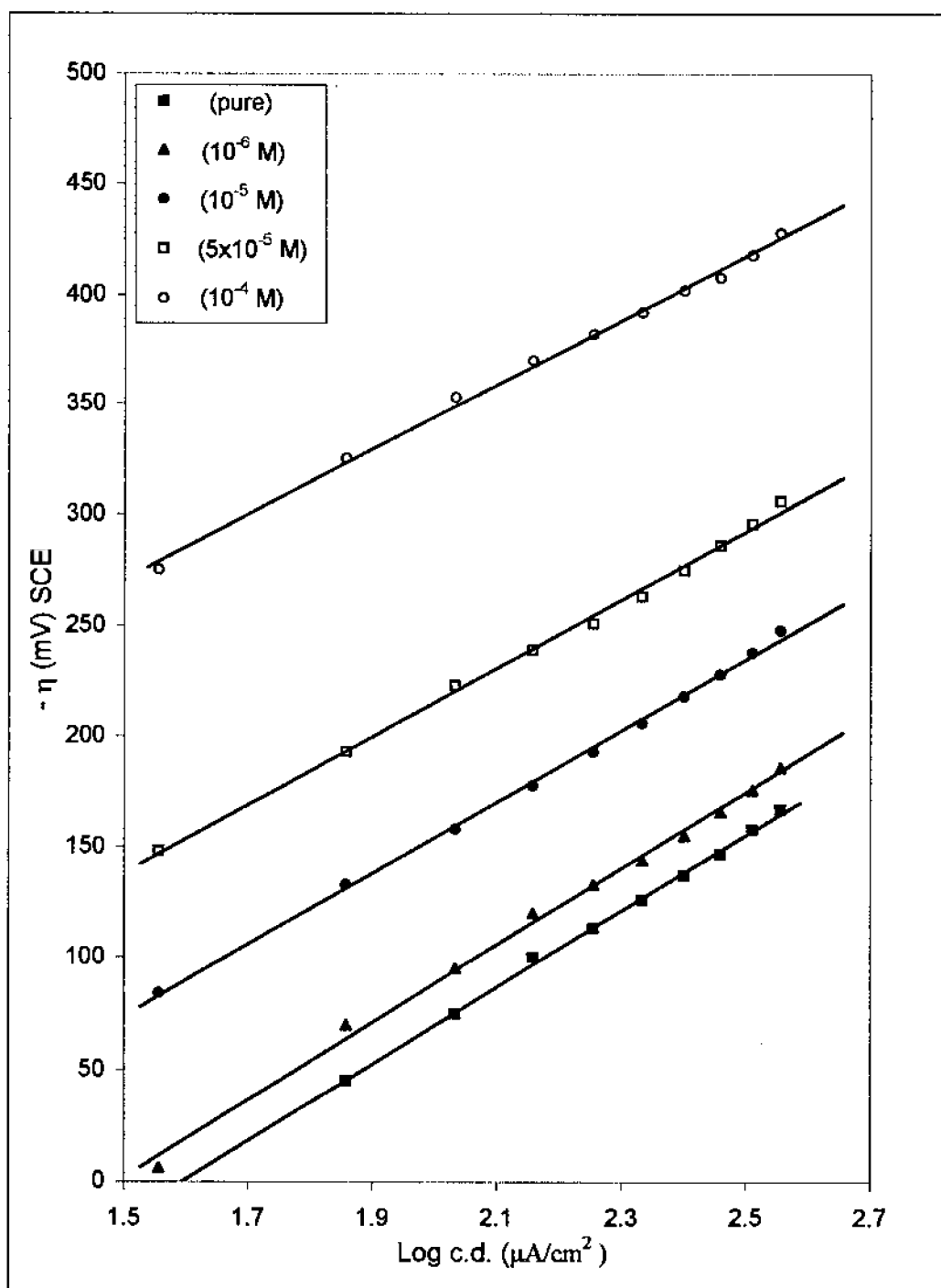


Figure (37): Cathodic Tafel lines for pure aluminium in 0.5M HClO<sub>4</sub> solution in presence of 3-mercapto-4-phenyl-5-p-tolyl-1,2,4-triazole.

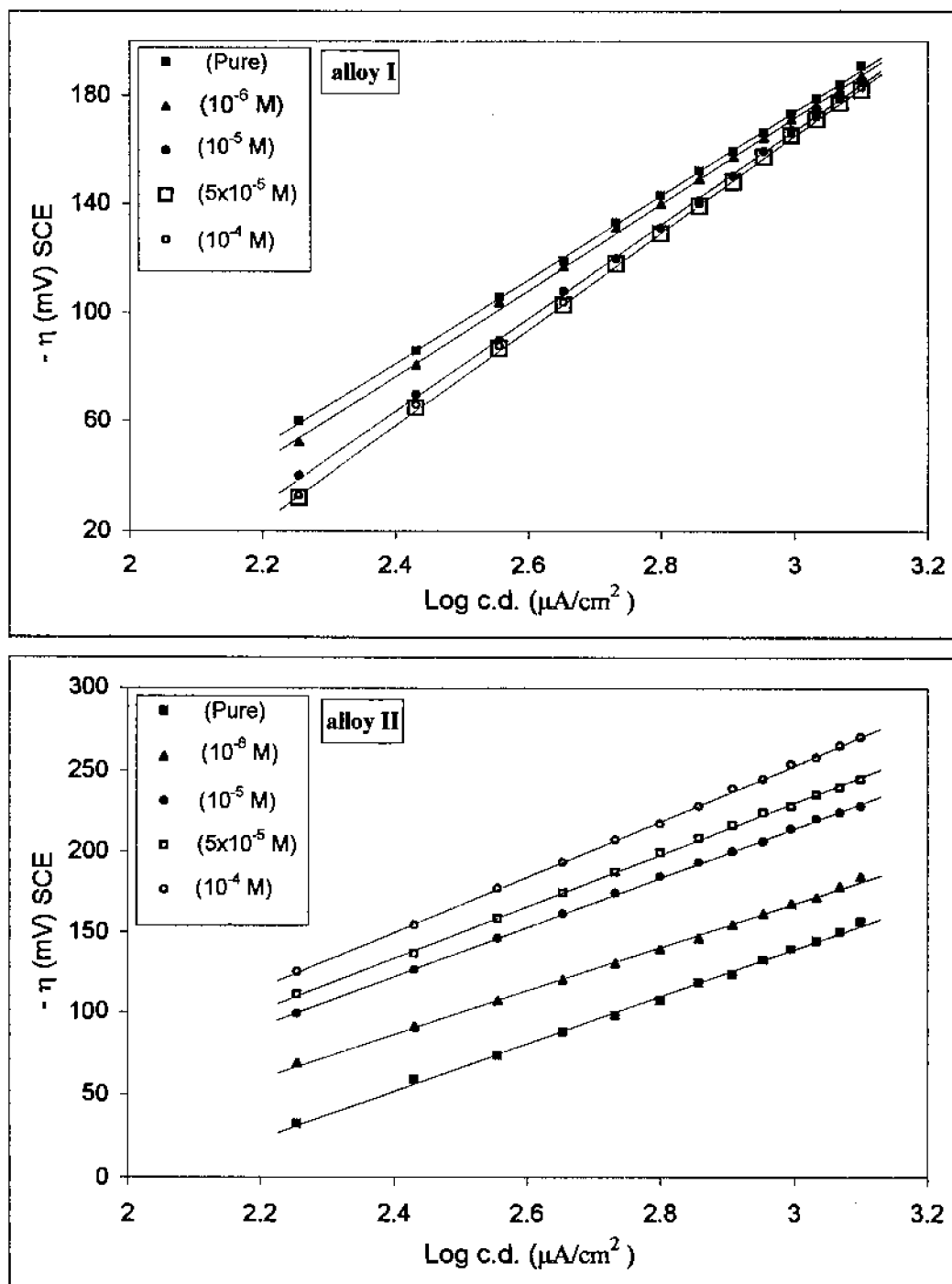


Figure (38): Cathodic Tafel lines for Al-alloys in 0.5 M  $\text{HClO}_4$  solution in presence of 3-mercapto-4-phenyl-5-p-tolyl-1,2,4-triazole.

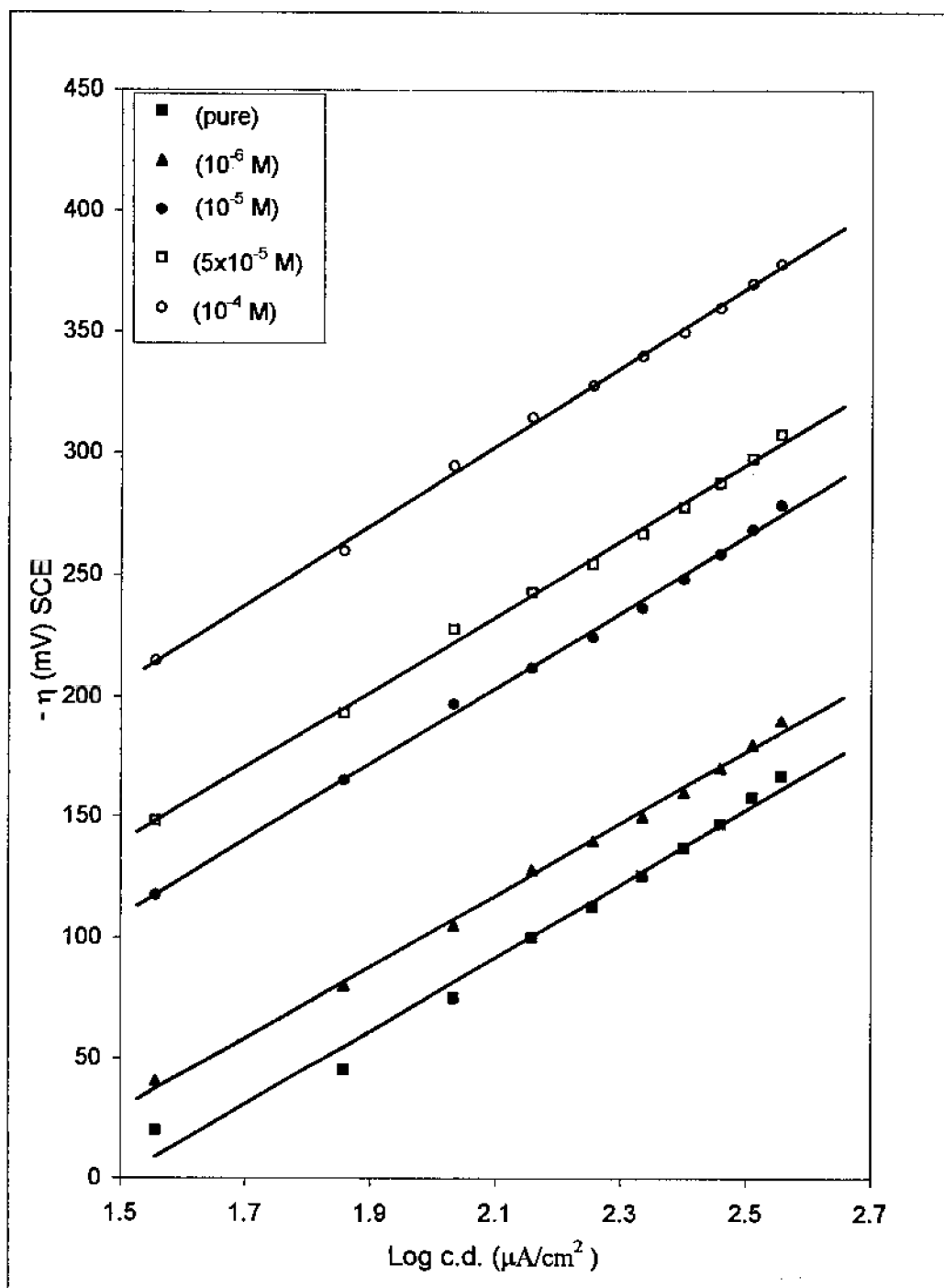


Figure (39): Cathodic Tafel lines for pure aluminium in 0.5 M  $\text{HClO}_4$  solution in presence of 3-mercapto-4-phenyl-5-p-nitrophenyl-1,2,4-triazole.

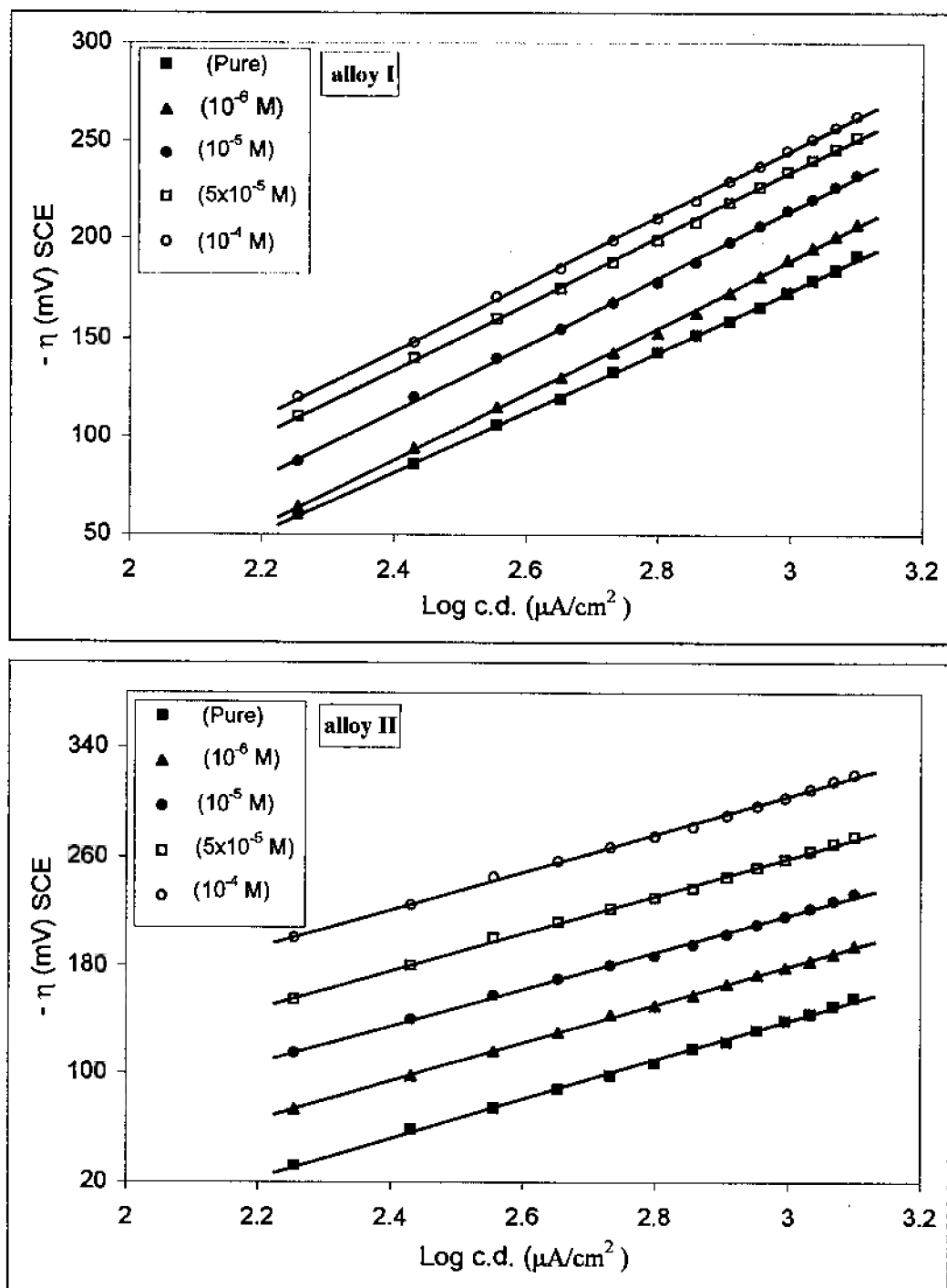


Figure (40): Cathodic Tafel lines for Al-alloys in 0.5 M  $\text{HClO}_4$  solution in presence of 3-mercapto-4-phenyl-5-p-nitrophenyl-1,2,4-triazole.

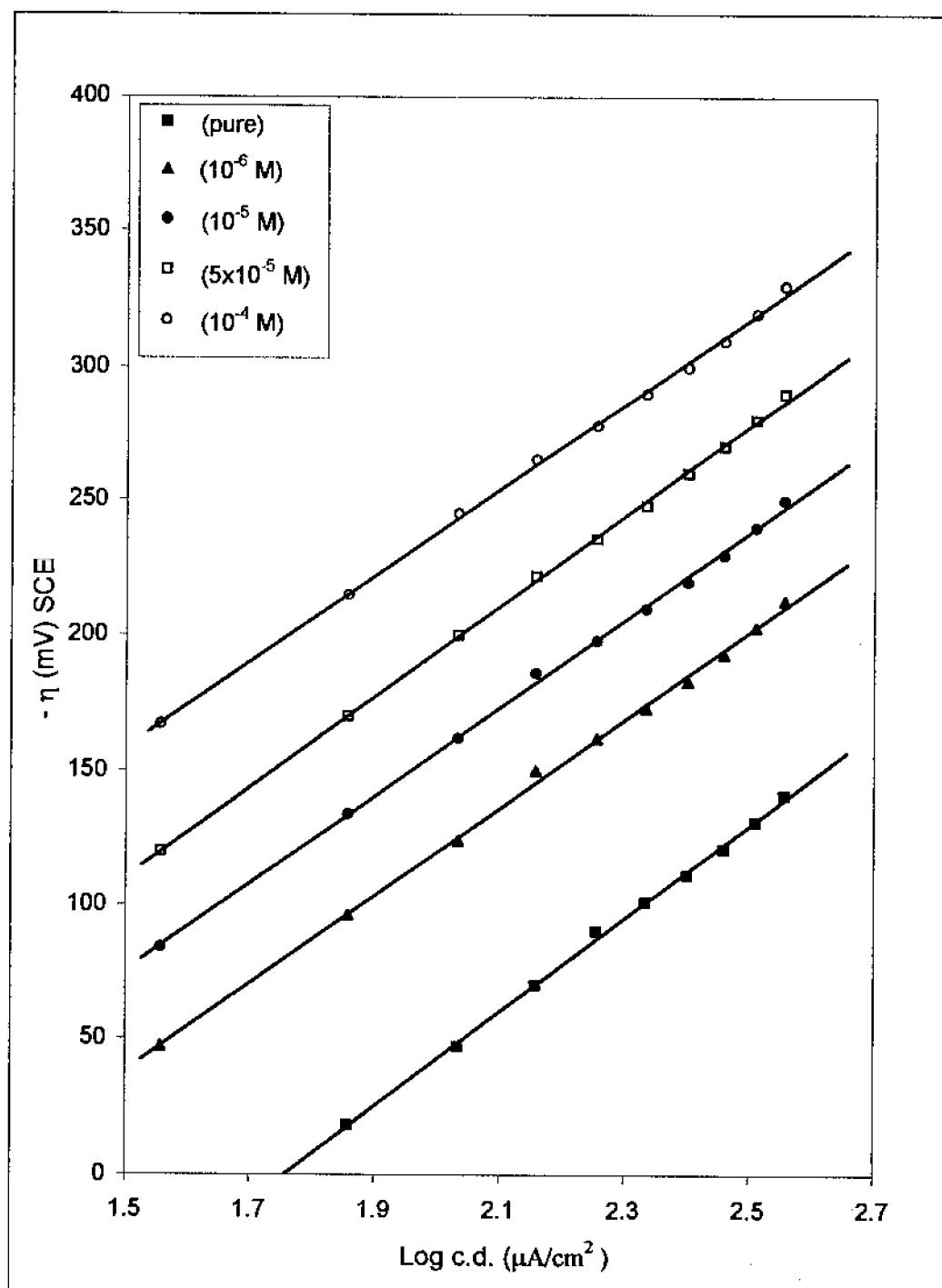


Figure (41): Cathodic Tafel lines for pure aluminium in 0.5M  $H_2SO_4$  solution in presence of 3-mercapto-4-phenyl-5-4-pyridyl-1,2,4-triazole.

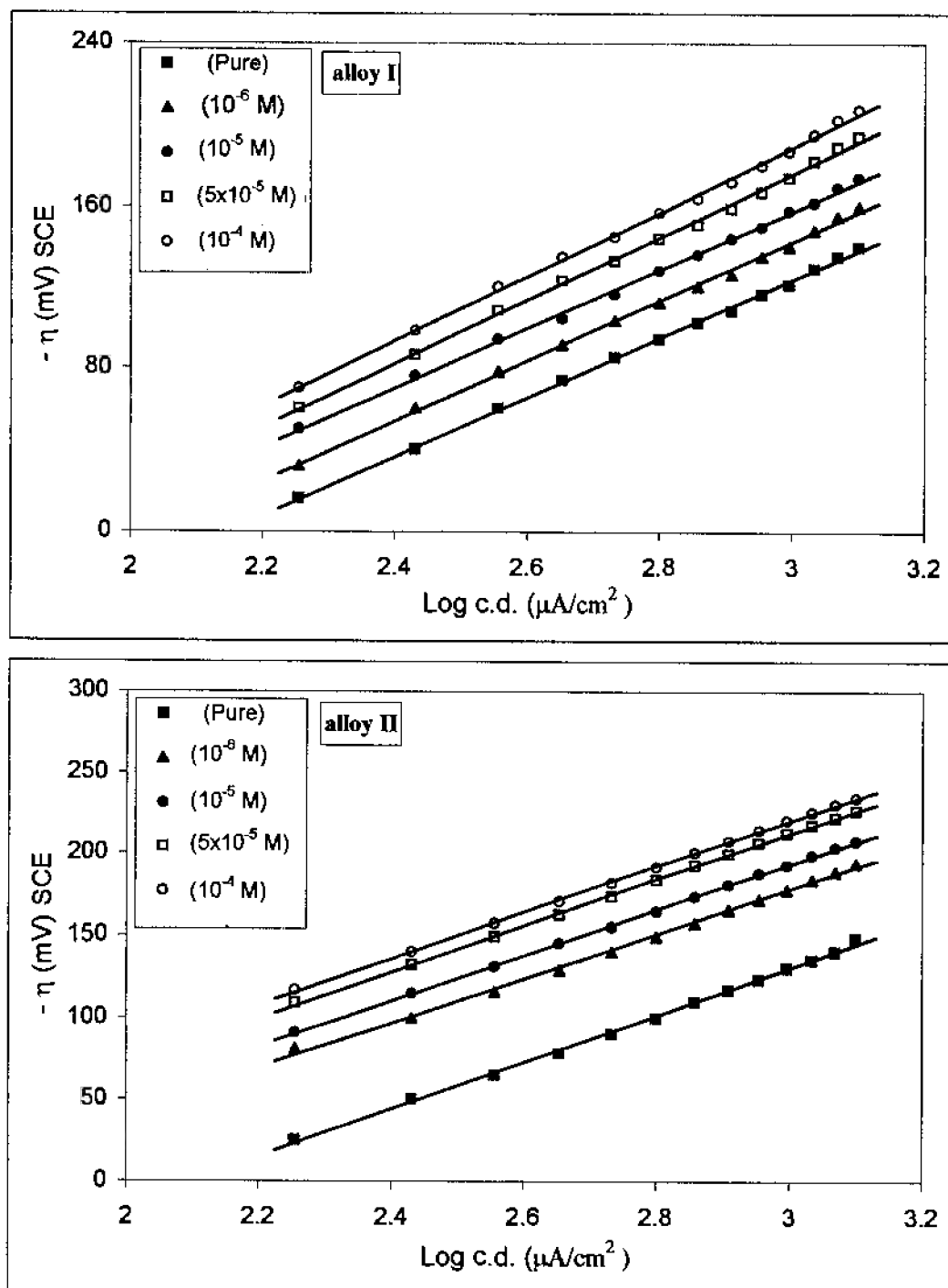


Figure (42): Cathodic Tafel lines for Al-alloys in 0.5 M H<sub>2</sub>SO<sub>4</sub> solution in presence of 3-mercapto-4-phenyl-5-4-pyridyl-1,2,4-triazole.

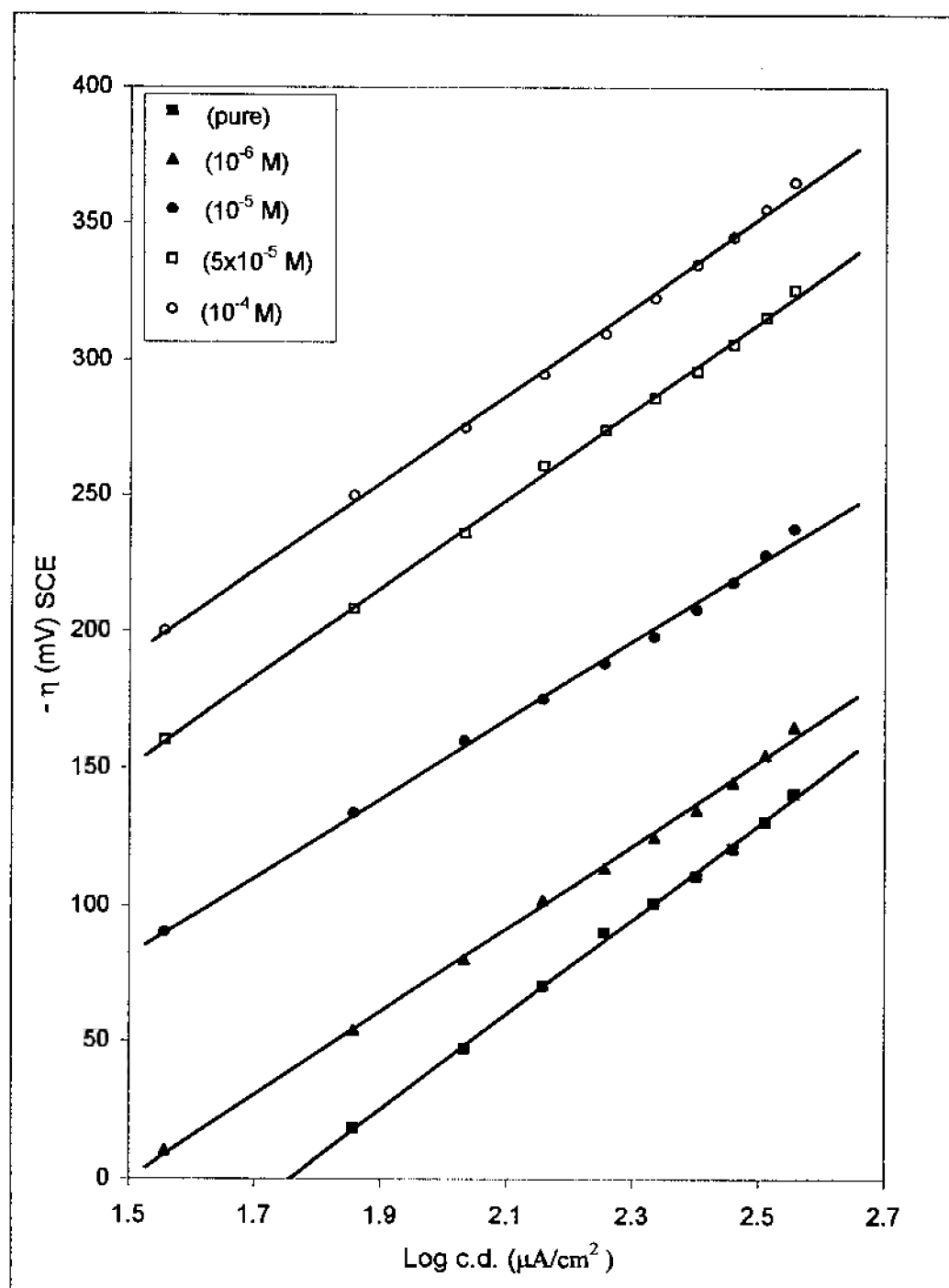


Figure (43): Cathodic Tafel lines for pure aluminium in 0.5M  $\text{H}_2\text{SO}_4$  solution in presence of 3-mercapto-4-phenyl-5-p-tolyl-1,2,4-triazole.

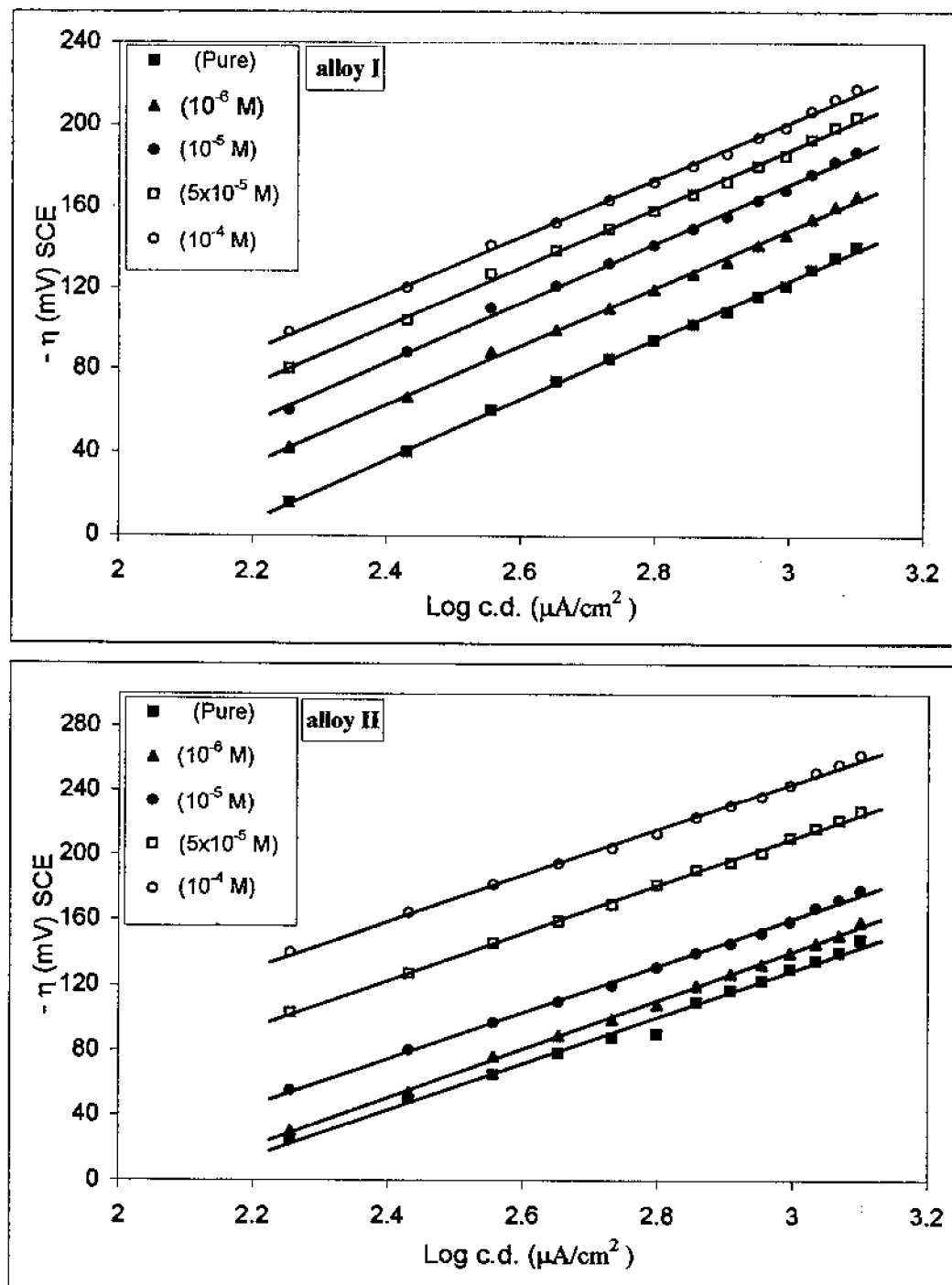


Figure (44): Cathodic Tafel lines for Al-alloys in 0.5 M  $\text{H}_2\text{SO}_4$  solution in presence of 3-mercapto-4-phenyl-5-p-tolyl-1,2,4-triazole.



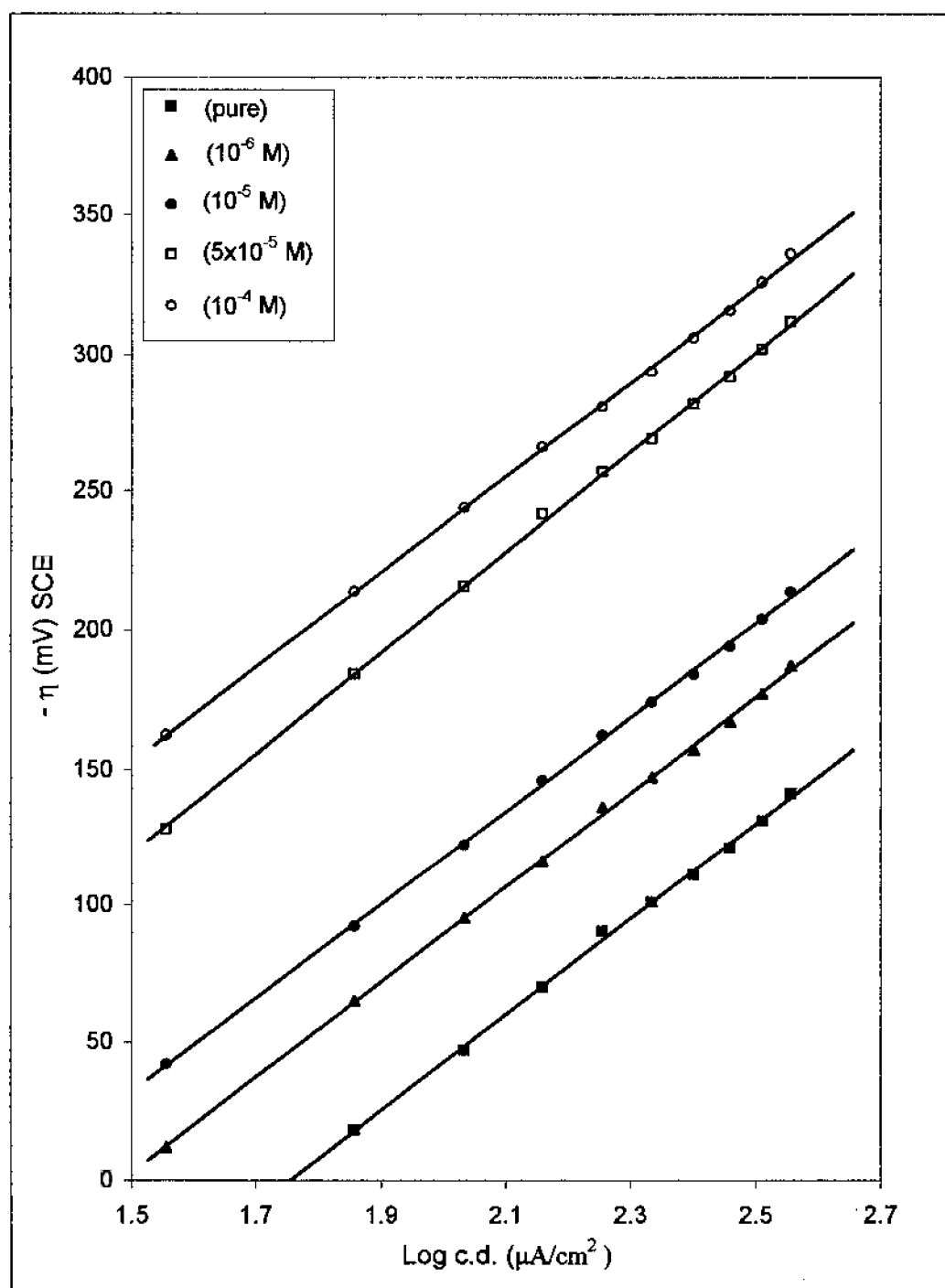


Figure (45): Cathodic Tafel lines for pure aluminium in 0.5 M  $\text{H}_2\text{SO}_4$  solution in presence of 3-mercapto-4-phenyl-5-p-nitrophenyl-1,2,4-triazole.

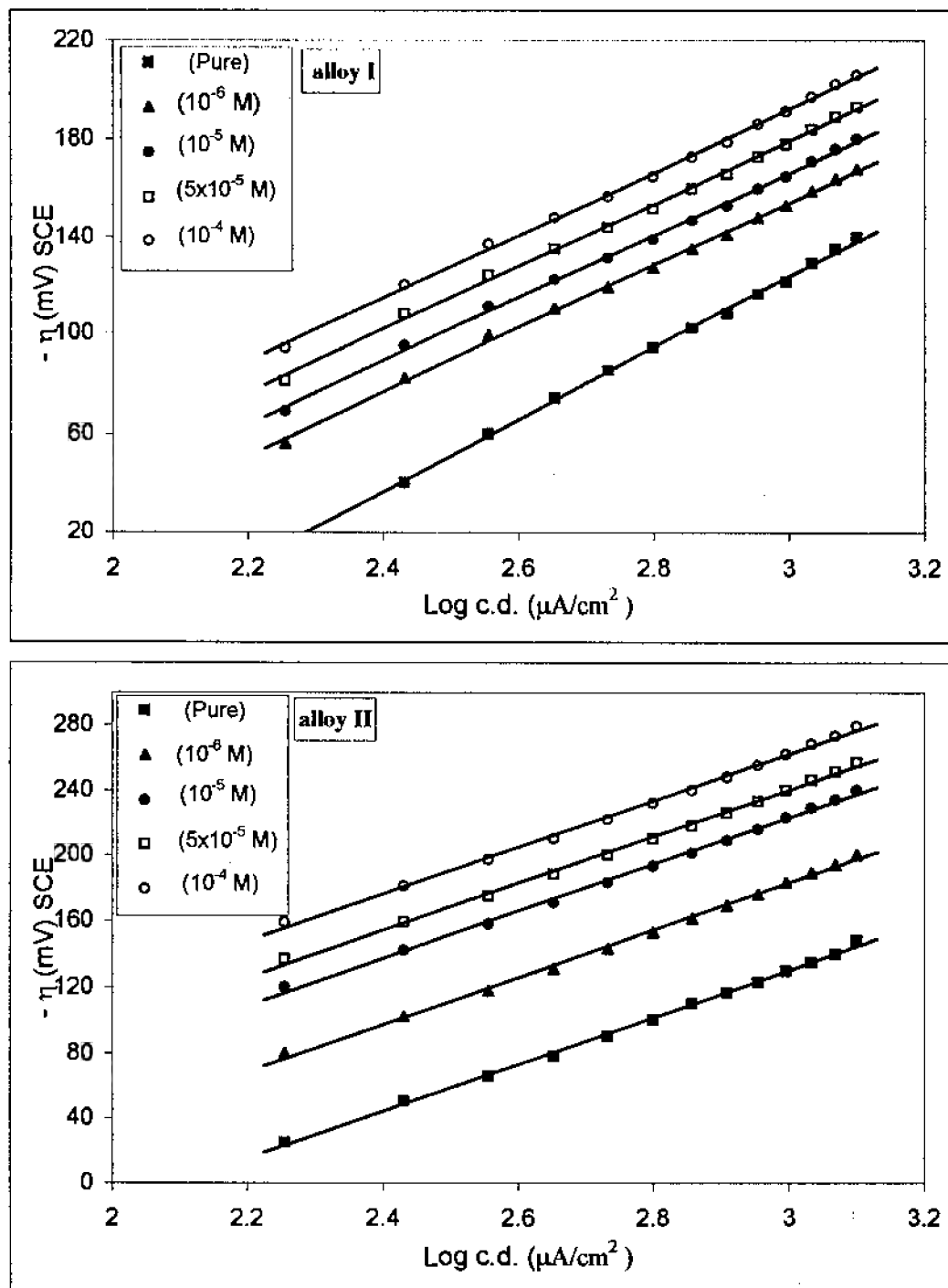


Figure (46): Cathodic Tafel lines for Al-alloys in 0.5 M  $\text{H}_2\text{SO}_4$  solution in presence of 3-mercaptop-4-phenyl-5-p-nitrophenyl-1,2,4-triazole.

## **2.2. Parameters for hydrogen evolution reaction:**

Values of the slope of the cathodic Tafel lines ( $b_c$ ) and transfer coefficient ( $\alpha$ ) for h.e.r. at both pure Al and its alloys in the presence of the investigated triazole derivatives within the concentration range  $10^{-6}$ - $10^{-4}$  M are given in Tables 29-37. The data obtained for triazole derivatives show that the presence of such compounds within the investigated concentration range slightly affected the values obtained in pure 0.5 M solutions of HCl, HClO<sub>4</sub> and H<sub>2</sub>SO<sub>4</sub>. Values of the Tafel slope for h.e.r. at the pure Al cathode in the presence of triazole derivatives at all examined concentrations amount to  $-160 \pm 20$  mV. The corresponding values of  $b_c$  in case of Al-alloys amount to  $-150 \pm 15$  mV. Values of  $\alpha$  (transfer coefficient) in case of Al in the presence of such organic compounds range from 0.33 to 0.38 for pure Al, and from 0.34 to 0.44 for its alloys in the investigated acids solutions.

## **2.3. Open circuit corrosion potentials:**

The values of open circuit corrosion potentials of Al and its alloys in the absence and presence of various concentrations of triazole derivatives in 0.5 M solutions of HCl, HClO<sub>4</sub> and H<sub>2</sub>SO<sub>4</sub> are given in Tables 29-37. It is observed that the value of  $E_{\text{corr}}$  for pure Al and its alloys shifts in the positive direction in the presence of all investigated triazole compounds in all investigated acids solutions. Such positive shift increases with the increase in concentration of such investigated compounds. The value of the positive shift in  $E_{\text{corr}}$  is higher for pure Al in HCl solution than for its alloys at the same concentration of the organic compounds. The phenomenon is reversed in the presence of the same investigated compounds in both

HClO<sub>4</sub> and H<sub>2</sub>SO<sub>4</sub> solution, that is, the positive shift in  $E_{\text{corr}}$  is more pronounced with Al-alloys than with pure Al.

#### 2.4. corrosion currents ( $i_{\text{corr}}$ ):

Corrosion currents ( $i_{\text{corr}}$ ) for both pure Al and its alloys in the investigated acids solutions determined as previously described (see part one) in the absence and presence of triazole derivatives within the concentration range  $10^{-6}$ - $10^{-4}$  M are given in Tables 29-37.

From these results it is observed that all investigated compounds decrease the value of  $i_{\text{corr}}$  for both pure Al and its alloys in H<sub>2</sub>SO<sub>4</sub> solution. The extent of decrease in  $i_{\text{corr}}$ , increases with the increase in the concentration of the organic compound. However, 3-mercapto-4-phenyl-5-p-tolyl-1,2,4-triazole increases  $i_{\text{corr}}$  of alloy I in HClO<sub>4</sub> solution and decreases for pure Al and alloy II. Although 3-mercapto-4-phenyl-5-4-pyridyl-1,2,4-triazole does not affect the value of  $i_{\text{corr}}$  for alloy I (except at  $10^{-6}$  M),  $i_{\text{corr}}$  decreases with increasing concentration for both pure Al and alloy II in HClO<sub>4</sub> solution. In HCl solution, 3-mercapto-4-phenyl-5-4-pyridyl-1,2,4-triazole has influence to decrease  $i_{\text{corr}}$  up to  $5 \times 10^{-5}$  M, however higher value of  $i_{\text{corr}}$  is obtained at  $10^{-4}$  M of both pure Al and its alloys.  $i_{\text{corr}}$  decreases with increasing the concentration of 3-mercapto-4-phenyl-5-p-tolyl-1,2,4-triazole in HCl solution of both pure Al and its alloys.  $i_{\text{corr}}$  decreases as an increase in the concentration of 3-mercapto-4-phenyl-5-p-nitrophenyl-1,2,4-triazole only of pure Al. While,  $i_{\text{corr}}$  decreases for its alloys with increasing the concentration up to  $5 \times 10^{-5}$  M and starts to increase at higher concentration ( $10^{-4}$  M). However, these values are still lower than that obtained in the pure medium.

### **2.5. Inhibition efficiency:**

Values of the inhibition efficiency expressed as %I determined by equation (3) given in part 1 are recorded in Tables 29-37, together with values of  $E_{\text{corr}}$  and  $i_{\text{corr}}$ .

All investigated triazole derivatives have higher inhibition efficiencies of pure Al than of its alloys in  $\text{H}_2\text{SO}_4$  solution. The inhibition efficiency increases with increasing the concentration of triazole derivative in  $\text{H}_2\text{SO}_4$  solution of both pure Al and its investigated alloys. In  $\text{HClO}_4$  solution, all investigated triazole derivatives, show that for pure Al and alloy II, inhibition efficiency increases as an increase of the inhibitor concentration. For alloy I, the inhibition efficiency is gradually increased as an increase in the concentration of 3-mercapto-4-phenyl-5-p-nitrophenyl-1,2,4-triazole. While, 3-mercapto-4-phenyl-5-p-tolyl-1,2,4-triazole has influence to increase %I in the negative direction ( catalytic effect ). On the other hand, with 3-mercapto-4-phenyl-5-4-pyridyl-1,2,4-triazole at lower concentration ( $10^{-6}\text{M}$ ), low %I ( 9% ) is observed, but at higher examined concentrations, the inhibition efficiencies range from zero to -1.3 % for alloy I.

### **2.6. Change in the hydrogen overpotential reaction:**

The values of change in the hydrogen overpotential reaction ( $\Delta\eta_c$ ) of pure Al and its investigated alloys in the presence of various concentrations from the investigated triazole derivatives in 0.5 M solutions of  $\text{HCl}$ ,  $\text{HClO}_4$  and  $\text{H}_2\text{SO}_4$  are given in Tables 29-37. The data exhibited that the value of  $\Delta\eta_c$  increases in the negative direction as an increase in

concentration of the investigated triazole derivatives in  $\text{H}_2\text{SO}_4$  solution. The value of  $\Delta\eta_c$  is greater for pure Al than of its alloys within the examined concentrations range of the inhibitor. The value of  $\Delta\eta_c$  increases with increasing the concentration of all investigated triazole derivatives for pure Al and alloy II in  $\text{HClO}_4$  solution. The value of  $\Delta\eta_c$  increases in the presence of 3-mercapto-4-phenyl-5-p-nitrophenyl-1,2,4-triazole, but the other investigated triazole derivatives have reverse effect, The value of  $\Delta\eta_c$  decreases as an increase in the concentration of the inhibitor at alloy I.

In  $\text{HCl}$  solution, the value of  $\Delta\eta_c$  increases in the negative direction with increasing of 3-mercapto-4-phenyl-5-p-tolyl-1,2,4-triazole concentration of both pure Al and its alloys. Similar effects (except at  $10^{-4}\text{M}$  of 3-mercapto-4-phenyl-5-4-pyridyl-1,2,4-triazole in case of pure Al, and at  $10^{-4}\text{M}$  of 3-mercapto-4-phenyl-5-p-nitrophenyl-1,2,4-triazole in case of alloy I) in the presence of the two other studied triazole compounds are observed.

### **2.7. Change in the overpotential of anodic dissolution reaction:**

The values of change in the overpotential anodic dissolution reaction ( $\Delta\eta_a$ ) of pure Al and its alloys in the presence of various concentrations of triazole derivatives in 0.5 M solutions of  $\text{HCl}$ ,  $\text{HClO}_4$  and  $\text{H}_2\text{SO}_4$  are given in Tables 29-37. It is observed that the value of  $\Delta\eta_a$  increases in the positive direction with increasing the inhibitor concentration of all the investigated triazole derivatives in acids solutions of both pure Al and its investigated alloys. Greater values of  $\Delta\eta_a$  are observed in  $\text{H}_2\text{SO}_4$  containing triazole derivatives than in both  $\text{HCl}$  and  $\text{HClO}_4$  solutions within the examined concentrations range ( $10^{-6}$ - $10^{-4}\text{M}$ ).

### **2.8. Adsorption isotherm:**

The degree of coverage  $\theta_{\text{org}}$  for compounds having inhibition efficiencies lying within the range 3-97 % were calculated according to the method recommended by Fischer <sup>(16)</sup>, applying equation (4). Values of  $\theta_{\text{org}}$  for triazole derivatives are given in Tables 29-37. Adsorption isotherms obtained by plotting  $C/\theta$  versus  $C$  for both pure Al and its alloys are shown in Figs.47-55.

Table (29): Effect of 3-mercapto-4-phenyl-5-4-pyridyl-1,2,4-triazole on the electrochemical and corrosion behaviour of aluminium and its alloys in 0.5 M HCl solution.

Electrode	Additive concn. (M)	-E <sub>corr.</sub> mV (SCE)	i <sub>corr.</sub> $\mu\text{A}/\text{cm}^2$	% I (inh.effec.)	Surf. Coverage ( $\theta$ )	$\Delta\eta_c$ (mV) at 360 $\mu\text{A}/\text{cm}^2$	$\Delta\eta_a$ (mV) at 162 $\mu\text{A}/\text{cm}^2$	Tafel slopes.		Transfer coeff. (a)
								b <sub>a</sub> (mV)	b <sub>c</sub> (mV)	
Aluminium	0	922	68	—	—	—	—	76	135	0.437
	$1 \times 10^{-6}$	917	45	33.8	0.338	-74	+5	78	150	0.393
	$1 \times 10^{-5}$	905	10	85.3	0.853	-208	+8	76	164	0.360
	$5 \times 10^{-5}$	900	1.5	97.8	0.978	-529	+8	76	180	0.328
	$1 \times 10^{-4}$	890	93	-36.8	—	-14	+9	77	130	0.454
Alloy I	0	774	122	—	—	—	—	47	131	0.450
	$1 \times 10^{-6}$	765	84	31.1	0.311	-11	+2	47	126	0.468
	$1 \times 10^{-5}$	762	78	36.1	0.361	-19	+6	46	126	0.468
	$5 \times 10^{-5}$	760	66	45.9	0.459	-31	+8	47	130	0.454
	$1 \times 10^{-4}$	757	73	40.2	0.402	-24	+10	46	127	0.465
Alloy II	0	767	200	—	—	—	—	31	131	0.450
	$1 \times 10^{-6}$	760	119	40.5	0.405	-27	+3	31	120	0.492
	$1 \times 10^{-5}$	758	100	50.0	0.500	-39	+6	31	123	0.480
	$5 \times 10^{-5}$	750	71	64.5	0.645	-57	+7	29	123	0.480
	$1 \times 10^{-4}$	745	130	35.0	0.350	-22	+8	30	120	0.492



Table (30): Effect of 3-mercapto-4-phenyl-5-p-tolyl-1,2,4-triazole on the electrochemical and corrosion behaviour of aluminium and its alloys in 0.5 M HCl solution.

Electrode	Additive concn. (M)	$-E_{\text{corr.}}$ mV (SCE)	$i_{\text{corr.}}$ $\mu\text{A}/\text{cm}^2$	%I (inh. effec.)	Surf. Coverage ( $\theta$ )	$\Delta\eta_c$ (mV) at 360 $\mu\text{A}/\text{cm}^2$	$\Delta\eta_a$ (mV) at 162 $\mu\text{A}/\text{cm}^2$	Tafel slopes.		Transfer coeff. ( $\alpha$ )
								$b_a$ (mV)	$b_c$ (mV)	
Aluminium	0	922	68	—	—	—	—	77	135	0.44
	$1 \times 10^{-6}$	918	48	29.4	0.294	-53	+ 3	75	143	0.41
	$1 \times 10^{-5}$	915	6	91.2	0.912	-259	+ 5	77	167	0.35
	$5 \times 10^{-5}$	905	2	97.1	0.971	-377	+ 6	78	167	0.35
	$1 \times 10^{-4}$	900	2	97.1	0.971	-391	+ 7	83	166	0.36
Alloy I	0	774	122	—	—	—	—	47	131	0.45
	$1 \times 10^{-6}$	771	101	17.2	0.172	-8	+ 2	47	129	0.46
	$1 \times 10^{-5}$	765	58	52.5	0.525	-34	+ 7	46	126	0.47
	$5 \times 10^{-5}$	764	26	78.7	0.787	-86	+ 11	49	126	0.47
	$1 \times 10^{-4}$	763	16	86.9	0.869	-116	+ 15	49	130	0.45
Alloy II	0	767	200	—	—	—	—	31	131	0.45
	$1 \times 10^{-6}$	766	119	40.5	0.405	-27	+ 4	28	121	0.49
	$1 \times 10^{-5}$	764	99	50.5	0.505	-34	+ 6	28	122	0.48
	$5 \times 10^{-5}$	761	92	54.0	0.540	-42	+ 8	28	122	0.48
	$1 \times 10^{-4}$	758	63	68.5	0.685	-51	+ 11	29	122	0.48

Table (31): Effect of 3-mercapto-4-phenyl-5-p-nitrophenyl-1,2,4-triazole on the electrochemical and corrosion behaviour of aluminium and its alloys in 0.5 M HCl solution.

Electrode	Additive concn. (M)	$-E_{corr.}$ mV (SCE)	$i_{corr.}$ $\mu A/cm^2$	% I (inh. effec.)	Surf. Coverage ( $\theta$ )	$\Delta\eta_c$ (mV) at 360 $\mu A/cm^2$	$\Delta\eta_a$ (mV) at 162 $\mu A/cm^2$	Tafel slopes.		Transfer coeff. ( $\alpha$ )
								$b_a$ (mV)	$b_c$ (mV)	
Aluminium	0	922	68	—	—	—	—	76	135	0.44
	$1 \times 10^{-6}$	910	54	20.6	0.206	-31	+ 3	76	165	0.36
	$1 \times 10^{-5}$	902	26	61.8	0.618	-89	+ 5	77	163	0.36
	$5 \times 10^{-5}$	895	10	85.3	0.853	-164	+ 8	77	169	0.35
	$1 \times 10^{-4}$	890	9	86.8	0.868	-181	+ 8	77	165	0.36
Alloy I	0	774	122	—	—	—	—	47	131	0.45
	$1 \times 10^{-6}$	771	82	32.8	0.328	-18	+ 2	46	124	0.48
	$1 \times 10^{-5}$	769	73	40.2	0.402	-25	+ 4	47	125	0.47
	$5 \times 10^{-5}$	767	87	28.7	0.287	-12	+ 5	47	124	0.48
	$1 \times 10^{-4}$	764	94	23.0	0.230	-7	+ 7	46	124	0.48
Alloy II	0	767	200	—	—	—	—	31	131	0.45
	$1 \times 10^{-6}$	760	89	55.5	0.555	-32	+ 3	32	122	0.48
	$1 \times 10^{-5}$	757	63	68.5	0.685	-39	+ 5	31	125	0.47
	$5 \times 10^{-5}$	752	55	72.5	0.725	-48	+ 8	31	122	0.48
	$1 \times 10^{-4}$	748	89	55.5	0.555	-25	+ 8	31	125	0.47

Table (32): Effect of 3-mercapto-4-phenyl-5-4-pyridyl-1,2,4-triazole on the electrochemical and corrosion behaviour of aluminium and its alloys in 0.5 M  $\text{HClO}_4$  solution.

Electrode	Additive concn. (M)	$-E_{\text{corr.}}$ mV (SCE)	$i_{\text{corr.}}$ $\mu\text{A}/\text{cm}^2$	% I (inh.effec.)	Surf. Coverage ( $\theta$ )	$\Delta\eta_c$ (mV) at 360 $\mu\text{A}/\text{cm}^2$	$\Delta\eta_a$ (mV) at 162 $\mu\text{A}/\text{cm}^2$	Tafel slopes.		Transfer coeff. ( $\alpha$ )
								$b_a$ (mV)	$b_c$ (mV)	
Aluminium	0	925	34	—	—	—	—	132	158	0.373
	$1 \times 10^{-6}$	915	28	17.6	0.176	-52	+ 12	139	159	0.371
	$1 \times 10^{-5}$	905	11	67.6	0.676	-111	+ 22	147	166	0.355
	$5 \times 10^{-5}$	900	5	85.3	0.853	-138	+ 29	149	166	0.355
	$1 \times 10^{-4}$	890	5	85.3	0.853	-195	+ 36	156	156	0.378
Alloy I	0	725	78	—	—	—	—	66	158	0.373
	$1 \times 10^{-6}$	712	71	9.0	0.090	+ 4	+ 7	73	151	0.391
	$1 \times 10^{-5}$	709	79	-1.3	—	+ 12	+ 9	74	155	0.381
	$5 \times 10^{-5}$	708	77	1.3	0.013	+ 9	+ 14	76	155	0.381
	$1 \times 10^{-4}$	707	78	0.0	0.000	+ 9	+ 50	81	155	0.381
Alloy II	0	712	135	—	—	—	—	28	160	0.369
	$1 \times 10^{-6}$	709	65	51.9	0.519	-33	+ 2	31	151	0.391
	$1 \times 10^{-5}$	690	35	74.1	0.741	-79	+ 22	43	151	0.391
	$5 \times 10^{-5}$	680	25	81.5	0.815	-106	+ 25	41	154	0.383
	$1 \times 10^{-4}$	650	13	90.4	0.904	-148	+ 25	37	153	0.386

Table (33): Effect of 3-mercapto-4-phenyl-5-p-tolyl-1,2,4-triazole on the electrochemical and corrosion behaviour of aluminium and its alloys in 0.5 M HClO<sub>4</sub> solution.

Electrode	Additive concn. (M)	-E <sub>corr.</sub> mV (SCE)	i <sub>corr.</sub> $\mu\text{A}/\text{cm}^2$	% I (inh.effec.)	Surf. Coverage ( $\theta$ )	$\Delta\eta_c$ (mV) at 360 $\mu\text{A}/\text{cm}^2$	$\Delta\eta_a$ (mV) at 162 $\mu\text{A}/\text{cm}^2$	Tafel slopes.		Transfer coeff. ( $\alpha$ )
								b <sub>a</sub> (mV)	b <sub>c</sub> (mV)	
Aluminium	0	925	34	—	—	—	—	134	158	0.373
	1x10 <sup>-6</sup>	920	34	0.0	0.000	-19	+ 6	135	176	0.335
	1x10 <sup>-5</sup>	917	15	55.9	0.559	-81	+ 15	145	178	0.331
	5x10 <sup>-5</sup>	912	7	79.4	0.794	-139	+ 20	147	177	0.333
	1x10 <sup>-4</sup>	905	2	94.1	0.941	-261	+ 21	153	176	0.335
Alloy I	0	725	78	—	—	—	—	66	158	0.373
	1x10 <sup>-6</sup>	710	84	-7.7	—	+ 2	+ 7	67	157	0.376
	1x10 <sup>-5</sup>	707	119	-52.6	—	+ 16	+ 10	67	177	0.333
	5x10 <sup>-5</sup>	703	117	-50.0	—	+ 19	+ 16	67	177	0.333
	1x10 <sup>-4</sup>	695	112	-43.6	—	+ 18	+ 16	67	178	0.331
Alloy II	0	712	135	—	—	—	—	31	160	0.369
	1x10 <sup>-6</sup>	700	59	56.3	0.563	-33	+ 17	40	135	0.437
	1x10 <sup>-5</sup>	695	43	68.1	0.681	-72	+ 17	40	155	0.381
	5x10 <sup>-5</sup>	690	37	72.6	0.726	-84	+ 17	40	160	0.369
	1x10 <sup>-4</sup>	687	34	74.8	0.748	-103	+ 19	41	171	0.345

Table (34): Effect of 3-mercapto-4-phenyl-5-p-nitrophenyl-1,2,4-triazole on the electrochemical and corrosion behaviour of aluminium and its alloys in 0.5 M HClO<sub>4</sub> solution.

Electrode	Additive concn. (M)	-E <sub>corr.</sub> mV (SCE)	i <sub>corr.</sub> $\mu\text{A}/\text{cm}^2$	% I (inh. effec.)	Surf. Coverage ( $\theta$ )	$\Delta\eta_c$ (mV) at 360 $\mu\text{A}/\text{cm}^2$	$\Delta\eta_a$ (mV) at 162 $\mu\text{A}/\text{cm}^2$	Tafel slopes.		Transfer coeff. ( $\alpha$ )
								b <sub>a</sub> (mV)	b <sub>c</sub> (mV)	
Aluminium	0	925	34	—	—	—	—	133	158	0.373
	1x10 <sup>-6</sup>	920	20	41.2	0.412	-23	+ 10	138	154	0.383
	1x10 <sup>-5</sup>	916	9	73.5	0.735	-112	+ 21	143	156	0.378
	5x10 <sup>-5</sup>	912	6	82.4	0.824	-141	+ 28	145	157	0.376
	1x10 <sup>-4</sup>	910	2	94.1	0.941	-211	+ 37	142	157	0.376
Alloy I	0	725	78	—	—	—	—	65	158	0.373
	1x10 <sup>-6</sup>	712	70	10.3	0.103	-9	+ 3	69	169	0.349
	1x10 <sup>-5</sup>	705	61	21.8	0.218	-34	+ 9	82	169	0.349
	5x10 <sup>-5</sup>	701	45	42.3	0.423	-54	+ 35	81	169	0.349
	1x10 <sup>-4</sup>	697	40	48.7	0.487	-65	+ 54	81	169	0.349
Alloy II	0	712	135	—	—	—	—	27	160	0.369
	1x10 <sup>-6</sup>	692	56	58.5	0.585	-42	+ 7	38	140	0.421
	1x10 <sup>-5</sup>	680	27	80.0	0.800	-84	+ 9	42	137	0.431
	5x10 <sup>-5</sup>	670	14	89.6	0.896	-126	+ 12	38	137	0.431
	1x10 <sup>-4</sup>	665	7	94.8	0.948	-171	+ 21	44	140	0.421

Table (35): Effect of 3-mercapto-4-phenyl-5-4-pyridyl-1,2,4-triazole on the electrochemical and corrosion behaviour of aluminium and its alloys in 0.5 M H<sub>2</sub>SO<sub>4</sub> solution.

Electrode	Additive concn. (M)	-E <sub>corr.</sub> mV (SCE)	i <sub>corr.</sub> $\mu\text{A}/\text{cm}^2$	% I (inh. effec.)	Surf. Coverage ( $\theta$ )	$\Delta\eta_c$ (mV) at 360 $\mu\text{A}/\text{cm}^2$	$\Delta\eta_a$ (mV) at 162 $\mu\text{A}/\text{cm}^2$	Tafel slopes.		Transfer coeff. ( $\alpha$ )
								b <sub>a</sub> (mV)	b <sub>c</sub> (mV)	
Aluminium	0	915	51	—	—	—	—	150	162	0.364
	1x10 <sup>-6</sup>	905	18	64.7	0.647	-72	+ 2	150	160	0.369
	1x10 <sup>-5</sup>	900	13	74.5	0.745	-109	+ 5	150	162	0.364
	5x10 <sup>-5</sup>	895	4	92.2	0.922	-149	+ 15	151	169	0.349
	1x10 <sup>-4</sup>	890	3	94.1	0.941	-189	+ 45	151	160	0.369
Alloy I	0	760	126	—	—	—	—	60	133	0.444
	1x10 <sup>-6</sup>	752	96	23.8	0.238	-18	+ 24	77	153	0.386
	1x10 <sup>-5</sup>	746	94	25.4	0.254	-34	+ 34	83	153	0.386
	5x10 <sup>-5</sup>	736	49	61.1	0.611	-48	+ 45	82	153	0.386
	1x10 <sup>-4</sup>	728	56	55.6	0.556	-60	+ 54	83	153	0.386
Alloy II	0	745	130	—	—	—	—	46	145	0.407
	1x10 <sup>-6</sup>	723	58	55.4	0.554	-51	+ 2	46	143	0.413
	1x10 <sup>-5</sup>	719	41	68.5	0.685	-66	+ 4	46	143	0.413
	5x10 <sup>-5</sup>	704	33	74.6	0.746	-84	+ 6	46	143	0.413
	1x10 <sup>-4</sup>	696	28	78.5	0.785	-92	+ 9	46	143	0.413

Table (36): Effect of 3-mercapto-4-phenyl-5-p-tolyl-1,2,4-triazole on the electrochemical and corrosion behaviour of aluminium and alloys in 0.5 M  $H_2SO_4$  solution.

Electrode	Additive concn. (M)	-E <sub>corr.</sub> mV (SCE)	i <sub>corr.</sub> $\mu A/cm^2$	% I (inh. effec.)	Surf. Coverage ( $\theta$ )	$\Delta\eta_c$ (mV) at 360 $\mu A/cm^2$	$\Delta\eta_a$ (mV) at 162 $\mu A/cm^2$	Tafel slopes.		Transfer coeff. ( $\alpha$ )
								b <sub>a</sub> (mV)	b <sub>c</sub> (mV)	
Aluminium	0	915	51	—	—	—	—	153	162	0.364
	$1 \times 10^{-6}$	910	38	25.5	0.255	-24	+ 5	153	166	0.355
	$1 \times 10^{-5}$	905	10	80.4	0.804	-97	+ 15	155	148	0.399
	$5 \times 10^{-5}$	902	3	94.1	0.941	-185	+ 27	158	165	0.358
	$1 \times 10^{-4}$	900	2	96.1	0.961	-224	+ 35	159	163	0.362
Alloy I	0	760	126	—	—	—	—	78	133	0.444
	$1 \times 10^{-6}$	757	81	35.7	0.357	-28	+ 1	82	131	0.450
	$1 \times 10^{-5}$	750	59	53.2	0.532	-50	+ 5	82	137	0.431
	$5 \times 10^{-5}$	746	45	64.3	0.643	-67	+ 7	70	139	0.424
	$1 \times 10^{-4}$	742	33	73.8	0.738	-81	+ 8	71	134	0.440
Alloy II	0	745	130	—	—	—	—	46	145	0.407
	$1 \times 10^{-6}$	760	103	20.8	0.208	-11	+ 5	46	142	0.415
	$1 \times 10^{-5}$	750	71	45.4	0.454	-32	+ 5	46	142	0.415
	$5 \times 10^{-5}$	723	46	64.6	0.646	-81	+ 20	48	143	0.413
	$1 \times 10^{-4}$	714	40	69.2	0.692	-116	+ 19	48	143	0.413

Table (37): Effect of 3-mercapto-4-phenyl-5-p-nitrophenyl-1,2,4-triazole on the electrochemical and corrosion behaviour of aluminium and its alloys in 0.5 M H<sub>2</sub>SO<sub>4</sub> solution.

Electrode	Additive concn. (M)	-E <sub>corr.</sub> mV (SCE)	i <sub>corr.</sub> $\mu\text{A}/\text{cm}^2$	% I (inh. effec.)	Surf. Coverage ( $\theta$ )	$\Delta\eta_c$ (mV) at 360 $\mu\text{A}/\text{cm}^2$	$\Delta\eta_a$ (mV) at 162 $\mu\text{A}/\text{cm}^2$	Tafel slopes.		Transfer coeff. ( $\alpha$ )
								b <sub>a</sub> (mV)	b <sub>c</sub> (mV)	
Aluminium	0	915	51	—	—	—	—	152	162	0.364
	1x10 <sup>-6</sup>	913	18	64.7	0.647	-46	+ 18	152	173	0.341
	1x10 <sup>-5</sup>	911	19	62.7	0.627	-73	+ 26	148	173	0.341
	5x10 <sup>-5</sup>	908	6	88.2	0.882	-171	+ 38	157	173	0.341
	1x10 <sup>-4</sup>	904	4	92.2	0.922	-195	+ 59	150	170	0.347
Alloy I	0	760	126	—	—	—	—	76	133	0.444
	1x10 <sup>-6</sup>	742	71	43.7	0.437	-39	+ 2	80	133	0.444
	1x10 <sup>-5</sup>	740	54	57.1	0.571	-51	+ 5	71	133	0.444
	5x10 <sup>-5</sup>	737	47	62.7	0.627	-64	+ 6	69	133	0.444
	1x10 <sup>-4</sup>	734	34	73.0	0.730	-77	+ 5	69	133	0.444
Alloy II	0	745	130	—	—	—	—	47	145	0.407
	1x10 <sup>-6</sup>	720	60	53.8	0.538	-53	+ 1	46	149	0.396
	1x10 <sup>-5</sup>	713	37	71.5	0.715	-93	+ 1	50	150	0.393
	5x10 <sup>-5</sup>	706	24	81.5	0.815	-110	+ 3	56	150	0.393
	1x10 <sup>-4</sup>	694	14	89.2	0.892	-132	+ 4	52	150	0.393



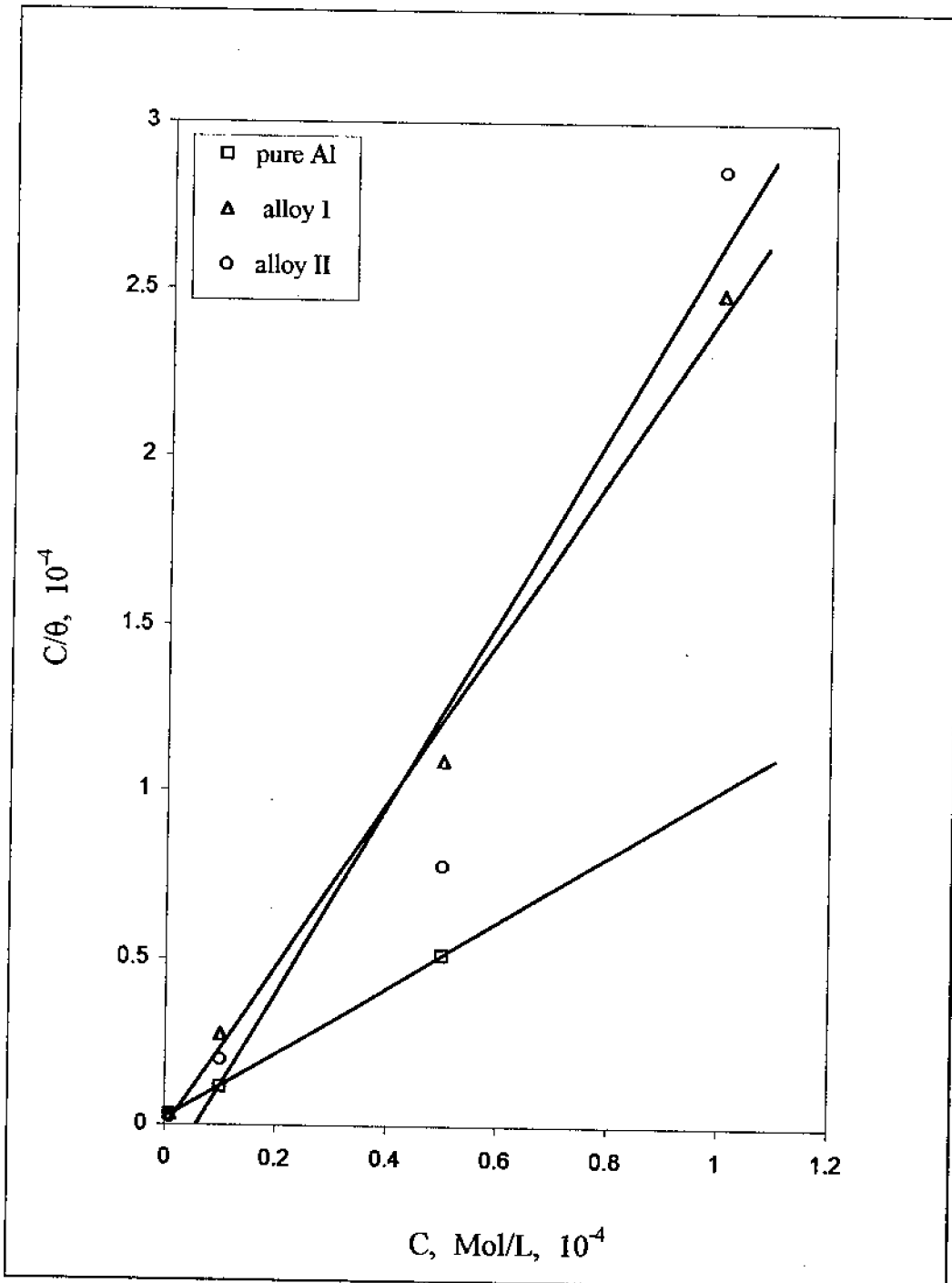


Figure (47): adsorption isotherm for 3-mercapto-4-phenyl-5-4-pyridyl-1,2,4-triazole on pure Al and its alloys in 0.5 M HCl solution.

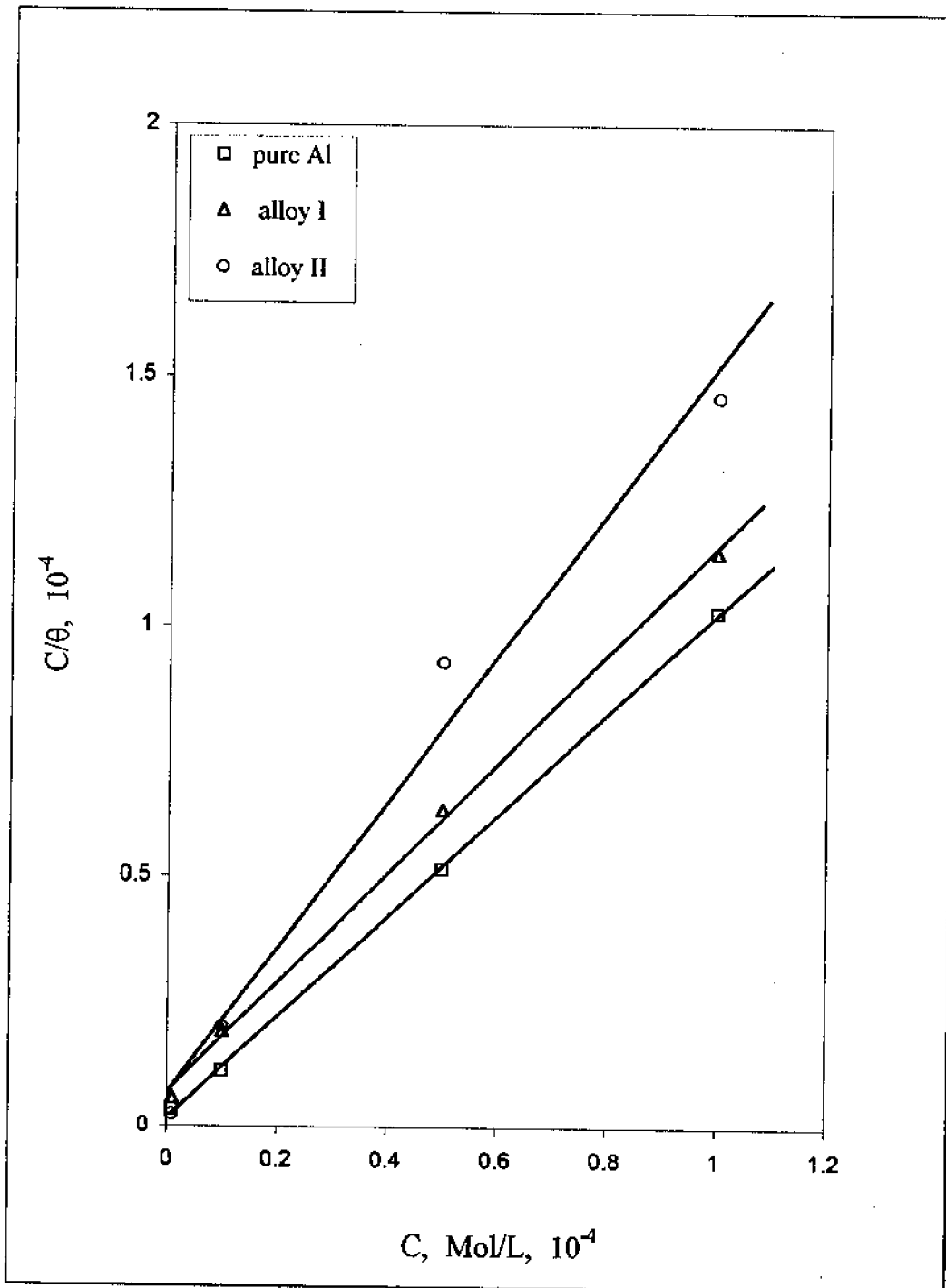


Figure (48): adsorption isotherm for 3-mercapto-4-phenyl-5-p-tolyl-1,2,4-triazole on pure Al and its alloys in 0.5 M HCl solution.

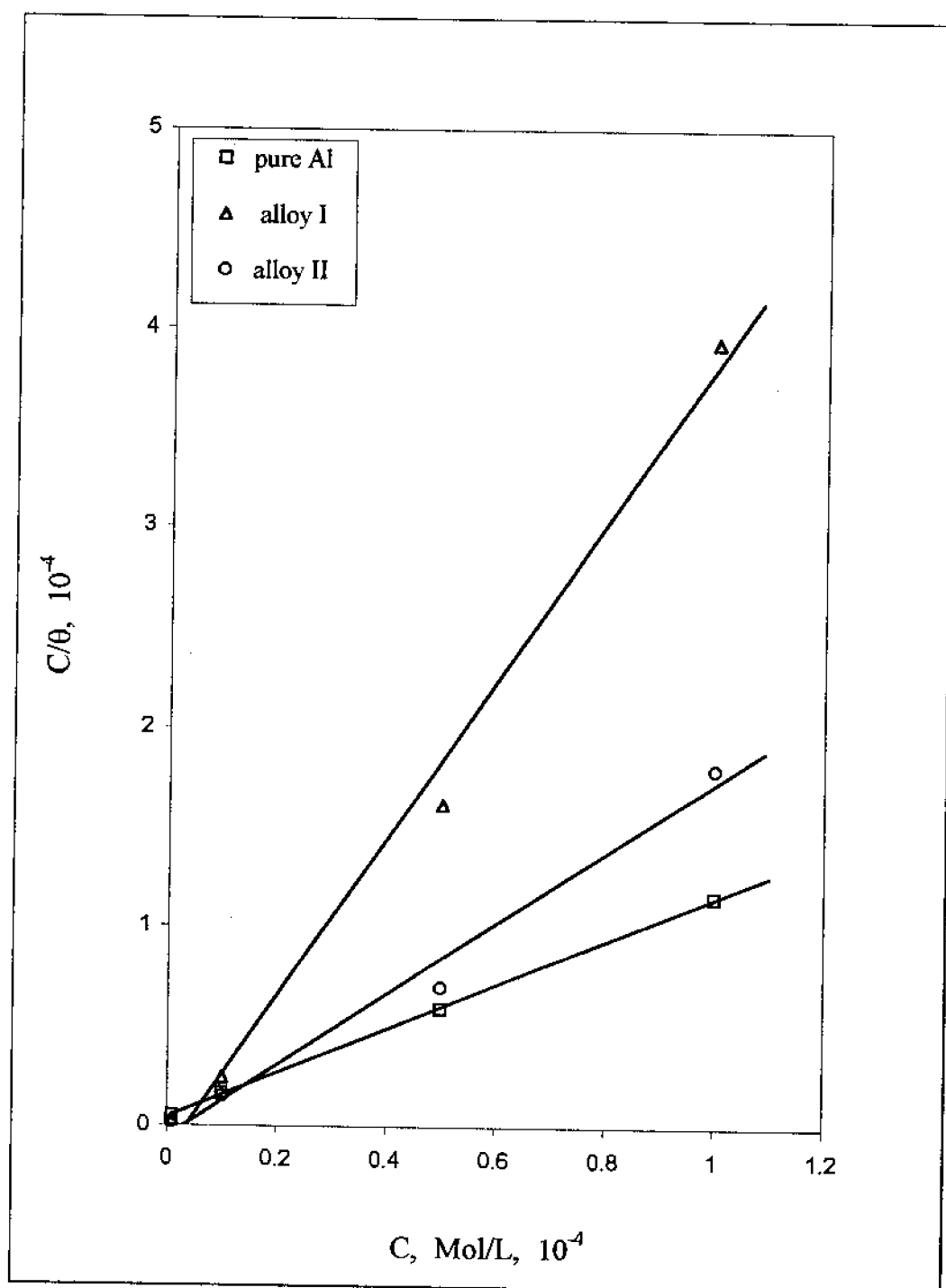


Figure (49): adsorption isotherm for 3-mercapto-4-phenyl-5-p-nitrophenyl-1,2,4-triazole on pure Al and its alloys in 0.5 M HCl solution.

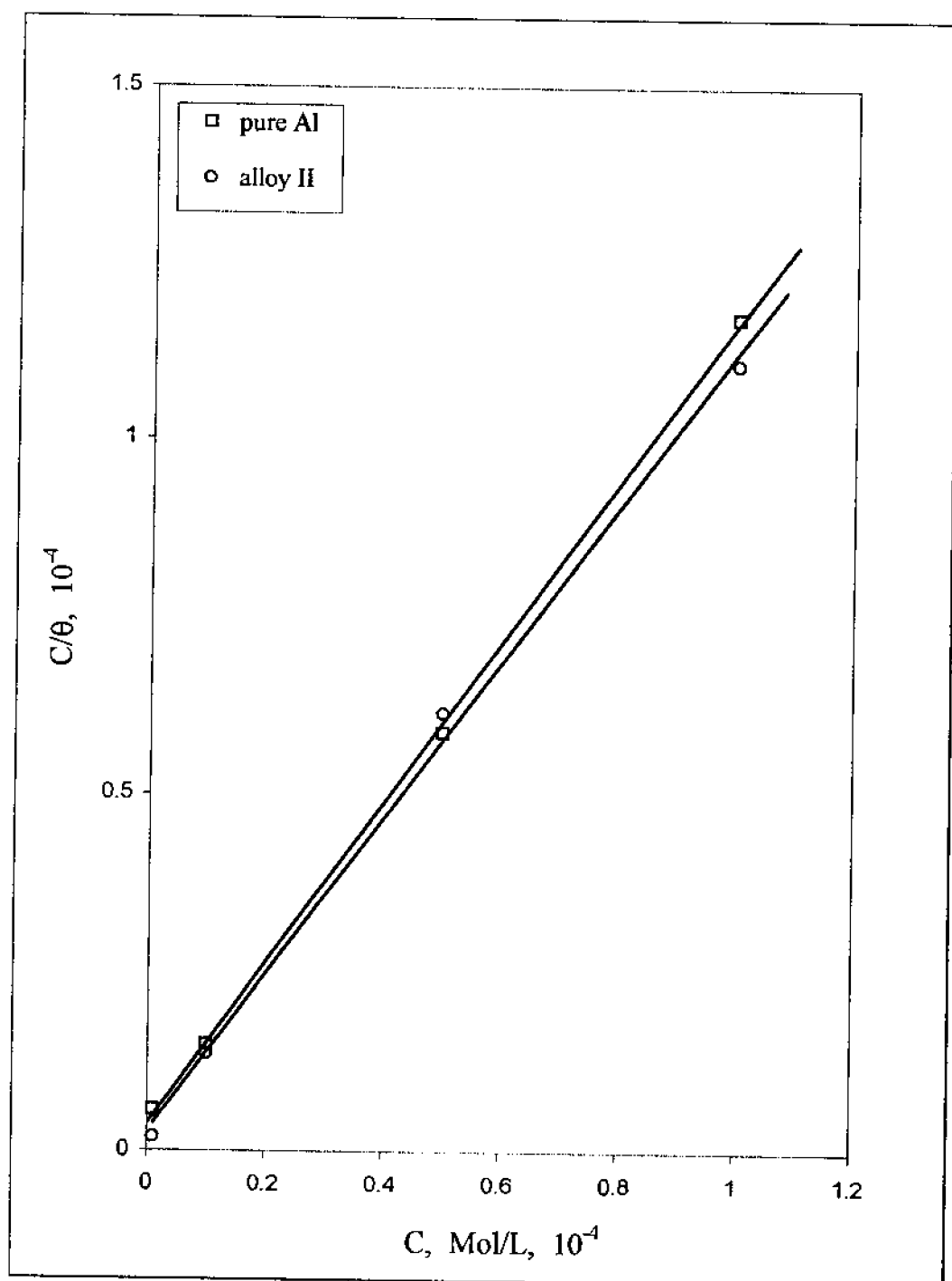


Figure (50): adsorption isotherm for 3-mercapto-4-phenyl-5-4-pyridyl-1,2,4-triazole on pure Al and its alloys in 0.5 M  $\text{HClO}_4$  solution.

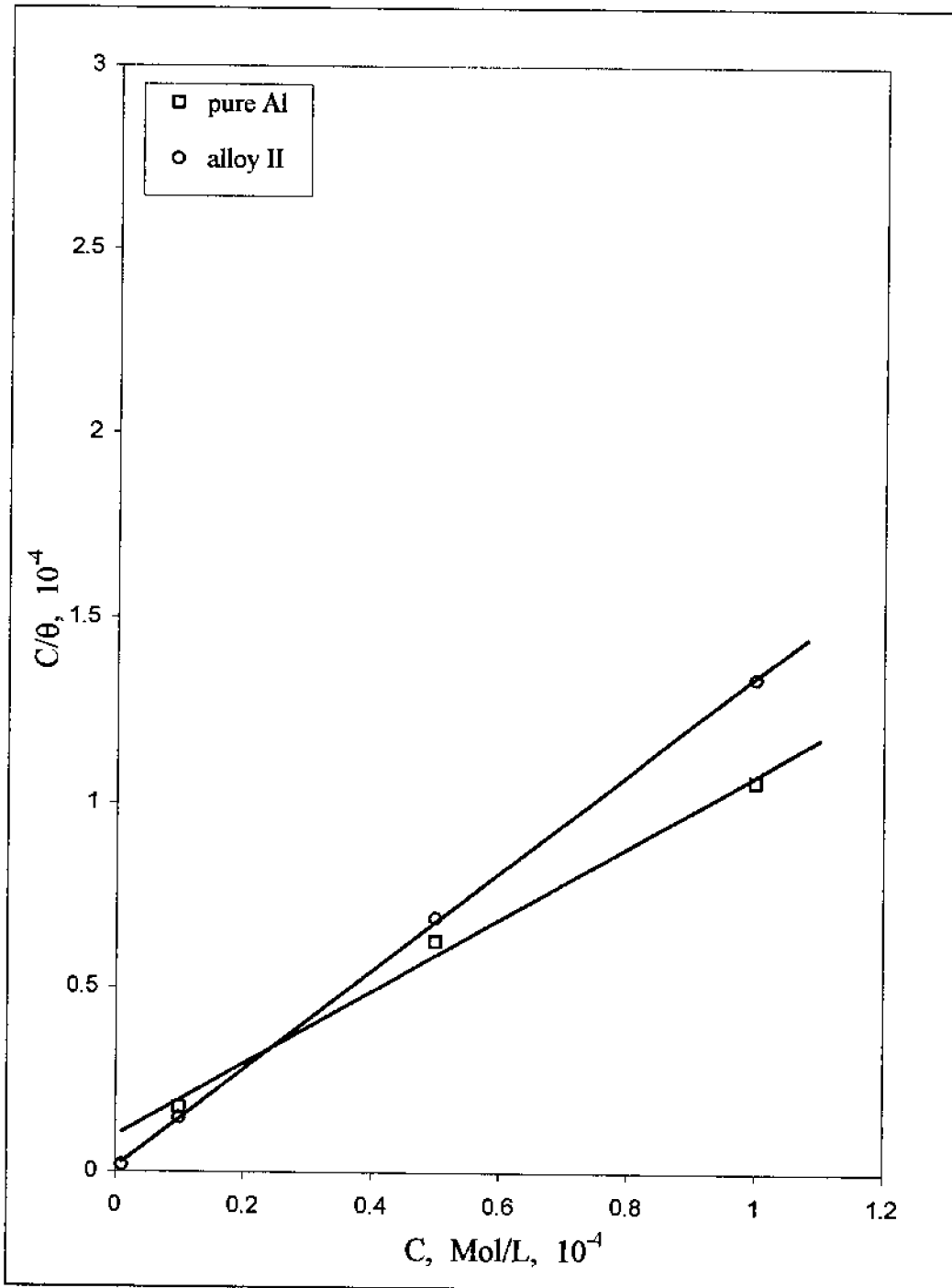


Figure (51): adsorption isotherm for 3-mercapto-4-phenyl-5-p-tolyl-1,2,4-triazole on pure Al and its alloys in 0.5 M HClO<sub>4</sub> solution.

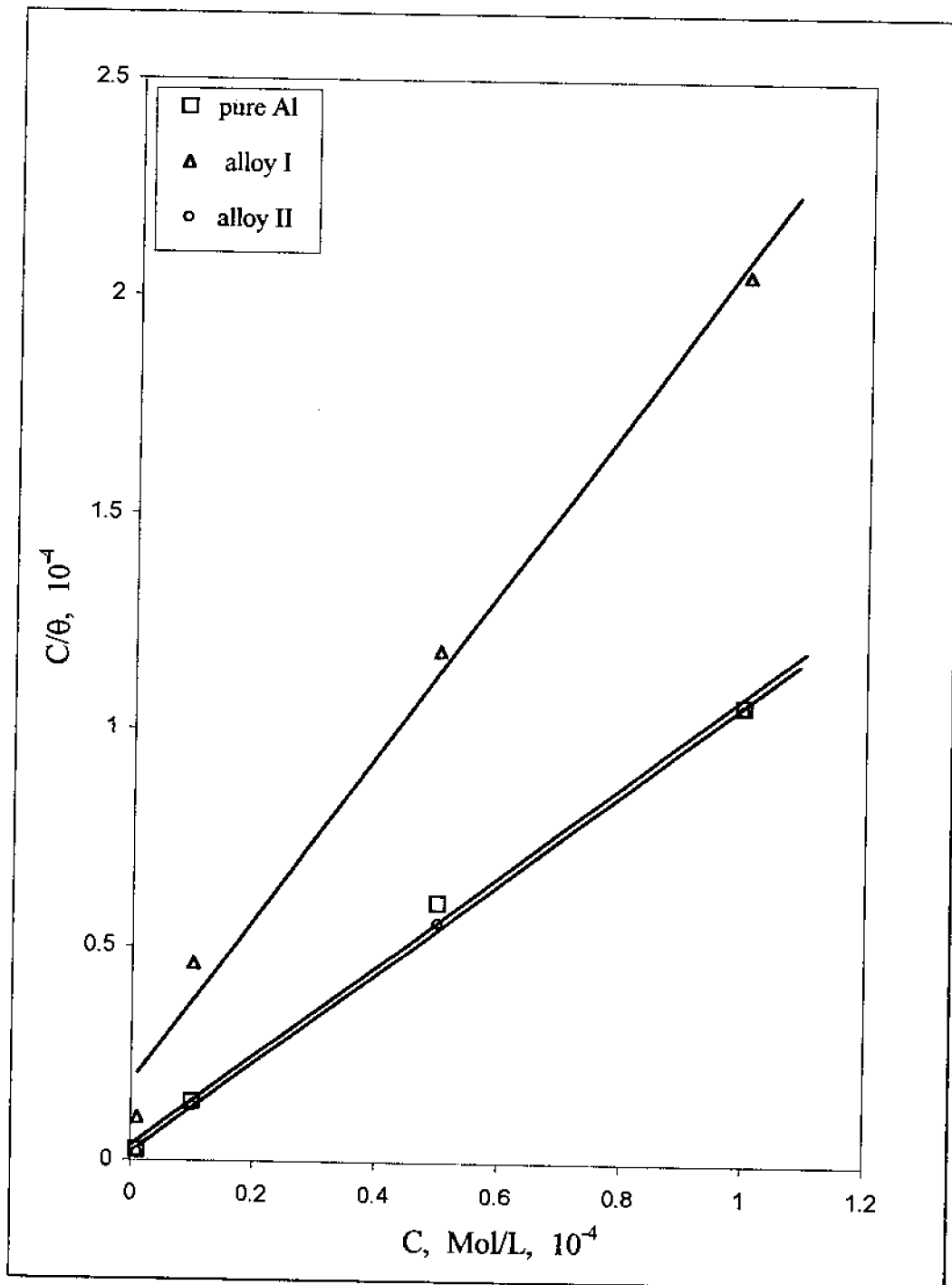


Figure (52): adsorption isotherm for 3-mercapto-4-phenyl-5-p-nitrophenyl-1,2,4-triazole on pure Al and its alloys in 0.5 M HClO<sub>4</sub> solution.

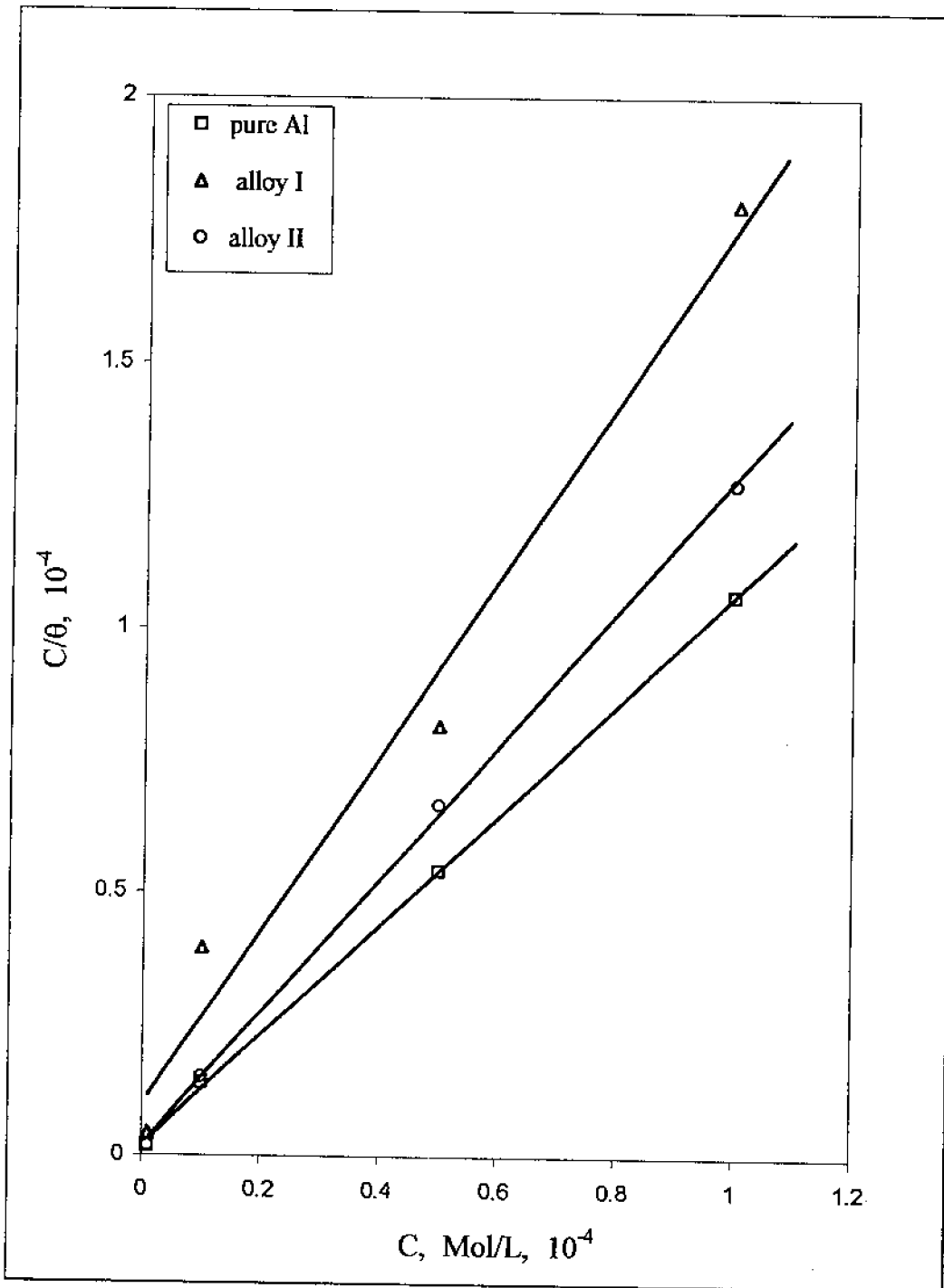


Figure (53): adsorption isotherm for 3-mercapto-phenyl-5-4-pyridyl-1,2,4-triazole on pure Al and its alloys in 0.5 M  $\text{H}_2\text{SO}_4$  solution.

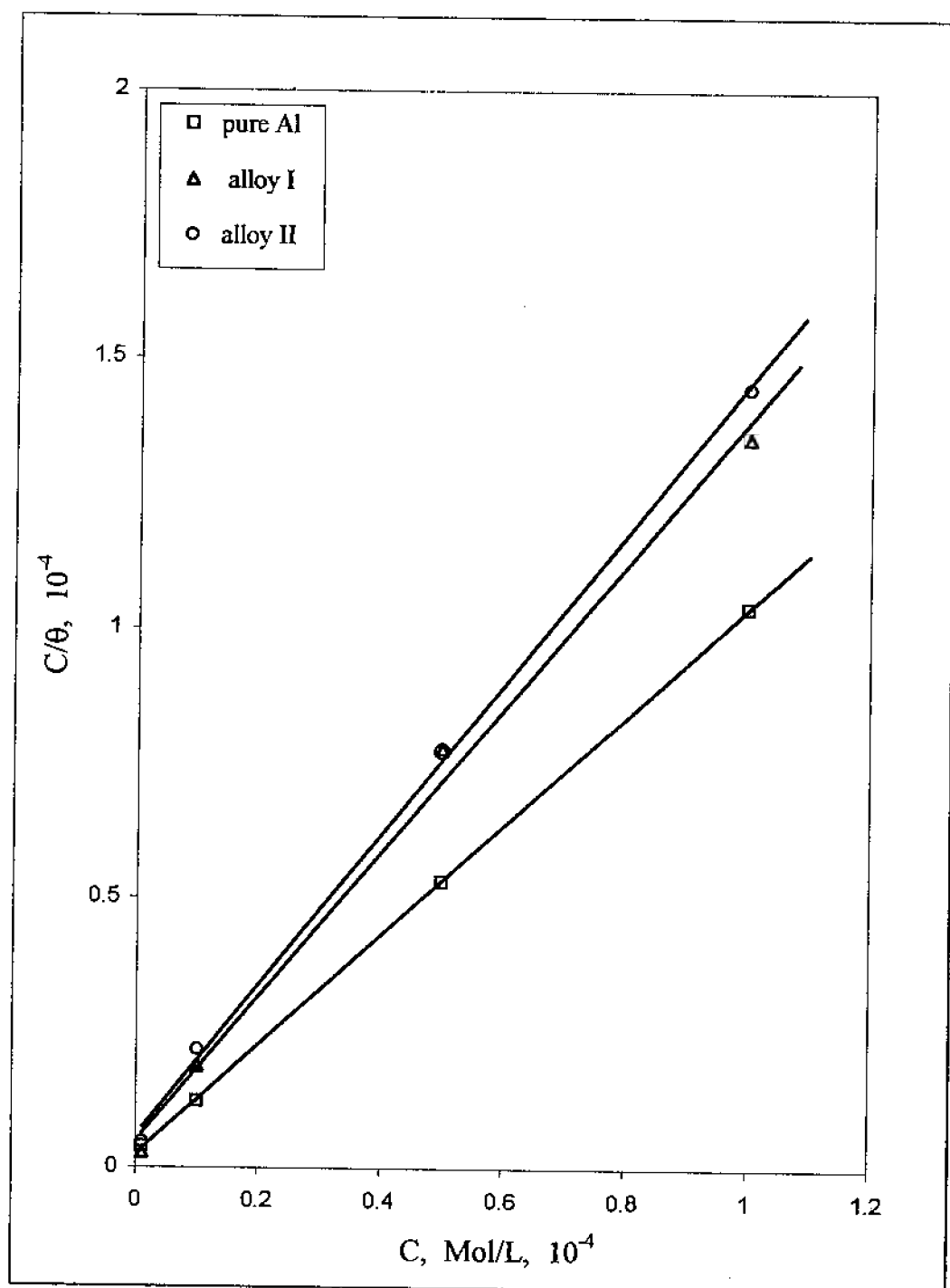


Figure (54): adsorption isotherm for 3-mercapto-4-phenyl-5-p-tolyl-1,2,4-triazole on pure Al and its alloys in 0.5 M H<sub>2</sub>SO<sub>4</sub> solution.



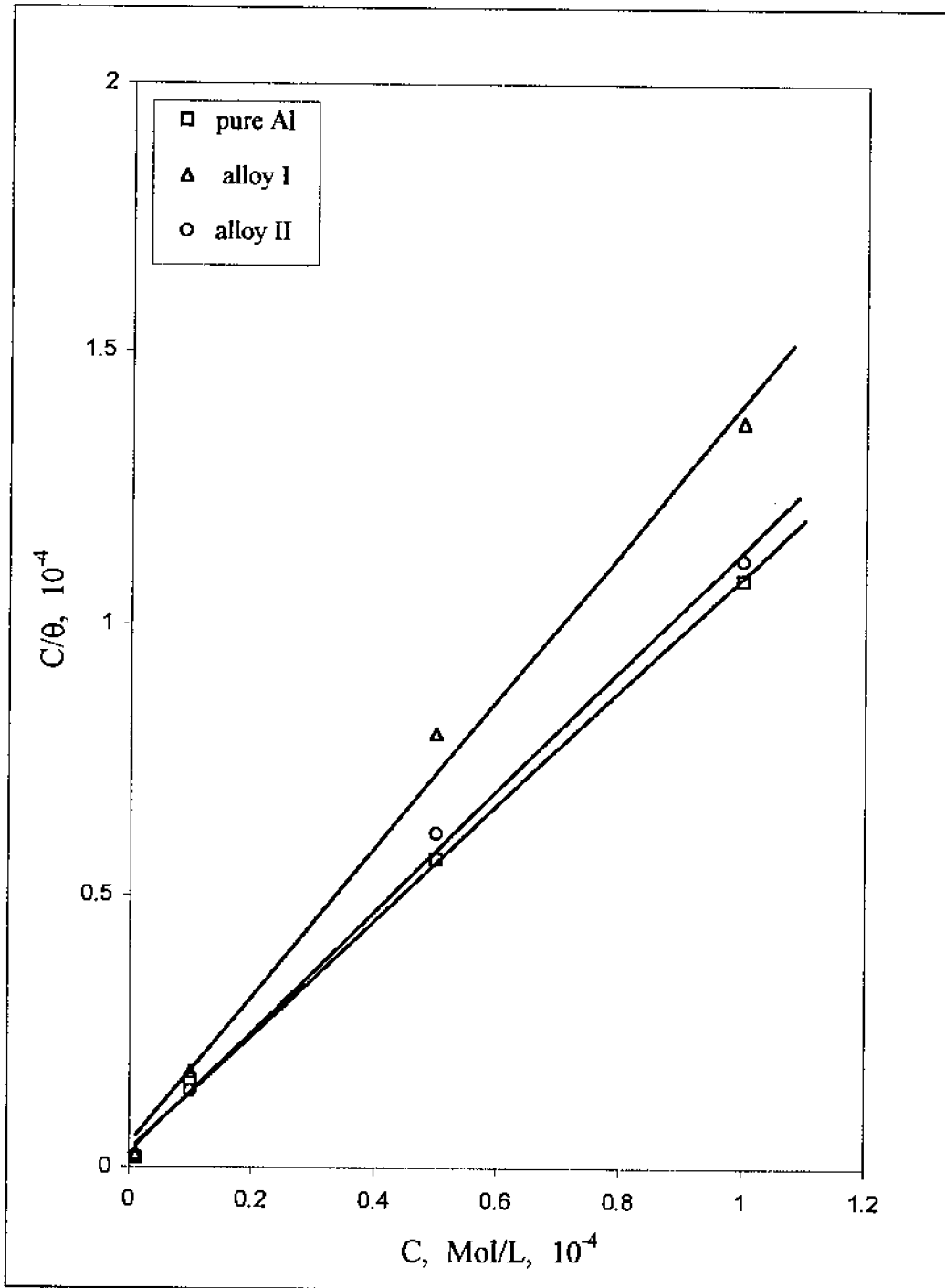


Figure (55): adsorption isotherm for 3-mercapto-4-phenyl-5-p-nitrophenyl-1,2,4-triazole on pure Al and its alloys in 0.5 M H<sub>2</sub>SO<sub>4</sub> solution.

DISCUSSION DISCUSSION DISCUSSION

DISCUSSION DISCUSSION

DISCUSSION DISCUSSION DISCUSSION

DISCUSSION DISCUSSION

DISCUSSION DISCUSSION DISCUSSION

DISCUSSION DISCUSSION

DISCUSSION DISCUSSION DISCUSSION

DISCUSSION DISCUSSION

DISCUSSION DISCUSSION DISCUSSION

DISCUSSION DISCUSSION

DISCUSSION DISCUSSION

# ***DISCUSSION***

DISCUSSION DISCUSSION

DISCUSSION DISCUSSION

DISCUSSION DISCUSSION DISCUSSION

DISCUSSION DISCUSSION

DISCUSSION DISCUSSION DISCUSSION

DISCUSSION DISCUSSION

DISCUSSION DISCUSSION DISCUSSION

DISCUSSION DISCUSSION

DISCUSSION DISCUSSION DISCUSSION

DISCUSSION DISCUSSION

DISCUSSION DISCUSSION DISCUSSION

## DISCUSSION

### *1. Effect of adenine, adenosine and pyrrole derivative on the electrochemical and corrosion behaviour of pure aluminium and its alloys in 0.5M solutions of HCl, HClO<sub>4</sub> and H<sub>2</sub>SO<sub>4</sub>.*

#### 1.1 Behaviour in HCl solution:

The data of Tafel lines for cathodic hydrogen evolution reaction indicate that in the pure HCl solution, although values of the cathodic Tafel slope for the alloys (I and II) are close or slightly higher than the values calculated from the equation  $b_c = 2.3(2RT/F) = 118 \text{ mV}$  at  $25^\circ\text{C}$  (the hydrogen evolution reaction on aluminium electrodes essentially free of "spontaneous oxide" was found to follow the slow discharge mechanism)<sup>(82)</sup>. Higher values of the cathodic Tafel slope in case of pure Al may be ascribed to the specific adsorption of chloride ions and/or the incomplete dissolution of the spontaneously formed oxide film (barrier type). It was reported that, if aluminium is left in the acid electrolyte for a long time, some but not all of the film dissolved<sup>(83)</sup>. Cathodic Tafel slopes of  $\sim 300 \text{ mV/decade}$  were obtained by Kunze<sup>(84)</sup> and by Hoggard and Egarl<sup>(85)</sup> for super-pure aluminium in aqueous solutions. A value of  $175 \text{ mV}$  of the cathodic Tafel slope for aluminium (99.6%) in NaCl solution was reported by Nisancioglu and Holtan<sup>(79)</sup>. Chakrabarty, Singh and Agarwal<sup>(86)</sup> reported values for the cathodic Tafel slope for Al (purity 99.26-99.82%) of  $160\text{-}210 \text{ mV/decade}$  in 20% nitric acid solution. Metikos et al.<sup>(75)</sup> reported that the values of the Tafel slopes for hydrogen evolution reaction (h.e.r.)  $> 2.3(2RT/F)$  ( $118 \text{ mV}$  at room temperature)

usually are regarded as anomalous since they can not be predicted. For any mechanism by the two well-known theoretical procedures, namely, the steady-state method and the quasi-equilibrium approach, without making assumptions that are easily contestable. Preparation of the working electrode involved exposure to air. Therefore, the electrodes undoubtedly had a thin oxide film on their surface before being introduced into the cell. The presence of a film could have influenced the reduction process at the surface by affecting the energetics of the reaction at the double layer, by imposing barrier to charge transfer through the film, or both. The barrier-film model was a consistent way of explaining the high Tafel slopes for the h.e.r. observed. This assumed that a fraction of the applied electrode solution overpotentials operated across the surface film and was not available to assist the charge transfer (h.e.r) at the film-solution interface<sup>(87)</sup>. For a typical electrode reaction (e.g., h.e.r on an oxide-covered electrode), the cathodic reaction of hydrogen evolution involved passage of electrons the potential energy barrier within the film to reach the film-solution interface at a rate influenced by part  $V_{\text{Film}}$  of the total potential difference ( $V_t$ ). The charge transfer of the other reactant hydrogen ion ( $\text{H}_3\text{O}^+$ ) across a separate barrier within the Helmholtz double layer was influenced by the potential  $V_{\text{H}^+}$ .

Thus,

$$i_{\text{H}} = K_{\text{H}} C_{\text{H}} \exp \left[ \frac{-\beta (\eta_t - \eta_{\text{Film}}) F}{RT} \right] \quad (5)$$

Where  $\beta$  was the charge transfer symmetry factor with the usual value equal to 0.5,  $\eta_t$  was the total overpotential across the metal-film solution interface, and  $\eta_{\text{Film}}$  was the potential drop across the film. According to equation (5), the Tafel slope was:

$$\frac{\partial \eta_i}{\partial \log i} = - \frac{2.303 RT}{\beta F (1 - \frac{\partial \eta_{\text{Film}}}{\partial \eta_i})} = \text{Tafel slope} \quad (6)$$

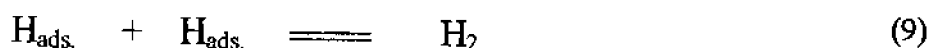
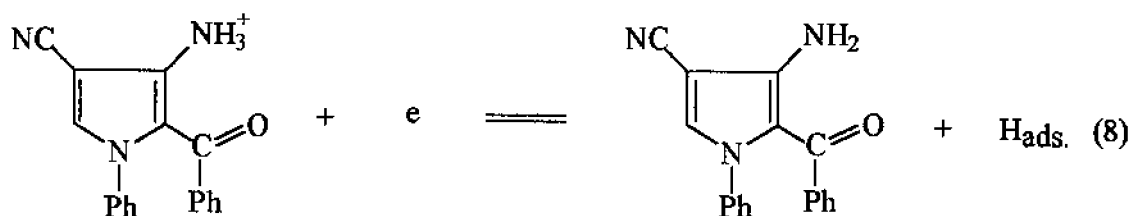
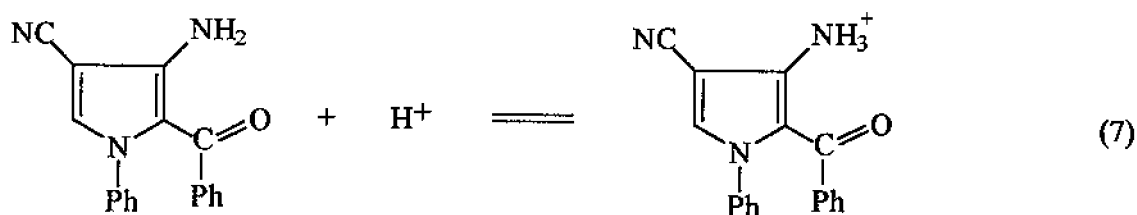
Thus, a slope with a value  $> 118$  mV/dec. was obtained when  $\partial \eta_{\text{Film}}/\partial \eta_i$  assumed a positive value. At  $\eta_i = 0.5$ , then the value of the slope from equation (6) was 236 at room temperature.

Presence of a semi conducting oxide on the electrode surface led to a higher overpotential at a given rate, that is, to an inhibition (or retardation) of the electrode reaction<sup>(88)</sup>. The semi conducting surface oxides also resulted in partial or complete inhibition of the electrode reaction even before the formation of a complete monolayer of the oxide. Further details on these inhibition effects were reviewed by Conway<sup>(89)</sup> and Gilroy and Conway<sup>(90)</sup>. Anodic Tafel slopes ( $b_a$ ) ranged from 130-150 mV in case of pure Al and from 40-60 mV in case of its alloys, indicating growth of the spontaneous oxide layer especially of pure Al during anodic polarization up to the breakdown potential<sup>(91)</sup>.

The corrosion current ( $i_{\text{corr.}}$ ), determined by extrapolation of the cathodic Tafel curves, the data show that all investigated organic compounds (except pyrrole derivative in case of alloy I) decrease the corrosion current of both pure aluminium and its alloys. For both pure aluminium and the investigated alloys in the presence of adenine, adenosine and pyrrole derivative shift the open circuit corrosion potential in the positive direction and such shift increases with the increase in inhibitor concentration. Based on the shift in corrosion potential and the increase in the cathodic overpotential in the presence of the organic additives (cathodic Tafel lines for pure aluminium and alloys I and II are

shown in Figs. 2-19 and  $\Delta \eta_c$  values at an applied c.d. of  $360 \mu\text{A}/\text{cm}^2$  are given in Tables 2-10). adenine, adenosine and pyrrole derivative can be considered as mixed type inhibitors<sup>(76)</sup> (at all examined organic compounds in case of pure aluminium and alloy II and in the presence of adenine and adenosine in case of alloy I only).

The results of inhibition efficiency ( %I ) in Table (13) indicate that 3-amino-4-cyano-2-benzoyl-N-phenyl pyrrole inhibits the corrosion of both pure aluminium and alloy II, and the inhibition efficiency also increases as an increase in the concentration of the inhibitor. But, such additive has influence to increase the corrosion current for alloy I in HCl solution, and the maximum value of  $i_{\text{corr.}}$  is obtained at higher concentration of such additive ( $10^{-4}$  M). This indicating that the addition of this compound catalyze the hydrogen evolution reaction on alloy I. This behaviour may be attributed to the presence of iron and silicon as  $\text{FeAl}_3$  and  $\text{Fe}_2\text{SiAl}_8$  intermetallic compounds<sup>(92)</sup> at the aluminium-alloy surface which cause high accelerating effect on the hydrogen evolution reaction in the presence of such additive. This may takes place according to the following reaction sequence:



Simple aminothiols were found to be protonated at the amino group, in acidic solutions<sup>(93)</sup>. On the other hand, the results exhibited that pyrrole derivative gives an opposite effect on alloy II compared to alloy I, that is, the inhibition efficiency increases as the concentration of such additive is increased. This behaviour may be attributed to the high density of cathodic active sites at the alloy II surface (iron-rich phases)<sup>(92)</sup>, which interact with inhibitor molecules to produce an insoluble complex, leading to coverage of the majority of those cathodic active sites<sup>(76)</sup>.

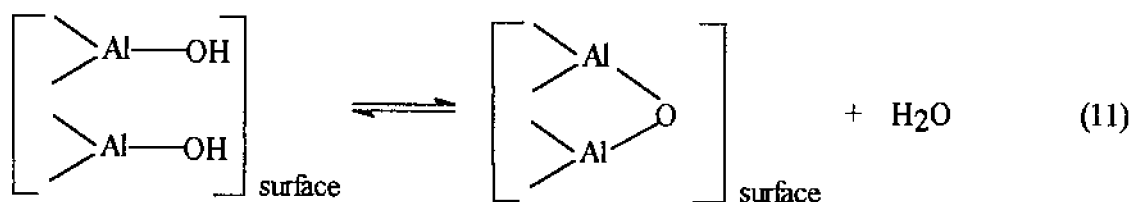
The data in Tables 11 and 12 showed that  $i_{\text{corr}}$  decreases and inhibition efficiency ( %I ) increases as the concentration of adenine or adenosine is increased in HCl solution of both pure aluminium and its investigated alloys. It is observed that, the inhibition efficiency of adenine and adenosine in case of pure Al is higher than that of corresponding obtained for alloys I and II at all examined concentrations. However, the inhibition efficiency of adenosine is higher than the adenine of both pure Al and its investigated alloys.

According to Vijh<sup>(82)</sup> and Desai et al.<sup>(94)</sup>, the potential of zero charge (PZC) of Al in acidic media  $E_{q=0} = -0.4$  V. Values of the  $\phi$  potential of pure Al and Al-alloys I and II were calculated according to the following equation:

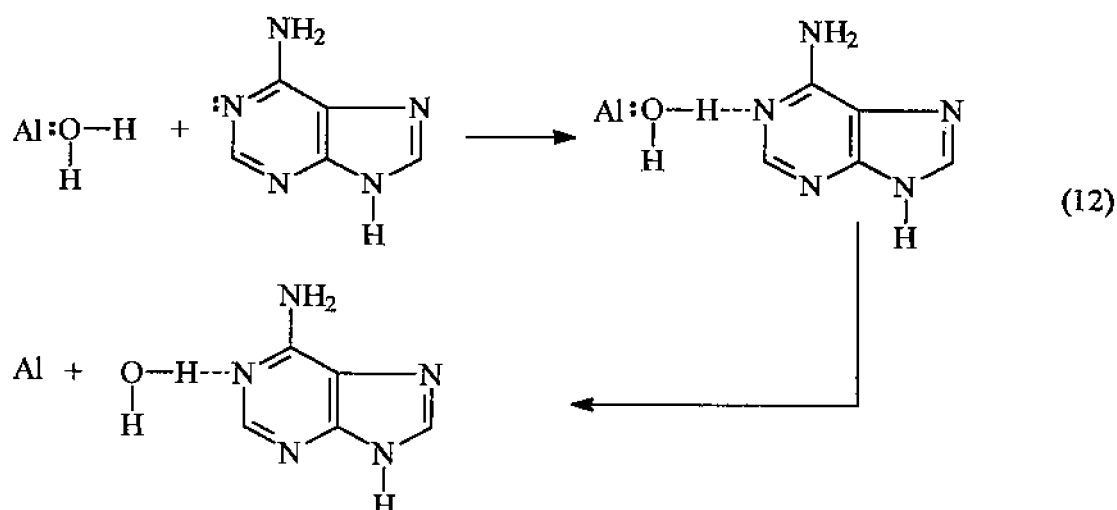
$$\phi = E_{\text{ocp}} - E_{q=0} \quad (10)$$

Hence, values of the  $\phi$  potential of pure Al and Al-alloys I and II are  $-0.28$ ,  $-0.133$ ,  $-0.126$  V, respectively. This indicate that pure Al and its alloys are negatively charged at the  $E_{\text{ocp}}$ . On the other hand, adenine and adenosine

undergo protonation in aqueous acidic solutions<sup>(34)</sup>, thus the initial step of adsorption may be involve the protonated molecules. According to Blomgren and Bockris<sup>(95)</sup> and Foroulis<sup>(96)</sup> aromatic amines (aniline, pyridine and quaternaries) which are preferentially adsorbed in the cation form, lie flat on the electrode surface and adsorption via a mechanism involving  $\pi$ -electron interactions between the aromatic nucleus and the metal surface is also possible. Before proceeding with a development of equations describing the mechanism of adsorption occurring at the electrolyte-oxide interface, a particular model for these processes is required. The following model will be assumed and is consistent with that arising from studies of double layer at oxide-solution interface<sup>(90)</sup>. Equilibrium is assumed with respect to reactions of the following type:

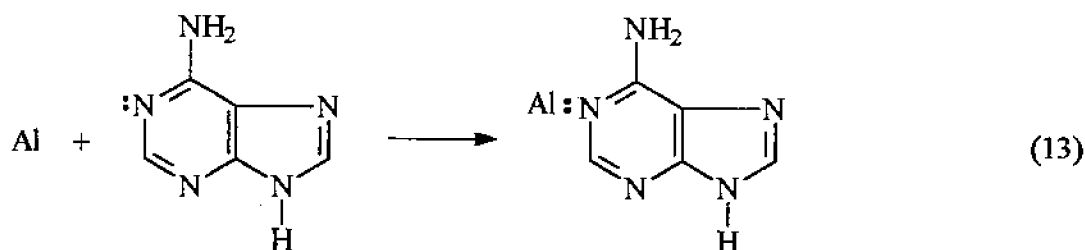


Adenine or adenosine molecules have electron-donating ability and can displace adsorbed water on the surface<sup>(91,97)</sup> by hydrogen bridging with its unshared electron pair as follows:





After losing adsorbed water the electrode surface becomes electron-acceptable, and inhibitor molecules can be easily adsorbed:



The adsorption of an organic adsorbate on the surface of a metal is regarded as a substitutional adsorption process between the organic compound in the aqueous phase  $\text{Org}_{(\text{aq})}$  and the water molecules adsorbed on the electrode surface  $\text{H}_2\text{O}_{(\text{s})}$ <sup>(21)</sup>:



Where  $n$  is the size ratio, which is the number of water molecules replaced by one molecule of organic adsorbate.

The data exhibit that adenosine is greater inhibitive action on both Al and its alloys than the adenine under the same conditions. This behaviour can be ascribed to adsorption of the larger molecules of adenosine compared to adenine molecules, so enhancing the inhibition efficiency of the cathodic process. Lower values for the inhibition efficiency in case of the investigated alloys compared to those of pure Al can be ascribed to the presence of iron as a minor alloying elements, thus, increasing the catalytic activity of Al-alloys (no silicon can be detected in the film above the aluminium matrix containing 1% Si).

The data of galvanostatic anodic polarization of pure Al and its investigated alloys in 0.5M HCl solution in the absence and presence of  $10^{-6}$ - $10^{-4}$  M in case of pyrrole derivative and  $10^{-5}$ - $10^{-3}$  M in case of both adenine and adenosine are shown in Tables 11,12 and 13 together with corrosion current, inhibition efficiency, the values of  $\Delta \eta_a$  and the values of  $\Delta \eta_c$  and corrosion potential. These results show that the anodic Tafel slope ( $b_a$ ) in case of pure Al is greater than of its alloys. On the other hand, value of  $b_a$  seems to be the same in the absence and presence of all investigated organic compounds. This indicates that anodic dissolution process takes place at the uncovered part of the electrode surface. The inhibition of anodic dissolution process is associated with the increase in the value of  $\Delta \eta_a$  in the presence of all investigated compounds of both pure Al and its alloys. These results suggested that retardation of the electrodes processes occurs, at anodic sites, as a result of coverage of the majority of anodic active sites of pure Al or its alloys by the inhibitor molecules.

### **1.2. Behaviour in HClO<sub>4</sub> solution:**

The data obtained for the electrochemical and corrosion behaviour of pure aluminium and its alloys, in 0.5 M HClO<sub>4</sub> solution in the absence and presence of pyrrole derivative, adenine and adenosine within the concentration range  $10^{-6}$ - $10^{-4}$  M in case of pyrrole derivative and  $10^{-5}$ - $10^{-3}$  M in case of adenine and adenosine are given in Tables 14-16. The results indicate that pyrrole derivative inhibits the corrosion (except at higher concentration,  $10^{-4}$  M, in case of alloy I) of both pure Al and the investigated alloys even at the lowest examined concentrations. The presence of pyrrole derivative shifts the open circuit corrosion potential in the positive direction and such shift increases with the increase in inhibitor

concentration. Based on the shift in corrosion potential and the increase in the cathodic overpotential in the presence of the inhibitor (cathodic Tafel lines for pure Al and its investigated alloys are shown in Figs. 12 and 13 and  $\Delta \eta_c$  and  $\Delta \eta_a$  values are given in Table 16 pyrrole derivative can be considered as mixed type inhibitor<sup>(76)</sup>. The data recorded in Table 16 indicate that for pure Al and its alloys (except at  $10^{-4}$ M in case of alloy I) the increase in the inhibition efficiency with concentration is associated with a decrease in the value of corrosion current ( $i_{corr.}$ ), denoting a decrease in the true surface area available for hydrogen deposition (hydrogen evolution occurs at the uncovered parts of the electrode surface). Both approximate constancy of both the cathodic Tafel slope ( $b_c$ ) and anodic dissolution Tafel slope in the absence and presence of the inhibitor suggest that the presence of pyrrole derivative does not affect the mechanism of both hydrogen evolution and anodic dissolution reactions.

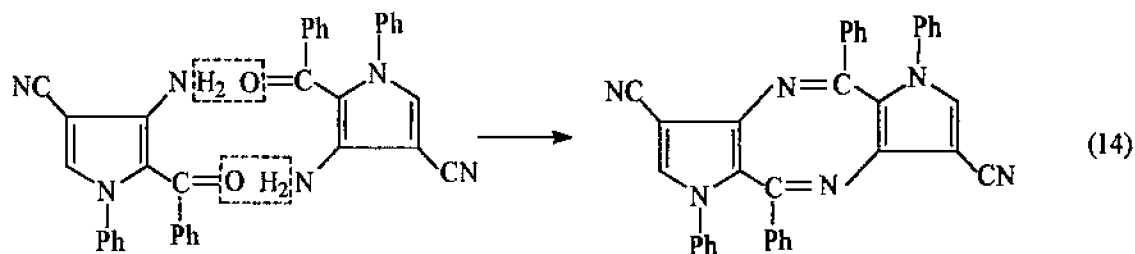
The increase in the corrosion current of alloy I in the presence of pyrrole derivative (at  $10^{-4}$ M) associated with positive value of change in hydrogen overpotential ( $\Delta \eta_c$ ) and corresponding to that inhibition efficiency becomes negative one. This indicates that catalytic effect on the hydrogen evolution reaction at higher concentration ( $10^{-4}$ M) of the additive is occurred. This behaviour may be attributed to the presence of iron in the alloy I (as  $FeAl_3$  intermetallic compound) at the alloy surface may catalyze the reduction of  $C \equiv N$  group for 3-amino-4-cyano-2-benzoyl-N-phenyl pyrrole. Cathodic overpotential values for pure Al and the investigated alloys at different current densities in 0.5 M  $HClO_4$  solution in the absence and presence of  $10^{-5}$ - $10^{-3}$ M adenine and adenosine are recorded in Tables 5 and 6. The parameters of both hydrogen evolution reaction and anodic dissolution reaction in the absence and presence of such compound are

given in Tables 14 and 15. The approximate constancy of the cathodic Tafel slopes for both pure Al and its alloys indicate that the mechanism of hydrogen evolution reaction is the same in the absence and presence of the investigated compounds. However, slight change in anodic dissolution Tafel slope ( $b_a$ ) in the presence of the additives is observed. This behaviour may be ascribed to a slight change in the true surface area available for anodic dissolution reaction.

The results of inhibition efficiency,  $i_{\text{corr}}$  and  $\Delta \eta_c$  values exhibited that adenine and adenosine inhibit the corrosion of pure Al and alloy II (except alloy II at  $10^{-3}\text{M}$  concentration of adenosine, %I decreases relatively). While, the same compounds have influence to increase the corrosion current and according to that, inhibition efficiency shifts to more negative values (catalytic effect) as an increase the concentration of the additive on alloy I. This indicates that the investigated compounds catalyze the hydrogen evolution reaction on alloy I surface due to the presence of iron as  $\text{FeAl}_3$  at the alloy surface. However,  $\Delta \eta_a$  values increase with increasing the concentration of adenine or adenosine in  $0.5\text{M HClO}_4$  solution on alloy I. This result suggests that specific interaction with anodic process and the investigated compounds act as an anodic inhibitor. One can concluded that the inhibitor becomes adsorbed on the metal surface and covers the anodic regions<sup>(39)</sup>. Based on the shift in corrosion potentials of pure Al and alloy II, the increase in cathodic overpotential in Figs. 8-11 and  $\Delta \eta_c$  and  $\Delta \eta_a$  values are given in Tables 14 and 15, adenine and adenosine can be considered as an inhibitor of the mixed type<sup>(98)</sup>. Comparison of the results obtained at higher concentration ( $10^{-3}\text{M}$ ) of both adenine and adenosine in  $0.5\text{M HClO}_4$  solution of pure Al indicated that the inhibition efficiency of adenosine is higher than that of adenine. These

results suggest that the covered area of the electrode surface by adenosine molecules is expected to be much larger than the covered area by adenine molecules, due to the larger molecular size of adenosine than that of adenine. Stupnisek-Lisac and Ademovic<sup>(99)</sup> stated that the size of the adsorbed molecule influences the inhibiting properties of compound. Bigger molecules have better adsorption on the metal surface. Similar results were obtained by Fouda et al.<sup>(100)</sup> for the corrosion inhibition of Al by thiosemicarbazide derivatives in 2N HCl solution that the inhibition efficiency of additive compounds depends on many factors which include the number of adsorption sites and their charge density, molecules size, heat of hydrogenation mode of interaction with the metal surface, and formation of metallic complexes. The relative decrease in the inhibition efficiency of adenosine at highest concentration ( $10^{-3}\text{M}$ ) on alloy II compared to its efficiency at lower concentrations of such compound, can be attributed to the decrease in electrode coverage with an increase in the concentration of adenosine. So supporting the fact on insoluble complex formed at lower concentrations of the investigated compound becomes soluble. This is due to the accumulation of a large number of molecules at higher concentrations which makes the complex soluble<sup>(76)</sup>.

For pure Al, pyrrole derivative has higher inhibition efficiency in  $\text{HClO}_4$  solution compared with its %I in HCl solution at concentration  $10^{-4}\text{M}$ . This behaviour may be ascribed to strong adsorption and blocking of the electrode surface by the condensation reaction of two molecules of the 3-amino-4-cyano-2-benzoyl-N-phenyl pyrrole in  $\text{HClO}_4$  solution, according to the following reaction:



A further increase of the double bonds between  $\text{-NH}_2$  and  $\text{-C=O}$  groups gave rise to the protection efficiency of the inhibitor as result of  $\pi$ -electron interaction between the molecules and the surface. Similar results were obtained by Metikos et al.<sup>(75)</sup>, for corrosion inhibition of Al in  $\text{HClO}_4$  solution by substituted N-aryl pyrroles containing carbaldehyde groups on pyrrole ring.

### 1.3. Behaviour in $\text{H}_2\text{SO}_4$ solution:

The results for the electrochemical and corrosion of pure Al and its investigated Al-alloys in 0.5M  $\text{H}_2\text{SO}_4$  solution in the absence and presence of pyrrole derivative, adenine and adenosine within the concentration range  $10^{-6}$ - $10^{-4}$ M of pyrrole derivative and  $10^{-5}$ - $10^{-3}$ M of adenine and adenosine are given in Tables 17, 18 and 19. These results indicate that the presence of pyrrole derivative causes parallel displacement of the cathodic Tafel lines (except alloy I at all examined concentrations) towards higher overpotential of both pure Al and its investigated alloys are given in Figs.18 and 19. Such displacement increases with the increase in the concentration of organic compound, However, pyrrole derivative exhibited reverse effect on alloy I to that observed of pure Al and alloy II. The cathodic Tafel lines of alloy I shift to less negative values in the presence of pyrrole derivative, and such shift increases as an increase in the concentration. This indicates that the adsorption of additive molecules on

the alloy I surface leads to catalyze hydrogen evolution reaction (see Fig. 19), and this behaviour is similar to that observed in HCl solution.

Comparison of the results obtained for pure Al and the investigated Al-alloy in the presence of pyrrole derivative indicates that, at higher concentration ( $10^{-4}$  M) the inhibition efficiency is higher in case of pure aluminium than with alloy II. These results indicate that pyrrole derivative inhibits the corrosion of pure Al and alloy II even at the lowest examined concentration. The open circuit corrosion potential is markedly shifted in the positive direction in the presence of examined organic compound of both pure Al and its investigated alloys (I and II). The increase in cathodic overpotential of pure Al and alloy II (Table I0), together with an increase of  $\Delta \eta_a$  values with increasing concentration of such organic compound, suggest that pyrrole derivative can be considered as an inhibitor of mixed type of pure Al and alloy II, and anodic inhibitor only of alloy I<sup>(61)</sup>. At the two higher concentrations of such organic compound ( $5 \times 10^{-5}$  and  $10^{-4}$  M) in case of alloy II, relative decrease in inhibition efficiency compared to that observed at lower concentrations. This behaviour may be attributed to the soluble complex formation which leads to less inhibition at higher concentrations<sup>(76)</sup>.

The less inhibitive action of the investigated compound in  $H_2SO_4$  solution compared with that in HCl solution may be ascribed to adsorption of  $SO_4^{=}$  ions at the electrode surface<sup>(101)</sup>, leading to the hindrance of the adsorption of organic molecules. Accordingly, it can be suggested that the interaction between the metal surface and the additive compounds will be of much less significance compared with HCl and  $HClO_4$  solutions.

The data in Tables 17 and 18 show the effect of adenine and adenosine on the corrosion inhibition of pure aluminium and its alloys. It can be seen that adenine and adenosine inhibit the corrosion at all examined concentrations. The inhibition efficiency (expressed as %I) increases with inhibitor concentration. This is associated with the decrease in corrosion current,  $\Delta \eta_c$  values shift to more negative,  $\Delta \eta_a$  values shift to more positive and  $E_{\text{corr}}$  shifts to more positive with increasing the concentration of the additives. Accordingly, adenine and adenosine can be considered as inhibitors of mixed type<sup>(61)</sup>. This indicates that the investigated compounds have influence to suppress the anodic partial process and cathodic partial one. These results suggest retardation of the electrode processes occurs at both anodic and cathodic sites of both pure Al and its investigated alloys, as a result of coverage the majority of active sites by the inhibitor molecules<sup>(102)</sup>. The fact that  $b_c$  and  $b_a$  are almost the same in uninhibited and inhibited solution suggests that the inhibitory action of such compounds reduces the surface area available for hydrogen evolution and anodic dissolution without affecting their mechanism. The inhibitive effect of adenine and adenosine molecules in  $\text{H}_2\text{SO}_4$  is probably caused by hindering the adsorption of sulphate ions on pure Al and its alloys, thus preventing dissolution. Similar behaviour was previously reported by Mrowczynski et al.<sup>(103)</sup> for corrosion inhibition of iron in sulphate solution. The obtained results are similar to that observed in both HCl and  $\text{HClO}_4$  solutions, in which adenosine is much better inhibitor especially for pure Al than adenine. Therefore, the covered area by adenosine molecules is expected to be much greater than the covered area by adenine, due to the largest molecular size of adenosine. However, the results obtained for Al-alloys indicate a decrease in inhibition efficiency compared with pure Al in the presence of adenine and adenosine. This



behaviour can be attributed to the presence of iron at the alloy surface may catalyze the hydrogen evolution reaction at the alloy surface in the presence of protonated molecules. Similar results were obtained by Chakrabarty, Singh and Agarwal<sup>(86)</sup> for the corrosion inhibition of aluminium in nitric acid solution using 1-aryl substituted-3-formamidine thiocarbamide. It was concluded by Vetter<sup>(104)</sup> that a catalytic effect is present only in the adsorbed state. The results obtained by Troquet, Labbe and Pagetti<sup>(105)</sup> indicate that commercially pure zinc is more effective catalyst for the reduction of  $\text{Ph}_3\text{PhCH}_2\text{-P}^+\text{Cl}^-$  than pure zinc. It can be concluded that lower values of inhibition efficiency in case of alloys I and II ascribe to the influence of iron and silicon in the alloy which consequently results in an their catalytic activity. Abdel-Aal et al.<sup>(92)</sup> stated that lower values for inhibition efficiency in case of the Al-alloys compared to those of pure Al using  $[(\text{PhCH}_2)_4\text{P}]^+\text{Cl}^-$  can be attributed to the presence of iron as minor alloying elements, thus, increasing the catalytic activity of aluminium for the reduction of the adsorbed organic onium cations.

#### 1.4. Adsorption isotherms:

The extent of corrosion inhibition depends on the surface conditions and mode of adsorption of inhibitors<sup>(106)</sup>. Assuming that the corrosion on the covered parts of the surface equal to zero and that the corrosion takes place only on the uncovered parts of the surface, the degree of coverage ( $\theta$ ) was calculated from:

$$\theta = 1 - \frac{i_{\text{inh}}}{i_{\text{uninh}}} \quad (4)$$

The obtained adsorption isotherms for pyrrole derivative, adenine

and adenosine from the above equation are represented graphically in Figs. 20-22 in case of HCl, Figs. 23-25 in case of HClO<sub>4</sub> and Figs. 26-28 in case of H<sub>2</sub>SO<sub>4</sub>. These isotherms follow that of Langmuir which characterises the chemisorption of additive compounds on heterogeneous surfaces. For such isotherm  $C/\theta$  is a linear function of  $C$ .

The agreement between cathodic Tafel slopes ( $b_c$ ) in the absence and presence of all investigated organic compounds within the examined concentration range, suggests primary interface inhibition<sup>(16,107)</sup>. Similar isotherms were obtained by El-Sayed<sup>(76)</sup> for the adsorption of some nitrogen-heterocyclic compounds on pure Al and the same investigated Al-alloys in HCl solution.

## ***2. Effect of some triazole derivatives on the electrochemical and corrosion behaviour of pure aluminium and its alloys in 0.5M solutions of HCl, HClO<sub>4</sub> and H<sub>2</sub>SO<sub>4</sub>.***

### **2.1. Behaviour in HCl solution:**

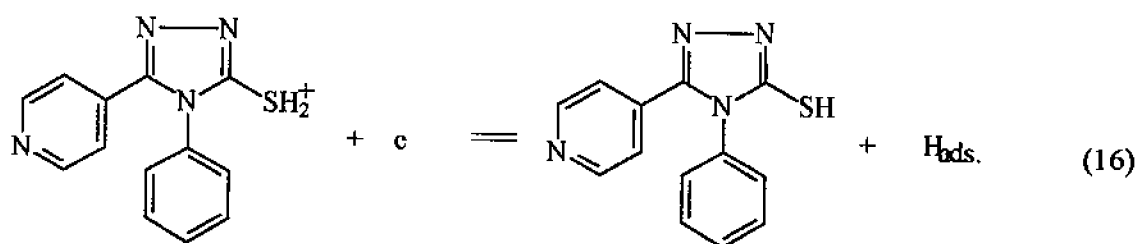
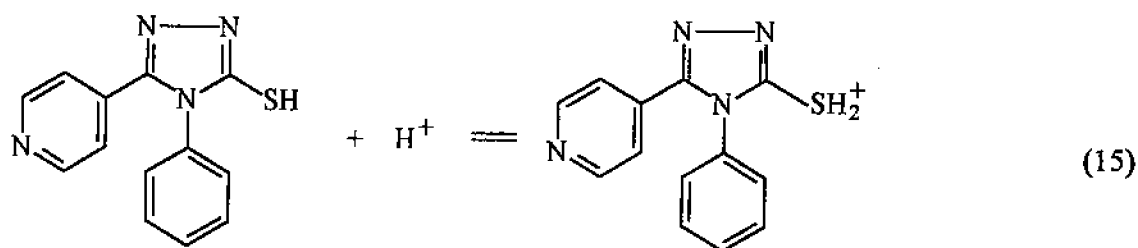
The data obtained for the electrochemical and corrosion behaviour of pure Al and its investigated alloys in 0.5M HCl solution in the absence and presence of 3-mercapto-4-phenyl-5-4-pyridyl-1,2,4-triazole indicate that the open circuit corrosion potential of both pure Al and the studied Al-alloys shift in the positive direction. Such potential shifts together with the increase of  $\eta_c$  cathodic overpotential (except at  $10^{-4}$  M in case of pure Al) and the change in overpotential of both cathodic hydrogen evolution ( $\Delta\eta_c$ ) and anodic dissolution ( $\Delta\eta_a$ ) on addition of the investigated compound, indicate that such compound can be considered as an inhibitor of mixed type. The results suggest that both cathodic and anodic partial processes are affected to the same extent<sup>(61)</sup>. The approximately constant values of the cathodic Tafel slope ( $b_c$ ) in the absence and presence of studied compound (especially in case of alloys I and II) suggests that the mechanism of hydrogen evolution reaction (h.e.r.) at the alloy surface is essentially unaffected. It can be concluded that the inhibition takes place by simple blocking of the surface, with subsequent decrease of the area available to respective partial process. Slight decrease in  $\eta_c$  values in case of alloys I and II, while sharp decrease in  $\eta_c$  values at higher concentration ( $10^{-4}$  M) are observed. This indicates that such compound at  $10^{-4}$  M is able to accelerate hydrogen evolution reaction particularly on pure Al surface.

The data in Table 29 show the decrease in the value of  $i_{\text{corr.}}$ , with the increase in  $\Delta\eta_c$  cathodic for pure Al in the presence of  $10^{-6}$  up to  $5 \times 10^{-5}$  M of 3-mercapto-4-phenyl-5-4-pyridyl-1,2,4-triazole reveal an inhibiting effect. While, a sudden increase in  $i_{\text{corr.}}$  at  $10^{-4}$  M of such compound which is associated with sharp decrease in  $\Delta\eta_c$  value, reveal a stimulating effect (catalytic of hydrogen evolution reaction). In case of alloys I and II, the  $i_{\text{corr.}}$  values decrease also with increasing concentration of such compound up to  $5 \times 10^{-5}$  M and then starts to increase again at higher concentration.

The data given in Table 29 reveal that the inhibition efficiency for the corrosion of pure Al and its investigated alloys in 0.5M HCl solution in the presence of 3-mercapto-4-phenyl-5-4-pyridyl-1,2,4-triazole increases gradually as an increase in the concentration of such compound up to  $5 \times 10^{-5}$  M. However, the inhibition efficiency becomes negative value at higher concentration ( $10^{-4}$  M) in case of pure Al, and decreases relatively in case of its alloys (I and II). The increase in inhibition efficiency (%I) as an increase in the concentration of such compound up to  $5 \times 10^{-5}$  M can be ascribed to the blocking of the surface, which enhances cathodic polarization and diminishes cathodic current density. Accordingly, hydrogen evolution reaction decreases as an increase in the inhibition efficiency because the organic compound molecules are adsorbed at the most active cathodic sites<sup>(108)</sup>. Such compound which inhibits both h.e.r. and anodic dissolution may adsorbed in flat form in case of pure Al, leading to more coverage of active cathodic and anodic sites. Accordingly, highest inhibition efficiency (97.8%) is observed at  $5 \times 10^{-5}$  M. However, adsorption of such compound on the surface in case of alloy I or alloy II is probably in the vertical position, leading to small coverage of the surface.

Therefore, lower inhibition efficiency values are observed in case of alloys I and II compared with pure Al at  $5 \times 10^{-5}$  M.

The increase in corrosion current in the presence of 3-mercapto-4-phenyl-5-4-pyridyl-1,2,4-triazole on pure Al at higher concentration ( $10^{-4}$  M) may be ascribed to a catalytic effect on the hydrogen evolution reaction. Accordingly, this may take place according to the following reaction sequence:



Similar behaviour was observed by Abdel Aal et al.<sup>(93)</sup> for the corrosion of zinc in HCl solution in the presence of benzenethiol, such a reaction results in a decrease in the cathodic overpotential ( $\Delta \eta_c$ ). The observed decrease in the cathodic Tafel slope compared with its slope at lower concentrations of the same compound, suggests a change in the mechanism of hydrogen evolution reaction, although the mechanism of the electrodisolution of pure Al remains the same.

The relative decrease in inhibition efficiency at higher concentration ( $10^{-4}$  M) in case of alloys I and II may be due to the complex formed between the iron traces in the alloy and the inhibitor. This may be ascribed to the accumulation of a large number of molecules at higher concentration which makes the complex soluble<sup>(109)</sup>.

The data given in Table 30 show the effect of 3-mercapto-4-phenyl-5-p-tolyl-1,2,4-triazole on the electrochemical and corrosion behaviour of pure Al and its investigated alloys in 0.5M HCl solution. The values of open circuit potential ( $E_{\text{corr}}$ ), corrosion rates ( $i_{\text{corr}}$ ), the change in overpotential of both cathodic hydrogen evolution reaction ( $\Delta\eta_c$ ) and anodic dissolution ( $\Delta\eta_a$ ) in the presence of the different concentrations of such compound together with the values of the inhibition efficiency, indicate that the investigated compound inhibits the corrosion of both pure Al and the investigated alloys at all examined concentrations. For both pure Al and its studied alloys, the corrosion potential is shifted in the positive direction in the presence of investigated compound, and such shift increases with the increase in the inhibitor concentrations. The marked increase in the cathodic overpotential values in the presence of such compound, together with the positive shift in  $E_{\text{corr}}$  and the increase in anodic dissolution overpotential ( $\Delta\eta_a$ ), suggest that the studied compound works by inhibiting both the anodic and cathodic reactions. Inhibitor function in this way are known as mixed type inhibitor. Figs.31 and 32 show the cathodic polarization of pure Al and its investigated alloys in the absence and presence of different concentrations of such studied compound. Similar effect of some triazole derivatives on the corrosion of steel in HCl solution was investigated by Quraishi et al.<sup>(110)</sup> They stated that all investigated triazoles are mixed type inhibitors, that is, inhibiting the

corrosion of mild steel by blocking the active sites of the metal surface.

The results obtained for the inhibitive effects of 3-mercapto-4-phenyl-5-p-tolyl-1,2,4-triazole on corrosion of pure Al and its studied alloys indicate high inhibition efficiency value, is observed in case of pure Al (97% at  $5 \times 10^{-5}$  M). While, lower values (54-78%) in case of alloys I and II are attained. The observed high inhibition efficiency on the hydrogen evolution reaction of the pure Al compared to the examined alloys, can be attributed to strong adsorption of such compound on the pure Al than of its alloys. Lower values of inhibition efficiency in case of Al-alloys compared to pure Al, may be due to the presence of iron and silicon as  $\text{FeAl}_3$  and  $\text{Fe}_2\text{SiAl}_8$  intermetallic compounds<sup>(92)</sup> at the Al-alloys surface. This leads to catalytic of the hydrogen evolution reaction and consequently low inhibition efficiency is observed. Lower inhibition efficiency in case of alloy II compared to alloy I, suggests that iron-rich phases (alloy II) have more catalytic ability<sup>(76)</sup>.

Higher values of inhibition efficiency of both pure Al and its studied alloys in the presence of 3-mercapto-4-phenyl-5-p-tolyl-1,2,4-triazole particularly at highest examined concentration ( $10^{-4}$  M) compared to that observed in the presence of 3-mercapto-4-phenyl-5-4-pyridyl-1,2,4-triazole, can be attributed to its stability toward surface protonation in HCl solution. Similar trend was observed by Abdel-Aal et al.<sup>(93)</sup> for corrosion inhibition of zinc by o-methyl benzenethiol and benzylthiol in HCl solution.

The data given in Table 31 show the effect of 3-mercapto-4-phenyl-5-p-nitrophenyl-1,2,4-triazole on the electrochemical and corrosion

behaviour of pure Al and its investigated alloys. Cathodic overpotential values for pure Al and its investigated alloys at different current densities in 0.5M HCl solution in the absence and presence of  $10^{-6}$ - $10^{-4}$  M from 3-mercapto-4-phenyl-5-p-nitrophenyl-1,2,4-triazole are recorded in Table 22. Cathodic Tafel lines for both pure Al and its investigated alloys are shown in Figs.33 and 34. Parameters for hydrogen evolution reaction including cathodic Tafel slope ( $b_c$ ) and transfer coefficient ( $\alpha$ ) in the absence and the presence of such investigated compound are given in Table 31. The approximate constancy of the cathodic Tafel slope especially for Al-alloys indicate that the mechanism of hydrogen evolution reaction is the same in the absence and presence of the investigated compound. However, the large increase in the cathodic Tafel slope in the presence of various concentrations of such organic compound, suggests a change in the mechanism of the hydrogen evolution reaction<sup>(111)</sup>. The results indicate that 3-mercapto-4-phenyl-5-p-nitrophenyl-1,2,4-triazole inhibits the corrosion of pure Al and its investigated alloys, and the inhibiting action increases as an increase in the inhibitor concentration, particularly in case of pure Al and up to  $10^{-5}$  M in case of alloy I and up to  $5 \times 10^{-5}$  M in case of alloy II. The open circuit corrosion potential is markedly shifted in the positive direction in the presence of such examined compound of both pure Al and its studied alloys. The increase in both cathodic and anodic overpotentials ( $\Delta\eta_c$  and  $\Delta\eta_a$  respectively) together with the shift in corrosion potential suggest that the studied compound can be considered as an inhibitor of the mixed type.

The data given in Table 31 indicate that the inhibition efficiency of such compound in case of pure Al at any particular concentration (except at  $10^{-6}$  M) is much higher than that of either alloy I and alloy II. These results



suggest that the adsorption in acidic solution, triazole derivative can exist as cationic species like amino acids<sup>(109)</sup>. These cationic species may adsorb on the cathodic sites of both pure Al and its investigated alloys, and decreases the evolution of hydrogen. The adsorption of triazole derivative molecules on the anodic sites through lone pairs of electrons of nitrogen and sulphur atoms may decrease anodic dissolution of pure Al and its studied alloys. On the other hand, lower values for the inhibition efficiency in case of the investigated alloys compared to those of pure Al can be attributed to the presence of small iron in the alloy, thus, increasing the catalytic activity on the surface of the alloys. In case of alloys I and II, increasing concentration (at  $5 \times 10^{-5}$  and  $10^{-4}$  M in case of alloy I and at  $10^{-4}$  M in case of alloy II) does not lead to a regular increase in inhibition, as might have been expected from the behaviour of the above mentioned triazole derivative. It may be less stable complexes are generated at higher concentrations<sup>(112)</sup>.

The cathodic polarization curve and inhibition efficiency for pure Al in HCl solution with 3-mercapto-4-phenyl-5-p-nitrophenyl-1,2,4-triazole exhibited a less inhibitive effect of this compound compared to the other examined triazole derivatives. This may be due to the reduction of  $-\text{NO}_2$  group to  $-\text{NHOH}$  group on the surface of pure Al<sup>(113)</sup>, during cathodic polarization or at the corrosion potential diminishes its efficiency.

## **2.2 Behaviour in $\text{HClO}_4$ solution:**

Cathodic overpotential values for pure Al and its investigated alloys at different current densities in 0.5M  $\text{HClO}_4$  solution in the absence and presence of  $10^{-6}$ - $10^{-4}$  M 3-mercapto-4-phenyl-5-4-pyridyl-1,2,4-triazole,

3-mercapto-4-phenyl-5-p-tolyl-1,2,4-triazole and 3-mercapto-4-phenyl-5-p-nitrophenyl-1,2,4-triazole are recorded in Tables 23,24 and 25 respectively. Cathodic Tafel lines for both pure Al and the investigated alloys are shown in Figs. 35-40. Parameters for hydrogen evolution reaction including cathodic Tafel slope ( $b_c$ ) and transfer coefficient ( $\alpha$ ) together with anodic Tafel slope and the change in both cathodic and anodic overpotentials ( $\Delta\eta_c$  and  $\Delta\eta_a$  respectively) in the absence and presence of such studied compounds are given in Tables 32, 33 and 34.

These results indicate that the presence of such investigated compounds cause parallel displacement (except in the presence of both 3-mercapto-4-phenyl-5-4-pyridyl-1,2,4-triazole and 3-mercapto-4-phenyl-5-p-tolyl-1,2,4-triazole in case of alloy I) of the cathodic Tafel lines towards higher overpotential. Such displacement increases with the increase in the concentration of organic additives.

The data given in Table 32 including values of the open circuit corrosion potential ( $E_{corr.}$ ), corrosion rates ( $i_{corr.}$ ), the change in both cathodic and anodic overpotentials ( $\Delta\eta_c$  and  $\Delta\eta_a$  respectively) in the presence of the different concentrations of 3-mercapto-4-phenyl-5-4-pyridyl-1,2,4-triazole together with the values of the inhibition efficiency, indicate that the investigated compound inhibits the corrosion of both pure Al and its investigated alloy II at all examined concentrations. Although the presence of such compound seems to be does not affect the cathodic hydrogen evolution reaction on the surface of alloy I. While the corrosion potential is shifted in the positive direction in the presence of the examined compound, and such shift increases with the increase in the inhibitor concentration. But, such shift is more pronounced in case of alloy II

compared with pure Al and alloy I. The marked increase in the cathodic overpotential value ( $\Delta\eta_c$  at  $360 \mu\text{A}/\text{cm}^2$  ranges from  $-33$  to  $-195$  mV), together with the positive shift in  $E_{\text{corr.}}$ , and the increase in anodic dissolution overpotential of pure Al and its investigated alloys. Such studied compound can be considered as an inhibitor of mixed type of pure Al and alloy II. On the other hand, such compound can be considered as anodic inhibitor of alloy I. Mernari et al.<sup>(114)</sup> studied the inhibiting effects of 3,5-bis(N-pyridyl)-4-amino-1,2,4-triazoles on the corrosion for mild steel in 1M HCl solution. They showed that the electrochemical study reveals that these compounds are anodic inhibitors. Indication of a strong adsorption of these compounds on the active anodic sites suppresses the dissolution reaction and adsorption leads to the formation of a protective film which grows with increasing exposure time. This indicates that such compound retards both cathodic and anodic partial processes in case of pure Al and alloy II. While anodic partial process is suppressed only in the presence of the investigated compound in case of alloy I.

The results obtained for the inhibitive effects of 3-mercapto-4-phenyl-5-4-pyridyl-1,2,4-triazole on the corrosion of pure Al and the investigated alloys, indicate that high inhibition efficiency in case of both pure Al and alloy II is observed. The inhibition efficiency increases with increasing inhibitor concentration. It is noteworthy to show that the inhibition efficiency is higher in case of alloy II than that of pure Al at maximum inhibitor concentration ( $10^{-4}$  M), which reaches a level of 90.4% for alloy II, while reaches to 85.3% in case of pure Al. The highest inhibition efficiency in the presence of such compound can be ascribed to chelation between the inhibitor and iron atoms in the alloy to form  $\text{Fe}^{\circ}$ -triazole complex. The latter is then oxidized to form insoluble complex,

leading to coverage of the most cathodic active sites. Lower values for the inhibition efficiency of such compound in case of pure Al than those obtained with alloy II, may be due to the partial solubility of an insoluble complex chelate which is formed when corrosion occurs in  $\text{HClO}_4$  in the presence of the investigated compound<sup>(71)</sup>.

The data also indicate that the investigated compound does not appreciably affect the value of corrosion current ( $i_{\text{corr.}}$ ) and cathodic overpotential in case of alloy I in such investigated acid. This suggests that such compound is adsorbed very weakly on the surface of alloy I, or its competition between simple blocking of the electrode surface and the accelerating effect of hydrogen evolution reaction by  $\text{FeAl}_3$  and  $\text{Fe}_2\text{SiAl}_8$  intermetallic compounds on the alloy surface. One can conclude that the inhibiting action and the catalytic effect of the hydrogen evolution reaction by the investigated compound in case of alloys in  $\text{HClO}_4$  are approximately equal. The electrochemical behaviour of both pure Al and its investigated alloys in the absence and presence of various concentrations of 3-mercapto-4-phenyl-5-p-tolyl-1,2,4-triazole are given in Table 33. It is seen that  $i_{\text{corr.}}$  values decrease significantly in the presence of such compound at all examined concentrations in case of pure Al and alloy II. This behaviour brings out the fact that such investigated compound is an effective corrosion inhibitor. For alloy I, such compound exhibited catalytic effect on the hydrogen evolution reaction, that is, values of  $i_{\text{corr.}}$  increase as an increase in the concentration of studied compound. This behaviour is associated with decrease in cathodic hydrogen overpotential ( $\Delta\eta_c$ ) and  $E_{\text{corr.}}$  shifts in the positive direction with increasing concentration of the organic compound. Accordingly, such compound can be considered as mixed type inhibitor for pure Al and alloy II, while it can be anodic inhibitor type in

case of alloy I.

The higher inhibition efficiency obtained in case of pure Al at maximum concentration ( $10^{-4}$  M) compared with that in case of alloy II, can be attributed to strong interaction between pure Al surface and inhibitor molecules. Tan and Lee<sup>(115)</sup> suggested that chemisorption is initiated by the partial transfer of electrons from the inhibitor to the metal. The ease of electron transfer depends upon the availability of electrons in inhibitor molecules and the surface metal atoms. A facile transfer is promoted by transition metals having vacant, low lying orbitals, and an inhibitor having high electron density at one of the surface metal atoms. Recently, it has been shown that adsorption also could be established by hydrogen bonding between hydrogen in N-H bonds and oxygen of the metal surface. A good inhibitor preferably should be a large molecule that remains water soluble, contains a large number of N donor atoms and NH bonds, and has an overall high  $pK_a$  value. Accordingly, the adsorption of such studied compound on pure Al or alloy II surface occurs either directly on the basis of donor-acceptor interactions between the  $\pi$ -electrons of the heterocycle or phenyl group of the compound and surface atoms, or interaction of the studied compound with the negatively charged surface. The performance of 3-mercapto-4-phenyl-5-p-tolyl-1,2,4-triazole in 0.5M  $HClO_4$  solution can be explained as follows. In aqueous acidic solutions, such investigated compound exists either as neutral molecules, sharing of electrons between the nitrogen or sulphur atoms, and the metal surface, could be adsorbed on the surface, and leads to displacement of water<sup>(116)</sup>. This organic compound can also adsorb through electrostatic interactions between the positively charged nitrogen (as a result of protonation) and the negatively surface<sup>(117)</sup>. In addition, these molecules possess an abundance of  $\pi$ -electrons and

unshared electron pairs which interact with the surface to provide a protective film. The ability of the molecule to chemisorb dependent on the position of methyl group on the aromatic substituent. The strong electron donor character of the substituent enhances the electronic density near the triazole. The accelerating effect of the same investigated compound in case of alloy I can be ascribed to protonation of  $-SH$  group attached to triazole compound to  $-SH_2^+$ , and the presence of  $FeAl_3$  and  $Fe_2SiAl_8$  intermetallic compounds at the alloy surface catalyze the reduction of hydrogen evolution on the cathodic sites. Such a reaction results in a decrease in the cathodic overpotential ( $\Delta \eta_c$ ) becomes positive values in the presence of such compound. However, such investigated compound exhibited inhibitive effect on the anodic dissolution process. Accordingly, the value of the anodic overpotential ( $\Delta \eta_a$ ) is increased and an appreciable positive shift in corrosion potential is occurred due to the addition of such organic compound. The results suggest that the adsorption of the investigated triazole compound on anodic sites through lone pairs of electron of nitrogen and sulphur atoms may decrease anodic dissolution of alloy I. Niu et al.<sup>(118)</sup> studied inhibitive effect of benzotriazole on the corrosion of Cr-Ni-Ti stainless steel in acidic solution. They found that adsorption and inhibiting the anodic dissolution of the metal by the effect of blocking the active sites on the metal surface. In light of the theory on the shift of the corrosion potential due to addition of inhibitors, it follows that the benzotriazole mainly inhibits the anodic reaction of corrosion process.

The data given in Table 34 show the effect of 3-mercapto-4-phenyl-5-p-nitrophenyl-1,2,4-triazole on the electrochemical and corrosion behaviour of pure Al and its investigated alloys in 0.5M  $HClO_4$  solution. These results indicate that  $i_{corr}$  decreases as an increase in the concentration

of such compound of both pure Al and the investigated alloys I and II. The results also show that values of  $E_{\text{corr}}$  are shifted to more positive values upon increasing the concentration of such compound. While values of both the anodic ( $b_a$ ) and cathodic ( $b_c$ ) Tafel slopes obtained in the absence and presence of the inhibitor are approximately the same of both pure Al and its investigated alloys. Addition of such compound leads to increase in both the overpotential of cathodic hydrogen evolution ( $\Delta \eta_c$ ) and the overpotential of anodic dissolution ( $\Delta \eta_a$ ). These observations are indicative of mixed-type inhibitor without changing the mechanism of the hydrogen evolution reaction (h.e.r.) or anodic dissolution of both pure Al and its investigated alloys.

The results given in Table 34 indicate that 3-mercapto-4-phenyl-5-p-nitrophenyl-1,2,4-triazole inhibits the corrosion of both pure Al and the studied alloys at all examined concentrations. It is observed that the inhibition efficiency gradually increased as an increase in the concentration of the inhibitor in the case of both pure Al and its alloys (I and II). It is interesting to note that inhibition efficiency values in case of pure Al and alloy II (reach to 95% at  $10^{-4}$  M) are higher than those obtained with alloy I (reaches to 48.7%) under the same conditions. The highest inhibition efficiency of pure Al in the presence of such investigated compound is expected, due to the strong interaction between the inhibitor molecules and Al surface. This suggests that the initial step of adsorption involves the protonated inhibitor molecules, which lie flat on the pure Al surface and adsorption via a mechanism involving  $\pi$ -electrons between the heterocycle and the electrode surface is occurred. Accordingly, the adsorption takes place at both anodic and cathodic sites consequently influence the anodic and cathodic partial reactions. On the other hand, lower values for the

inhibition efficiency in case of the investigated alloys compared to those of pure Al are expected due to the presence of iron as minor alloying elements. But, high inhibition efficiency in presence of such compound in case of alloy II is obtained (94.8% at  $10^{-4}$  M). This behaviour may be attributed to chelate formation between the iron atoms in the alloy surface and the inhibitor molecules to form insoluble complex which adsorb very strongly at surface and becomes protecting for the alloy surface. Bentiss et al.<sup>(116)</sup> studied the effect of some triazole derivatives on the corrosion of mild steel in HCl, showed that these compound are very good inhibitors. The inhibition efficiency increases with increasing concentration of such investigated compounds and reaches a level of 98.9% for the inhibitor concentration of  $300 \text{ mg dm}^{-3}$ . Lower values of inhibition efficiency in case of alloy I are expected due to the presence of  $\text{FeAl}_3$  phases which catalyze the hydrogen evolution reaction. The highest inhibiting action of such investigated in case of pure Al and alloy II compared to that observed in HCl solution, may be attributed to the reduction of  $-\text{NO}_2$  group during cathodic polarization in  $\text{HClO}_4$  solution does not take place due to the slow discharge of hydrogen ions on the surface.

## **2.2. Behaviour in $\text{H}_2\text{SO}_4$ solution:**

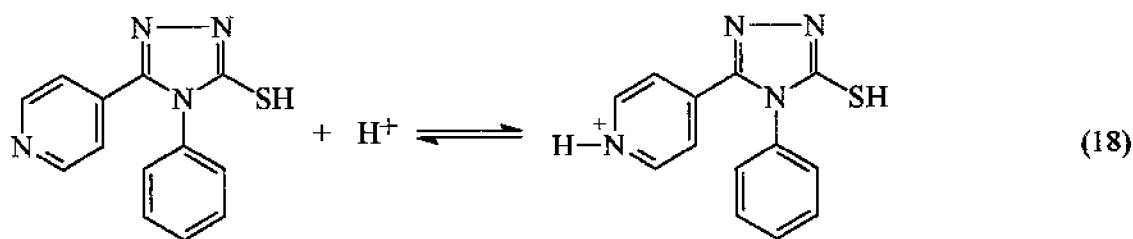
The data obtained from the electrochemical and corrosion behaviour of pure Al and its investigated alloys in 0.5M  $\text{H}_2\text{SO}_4$  solution in the absence and presence of  $10^{-6}$ - $10^{-4}$ M of the investigated triazole derivatives such as : 3-mercapto-4-phenyl-5-4-pyridyl-1,2,4-triazole, 3-mercapto-4-phenyl-5-p-tolyl-1,2,4-triazole and 3-mercapto-4-phenyl-5-p-nitrophenyl-1,2,4-triazole are given in Tables 35, 36 and 37. These results show the



corrosion potential ( $E_{\text{corr.}}$ ) is shifted in the positive direction in the presence of such investigated compounds. The positive shift increases with increasing concentration of the inhibitors of both pure Al and its investigated alloys. However,  $E_{\text{corr.}}$  of Al-alloys is more shifted to positive direction in the presence of such investigated compounds compared with the positive shift in  $E_{\text{corr.}}$  for pure Al. The values of corrosion current ( $i_{\text{corr.}}$ ) are appreciably decreased on addition of all investigated compounds even at the lowest examined concentration ( $10^{-6}$  M). such compounds increased both cathodic and anodic overpotentials ( $\Delta \eta_c$  and  $\Delta \eta_a$  respectively) at all examined concentrations.

Based on the potential shift in  $E_{\text{corr.}}$  and the change in both  $\eta_c$  and  $\eta_a$  of all examined compounds can be considered as an inhibitors of mixed type (affects both cathodic and anodic partial processes). However, the approximate constancy of the anodic ( $b_a$ ) and cathodic ( $b_c$ ) Tafel slopes with increasing concentration of each one of the investigated compounds, indicate that the mechanism of both cathodic hydrogen evolution reaction (h.e.r.) and the anodic dissolution of both pure and its studied alloys are not affected by the presence of any one of such investigated compounds.

Comparison of the results obtained for pure Al and the investigated Al-alloys in the presence of 3-mercapto-4-phenyl-5-4-pyridyl-1,2,4-triazole indicates that at one and the same concentration of the investigated compound, the inhibition efficiency is higher in case of pure Al than that with alloys I and II. Values of inhibition efficiency in case of alloy II is higher than that of alloy I. It may be the pyridyl group attached to triazole compound undergo protonation in aqueous acidic solutions<sup>(1)</sup> according to the following equation:



Thus the initial step of adsorption may involve the protonated molecules of the investigated compound on the negatively charged surface of pure Al. The rapid attainment of the steady state corrosion potential in the presence of such inhibitor (3-4 min) suggests that the initial step of adsorption involves the protonated compound (such adsorption is determined mainly by electrostatic forces). Thus, the inhibition of the studied compound suggests an appreciable contribution to the inhibition process via interaction of  $\pi$ -electrons of aromatic nuclei with the electrode surface<sup>(76)</sup>. Blomgren and Bockris<sup>(95)</sup> and Foroulis<sup>(96)</sup> stated that aromatic amines such aniline and pyridine which are preferentially adsorbed in the cationic form, lie flat on the electrode surface and adsorption via a mechanism involving  $\pi$ -electron interactions between the aromatic nucleus and the metal surface is also possible.

Lower values, for the inhibition of 3-mercapto-4-phenyl-5-(4-pyridyl)-1,2,4-triazole in case of the alloys can be ascribed to the more positive  $\phi$  potential (rational corrosion potential) of the alloy ( $\phi$  potentials for alloys I and II are 155 and 170 mV more positive than that of pure Al). On the other hand, the inhibition efficiency in case of alloy II is higher than that of alloy I which may be due to high density of cathodic active sites on the alloy surface interact with the additive molecules to produce an insoluble complex. It is noteworthy that iron (in alloy II) has an increasing complexing ability with studied additive. This may be explained by the

formation of an adsorbed intermediate on the alloy surface by the interaction of the surface with the investigated additive. Probably an insoluble complex, leading to very high values of inhibition efficiency. However, the efficiency is dependent on the nature of the complex formed and its formation stability constant.

The data given in Table 36 reveal that the inhibition efficiency increases with the increase of 3-mercapto-4-phenyl-5-p-tolyl-1,2,4-triazole concentration in 0.5M  $\text{H}_2\text{SO}_4$  solution of both pure Al and its investigated alloys. Similar trend is observed in the presence of such compound with that of 3-mercapto-4-phenyl-5-4-pyridyl-1,2,4-triazole. High inhibition efficiency of pure Al (96.1% at  $10^{-4}\text{M}$ ) in the presence of studied compound for its investigated alloys (70% at  $10^{-4}\text{M}$ ) is observed. As mentioned above, lower values of inhibition efficiency in case of studied Al-alloys compared with pure Al in the presence of such compound may be due to the ability of the protonated molecules to provide a catalytic path for the hydrogen evolution reaction under cathodic polarization conditions<sup>(119)</sup>. It can be suggested that such reaction is catalyzed by  $\text{FeAl}_3$  present at the alloy surface. The adsorption of such studied compound on the surface can occur either directly on the basis of donor-acceptor interaction between the  $\pi$ -electrons of the heterocycle compound and the surface atoms, or the interaction of such compound with already adsorbed sulphate ions<sup>(120)</sup>. The better performance of triazole derivative can be explained in the following way. In aqueous acidic solutions, such studied compound exist either as neutral molecules or in the form of protonated cation. It may be adsorbed on the metal surface in the form of neutral molecules, involving the displacement of water molecules from the metal surface and sharing of electrons between nitrogen atoms and the metal

surface<sup>(121)</sup>. Heterocyclic nitrogen compounds may also adsorbed through electrostatic interactions between the positively charged nitrogen atom and the negatively charged metal surface<sup>(108)</sup>. It has been observed that the adsorption of such compound can be influenced by the nature of anions in acidic solution<sup>(96,122)</sup>, the specific adsorption of anions having a smaller degree of hydration. Strong adsorption of organic molecules is not always a direct combination of the molecule with metal surface. In some cases, the adsorption can occur through the already chloride or sulphate ions, which interfere with the adsorbed organic molecules. The molecular structure of the organic compound is important in inhibition. On the other hand, it may be -p-tolyl group attached to five position of triazole derivative enhances the electronic density of the ring and in turn, strong ability of the molecule to chemisorb on the surface takes place. In addition, introduction of the electron donating methyl group in the para position in the phenyl group should lead to an increase in the strength of coordination especially with pure Al due to overall increase in electron density in the triazole ring.

The data in Table 37 exhibited that 3-mercapto-4-phenyl-5-p-nitrophenyl-1,2,4-triazole has inhibitive effect on the corrosion of both pure Al and its investigated alloys in 0.5M H<sub>2</sub>SO<sub>4</sub> solution at all examined concentrations. It is observed that the inhibition efficiency of pure Al is higher in the presence of such compound compared with that in case of its studied alloys at all examined concentrations. As mentioned above, the observed lower inhibition efficiency of the studied Al-alloys compared with pure Al in the presence of such studied compound at cathodic potential can be attributed to the presence of iron and silicon as FeAl<sub>3</sub> and Fe<sub>2</sub>SiAl<sub>3</sub> intermetallic compounds at the alloy surface have catalytic effect on the hydrogen evolution reaction. It is noteworthy that iron-rich alloy

(alloy II) exhibited highest inhibition efficiency in the presence of such compound to that observed in case of alloy I. This may be explained by the formation of an adsorbed intermediate on the alloy surface by the interaction of the surface with the studied compound. Probably an insoluble complex, leads to higher values of inhibition efficiency in case of alloy II compared with that of alloy I.

Higher inhibition efficiency values in the presence of such investigated compound in  $\text{H}_2\text{SO}_4$  solution especially in case of the studied alloys compared with the inhibition efficiency values in  $\text{HCl}$  solution are observed. This suggests that the formation of an insoluble complexes in  $\text{H}_2\text{SO}_4$  is stable, and the inhibiting action occurs by strong adsorption of these complexes on the surface, thus decreasing the surface area available for hydrogen deposition without affect in its reaction mechanism. The rate determining step for the hydrogen evolution reaction on the surface in acidic sulphate solution assumed to be slow discharge<sup>(123)</sup>, accordingly reduction of  $-\text{NO}_2$  group does not take place in  $\text{H}_2\text{SO}_4$  solution.

#### **2.4. Adsorption isotherms:**

As assuming no change in the mechanism of both hydrogen evolution reaction (h.e.r.) and anodic dissolution of pure Al and its investigated alloys in 0.5M solutions of  $\text{HCl}$ ,  $\text{HClO}_4$  and  $\text{H}_2\text{SO}_4$  (as previously suggested). Adsorption isotherm obtained from equation (4) are shown in Figs. 47-49 in case of  $\text{HCl}$ , Figs. 50-52 in case of  $\text{HClO}_4$  and Figs. 53-55 in case of  $\text{H}_2\text{SO}_4$  solutions. These isotherms conform approximately to the Langmuir type, in which  $C/\theta$  is a linear function of  $C$ . the same relation was observed by El-Sayed<sup>(76)</sup> for the corrosion inhibition of pure Al and

the same investigated alloys in HCl solution. Similar results were obtained by Bentiss et al.<sup>(116)</sup> for the corrosion inhibition of some triazole derivatives of mild steel in HCl solution, by Syed et al.<sup>(109)</sup> for corrosion inhibition of mild steel using dicyclohexylamine in H<sub>2</sub>SO<sub>4</sub> solution and by Zhao and Mu<sup>(124)</sup> for the adsorption of anion surfactants on Al in HCl solution.



## ***SUMMARY***

**1-** A general survey of the literature deals with the different theories concerning the mechanism of corrosion inhibition by organic inhibitors, and the work is done on such subjects up to the end of 1999. It is shown that although much attention has been paid to the corrosion inhibition of pure Al and its alloys in mineral acidic solutions, few studies on the corrosion inhibition of pure Al and its alloys using triazole compounds were carried out. Careful examination of literature reveals that some studied additives such as adenine and adenosine compounds have not almost yet been used as corrosion inhibitors especially for Al and its alloys.

**2-** The experimental parts deal with the preparation and purification of triazole derivatives and pyrrole derivative compounds used as inhibitors. Adenine and Adenosine compounds were reagent grade (Merck) and used without further purification. Pure Al electrode was cast from extra pure Al rod. Alloy I contains 0.08% Si, 0.1% Fe and the rest Al and alloy II contains 0.25% Si, 0.32% Fe and the rest Al. Preparation of electrolytes, (These were solutions of HCl, HClO<sub>4</sub> and H<sub>2</sub>SO<sub>4</sub>), description of the technique and the apparatus used for galvanostatic was mentioned. Full description of the polarization cell and the preparation of the cell for potential measurement was given. The preparation of organic inhibitor solutions used in this investigation was stated.

**3-** The effect of pyrrole derivative, adenine and adenosine on the electrochemical and corrosion behaviour of pure aluminium and its alloys in 0.5 M solutions of HCl, HClO<sub>4</sub> and H<sub>2</sub>SO<sub>4</sub> has been studied. The results can be summarized as follows:



### **a- Behaviour in HCl solution:**

For both pure Al and the investigated alloys, the studied compounds used as inhibitors shift the corrosion potential in the positive direction. Based on the shift in corrosion potential and the increase in the cathodic overpotential in the presence of organic additives such as, adenine, adenosine and pyrrole derivative can be considered as mixed type inhibitors. But, pyrrole derivative has influence to increase the corrosion current for alloy I in HCl solution, and the maximum value of  $i_{\text{corr}}$  is obtained at higher concentration. This indicates that the addition of this compound catalyzes the hydrogen evolution reaction on alloy I. This behaviour may be attributed to the presence of iron and silicon as  $\text{FeAl}_3$  and  $\text{Fe}_2\text{SiAl}_8$  intermetallic compounds at the alloy surface, which cause high accelerating effect on the hydrogen evolution reaction in the presence of such additive. However, such compound gives an opposite effect on alloy II compared to alloy I, that is, the inhibition efficiency increases as the concentration is increased. Also, the inhibition efficiency increases with increasing the concentration of adenine or adenosine of pure Al and its studied alloys. This inhibition efficiency of adenine and adenosine in case of pure Al is higher than that of corresponding obtained for alloys I and II at all examined concentrations.

### **b- Behaviour in $\text{HClO}_4$ solution:-**

The data indicate that for pure Al and its alloys (except at  $10^{-4}$  M in case of alloy I), the increase in inhibition efficiency with concentration of pyrrole derivative is associated with a decrease in the value of corrosion current ( $i_{\text{corr}}$ ), denoting a decrease in the true surface area available for hydrogen deposition. The increase in the corrosion current of alloy I in the presence of pyrrole derivative (at  $10^{-4}$  M) associated with positive value of change in hydrogen

overpotential( $\Delta\eta_c$ ), and corresponding to that %I becomes negative one. This behaviour may be due to catalytic effect on the hydrogen evolution reaction at higher concentration ( $10^{-4}$  M).

The results as inhibition efficiency,  $i_{corr.}$ , and  $\Delta\eta_c$  values exhibited that adenine and adenosine inhibit the corrosion of pure Al and alloy II (except in case of alloy II at  $10^{-3}$  M of adenosine, %I decreases relatively). While, the same compounds have influence to increase the corrosion current and according to that, inhibition efficiency shifts to more negative values (catalytic effect) as an increase the concentration of the additive on alloy I. Comparison of the results obtained at higher concentration ( $10^{-3}$  M) of both adenine and adenosine in 0.5 M  $HClO_4$  solution of pure Al, indicated that the inhibition efficiency of adenosine is higher than that of adenine, due to the larger molecular size of adenosine than that of adenine. For pure Al, pyrrole derivative has higher inhibition efficiency in  $HClO_4$  solution compared with its %I in HCl solution at concentration of  $10^{-3}$ M. This behaviour may be ascribed to strong adsorption and blocking of the electrode surface by condensation reaction of two molecules of the 3-amino-4-cyano-2-benzoyl-N-phenyl pyrrole in  $HClO_4$  solution.

### **C- Behaviour in $H_2SO_4$ solution:**

Comparison of the results obtained for pure Al and the studied Al-alloyII in the presence of pyrrole derivative indicates that, at higher concentration ( $10^{-4}$  M) the inhibition efficiency is higher in case of pure Al than with alloy II. These results also indicate such compound inhibits the corrosion of pure Al and alloy II even at the lowest examined concentration. The less inhibitive action of the investigated compound in  $H_2SO_4$  solution may be ascribed to adsorption of

$\text{SO}_4^{=}$  ions at the electrode surface, leading to the hinderance of the adsorption of organic molecules. Accordingly, it can be suggested that the interaction between the metal surface and the additive compound will be of much less significance compared with HCl and  $\text{HClO}_4$  solutions.

It can be seen that adenine and adenosine inhibit the corrosion of pure Al and its studied alloys at all examined concentrations. This indicates that the investigated compounds have influence to suppress the anodic partial process and cathodic partial one. The inhibitive effect of adenine and adenosine molecules in  $\text{H}_2\text{SO}_4$  is probably caused by hindering the adsorption of sulphate ions on both pure Al and its alloys, thus preventing dissolution.

#### Adsorption isotherms :

Adsorption isotherms obtained from  $\theta = 1 - \frac{i_{\text{inh.}}}{i_{\text{uninh.}}}$  equation and presented graphically in the presence of all studied compounds in HCl,  $\text{HClO}_4$  and  $\text{H}_2\text{SO}_4$  solutions. These isotherms follow that of Langmuir which characterises the chemisorption of additive compounds on heterogeneous surfaces. For such isotherm  $C/\theta$  is a linear function of  $C$ .

**4- The effect of some triazole derivatives on the eletrochemical and corrosion behaviour of pure aluminium and its alloys in 0.5 M HCl,  $\text{HClO}_4$  and  $\text{H}_2\text{SO}_4$ , has been investigated as the following:**

#### a- Behaviour in HCl solution:

The results reveal the inhibition efficiency for the corrosion of pure Al and its studied alloys in 0.5 M HCl in the presence of 3-mercapto-4-phenyl-5-4-

pyridyl-1,2,4-triazole increases gradually as an increase in the concentration of such compound up to  $5 \times 10^{-5} \text{ M}$ . However the inhibition efficiency becomes negative value at higher concentration ( $10^{-4} \text{ M}$ ) in case of its alloys (I and II). The increase in %I as an increase in the concentration of such compound up to  $5 \times 10^{-5} \text{ M}$  can be ascribed to blocking of the surface, which enhances cathodic polarization and diminishes cathodic current density. Such compound which inhibits both h.e.r. and anodic dissolution may be adsorbed in flat form in case of pure Al, leading to more coverage of active cathodic and anodic sites. The increase in corrosion current in the presence of 3-mercapto-4-phenyl-5-4-pyridyl-1,2,4-triazole on pure Al at higher concentration ( $10^{-4} \text{ M}$ ) may be ascribed to a catalytic effect on the hydrogen evolution reaction.

The results obtained for the inhibitive effects of 3-mercapto-4-phenyl-5-p-tolyl-1,2,4-triazole on corrosion of pure Al and its alloys, indicate high inhibition efficiency is observed in case of pure Al. While lower values (54-78% ) in case of Al-alloys (I and II) are attained. The observed high inhibition efficiency on the hydrogen evolution reaction of pure Al compared to the examined alloys, can be attributed to strong adsorption of such compound on the pure Al. Lower values of inhibition efficiency in case of Al-alloys compared with pure Al may be due to the presence of iron and silicon as  $\text{FeAl}_3$  and  $\text{Fe}_2\text{SiAl}_8$  intermetallic compounds at the alloy surface lead to catalytic of the hydrogen evolution. Lower inhibition in case of alloy II compared to alloy I, suggesting that iron-rich phases (alloy II) have more catalytic ability.

3-mercapto-4-phenyl-5-p-nitrophenyl-1,2,4-triazole shifts the open circuit corrosion potential in the positive direction of both pure Al and its investigated alloys. The inhibition efficiency of such compound in case of pure Al at any

examined concentration (except at  $10^{-6}\text{M}$ ) is much higher than that of either alloy I or alloy II. These results suggest that the adsorption in acidic solutions triazole derivative can exist as cationic species like amino compounds. These cationic species may adsorb on the cathodic sites of both pure Al and its investigated alloys and decrease the evolution of hydrogen. The adsorption of triazole derivative molecules on the anodic sites through lone pairs of electrons of nitrogen and sulphur atoms may decrease anodic dissolution of pure Al and its studied alloys. Less inhibitive effect of this compound on pure Al compared with the other examined triazole derivatives is observed. This behaviour may be attributed to the reduction of  $-\text{NO}_2$  group to  $-\text{NHOH}$  group on the surface of pure Al during cathodic polarization or at the corrosion potential diminishes its efficiency.

#### **b- Behaviour in $\text{HClO}_4$ solution:**

3-mercapto-4-phenyl-5-4-pyridyl-1,2,4-triazole seems to be does not affect the cathodic hydrogen evolution reaction in case of alloy I. The corrosion potential is shifted in the positive direction in the presence of the examined compound, and such shift increases with the increase in the inhibitor concentration. The inhibition efficiency is higher in case of alloy II than that of pure Al at maximum inhibitor concentration ( $10^{-4}\text{M}$ ), which reaches a level of 90.4% for alloy II, and 85.3% only in case of pure Al. The investigated compound does not appreciably affect the value of corrosion current ( $i_{\text{corr}}$ ) and cathodic overpotential in case of alloy I, which may be due to very weak adsorbability on the alloy surface.

At maximum concentration ( $10^{-4}\text{M}$ ) of 3-mercapto-4-phenyl-5-p-tolyl-

1,2,4-triazole, higher inhibition efficiency is obtained in case of pure Al compared with that in case of alloy II. This behaviour can be attributed to strong adsorption of the inhibitor molecules on the pure Al surface. The adsorption of such investigated compound on the pure Al or alloy II surface occurs either directly, on the basis of donor-acceptor interactions between the  $\pi$ -electrons of the heterocycle or phenyl group of the compound and surface atoms, or interaction of the investigated compound with the negatively charged surface. The accelerating effect of the same studied compound in case of alloy I can be ascribed to protonation of -SH group to  $-SH_2^+$  group, and the presence of  $FeAl_3$  and  $Fe_2SiAl_8$  phases at the alloy surface catalyze the hydrogen evolution on the cathodic sites. However, such compound exhibited inhibitive effect on the anodic dissolution process.

The results indicate that 3-mercapto-4-phenyl-5-p-nitrophenyl-1,2,4-triazole inhibits the corrosion of both pure Al and its studied alloys at all examined concentrations. The values of inhibition efficiency are higher in case of pure Al and alloy II (reaches to 95% at  $10^{-4}$  M) than those obtained with alloy I (reaches to 48.7%). Lower values for the inhibition efficiency in case of the investigated alloys compared to those of pure Al are expected due to the presence of iron as minor alloying elements. But, high inhibition efficiency in the presence of such compound in case of alloy II is obtained. This behaviour may be attributed to chelate formation between the iron atoms in the alloy surface and the inhibitor molecules to form insoluble complex which strongly adsorbed on the surface and becomes protective for the alloy surface.

### C- Behaviour in $H_2SO_4$ solution:

Comparison of the results obtained for pure Al and the studied Al-alloys in the presence of 3-mercapto-4-phenyl-5-4-pyridyl-1,2,4-triazole indicates that at one and the same concentration of the investigated compound, the inhibition efficiency is higher in case of pure Al than in case of alloys I and II. Values of inhibition efficiency in case of alloy II are higher than that of alloy I. Lower values for the inhibition efficiency of such compound in case of the alloys can be considered as more positive potential (rational corrosion potential) of the alloys ( $\phi$  potentials for alloys I and II are 155 and 170 mV more positive than that of pure Al).

3-mercapto-4-phenyl-5-p-tolyl-1,2,4-triazole inhibited the corrosion of pure Al and its alloys at all examined concentrations. The mechanism of hydrogen evolution reaction was found to be the same in the absence and presence of the inhibitor. The results showed that such compound is an inhibitor of the mixed type. Lower values of inhibition efficiency in case of studied alloys compared with pure Al in the presence of such compound may be due to the ability of the protonated molecules to provide a catalytic path for the hydrogen evolution reaction under cathodic polarization conditions.

The data exhibited that 3-mercapto-4-phenyl-5-p-nitrophenyl-1,2,4-triazole has inhibitive effect on the corrosion of both pure Al and its alloys in 0.5M  $H_2SO_4$  solution at all examined concentrations. Iron rich alloy(II) exhibited highest inhibition efficiency in the presence of such compound to that observed in case of alloy I. Higher inhibition efficiency in the presence of the investigated compound in  $H_2SO_4$  solution especially in case of Al-alloys

compared with the values of inhibition efficiency in HCl solution are observed. This suggests that the rate determining step for the hydrogen evolution reaction on the surface in acidic sulphate solution is assumed to be slow discharge. Accordingly, reduction as  $-\text{NO}_2$  group does not take place in  $\text{H}_2\text{SO}_4$  solution.

### Adsorption isotherms:

Assuming no change in the mechanism of both h.e.r. and anodic dissolution of pure Al and its alloys in all investigated acids. Adsorption isotherms are obtained from equation  $\theta = 1 - \frac{i_{\text{inh.}}}{i_{\text{uninh.}}}$ . These isotherms conform approximately to the Langmuir type in which  $C/\theta$  is a linear function of C.





## REFERENCES

1. Aluminium Alloys: structure and properties, L. F. Mondolfo P. 122, 282, 368, 120, Butter Worth & Co. (publisher) Ltd, 1976 Beccles and London.
2. Metallurgy of Aluminium Alloys, Ir. E. More Van Laneker p. 35, 37, Chapman and Hall Ltd, London (1967).
3. Aluminium Vol.1, Properties, Physical Metalurgy and Phase Diagram, K. R. Van. Horn (editor), p.212, ASM, Ohio (1971).
4. L. F. Mondolfo, Light Met. Age, **37** (1979) 20.
5. W. A. Anderson and H. C. Stumpf, Corrosion **36** (1980) 212.
6. M. Zamin, Corrosion-NACE, **37** (1981) 627.
7. S. M. Aleikina, Chem. Abst. **75** (1971) 29199f.
8. J. Cote, E. E. Howlette and H. J. Lamb Plating, **57** (1970) 484.
9. J. A. Isasi and M. Metzger, Corros. Sci., **11** (1971) 631.
10. G. TrabANELLI and V. Carassiti in Advances in Corrosion Science and Technology (M. G. Fontana and R. W. Staehle, eds.), Plenum, New York, **1** (1970) 147.
11. Z. A. Foroulis, in Proceedings of Symposium on Basic and Applied Corrosion Research, National Association of Corrosion Engineers, Houston, 1969.
12. O. L. Riggs, Jr., in Corrosion Inhibitors (C. C. Nathan, ed.), National Association of Corrosion Engineers, Houston, 1973, p.7.
13. J. G. Thomas, in Corrosion (L. L. Shreir, ed.), Newnes-Butterworths, London, **2** (1976) 183.
14. E. McCafferty, in Corrosion Control by Coatings (H. Leidheiser, Jr. ed.), Science Press, Princeton, 1979, p. 279.
15. I. L. Rosenfeld, in Corrosion Inhibitors, McGraw-Hill, New York, 1981.

16. H. Fischer, *Werkst. Korros.*, **23** (1972) 445.
17. W. J. Lorenz and F. Mansfeld, International Conference on Corrosion Inhibition, National Association of Corrosion Engineers, Dallas, 1983, paper 2.
18. W. J. Lorenz and F. Mansfeld 31<sup>st</sup> ISE Meeting, Venice, 1980.
19. P. Lorbeer and W. J. Lorenz, *Electrochim. Acta*, **25** (1980) 375.
20. R. H. Hausler, International Conference on Corrosion Inhibition, National Association of Corrosion Engineers, Dallas, 1983, Paper 19.
21. J. O'M. Bockris and D. A. J. Swinkels, *J. Electrochem. Soc.*, **111** (1964) 736.
22. L. I. Antropov, in First International Congress of Metallic Corrosion, Butterworths, London, 1962, p.147.
23. W. Lorenz, *Z. Phys. Chem.*, **219** (1962) 421.
24. W. Lorenz, *Z. Phys. Chem.*, **224** (1963) 145.
25. W. Lorenz, *Z. Phys. Chem.*, **244** (1970) 65.
26. K. J. Vetter and J. W. Schulze, *Ber. Bunsenges Phys. Chem.*, **76** (1972) 920, 927.
27. G. W. Schulze and K. J. Vetter, *J. Electroanal. Chem. Interfacial Electrochem.*, **44** ( 1973) 63.
28. K. J. Vetter and J. W. Schulze, *J. Electroanal. Chem. Interfacial Electrochem.*, **53** ( 1974) 67.
29. J. W. Schulze and K. D. Koppitz, *Electrochim. Acta*, **21** (1976) 327,337.
30. A. Frignani, G. Trabanelli, F. Zucchi and M. Zucchini, *Proc. 5<sup>th</sup> Eur. Symp. Corros. Inhibitors, Ann. Univ. Ferrara, N. S., Sez. V. Suppl.*, **7** (1980) 1185.
31. N. Hackerman and R. M. Hurd, in First International Congress on Metallic Corrosion, Butterworths, London, 1962, p.166.

32. R. G. Pearson, J. Am. Chem. Soc., **85** (1963) 3533; Science, **151** (1966) 172
33. L. Horner, Chem. Ztg., **100** (1976) 247.
34. J. D. Talati and D. K. Gandhi, Corros. Sci., **26** (1983) 1315.
35. S. W. Makwana, N. K. Patel and J. C. Vora Werkst. Korros., **24** (1973) 1036.
36. M. N. Desai, R. R. Patel and D. K. Shah, J. Inst. Chem., Calcutta, **45** (pt. 3), (1973) 87.
37. K. Ramakrishnaiah, N. Subramanyan Trans. Soc. Advan. Electrochem. Sci. Technol., **6** (1971) 87.
38. M. N. Desai, C. B. Shah and S. M. Deasi, J. Electrochem. Soc. India, **32** (1984) 317.
39. J. D. Talati and D. K. Gandhi, Corros. Sci., **23** (1983) 1315.
40. J. D. Talati, D. K. Gandhi, J. Electrochem. Soc. India, **32** (1983) 380.
41. R. B. Patel, J. M. Pandya and K. Lal, Trans. SAEST, **17** (1982) 321.
42. P. N. S. Yadav, R. S. Chaudhary and C. V. Agarwal, Corros. Prev. Control, **30** (1983) 9.
43. Abo El-Khair and B. Mostafa, Corros. Prev. Control., **30** (1983) 15.
44. B. A. Abd El-Nabey, M. M. Essa and M. A. E. Shaban, Surface Technol, **26** (1985) 165.
45. J. D. Talati and J. M. Daraji, Trans. SAEST, **21** (1986) 233.
46. A. E. Fouda, A. M. El-Asklany, L. H. Madkour and K. M. Ibrahim, Acta Chim. Hung., **124** (1987) 377.
47. S. M. Hassan, M. N. H. Moussa, F. I. M. Taha and A. S. Fouda, Corros. Sci., **21** (1981) 439.
48. J. B. Bessone, D. R. Salinas, C. E. Mayer, M. Ebert and W. J. Lorenz, Electrochim. Acta, **34** (1992) 2283.
49. F. D. Bogar and R. T. Foley, J. Electrochem. Soc., **119** (1972) 462.

50. W. M. Moore, C. T. Chen and G. A. Shirm, *Corrosion*, **40** (1984)644.
51. T. R. Beck, *Electrochim. Acta*, **33** (1988) 1321.
52. L. Tomcsanyi, K. Varga, I. Bartik, G. Horanyi and E. Maleczki, *Electrochim. Acta*, **34** (1989) 855.
53. S. Szklarska-Smialowska, *Corros. Sci.*, **33** (1992) 1193.
54. C. Brett, *Corros. Sci.*, **33** (1992) 203.
55. Sklarska-Smialowska, *Pitting Corrosion of Metals*, NACE, Houston, Texas, 1986, p.296.
56. M. Metikos-Hukovic, R. Babic, Z. Grubac and S. Brinic, *J. Appl. Electrochem.*, **24** (1994) 325, 772.
57. R. Babic, M. Metikos-Hukovic, S. Omanovic, Z. Grubac and S. Brinic, *Br. Corros. J.*, **30** (1995) 288.
58. M. N. Desai, B. C. Thakar, P. M. Chiaya and M. H. Gandi, *Corros. Sci.*, **16** (1976) 9.
59. N. Hackerman and A. C. Makrides, *Ind. Eng. Chem.*, **46** (1954) 523.
60. S. L. Granese and B. M. Rosales, *Proc. 7<sup>th</sup> European Symp. Corrosion Inhibitors*, Ann. Univ. Ferrara, N. S., Sez. V, Suppl. N. 9, 1990, P.73.
61. N. Hackerman and H. Kaesche, *J. Electrochem. Soc.*, **105** (1958)191.
62. C. Monticelli, G. Brunoro and G. Trabanelli, *Proceedings of the 7<sup>th</sup> European Symposium on Corrosion Inhibitors (7 SEIC)*, Ann. Univ. Ferrara, N. S., Sez. V, Suppl. 9, 1990, 1125.
63. J. D. Taladi and J. D. Daraji, *J. Indian Chem. Soc.*, **115** (1988) 94.
64. F. Tribonod and C. Fiaud, *Corros. Sci.*, **18** (1978) 139.
65. T. M. Salem, J. Horvath and P. S. Sidky, *Corros. Sci.*, **18** (1978) 363.
66. Y. Isobe, S. Tanaka and F. Hine, *Boshoka Gijutsu*, **39** (1990) 185.
67. H. Leidheiser and H. Konno, *J. Electrochem. Soc.*, **30** (1983) 747.
68. H. Konno, Z. Zhu. and M. Nagayama, *Plating and Surface Finishing*, **40** (1987).

69. K. Niki, F. M. Delnick and N. Hackerman, *J. Electrochem. Soc.*, **122** (1975) 855.
70. C. Casenave, N. Pebere and F. Dabosi, *Materials Science Forum*, *Electrochemical Method in Corrosion Research*, Edited by Ma'rio G. S. Ferreira and Alda M. P. Simo'es (1995).
71. L. Garrigues, N. Pebere and F. Dabosi, *Electrochim. Acta*, **41** (1996) 1209.
72. M. A. Paez, J. H. Zagal, O. Bustos, M. J. Aguirre, P. Skeldon and G. E. Thompson, *Electrochim. Acta*, **42** (1997) 3453.
73. A. A. El-Warraky and H. A. Eldahan, *J. Materials Science*, **32** (1997) 3693.
74. I. Popova and J. T. Yates, *Langmuir*, **13** (1997) 6169.
75. M. Metikos-Hukovic, Z. Grubac and E. Stupnisek-Lisac, *Corrosion*, **50** (1994) 146.
76. A. El-Sayed, *Denki Kagaku*, **66** (1998) 176.
77. E. A. Ashour, S. M. Sayed and B. G. Ateya, *J. Appl. Electrochem.*, **25** (1995) 137.
78. A. K. Vijh, *J. Phys. Chem.*, **73** (1969) 506.
79. K. Nisancioglu and H. Holtan, *Corros. Sci.*, **19** (1979) 537.
80. H. Abdel-Ghany, A. M. El-Sayed and A. K. El-Shafei, *Synthetic communications*, **25** (1995) 119.
81. M. Tandon, J. P. Banthwal, T. N. Bhallaf and K. B. P. Bhargava, *Indian. J. Chem.*, **20B** (1981).
82. A. K. Vijh, *J. Phys. Chem.*, **72** (1968) 1148.
83. *Oxides and Oxide Films*. Edited by John W. Diggle Marcel Dekker, INC, New York (1973) P.174, 176, 188, 199, 226.
84. J. Kunze, *Corros. Sci.*, **7** (1967) 273.
85. T. Hoggard and W. B. Earle, *J. Electrochem. Soc.*, **114** (1967) 694.

86. C. Chakrabarty, M. M. Singh and C. V. Agarwal "Corrosion Inhibition Theory and Practice". NACE paper No. 15 (1987) Houston, Texas.
87. R. E. Mayer, J. Electrochem. Soc., **113** (1966) 1158.
88. A. K. Vijh, Oxide Films; Influence of Solid State Properties on Electrochemical Behaviour, Vol. 2, in oxide and oxides films, ed. J. W. Diggle (New York, NY: Marcel Dekker, Inc.) (1972) 1.
89. B. E. Conway, Theory and Principles of Electrode Processes (New York, NY: Ronald press Co.) (1964) 170.
90. D. Gilroy, B. E. Conway, J. Phys. Chem., **69** (1965) 1259.
91. M. J. Dignam, Mechanism of Ionic Transport Through Oxide Films, Vol. 1, in Oxide and Oxides Films, ed. J. W. Diggle (Author: CITY) NY: Marcel Dekker, Inc., (1972) 92.
92. M. S. Abdel-Aal, M. Th. Makhlof and A. A. Hermas, Proc. 7<sup>th</sup> European Symposium Corrosion Inhibitors, Ann. Univ. Ferrara, N. S. Sez. V., Suppl. N. 9 (1990) 1143.
93. M. S. Abdel-Aal, A. A. Abdel-Wahab and A. El-Saied, Corrosion, **37** (1981) 557.
94. M. N. Desai, Werkstoffe Und Korrosion, **23** (1972) 475.
95. E. Blomgren and J. O.'M. Bockris, J. Phys. Chem., **63** (1959) 1475.
96. Z. A. Foroulis, Proceeding of The 6<sup>th</sup> European Symp. on Corrosion Inhibition, Ann. Univ. Ferrara, N. S. Sez. V, suppl. No. 8 (1985) 130.
97. E. M. Kosower, An Introduction to Physical Organic Chemistry (New York, NY: J. Wiley & Sons, Inc., 1968) p.45.
98. J. Uehara, K. Aramaki, J. Electrochem. Soc., **138** (1991) 3245.
99. E. Stupnisek-Lisac and Z. Ademovic, Proc. 8<sup>th</sup> European Symposium Corrosion Inhibitor, Ann. Univ. Ferrara, N. S. Sez. V, suppl. No. 10 (1995) 257.

100. A. S. Fouda, M. N. Moussa, F. I. Taha and A. I. Elneanaa, *Corros. Sci.*, **26** (1986) 719.
101. A. El-Sayed, *Corrosion Prevention & Control*, **43** (1996) 27.
102. A. El-Sayed, *J. Appl. Electrochem.*, **27** (1997) 193.
103. G. Mrowczynski and Z. Szklarska-Smialowska, *J. Appl. Electrochem.*, **9** (1979) 201.
104. K. J. Vetter ("Electrochem. Kinetics"), Academic Press, New York (1967) 572.
105. M. Troquet, J. P. Labbe and J. Pagetti, *Corros. Sci.*, **21** (1981) 101.
106. N. C. Sobramanyam and S. M. Mayanna, *J. Electrochem. Soc. India*, **33** (1984) 273.
107. H. Yamaoka and H. Fischer, *Electrochim. Acta*, **10** (1965) 679.
108. R. Agrawal and T. K. G. Namloodhiri, *J. Appl. Electrochem.*, **27** (1997) 1265.
109. S. Syed. Azim, S. Muralidharan and S. Venkatakrishna, *J. Appl. Electrochem.*, **25** (1995) 495.
110. M. A. Quraishi, S. Ahmed and M. Q. Ansari, *Br. Corros. J.*, **32** (1997) 297.
111. M. S. Abdel-Aal and M. H. Wahdan, *Br. Corros. J.*, **23** (1988) 25.
112. V. Otieno-Alego, N. Huynh, T. Notoya and S. E. Bottle, *Corros. Sci.*, **41** (1999) 685.
113. K. Aramaki, T. Kiuchi, T. Sumiyoshi and H. Nishihara, *Corros. Sci.*, **32** (1991) 593.
114. B. Mernari, H. Elattari, M. Traisnel, F. Bentiss and M. Lagrenee, *Corros. Sci.*, **40** (1998) 391.
115. P. Li, T. C. Tan and J. Y. Lee, *Corrosion*, **53** (1997) 186.
116. F. Bentiss, M. Lagrenee, M. Traisnel, B. Mernari and H. Elattari, *J. Appl. Electrochem.*, **29** (1999) 1073.



117. C. A. Mann, *Trans. Electrochem. Soc.*, **69** (1936) 105.
118. L. Niu, C. N. Cao, H. C. Lin and G. L. Song, *Corros. Sci.*, **40** (1998) 1109.
119. M. S. Abdel-Aal, M. S. Morad and Z. A. Ahmed, *Proceeding of the 8<sup>th</sup> European Symp. on Corrosion Inhibition*, *Ann. Univ. Ferrara, N. S.*, Sez. V, suppl. No. 10 (1995).
120. N. Hackerman, E. Snively Jr. and J. S. Paynejr., *J. Electrochem. Soc.*, **113** (1966) 677.
121. N. Hackerman and A. C. Makrides, *J. Phys. Chem.*, **59** (1955) 707.
122. S. Rengamati, S. Muralidharan, M. Kulandainathan and S. Venkatakrishna Iyer, *J. Appl. Electrochem.*, **24** (1994) 355.
123. M. Gmytryk and J. Sedzimir, *Corros. Sci.*, **7** (1967) 683.
124. T. Zhao and G. Mu, *Corros. Sci.*, **41** (1999) 1937.



وَقُلْ رَبِّ ادْخُلْنِيْ مُدْخَلَ صِدْقٍ وَّاُخْرِجْنِيْ  
مُخْرَجَ صِدْقٍ وَّاجْعَلْ لِّىْ مِنْ لَّدُنْكَ سُلْطٰنًا  
تَّصِيْرًا



A word cloud of the phrase "ARABIC SUMMARY" in various sizes and orientations, with a central box containing the phrase in a large, bold, italicized font.